

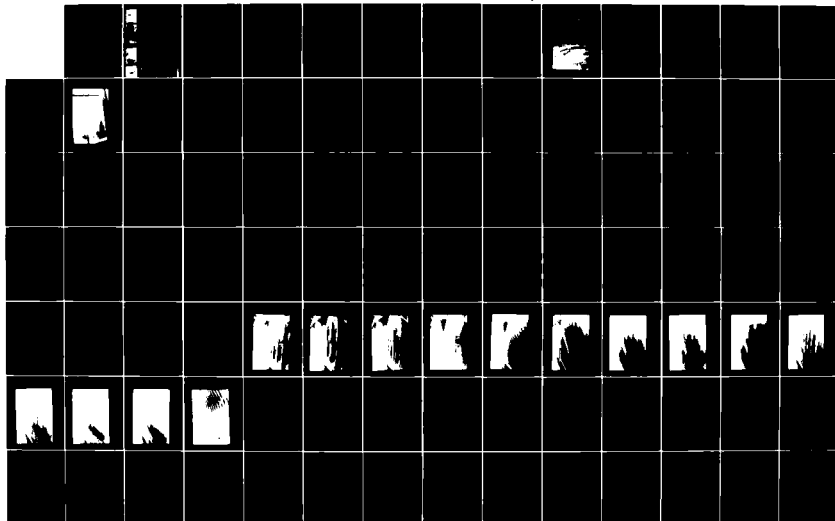
AD A157 888

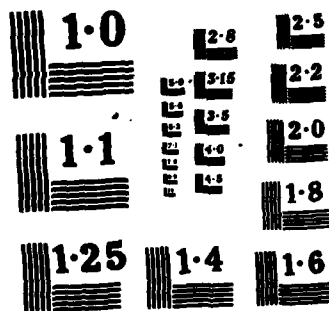
EFFECTS OF PROPOSED HARBOR MODIFICATIONS ON WAVE
CONDITIONS HARBOR RESONANCE (U) COASTAL ENGINEERING
RESEARCH CENTER VICKSBURG MS R R BOTTIN ET AL. JUN 85
CERC-85-2 F/G 13/2

112

UNCLASSIFIED

NL







US Army Corps
of Engineers

AD-A157 888



DTIC FILE COPY

TECHNICAL REPORT CERC-85-2

2

EFFECTS OF PROPOSED HARBOR MODIFICATIONS ON WAVE CONDITIONS, HARBOR RESONANCE, AND TIDAL CIRCULATION AT FISH HARBOR, LOS ANGELES, CALIFORNIA

PHYSICAL AND NUMERICAL MODEL INVESTIGATIONS

by

Robert R. Bottin, Jr., Douglas G. Outlaw,
William C. Seabergh

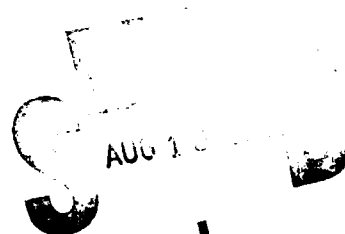
Coastal Engineering Research Center

DEPARTMENT OF THE ARMY
Waterways Experiment Station, Corps of Engineers
PO Box 631
Vicksburg, Mississippi 39180-0631



June 1985
Final Report

Approved For Public Release; Distribution Unlimited



Prepared for Port of Los Angeles
San Pedro, California 90733

Under Contract No. 81-22

85 8 6 055

Destroy this report when no longer needed. Do not return
it to the originator.

The findings in this report are not to be construed as an official
Department of the Army position unless so designated
by other authorized documents.

The contents of this report are not to be used for
advertising, publication, or promotional purposes.
Citation of trade names does not constitute an
official endorsement or approval of the use of
such commercial products.

Unclassified

SECURITY CLASSIFICATION OF THIS PAGE (When Data Entered)

REPORT DOCUMENTATION PAGE		READ INSTRUCTIONS BEFORE COMPLETING FORM
1. REPORT NUMBER Technical Report CERC-85-2	2. GOVT ACCESSION NO. AD-A151 888	3. REPORT'S CATALOG NUMBER
4. TITLE (and Subtitle) EFFECTS OF PROPOSED HARBOR MODIFICATIONS ON WAVE CONDITIONS, HARBOR RESONANCE, AND TIDAL CIRCULA- TION AT FISH HARBOR, LOS ANGELES, CALIFORNIA; PHYSICAL AND NUMERICAL MODEL INVESTIGATIONS	5. TYPE OF REPORT & PERIOD COVERED Final report	
7. AUTHOR(s) Robert R. Bottin, Jr., Douglas G. Outlaw, William C. Seabergh	6. PERFORMING ORG. REPORT NUMBER	
9. PERFORMING ORGANIZATION NAME AND ADDRESS US Army Engineer Waterways Experiment Station Coastal Engineering Research Center P. O. Box 631, Vicksburg, Mississippi 39180-0631	8. CONTRACT OR GRANT NUMBER(s) Contract No. 81-22	
11. CONTROLLING OFFICE NAME AND ADDRESS Port of Los Angeles San Pedro, California 90733	10. PROGRAM ELEMENT, PROJECT, TASK AREA & WORK UNIT NUMBERS	
14. MONITORING AGENCY NAME & ADDRESS (if different from Controlling Office)	12. REPORT DATE June 1985	
	13. NUMBER OF PAGES 180	
	15. SECURITY CLASS. (of this report) Unclassified	
	16. DECLASSIFICATION/DOWNGRADING SCHEDULE	
16. DISTRIBUTION STATEMENT (of this Report) Approved for public release; distribution unlimited.		
17. DISTRIBUTION STATEMENT (of the abstract entered in Block 20, if different from Report)		
18. SUPPLEMENTARY NOTES Available from National Technical Information Service, 5285 Port Royal Road, Springfield, Virginia 22161.		
19. KEY WORDS (Continue on reverse side if necessary and identify by block number) Channels (Hydraulic engineering) (LC) Fish Harbor (Los Angeles, Calif.) (LC) Harbors--California--Los Angeles (LC) Oscillations (LC)		
20. ABSTRACT (Continue on reverse side if necessary and identify by block number) The Port of Los Angeles has embarked upon a program to improve wave and current conditions at Fish Harbor, Los Angeles, California. To achieve this, field measurements (both wave heights and currents) for the existing harbor were obtained and analyzed and a physical hydraulic model for short-period wave tests and numerical models for harbor oscillation and tidal circulation were used to investigate the effects of proposed harbor improvements. The proposed improvements consisted of dredging deeper channels and berthing areas to (Continued)		

DD FORM 1 JAN 73 1473 EDITION OF 1 NOV 65 IS OBSOLETE

Unclassified

SECURITY CLASSIFICATION OF THIS PAGE (When Data Entered)

SECURITY CLASSIFICATION OF THIS PAGE(When Data Entered)

accommodate the larger, deeper draft vessels using the harbor and the creation of landfills to provide for expansion of local industry. The physical model was constructed to an undistorted scale of 1:60, model to prototype, and included the entire harbor and approximately 1,500 ft of underwater contours to the south and east of the entrance. A 30-ft-long wave generator and an Automated Data Acquisition and Control System were utilized in model operation. A hybrid finite element numerical model (capable of calculating forced harbor oscillations for harbors of arbitrary shape and variable depth) was used to calculate harbor resonance at Fish Harbor. Four numerical finite element grids were used to compute wave-height amplification factors and normalized maximum current velocities associated with the harbor's response to incident waves ranging from 20 to 160 sec. A two-dimensional depth-averaged formulation of the hydrodynamic equations was used in the tidal circulation model, and an implicit-explicit finite difference scheme was used to numerically solve the equations.

An optimum improvement plan was developed during the physical model wave tests which met the established wave-height criteria and provided increased area for mooring small craft in the lee of the harbor breakwater. The results of the long-period prototype data analysis and numerical harbor oscillation study indicated a decrease in long-period wave energy for this optimum plan. The tidal circulation study indicated that changes in tidal circulation characteristics were limited to the vicinity of Fish Harbor and included a slight shift in flood and ebb flow patterns due to the breakwater location for the optimum plan. Tidal flushing in Fish Harbor was influenced by the optimum plan but was similar to existing conditions for successive low waters.

Accession For	
NTIS GRA&I	<input checked="" type="checkbox"/>
DTIC TAB	<input type="checkbox"/>
Unannounced	<input type="checkbox"/>
Justification	

SECURITY CLASSIFICATION OF THIS PAGE (When Data Entered)

PREFACE

The investigation reported herein was authorized by the Harbor Department of the City of Los Angeles, California, under a contract with the US Army Engineer Waterways Experiment Station (WES), Agreement No. 81-22, dated 16 January 1982.

The studies were conducted during the period April 1982-May 1984 by personnel of the Wave Dynamics Division (WDD), Wave Processes Branch (WPB), under the direction of Messrs. C. E. Chatham, Jr., Chief of the WDD, and D. G. Outlaw, Chief of the WPB. The model investigations were initiated in the Hydraulics Laboratory (HL) under the general direction of Messrs. H. B. Simmons and F. A. Herrmann, Jr., Chief and Assistant Chief, respectively, HL. On 1 July 1983, WDD was transferred to the Coastal Engineering Research Center (CERC) under the general direction of Dr. R. W. Whalin and Dr. L. E. Link, Jr., Chief and Assistant Chief, respectively, CERC. The hydraulic model tests and the numerical analyses of harbor oscillations were conducted by Messrs. H. F. Acuff and M. G. Mize, Civil Engineering Technicians, and Mrs. M. L. Hampton, Computer Technician, under the supervision of Mr. R. R. Bottin, Jr., Project Manager. The tidal circulation study was conducted by Mr. W. C. Seabergh, Research Hydraulic Engineer. The prototype data acquisition and analyses were performed by CPT George Horsham, CE, and Messrs. L. A. Barnes and R. E. Ankeny, Civil Engineering Technicians, under the supervision of Mr. A. W. Garcia, Research Oceanographer. This report was prepared by Messrs. Bottin, Outlaw, and Seabergh.

During the course of the investigation, liaison between the City of Los Angeles and WES was maintained by means of conferences, telephone communications, and monthly progress reports.

Messrs. Ed Gorman, Vern Hall, and Roy Lawler of the City of Los Angeles Harbor Department, and Mr. Charlie Fisher of the US Army Engineer District, Los Angeles, visited WES to observe model operation and/or participate in conferences during the course of the various studies.

Commanders and Directors of WES during the conduct of this investigation and the preparation and publication of this report were COL Tilford C. Creel, CE, and COL Robert C. Lee, CE. Technical Director was Mr. F. R. Brown.

CONTENTS

	<u>Page</u>
PREFACE.	1
CONVERSION FACTORS, NON-SI TO SI (METRIC)	
UNITS OF MEASUREMENTS.	3
PART I: INTRODUCTION.	5
The Prototype.	5
Proposed Improvements.	5
Purpose of the Investigation	6
PART II: SHORT-PERIOD WAVE TESTS IN THE PHYSICAL MODEL.	7
The Physical Model	7
Test Conditions and Procedures	12
Tests and Results.	16
PART III: HARBOR OSCILLATION RESULTS.	21
Prototype Wave Data Acquisition.	21
Prototype Wave Data Analysis Results	22
Harbor Oscillation Numerical Model	25
Model Tests and Results.	28
Comparison of Prototype Data and Numerical Model Results	30
Plan Evaluation.	31
Wave and Current Design Parameters	32
PART IV: TIDAL CIRCULATION RESULTS.	34
The Numerical Model.	34
Tests and Results.	34
PART V: CONCLUSIONS	43
REFERENCES	45
TABLES 1-13	
PHOTOS 1-14	
PLATES 1-109	
APPENDIX A: NOTATION.	A1

CONVERSION FACTORS, NON-SI TO SI (METRIC)
UNITS OF MEASUREMENTS

Non-SI units of measurement used in this report can be converted to SI (metric) as follows:

<u>Multiply</u>	<u>By</u>	<u>To Obtain</u>
acres	4046.856	square metres
cubic feet	0.02831685	cubic metres
feet	0.3048	metres
feet per second	0.3048	metres per second
miles (US statute)	1.609347	kilometres
pounds (mass) per cubic foot	16.01846	kilograms per cubic metre
square feet	0.09290304	square metres
square feet per second	0.09290304	square metres per second
square miles (US statute)	2.589988	square kilometres

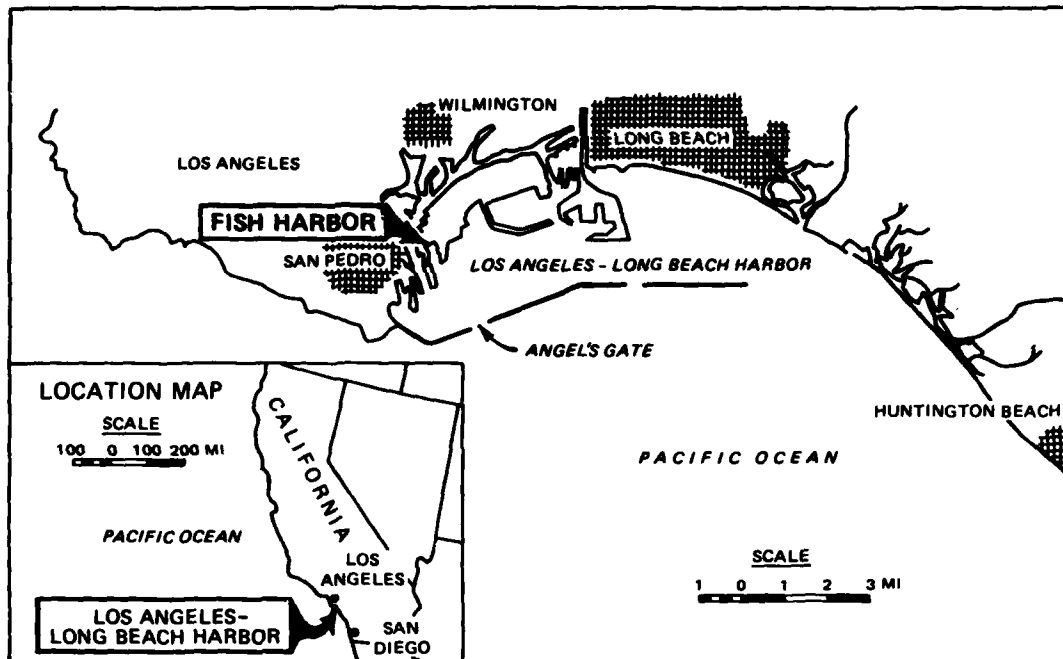


Figure 1. Project location



Port of Los Angeles The Port of the Pacific

Figure 2. Aerial photograph of Fish Harbor

EFFECTS OF PROPOSED HARBOR MODIFICATIONS ON WAVE
CONDITIONS, HARBOR RESONANCE, AND TIDAL CIRCULATION AT
FISH HARBOR, LOS ANGELES, CALIFORNIA
Physical and Numerical Model Investigations

PART I: INTRODUCTION

The Prototype

1. Fish Harbor is located within Los Angeles Harbor, California, about 2 miles* north-northwest of Angel's Gate (Figure 1). Approximately 4,000 ft of water frontage in Fish Harbor is used for commercial fishing and cannery purposes. Many of the waterfront structures were constructed in the early 1900's and now require replacement due to deterioration and obsolescence.

2. Present depths in the Fish Harbor channel and berthing area range from 15 to 22 ft and cannot accommodate the larger, deeper draft fishing vessels now being used in the area. In addition, unfavorable wave conditions during storms prevent the expansion of small-boat moorings. An aerial photograph of Fish Harbor is shown in Figure 2.

Proposed Improvements

3. Improvements for Fish Harbor proposed by the Port of Los Angeles consist of the following:

- a. Removing a portion of the existing outer harbor west breakwater and the inner harbor east breakwater.
- b. Deepening of the entrance channel to -30 ft and increasing its width to 240 ft.
- c. Deepening of the entire existing inner harbor and the northeasternmost portion of the existing outer harbor to -30 ft.
- d. Excavating land at the southeastern portion of the harbor and constructing a 190-acre landfill extending in an easterly direction. A 3-acre landfill on the western side of the harbor is also proposed.

* A table of factors for converting non-SI units of measurement to SI (metric) units is presented on page 3.

- e. Deepening of areas on the east and west sides of the existing outer harbor to -20 ft for commercial fishing vessels.
- f. Deepening an area on the west side of the existing outer harbor to -15 ft for recreational small craft.
- g. Installing adequate breakwaters for protection of craft against storm wave attack.

Purpose of the Investigation

4. At the request of the Port of Los Angeles, Los Angeles, California, an investigation was conducted by WES to:

- a. Determine, through field measurements, wave conditions in the existing harbor. Prototype data would be obtained over a 6-month period.
- b. Determine, through the use of a small-scale physical hydraulic model, breakwater modifications required to provide short-period (4 to 18 sec) wave protection for the proposed development project.
- c. Determine, through the use of a harbor resonance numerical model, the response of the existing and proposed configurations to wave excitation for long-period waves ranging from 20 to 160 sec. The response of the existing configuration would maximize usefulness of data from the field program.
- d. Determine, through the use of a numerical tidal circulation model, the effects of the proposed plan on tidal circulation.
- e. Develop remedial plans in the various models, as necessary to alleviate undesirable conditions.
- f. Determine if design modifications to the proposed plans could be made that would significantly reduce construction costs and still provide adequate protection.

PART II: SHORT-PERIOD WAVE TESTS IN THE PHYSICAL MODEL

The Physical Model

Design of model

5. The Fish Harbor model (Figure 3) was constructed to an undistorted linear scale of 1:60, model to prototype. Scale selection was based on such factors as:

- a. Depth of water required in the model to prevent excessive bottom friction.
- b. Absolute size of model waves.
- c. Available shelter dimensions and area required for model construction.
- d. Efficiency of model operation.
- e. Available wave-generating and wave-measuring equipment.
- f. Model construction costs.

A geometrically undistorted model was necessary to ensure accurate reproduction of short-period wave patterns. Following selection of the linear scale, the model was designed and operated in accordance with Froude's model law (Stevens et al. 1942). The scale relations used for design and operation of the model were as follows:

<u>Characteristic</u>	<u>Dimension*</u>	<u>Model:Prototype Scale Relation</u>
Length	L^{**}	$L_r = 1:60$
Area	L^2	$A_r = L_r^2 = 1:3,600$
Volume	L^3	$V_r = L_r^3 = 1:216,000$
Time	T	$T_r = L_r^{1/2} = 1:7.75$
Velocity	L/T	$V_r = L_r^{1/2} = 1:7.75$

* Dimensions are in terms of length and time.

** For convenience, symbols and unusual abbreviations are listed and defined in Appendix A.

6. The proposed improvement plans for Fish Harbor included the use of rubble-mound breakwaters. The existing breakwaters and revetments are rubble-mound structures. Based on past experience, 1:60-scale model structures

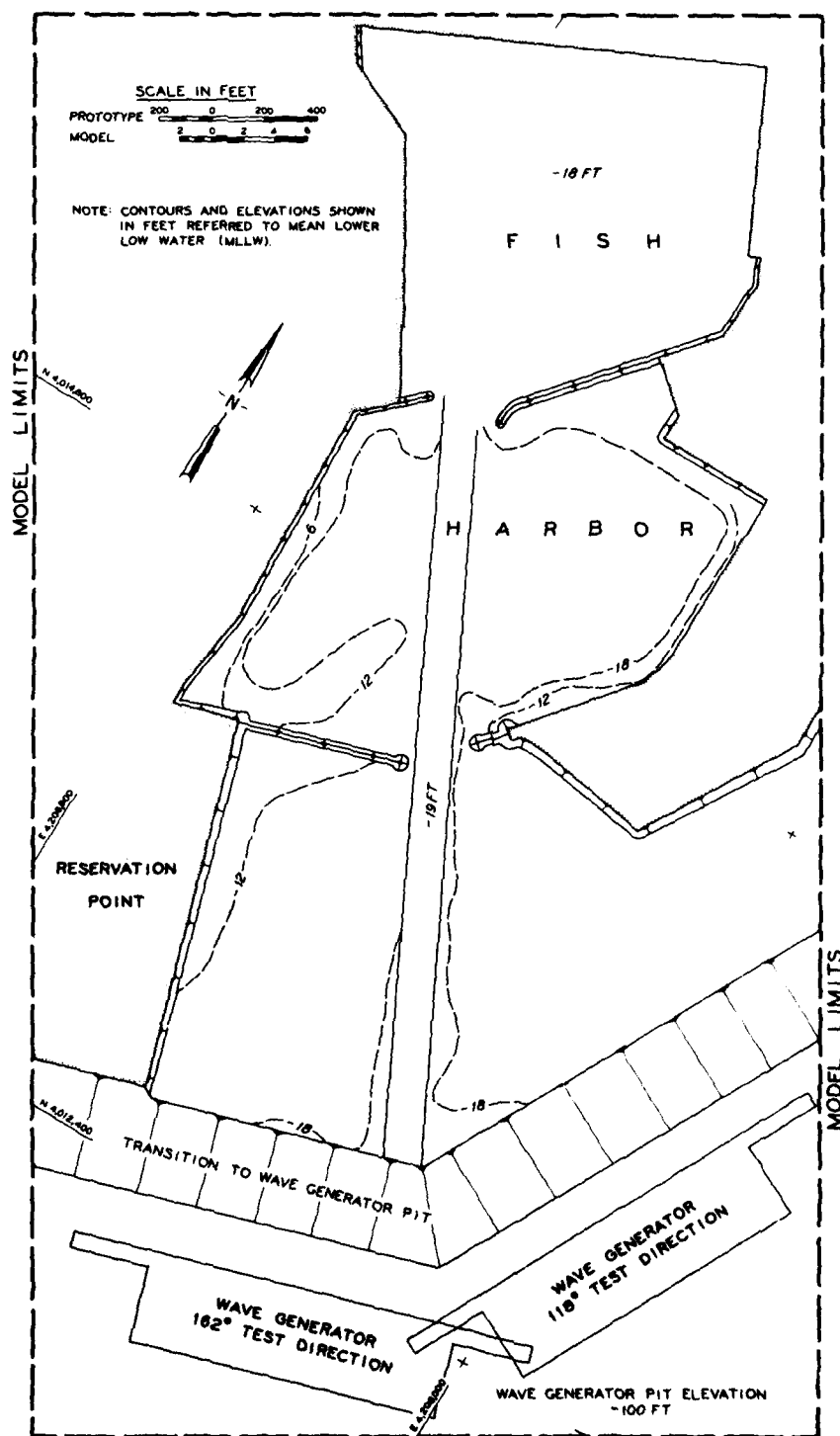


Figure 3. Model layout

should not create sufficient scale effects to warrant geometric distortion of rock sizes to ensure proper transmission and reflection of wave energy. Therefore stone size selection was based on linear scale relations and an assumed specific weight of 165 lb/ft^3 for the prototype rock.

The model and appurtenances

7. The model, which was molded in cement mortar, reproduced all of Fish Harbor and approximately 1,500 ft of the underwater topography to the south and east of the entrance (in the Los Angeles outer harbor), with a sloping transition to the wave generator pit elevation (el) of -100 ft. The total area reproduced in the model was approximately 4,750 sq ft, representing about 0.6 square mile in the prototype. A general view of the model is shown in Figure 4. Vertical control for model construction was based on mean lower low water (mllw)* datum. Horizontal control was referenced to a local prototype grid system.

8. Model waves were generated by a 30-ft-long wave generator with a trapezoidal-shaped, vertical-motion plunger. The vertical movement of the plunger caused a periodic displacement of water incident to this motion. The length of the stroke and the period of the vertical motion were variable over the range necessary to generate waves with the required characteristics.

9. An Automated Data Acquisition and Control System (ADACS), designed and constructed at WES (Figure 5), was used to secure wave-height data at selected locations in the model. Basically, through the use of a mini-computer, ADACS recorded onto magnetic tape the electrical output of parallel-wire resistance-type wave gages that measured the change in water-surface elevation with respect to time. The magnetic tape output of ADACS was then analyzed to obtain the wave-height data.

10. A 2-ft (horizontal) solid layer of fiber wave absorber was placed around the inside perimeter of the model to damp any wave energy that might otherwise be reflected from the model walls. In addition, guide vanes were placed along the wave generator sides to ensure proper formation of the wave train incident to the model contours.

* All elevations (el) cited herein are in feet referred to mean lower low water (mllw) unless otherwise defined.



Figure 4. General view of model

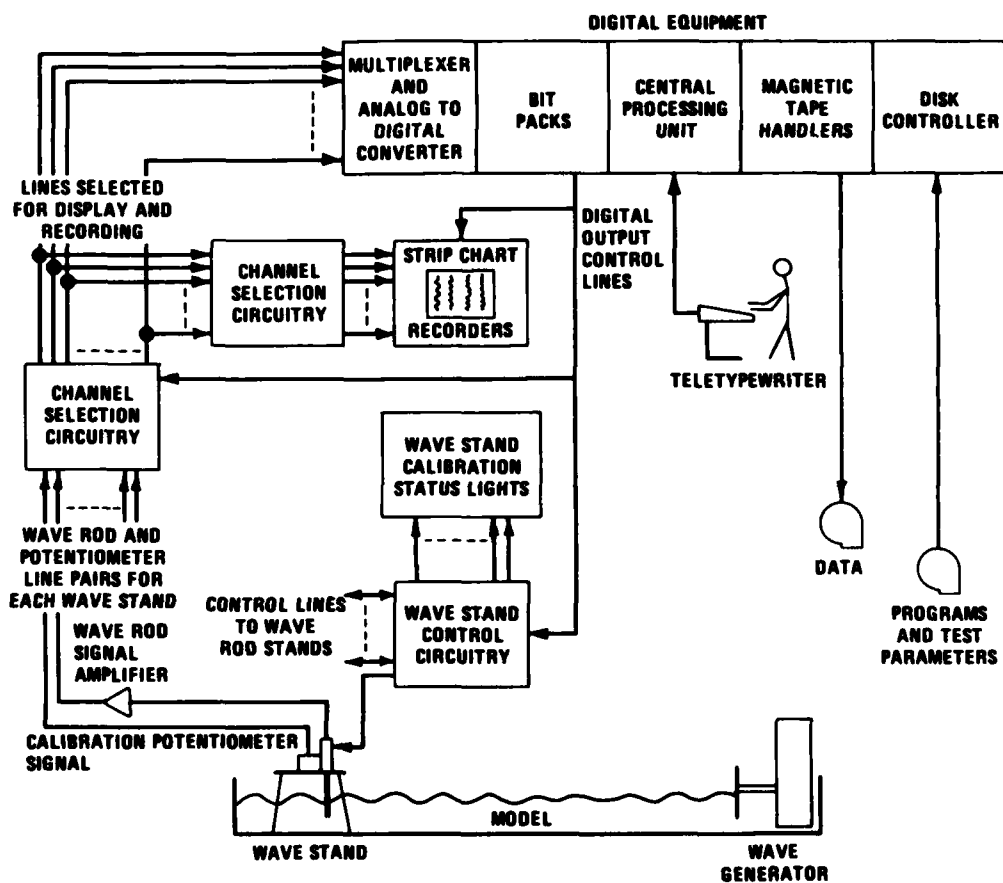


Figure 5. Automated Data Acquisition and Control System (ADACS)

Test Conditions and Procedures

Selection of test conditions

11. Still-water levels. Still-water levels (swl's) for harbor wave-action models are selected so that various wave-induced phenomena dependent on water depths are accurately reproduced in the model. These phenomena include the refraction of waves in the harbor area, overtopping of harbor structures by waves, reflection of wave energy from harbor structures, and transmission of wave energy through porous structures.

12. It was desirable to select a model swl that closely approximated the higher water stages which normally occur in the prototype for the following reasons:

- a. The maximum amount of wave energy reaching a coastal area normally occurs during the higher water phase of the local tide cycle.
- b. Most storms moving onshore are characteristically accompanied by a higher water level due to wind, tide, and shoreward mass transport.
- c. The selection of a high swl helps to minimize model scale effects due to viscous bottom friction.
- d. When a high swl is selected, a model investigation tends to yield more conservative results.

13. A swl of +5.4 ft mllw was selected for use during model testing. This value (+5.4 ft) represents mean higher high water (mhhw).

14. Factors influencing selection of test wave characteristics. In planning the testing program for a model investigation of harbor wave-action problems, it is necessary to select dimensions and directions for the test waves that will allow a realistic test of the proposed improvement plans and an accurate evaluation of the elements of the various proposals. Surface wind waves are generated primarily by the interactions between tangential stresses of wind flowing over water, resonance between the water surface and atmospheric turbulence, and interactions between individual wave components. The height and period of the maximum wave that can be generated by a given storm depend on the wind speed, the length of time that wind of a given speed continues to blow, and the water distance (fetch) over which the wind blows.

Selection of test conditions entails evaluation of such factors as:

- a. The fetch and decay distances (the latter being the distance over which waves travel after leaving the generating area) for

various directions from which waves can attack the problem area.

- b. The frequency of occurrence and duration of storm winds from the different directions.
- c. The alignment, size, and relative geographic position of the navigation entrance to the harbor.
- d. The alignments, lengths, and locations of various reflecting surfaces inside the harbor.
- e. The refraction of waves caused by differentials in depth in the area seaward of the harbor, which may create either a concentration or diffusion of wave energy at the harbor site.

15. Wave refraction. When waves move into water of gradually decreasing depth, transformations take place in all wave characteristics except wave period (to the first order of approximation). The most important transformations with respect to selection of test wave characteristics are the changes in wave height and direction of travel due to the phenomenon referred to as wave refraction. The change in wave height and direction can be determined by plotting refraction diagrams and calculating refraction coefficients. These diagrams are constructed by plotting the position of wave orthogonals (lines drawn perpendicular to wave crests) from deep water into shallow water. If it is assumed that waves do not break and there is no lateral flow of energy along the wave crest, the ratio between the wave height in deep water (H_0) and the wave height at any point in shallow water (H) is inversely proportional to the square root of the ratio of the corresponding orthogonal spacings (b_0 and b), or $H/H_0 = K_R (b_0/b)^{1/2}$. The quantity $(b_0/b)^{1/2}$ is the refraction coefficient K_R ; K_S is the shoaling coefficient. Thus the refraction coefficient multiplied by the shoaling coefficient gives a conversion factor for transfer of deepwater wave heights to shallow-water values. The shoaling coefficient, which is a function of wavelength and water depth, can be obtained from the Shore Protection Manual (SPM) (USAEWES, CERC 1984).

16. A wave refraction and shoaling analysis was performed at the site in connection with the design of the Los Angeles-Long Beach (LA-LB) Harbors' three-dimensional model investigation at WES (Outlaw et al. 1977). This analysis indicated, in general, a convergence of energy at the LA-LB breakwaters. It was determined that up to a 50 percent increase in amplitude could be expected at the breakwater for various wave periods.

17. Prototype wave data and selection of test waves. Measured prototype wave data on which a comprehensive statistical analysis of short-period

wave conditions could be based were unavailable for the LA-LB Harbor area. However, statistical deepwater wave hindcast data representative of this area were obtained from National Marine Consultants (1960). An analysis of these data (based on meteorological records and charts) indicates an envelope for wave period versus wave height for the unrefracted open-ocean wave statistics, as shown in Figure 6. By application of refraction and shoaling coefficients, shallow-water wave heights at the LA-LB breakwater were determined (Figure 6). These shallow-water wave values were then diffracted through Angel's Gate (using procedures from the SPM (USAEWES, CERC 1984) and transmitted through and over the middle breakwater (using coefficients obtained from Hales (1976) to obtain wave characteristics at Fish Harbor (Table 1)). In addition, the characteristics of locally generated wind waves (i.e., generated inside the LA-LB middle breakwater) were obtained by the application of hindcasting techniques from the SPM (USAEWES, CERC 1984) to wind data acquired at the Los Angeles International Airport during the period 1947-1975. The characteristics of waves selected for use in the model (based on the above-mentioned analyses)

are shown in the following tabulation:

Selected Test Direction	Selected Test Waves	
	Period, sec	Height, ft
162 deg (deepwater waves)	5	2
	7	5
	9	3,7
	11	5
	13	5
	15	3
	17	3
	19	3
118 deg (locally generated waves)	4	3

Analysis of model data

18. Relative merits of the various plans tested were evaluated by:

- a. Comparison of wave heights at selected locations in the model.
- b. Visual observations and wave pattern photographs.

In analyzing the wave-height data, the average height of the highest one-third of the waves recorded at each gage location was selected. All wave heights thus selected were adjusted to compensate for wave-height attenuation due to viscous bottom friction in the model by application of Keulegan's equation (Keulegan 1950). From this equation, reduction of wave heights in the model

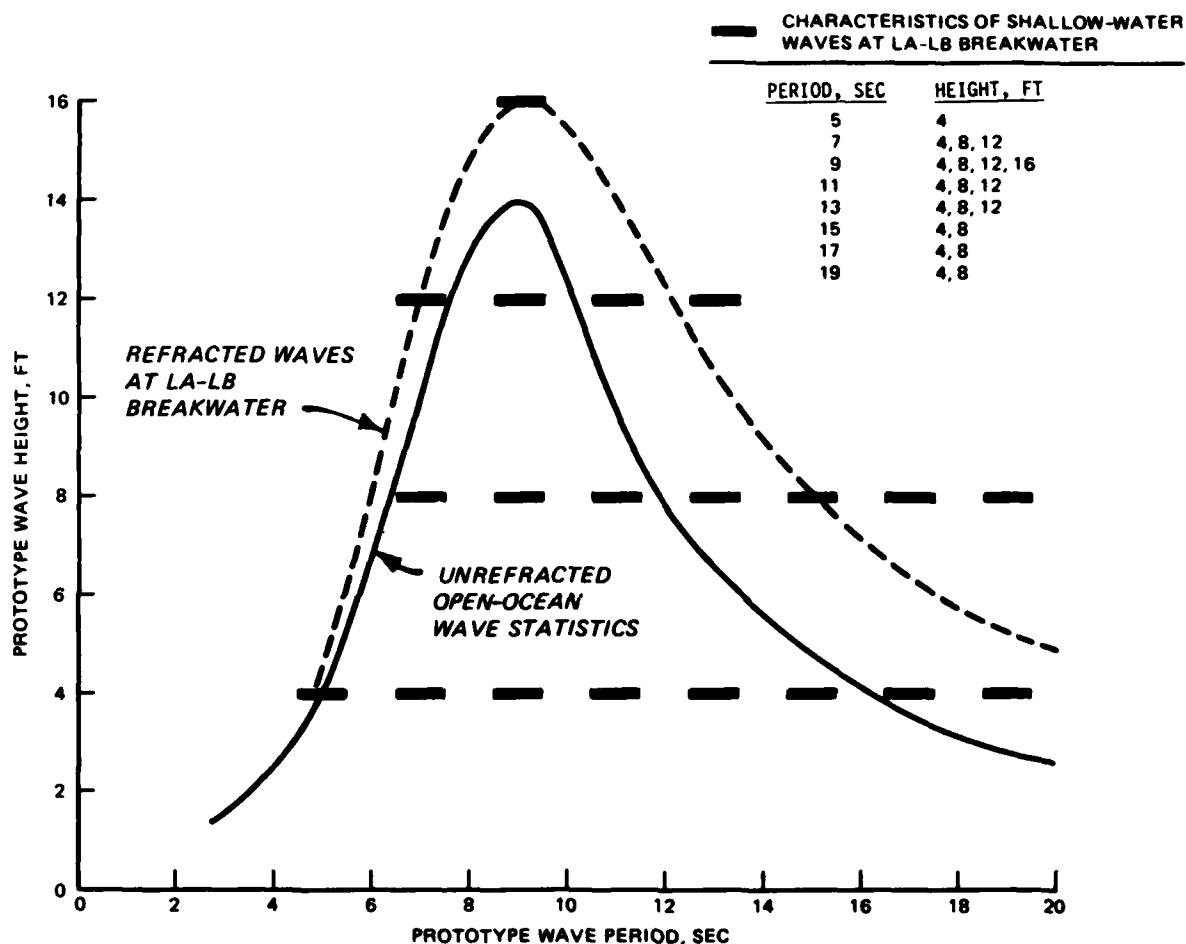


Figure 6. Characteristics of wave statistics (open ocean and refracted waves at LA-LB breakwater)

can be calculated as a function of water depth, width of wave front, wave period, water viscosity, and distance of wave travel.

Tests and Results

Description of tests

19. Existing conditions. Prior to tests of various improvement plans, comprehensive tests were conducted for existing conditions. Wave-height data

were obtained at various locations in the harbor (Plate 1) for the test waves listed in paragraph 17. Wave pattern photographs were secured for representative test waves.

20. Improvement plans. Wave-height tests were conducted for 18 variations in the design elements of one major improvement plan. Variations consisted of changes in the length of the breakwater, alignment of the entrance channel, and length and location of a breakwater spur. Wave pattern photographs were obtained for the initial test plan and what was considered the optimum test plan. Brief descriptions of the improvement plans are presented in the following subparagraphs; dimensional details are presented in Plates 2-9.

- a. Plan 1 (Plate 2) consisted of the initially proposed improvement plan. This included removal of the existing east inner breakwater and a 150-ft-long portion of the west outer structure, the removal of the existing east outer breakwater, and excavation of a portion of the existing overbank. A new landfill extending easterly increased the overbank area on the eastern side of the outer harbor, and a new landfill was installed in the western portion of the harbor adjacent to the remaining west outer breakwater. The plan also entailed a 240-ft-wide, 30-ft-deep entrance channel and a 30-ft-deep inner harbor. Areas in the east and west portions of the outer harbor were increased to 20-ft depths for a commercial fishing basin and commercial fishing piers, respectively, and another area in the southwestern portion of the outer harbor was dredged to a 15-ft depth for recreational craft. Wave protection was provided by a 1,200-ft-long breakwater installed at an elevation of +15 ft. The structure originated at the southeastern corner of the outer harbor and extended in a southwesterly direction.
- b. Plan 1A (Plate 2) entailed the elements of Plan 1 with a 210-ft-long revetment installed along the vertical wall adjacent to the commercial fishing basin.
- c. Plan 1B (Plate 2) involved the elements of Plan 1 with a 420-ft-long revetment installed along the vertical wall adjacent to the commercial fishing basin.
- d. Plan 1C (Plate 2) included the elements of Plan 1 with a 630-ft-long revetment installed along the vertical wall adjacent to the commercial fishing basin.
- e. Plan 1D (Plate 3) consisted of the elements of Plan 1 and the 630-ft-long revetment of Plan 1C with a 100-ft-long spur installed on the breakwater originating 300 ft west of the vertical wall and extending northwesterly.
- f. Plan 1E (Plate 3) entailed the elements of Plan 1 and the 630-ft-long revetment of Plan 1C with a 150-ft-long spur

installed on the breakwater originating 300 ft west of the vertical wall and extending northwesterly.

- g. Plan 1F (Plate 4) included the elements of Plan 1 and the 630-ft-long revetment of Plan 1C with a 150-ft-long spur originating on the breakwater 960 ft from the vertical wall and extending northwesterly.
- h. Plan 1G (Plate 4) involved the elements of Plan 1 and the 630-ft-long revetment of Plan 1C with a 150-ft-long spur originating on the breakwater at a point 600 ft from the vertical wall and extending northwesterly.
- i. Plan 1H (Plate 5) consisted of the elements of Plan 1 and the 420-ft-long revetment of Plan 1B with a 150-ft-long spur originating on the breakwater at a point 300 ft from the vertical wall and extending northwesterly.
- j. Plan 1I (Plate 5) entailed the elements of Plan 1 and the 210-ft-long revetment of Plan 1A with a 150-ft-long spur originating on the breakwater at a point 300 ft from the vertical wall and extending northwesterly.
- k. Plan 1J (Plate 5) involved the elements of Plan 1 with a 150-ft-long spur originating on the breakwater at a point 300 ft from the vertical wall and extending northwesterly.
- l. Plan 1K (Plate 6) included the elements of Plan 1 with a 240-ft-long spur originating on the breakwater at a point 600-ft seaward of the vertical wall and extending northwesterly.
- m. Plan 1L (Plate 6) consisted of the elements of Plan 1 with a 200-ft-long spur originating at a point 700 ft seaward of the vertical wall and extending northwesterly.
- n. Plan 2 (Plate 7) involved the elements of Plan 1, but the breakwater was decreased by 200 ft in length resulting in a 1,000-ft-long structure and the entrance channel was shifted easterly.
- o. Plan 3 (Plate 8) entailed the elements of Plan 1, but the breakwater was decreased by 100 ft in length resulting in a 1,100-ft-long structure and the entrance channel was shifted easterly.
- p. Plan 4 (Plate 9) included the elements of Plan 1, but 200 ft of the breakwater length was removed from the shoreward end of the structure resulting in a 1,000-ft-long breakwater.
- q. Plan 4A (Plate 9) consisted of the elements of Plan 1 with 200 ft of breakwater length removed from the shoreward end of the structure and a 150-ft-long spur originating on the breakwater at a point 300 ft seaward of the vertical wall (100 ft from the shoreward end of the structure) and extending northwesterly.
- r. Plan 4B (Plate 9) involved the elements of Plan 1 with 200 ft of breakwater length removed from the shoreward end of the

structure and the 150-ft-long spur of Plan 4A. In addition, a 630-ft-long revetment was installed along the vertical wall adjacent to the commercial fishing basin.

21. Wave-height tests involving most of the improvement plans were limited to the most critical direction of wave approach (i.e., 162 deg). The most promising improvement plan (Plan 1L), however, was subjected to wave-height tests from both the 162- and 118-deg test directions. Wave gage locations for the various test plans are shown in Plates 2-9.

Test results

22. In evaluating test results, the relative merits of each plan were based on an analysis of measured wave heights. Model wave heights (significant wave height or $H_{1/3}$) were tabulated (Tables 2-10) to show measured values at selected locations. For an improvement plan to be acceptable, it was specified that wave heights not exceed 1.5 ft in the commercial fishing areas or 1.0 ft in the recreational boating area.

23. Existing conditions. Wave-height measurements secured for existing conditions are presented in Table 2. Maximum wave heights obtained were 4.9 ft in the entrance to the outer harbor (gage 1) for 9-sec, 7-ft and 19-sec, 3-ft test waves from 162 deg; 4.1 ft in the mooring area of the outer harbor (gage 4) for 9-sec, 7-ft test waves from 162 deg; 2.3 ft in the entrance to the inner harbor (gage 8) for 13-sec, 5-ft test waves from 162 deg; and 3.2 ft in the inner harbor (gage 12) for 13-sec, 5-ft test waves from 162 deg. Typical wave patterns obtained for existing conditions are shown in Photos 1-5.

24. Improvement plans. Results of wave-height tests with Plan 1 installed in the model for test waves from 162 deg are presented in Table 3. Maximum wave heights were 1.3 ft in the commercial fishing basin (gages 8 and 9) for 17-sec, 3-ft test waves; 1.0 ft in the recreational boating area (gages 5 and 6) for 9-sec, 7-ft test waves; and 0.9 ft in the inner portion of the harbor (gages 11-20) for 9-sec, 7-ft and 17-sec, 3-ft test waves. Wave pattern photographs secured for representative test waves for Plan 1 are shown in Photos 6-9.

25. Results of wave-height tests conducted for Plans 2 and 3 are presented in Tables 4 and 5 for test waves from 162 deg. Maximum wave heights obtained were 2.3 and 2.0 ft in the commercial fishing basin (gages 8 and 9); 1.4 and 1.3 ft in the recreational boating area (gages 5 and 6); and 1.7 and

1.5 ft in the inner portion of the harbor (gages 11-20) for Plans 2 and 3, respectively.

26. Wave-height measurements obtained for Plan 4 for test waves from 162 deg are presented in Table 6. Maximum wave heights were 1.4 ft in the commercial fishing basin (gages 8 and 9) for 7-sec, 5-ft test waves; 0.9 ft in the recreational boating area (gages 5 and 6) for 17-sec, 3-ft test waves; and 1.5 ft in the inner harbor (gages 11-20) for 15-sec, 3-ft test waves. Visual observation revealed, however, what appeared to be excessive wave heights along the vertical wall adjacent to the commercial fishing basin. A wave gage was placed in this area, and wave heights of 3.5 ft were recorded.

27. Additional wave heights were obtained along the vertical wall adjacent to the commercial fishing basin (gages 21-25). These data were obtained for Plan 4A and 4B and Plans 1-IJ for test waves from 162 deg. Results of these tests are shown in Table 7. Maximum wave heights obtained along the vertical wall were 2.9 and 3.0 ft for Plans 4A and 4B, respectively, and 3.2, 3.2, 3.0, 3.0, 1.8, 1.5, 2.1, 2.0, 1.4, 1.5, and 1.5 ft for Plans 1-IJ, respectively. Considering wave protection provided and construction costs, Plan 1J appeared to be optimum at this point.

28. Wave-height data were obtained for Plans 1K and 1L in an effort to provide a larger area for mooring small craft in the lee of the breakwater. A comparison of wave heights obtained for Plans 1J-1L along the vertical wall adjacent to the commercial fishing basin (gages 21-25) for test waves from 162 deg is presented in Table 8. Maximum wave heights were 1.5, 1.1, and 1.3 ft for Plans 1J-1L, respectively.

29. Results of comprehensive wave-height tests (gages 1-20) for Plans 1J and 1L are presented in Tables 9 and 10. Maximum wave heights obtained were 1.5 and 1.1 ft in the commercial fishing basin (gages 8 and 9); 0.8 and 0.9 ft in the recreational boating area (gages 5 and 6); and 0.8 and 0.9 ft in the inner portion of the harbor (gages 11-20) for Plans 1J and 1L, respectively. Typical wave patterns obtained for Plan 1L are shown in Photos 10-14.

30. Discussion of test results. Test results for existing conditions revealed rough and turbulent wave conditions in the harbor with wave heights in excess of 4 ft in the mooring areas of the outer harbor and 3 ft in the inner harbor.

31. Initial wave-height tests with Plan 1 installed in the model

indicated that this plan met the established wave-height criteria (maximum wave heights of 1.5 ft in the commercial fishing basin and 1.0 ft in the recreational boating area).

32. With the breakwater length decreased on the seaward end and the entrance channel shifted easterly (Plans 2 and 3), wave heights in both the commercial fishing basin and the recreational boating area increased and failed to meet the specified wave-height criteria.

33. Initial wave-height measurements for Plan 4 (breakwater length decreased from shoreward end) indicated that this test plan was acceptable with respect to the established wave-height criteria; however, visual observations revealed what appeared to be excessive wave heights along the vertical wall adjacent to the eastern commercial fishing area. Additional measurements confirmed wave heights in excess of 3 ft in this area. Installation of a revetment along the vertical wall (Plan 4A), and a spur on the breakwater (Plan 4B) did not reduce wave heights to the 1.5-ft wave-height criterion in the area.

34. At this point Plan 1 was reinstalled in the model, and wave heights were obtained along the vertical wall adjacent to the eastern commercial fishing basin. Wave heights in excess of 3.0 ft were recorded. A series of test plans (Plans 1A-1J), which entailed revetment along the vertical wall and/or the installation of spurs on the breakwater, was tested. Tests indicated that several plans (Plan 1E, 1H, 1I, 1J, 1K, and 1L) would meet the established wave-height criterion of 1.5 ft in the commercial fishing basin. After further evaluation, it appeared that Plans 1J and 1L were optimum. Plan 1J provided adequate wave protection with a minimum of breakwater spur length (the Plan 1J spur was 50 ft shorter than that of Plan 1L); however, Plan 1L provided a much larger area for mooring small craft in the lee of the breakwater (leaving an area for future expansion of the basin).

35. Wave heights for Plans 1J and 1L for the original gage locations (gages 1-15) revealed that both plans met the specified wave-height criteria.

PART III: HARBOR OSCILLATION RESULTS

Prototype Wave Data Acquisition

36. The wave data acquisition system consisted of completely submerged pressure gages at three locations (sta FH1-FH3) and a directional wave gage at one location (sta FH4), as shown in Plate 10. The gages, manufactured by SEA DATA and available commercially, are self-contained, pressure-sensing instruments that record on magnetic tape cassettes. Pressure gages were mounted on piling beneath the piers at each station and the directional gage was mounted on a submerged platform. Wave gage operational status for the measurement period is shown in Plate 11. Gage installation and service interval dates are shown in Table 11. Periods of time during which the gages were not operational were caused by either meter electronic-circuit malfunction or tape-drive malfunction.

37. Data tapes retrieved from the gages were processed and wave spectra were computed using a discrete Fast Fourier Transform and corrected for depth attenuation according to linear wave theory as a function of frequency. The pressure response factor P is computed as

$$P = \frac{\cosh kh}{\cosh kD} \quad (1)$$

where

k = local wave number

h = local water depth

D = height of the wave sensor above the bottom

The spectral energy density of the sea surface is thus related to the pressure spectrum by the equation

$$E_s(f) = \left(\frac{\cosh kh}{\cosh kD} \right)^2 E_p(f) \quad (2)$$

where

subscripts s , p are sea surface energy spectra and the energy spectra prior to correcting for pressure response, respectively. The significant wave height H_{m0} is computed as

$$H_{m_0} = 4 \left[\frac{1}{\frac{1}{T} \int_0^T E_s(f) df} \right]^{1/2} \quad (3)$$

where

Δt = sampling interval, sec

T = length of a wave record, sec

The significant wave height is used in the sea and swell period range. In the longer period range (approximately 25 sec and greater), the wave energy is separated into period bands where the energy is summed over eight spectral lines for each band. The spectral energy density E_b for each band is:

$$E_b(f_j) = \frac{1}{\Delta f} \sum_{k=Ml+1}^{M(l+1)} A_k^2 \quad \text{for } l = 0, 1, 2, 3, \dots, \left(\frac{N}{2M} - 1 \right) \quad (4)$$

where

$$j = l+1$$

$$M = 8$$

38. The length of the wave record for the pressure cells was 1.138 hr (2,048 data samples at a 2-sec time interval). The time interval between the start of each 2,048-point wave record was 2 hr. Pressure gages were set to start so that one of the three gages was acquiring data at all times. The directional gage was operated continuously with a 4-sec interval between data samples.

Prototype Wave Data Analysis Results

39. Waves in the shorter period sea and swell range were relatively small in Fish Harbor during the data acquisition period for all wave records analyzed. The maximum significant wave height was 0.28 ft during the data acquisition period and occurred at sta FH1 on 1 March 1983, at 2045 P.s.t. At approximately the same time, the significant wave height at sta FH2 was 0.37 ft. Sta FH3 was not on-line during the same time period. The maximum significant wave height for the available data analysis records at sta FH2 was 0.48 ft and occurred on 4 March 1983 at 1745 P.s.t. The significant wave

height at sta FH1 was less than 0.09 ft during the same time period.

40. For the available record at sta FH3 in the outer harbor, the maximum wave height was 0.68 ft and occurred on 21 November at 1645 P.s.t. The significant wave height at sta FH2 (sta FH1 was not on-line) was less than 0.09 ft during the same time period.

41. The sea and swell shorter period significant wave-height data indicate that Fish Harbor is protected against incident sea and swell at the wave gage stations. The maximum significant wave heights observed were less than 1 ft although the outer harbor station, FH3, was not operational during the period of maximum significant wave heights in the inner harbor. Physical model wave test data for existing conditions (Table 2) indicate that larger wave heights would have been observed near the outer harbor entrance and at the model gage 4 position near the northwest corner of the outer harbor.

42. Data analysis for long-period surge included the 24.3- to 248-sec-period range. In the analysis, spectral wave data results were grouped into period bands with equal width in frequency. The equal frequency bands were selected to provide sufficient definition of the wave energy and to limit the number of bands to the minimum required. The period bands for an equal frequency width of 0.001955 Hz are:

Period Band, sec

248.2 - 167.2
167.2 - 126.0
126.0 - 100.1
100.1 - 84.5
84.5 - 72.5
72.5 - 63.5
63.5 - 56.5
56.5 - 50.8
50.8 - 46.3
46.3 - 42.4
42.4 - 39.2
39.2 - 36.4
36.4 - 34.0
34.0 - 31.9
31.9 - 30.0
30.0 - 28.3
28.3 - 26.9
26.9 - 25.5
25.5 - 24.3

Although equal in frequency, the period bands are narrower as the period decreases. In the long-period surge range, the wave energy density in each

period band will be used as a measure of the wave energy in the band.

43. The maximum wave energy density for sta FH2 (northeast corner of the inner harbor) is plotted in Plates 12-16 for each period band. In each case, the wave energy density reaches a peak during data acquisition Interval 4 or 5, except for the 36.4- to 34.0-sec-period band which reaches a maximum during Interval 3. Intervals 4 and 5 correspond with the mid-January to mid-March winter storm period during the winter of 1983 and show the increase in long-period wave energy during the winter. The increased wave energy is particularly noticeable for the period bands near 50 sec and longer. In the first period band (248.2 to 167.7 sec), maximum wave energy density increased from Interval 1 to Interval 4 approximately 77 times (from $0.050 \text{ ft}^2/\text{sec}$ to $3.851 \text{ ft}^2/\text{sec}$). In the remaining period bands, the increase was smaller and was a minimum of 21 percent for the lowest period band (25.5 to 24.3 sec).

44. The observed wave spectra from the wave data analysis are, of course, affected by the offshore incident wave spectra, and the Fish Harbor analyses results will be dependent on the incident wave energy distribution. Amplification of wave energy at sta FH1, FH2, and FH3 is shown in Plates 17-19 for selected storms. The wave energy data in each period band have been normalized by the wave energy data observed at the directional wave gage location.

45. The directional gage data are used as a measure of the wave energy at a station that is not strongly affected by resonant oscillations. Wave energy amplification for each period band is shown in Plate 17 for sta FH1 and FH2 for 27 January 1983 at approximately 1045 P.s.t. This time period coincides with maximum wave energy observed during the storm of 27 January 1983 at Sunset Beach, Calif. The Sunset Beach data were available from the California Coastal Data Collection Program and were used to indicate periods of maximum incident storm wave energy. Wave energy amplification results for the same two gages are also shown in Plate 18 for data from the 2 March 1983 storm, again near the peak wave energy observed at Sunset Beach, Calif. Similar data for sta FH2 and FH3 are shown in Plate 19 for the approximate time of maximum wave energy at Sunset Beach, Calif., during the 30 November-1 December 1982 storm.

46. The average wave-height amplification data for sta FH1 and FH2 in the inner harbor relative to sta FH4 show maximum wave-height amplification in the 100- to 150-sec-period range with a smaller peak in the 50- to

70-sec-period range. A third amplification peak is present near 27 sec, particularly for the 1 December 1982 and 27 January 1983 storms. The average wave-height amplification for sta FH3 in the outer harbor is shown in Plate 19 for the 1 December 1982 storm. The periods of resonant amplification are similar to the periods at sta FH1 and FH2 but are higher near 27 and 50 to 70 sec. The maximum amplification is similar to sta FH2 for the longer period peaks but extends over a broader period range. The amplification data for sta FH1 and FH2 vary in amplification relative to sta FH4 and are probably due both to variation in the frequency distribution of the incident wave energy in the summed bands and to variation in the incident wave direction of approach.

Harbor Oscillation Numerical Model

47. The response of Fish Harbor to long wave excitation was determined by using a hybrid finite element numerical model developed by Chen and Mei at the Massachusetts Institute of Technology (Chen and Mei 1974). The model solves the following generalized Helmholtz equation:

$$\nabla \cdot [h(x,y) \nabla \phi(x,y)] + \frac{w^2}{g} \phi(x,y) = 0 \quad (5)$$

where $\phi(x,y)$ is the velocity potential defined by $u(x,y) = -\nabla \phi(x,y)$, with $u(x,y)$ being a two-dimensional velocity vector and w an angular frequency. Equation 5 governs small amplitude undamped oscillations of water in a basin of arbitrary shape and variable depth forced by periodic long waves. It has been further assumed that the flow is irrotational. The boundary condition along the shoreline and along the breakwaters is that the normal component of the velocity be equal to zero. Therefore the breakwater is considered as a solid barrier.

48. The Helmholtz equation:

$$\nabla^2 \phi(x,y) + \frac{w^2}{gh} \phi(x,y) = 0 \quad (6)$$

is the governing equation for a constant-depth ocean region outside the basin.

49. For a harbor in a semi-infinite ocean with a straight coastline there is an incident, reflected, and scattered wave. The scattered wave has a velocity potential ϕ_s given by

$$\phi_s = \sum_{n=0}^{\infty} \alpha_n H_n(kr) \cos n\theta \quad (7)$$

where α_n are unknown coefficients and $H_n(kr)$ are Hankel functions of the first kind of order n .

50. ϕ_s satisfies the radiation condition that the scattered wave must behave as an outgoing wave at infinity. This condition is known as the Sommerfeld radiation condition and may be expressed mathematically as follows:

$$\lim_{r \rightarrow \infty} \sqrt{r} \left(\frac{\partial}{\partial r} - ik \right) \phi_s = 0 \quad (8)$$

51. Chen and Mei (1974) used a calculus-of-variations approach and obtained a Euler-Lagrange formulation of the boundary value problem. The following functional, with the property that it is stationary with respect to arbitrary first variations of $\phi(x,y)$, was constructed by Chen and Mei:

$$\begin{aligned} F(\phi) = & \iint 1/2 \left[h(\nabla\phi)^2 - \frac{w^2}{g} \phi^2 \right] dA \\ & + 1/2 \oint \left[h(\phi_R - \phi_I) \frac{\partial(\phi_R - \phi_I)}{\partial n_a} \right] da - \oint \left[h\phi_a \frac{\partial(\phi_R - \phi_I)}{\partial n_a} \right] da \\ & - \oint \left[h\phi_a \frac{\partial\phi_I}{\partial n_a} \right] da + \oint \left[h\phi_I \frac{\partial(\phi_R - \phi_I)}{\partial n_a} \right] da \end{aligned} \quad (9)$$

where

A = region inside the harbor

\oint = line integral

ϕ_R = far-field velocity potential

ϕ_I = velocity potential of the incident wave

n_a = unit normal vector outward from Region A

a = boundary of Region A

ϕ_a = total velocity potential evaluated on Boundary a

Proof was given by Chen and Mei that the stationarity of this functional is equivalent to the original boundary value problem.

52. The integral equation obtained from extremizing the functional is solved by utilizing the finite element method. This method is a technique of numerical approximation that involves dividing a domain into a number of non-overlapping subdomains which are called elements.

53. The solution of the problem is approximated within each element by

suitable interpolation functions in terms of a finite number of unknown parameters. These unknown parameters are values of the field variable $\phi(x,y)$ at a finite number of points which are called nodes. The relations for individual elements are combined into a system of equations for all unknown parameters.

54. In the region outside the basin, the velocity potentials are solved analytically in terms of unknown coefficients. The region is considered a single element with an "interpolation function" given by Equation 7. The infinite series is terminated at some finite value so that the addition of further terms does not significantly influence the calculated values of $\phi(x,y)$. The resulting equation is combined with the system of equations for unknown parameters at nodal points within the basin and this complete system is solved using Gaussian elimination matrix methods.

55. $\eta(x,y)$ is related to $\phi(x,y)$ through the linearized dynamic free-surface boundary condition.

$$\eta(x,y) = - \frac{1}{g} \frac{\partial \phi(x,y)}{\partial t} \quad (10)$$

The horizontal velocity components have the following form:

$$u(x,y) = - \frac{g}{w} \frac{\partial \eta(x,y)}{\partial x}; \quad v(x,y) = - \frac{g}{w} \frac{\partial \eta(x,y)}{\partial y} \quad (11)$$

The hybrid finite element method (so named by Chen and Mei because the method involves the combination of analytical and finite element numerical solutions) is a steady-state solution of the boundary value problem. The response of a harbor to an arbitrary forcing function can easily be determined within the framework of a linearized theory.

Application of numerical model

56. The numerical grids used in the numerical model computations consisted of elements that were triangular and often equilateral. The lengths of the triangle sides were selected so that the largest elements had lengths equal to or less than one-eighth of the local wavelength. Such element lengths were determined to provide sufficient accuracy (Houston 1976) for this study. Smaller dimensions were selected for elements along docking facilities and breakwaters as well as in the vicinity of changes in depths and alignment of channels and basins. These smaller elements were chosen to allow

spatial resolution of geometric changes or variations in water depths.

57. The water depths in the numerical model were represented by discrete values at the centroid of each element. For each element, the chosen water depth represented an average value over the element.

58. Incident waves from south with periods ranging from 20 to 160 sec were considered in this study. Wave amplitudes at each nodal point and current velocities at the centroid of each element were calculated for various increments in wave period. Resonant peaks were identified by considering incident wave periods in increments of 0.25 sec.

Model Tests and Results

The tests

59. Numerical harbor oscillation tests were conducted for existing conditions and revised conditions. Revised conditions used were the optimum plan (Plan 1L) based on the short-period wave tests discussed in PART II. Four finite element grids (Plates 20-23) were used during the course of the study and are described as follows:

<u>Grid Number</u>	<u>Number of Elements</u>	<u>Number of Nodal Points</u>	<u>Harbor Configuration</u>	<u>Range of Periods Tested, sec</u>
I	2,614	1,400	Existing conditions	20 to 30
II	839	463	Existing conditions	30 to 160
III	2,325	1,253	Plan 1L	20 to 30
IV	840	474	Plan 1L	30 to 160

60. The smaller elements of Grids I and III were used for the 20- to 30-sec wave period range, and the larger elements of Grids II and IV were used for wave periods ranging from 30 to 160 sec to reduce computational costs.

61. Harbor response data were initially calculated for existing conditions and Plan 1L for 0.5-sec increments for wave periods ranging from 30 to 60 sec, 1-sec increments for wave periods ranging from 60 to 100 sec, and 2-sec increments for wave periods ranging from 100 to 160 sec. Data for additional wave periods were then calculated, as necessary, to define resonant peaks.

62. Stations for which wave-height amplification factors and normalized maximum current velocities were obtained for existing conditions and Plan 1L are shown in Plates 24 and 25, respectively. The wave-height amplification factor is defined at any point inside the harbor as the wave height at that

point divided by twice the incident wave height. This traditional definition results from the fact that the standing wave height for a straight coast with no harbor would be twice the incident wave due to the superposition of the incident and reflected waves. The normalized maximum current velocity at any point in the harbor is defined as the maximum current velocity over one period of the standing wave (oscillation) in the harbor divided by the amplitude of the incident wave. Since the numerical harbor oscillation model is based on the linearized long-wave equation, the velocities have no vertical variation. In addition, the mathematical form of the current velocity of a harmonic, long-period wave is directly proportional to the amplitude of the long-period wave in the harbor. Hence the current velocity associated with the harbor oscillation can be normalized, for convenience, by the incident wave amplitude. Therefore the normalized maximum current velocity at any point in the harbor multiplied by the incident wave amplitude in feet gives maximum current velocity in feet per second. Wave-height amplification factors and normalized maximum current velocity versus wave period were plotted for the elevation and velocity stations shown in Plates 24 and 25.

63. Based on frequency (wave period) response curves for wave-height amplification and normalized maximum current velocity, the wave periods of peak responses can be determined. These peak responses represent resonant effects of the harbor response to incident long-period wave energy.

Test results

64. Frequency response curves of wave-height amplification and normalized maximum current velocity versus wave period (periods ranging from 20 to 160 sec) are shown in Plates 26-41 for selected elevation and velocity stations for existing conditions and Plan 1L. Based on these curves, resonant peaks were identified at various stations for existing conditions for wave periods of 42.5, 43, 80, 103, 110, and 134.5 sec and various stations for Plan 1L for 44.5-, 53.5-, 54.5-, 64.5-, 75-, and 152-sec wave periods. The following tabulation shows the resonant peak, the maximum wave-height amplification factor, and the station location at which it occurred in the harbor for existing conditions and Plan 1L. Corresponding normalized maximum current velocities for the defined resonant peaks are also shown along with the station location where the maximum velocity occurred in the harbor.

<u>Period</u> <u>sec</u>	<u>Maximum</u> <u>Amplification</u>	<u>Station</u> <u>Location</u>	<u>Normalized</u> <u>Maximum</u> <u>Velocity</u>	<u>Station</u> <u>Location</u>
<u>Existing Conditions</u>				
42.5	6.50	1	8.49	1
43.0	6.00	10	5.44	1
80.0	2.89	4	5.04	1
103.0	13.37	6	34.80	5
110.0	3.96	11	6.05	10
134.5	14.01	1	19.88	1
<u>Plan 1L</u>				
44.5	5.98	11	9.30	11
53.5	6.91	3	14.72	1
54.5	14.27	10	21.69	12
64.5	3.83	1	6.24	4
75.0	6.04	8	8.61	7
152.0	1.38	1	5.12	2

65. Contours of wave-height amplification factors over the entire grid are an excellent technique of representing the model configuration of a harbor response. This graphic technique depicts very well the spatial variation of wave-height amplification throughout the harbor. Contours of wave-height amplification for the resonant peaks identified in paragraph 64 are shown in Plates 42-47 and Plates 48-53 for existing conditions and Plan 1L, respectively.

66. At any point in the harbor, horizontal velocities can be calculated from the pressure gradients associated with the spatial changes of the water-surface elevations or wave-height amplification factors. For each of the resonant peaks listed in paragraph 64, vector plots of the normalized maximum current velocities throughout the harbor are plotted in Plates 54-59 and Plates 60-65 for existing conditions and Plan 1L, respectively. Velocities are represented by lines whose centers lie at the elements centroids. Water particles move horizontally back and forth in a direction parallel to the lines. Since the velocities have been normalized by the amplitude of the incident wave, the velocities are in units of feet per second per foot of incident wave amplitude.

Comparison of Prototype Data and Numerical Model Results

67. Comparison of numerical model results for existing conditions at

sta 11 and 13 (Plates 32 and 33) with the prototype data at sta FH1 and FH2 indicates resonant wave-height amplification at similar periods. However, the prototype data results generally occur at a longer period, are lower in amplitude, and occur over a broader band. For example, the numerical model indicates resonant peaks near 43, 103, and 110 sec but the prototype maximum amplification occurs near 60 sec and in the 100- to 150-sec range.

68. At sta FH3 (corresponding to sta 8 in the numerical study) amplification peaks (Plate 30) for existing conditions again occur at longer periods than in the numerical data, are lower in amplitude, and the resonant amplification covers a broader period range. The prototype data indicate that the numerical results show periods near which resonant amplification can be expected to occur. The amplitude of the wave-height amplification data from the numerical data should be used cautiously and as a relative comparison of changes in amplification. The differences between the numerical model test results and the prototype data analysis results can be attributed to the following factors:

- a. Frictional effects are not incorporated in the numerical harbor oscillation model (wave-height amplification is limited by radiation out of the harbor).
- b. Limitation of the numerical Fish Harbor grid to the harbor and immediate vicinity.
- c. Prototype wave-height amplification analysis results are dependent on the frequency distribution and direction of approach of the incident wave.
- d. Location of sta FH4 in the harbor and consequent influence of the harbor on the observed data.

Plan Evaluation

69. The two peaks in the resonant response (103 and 134.5 sec) at sta 8 for existing conditions in the outer harbor area do not develop for Plan 1L. Below 80 sec, however, two resonant peaks develop at sta 8 for Plan 1L near 54.5 and 75 sec. The total wave energy in the two resonant peaks for Plan 1L is decreased approximately 93 percent in comparison with the two longer period peaks for existing conditions for similar incident wave conditions. The substantial decrease in wave energy is due to the sharpness of the shorter period peaks. The resonant peak at 42.5 sec for existing conditions is matched by a smaller peak (decrease in amplitude of approximately 40 percent) at a slightly

longer period. At sta 11 and 13 in the inner harbor, the resonant wave-height amplification peak for existing conditions near 103 sec did not develop for Plan 1L, but a resonant maximum peak did develop near 54.5 sec. At sta 13 the amplitude of the 54.5-sec resonant maximum amplification decreased approximately 10 percent in comparison with existing conditions for the 103-sec maximum amplification but increased for Plan 1L at sta 11 approximately 80 percent. The resonant amplification peak near 54.5 sec at sta 11 and 13 is more sharply peaked and results in less total wave energy near the amplification peak for Plan 1L than for existing conditions, even though the amplification amplitude is larger (provided the incident wave energy levels are the same for the two period bands). The total wave energy calculated from the normalized amplification data decreased for Plan 1L approximately 45 percent at sta 11 and 87 percent at sta 13. The period bands used to compare the normalized wave energy included all amplification energy values exceeding 10 percent of the maximum resonant amplification energy level.

70. In comparison with existing conditions, the resonant response for Plan 1L has been shifted from the period range greater than 100 sec to the period range less than 80 sec. The shift in response primarily affects the 103-sec mode of oscillation for existing conditions and the 54.5-sec mode of response for Plan 1L in the inner area of the existing harbor. In the outer harbor area, the two resonant maximum amplification peaks above 100 sec are shifted to the period range below 80 sec. The shift in period of the resonant peaks results in decreased wave energy at the resonant peaks for Plan 1L for similar incident wave energy levels, and correspondingly, reduces the wave energy available to adversely impact ship mooring.

71. Based on the relative comparison of wave energy data from the numerical model results, short-period sea and swell model test results, and prototype data results, Plan 1L will result in decreased surge energy in the harbor and is recommended as the best plan tested.

Wave and Current Design Parameters

72. The maximum short-period wave heights obtained in mooring areas for Plan 1L were 1.3 ft or less, and a conservative short-period wave height of 1.5 ft is recommended for design of small-boat facilities.

73. For long-period resonant modes of oscillation, wave-height

amplification results, normalized maximum current velocity data, and the observed prototype data can be used to predict maximum current amplitudes and locations. Regions of maximum currents for the 54.5- and 75-sec modes of oscillation for Plan 1L are shown in Plates 62 and 64. The current values for the 54.5- and 75-sec modes of oscillation for Plan 1L are normalized by a unit incident wave amplitude. From comparison of wave-height amplification for existing conditions and Plan 1L at sta 13 corresponding with prototype wave data acquisition sta FH2 (continuous observed wave data are available for sta FH2), peak resonant wave-height amplification increased by a factor of approximately 5.2 at sta FH2, the maximum average wave height observed over the analysis period band of 50.8- to 56.5-sec was approximately 0.04 ft (wave energy density of $0.40 \text{ ft}^2/\text{sec}$ as shown in Plate 13) during prototype Service Interval 5. For Plan 1L, the wave height for the 54.5-sec mode of oscillation should increase by the factor of 5.2 to 0.21 ft. Therefore the normalized maximum currents shown in Plate 62 may be scaled by the 0.21-ft wave height for Plan 1L. Similarly, the peak resonant wave-height amplification for the 75-sec mode of oscillation increased by a factor of approximately 2.1. The maximum average wave height observed over the analysis period band of 72.5 to 84.5 sec was 0.06 ft based on the maximum energy density of $0.84 \text{ ft}^2/\text{sec}$. For Plan 1L, the wave height for the 75-sec mode of oscillation should increase by the factor of 2.1 to 0.13 ft and the 0.13-ft wave height may be used to scale the normalized maximum velocities shown in Plate 64.

74. For example, the maximum currents for the 54.5-sec mode of oscillation will be 21 percent of the normalized maximum currents shown in Plate 62. Design current values, however, will depend on the location of the proposed small-boat facilities. The prototype data available for estimating current velocities are limited to the winter of 1982-1983 but do represent observed results for unusually severe incident storm wave conditions. In summary, small-boat facilities in Fish Harbor should be designed for a maximum short-period wave height of 1.5 ft. For long-period wave conditions the boat facilities should be designed for the 54.5- and 75-sec periods of oscillation.

PART IV: TIDAL CIRCULATION RESULTS

The Numerical Model

75. The investigation of tidal circulation for Fish Harbor Plan 1L was conducted with a numerical model previously used in other LA-LB Harbor tidal circulation studies (Seabergh and Outlaw 1984) and is documented there. The numerical tidal circulation model used in this study provides a two-dimensional, depth-averaged, second order finite difference solution to the hydrodynamic equations and is referred to as the Waterways Experiment Station Implicit Flooding Model (WIFM). The version used in this study also provides a two-dimensional solution to the transport equation for a conservative constituent. The study area included in the model and the smoothly varying finite difference grid used are shown in Figure 7; the grid contains 12,032 cells, covering 146 square miles. Minimum cell width was 235 ft and the maximum width was 1,463 ft, with smaller cells concentrated in the interior channels and basins.

Tests and Results

76. Tidal elevation stations, velocity stations, and discharge/flow volume ranges for the numerical simulation of tidal hydrodynamics are shown in Figures 8-11 for existing conditions and Plan 1L, as described previously. A spring tide was input at the model ocean boundary and the tidal simulation was 70 prototype hours in duration. At hour 18 of each simulation, Fish Harbor was filled with a 10 parts per thousand (ppt) concentration of dye which was allowed to disperse during the remainder of the test run.

77. Tide elevation and phase. Tide elevation data for existing conditions and Plan 1L are compared in Plates 66-73 for sta 9, 11, 16, 18, 19, F1, F2, and F3. The tide curves for the existing conditions and Plan 1L plot identically for all gages, indicating the Plan 1L will create no change in tide range or phase inside or outside of Fish Harbor.

78. Tidal velocity. Velocity data are presented in Plates 74-82. Velocity stations at the entrances to the harbor (sta 1B, 2E, and 3H in Plates 74-76, respectively), in the transitions between outer harbor and inner harbor (sta 5M and 8Y in Plates 77 and 78), and in the inner harbor (sta 8A-P

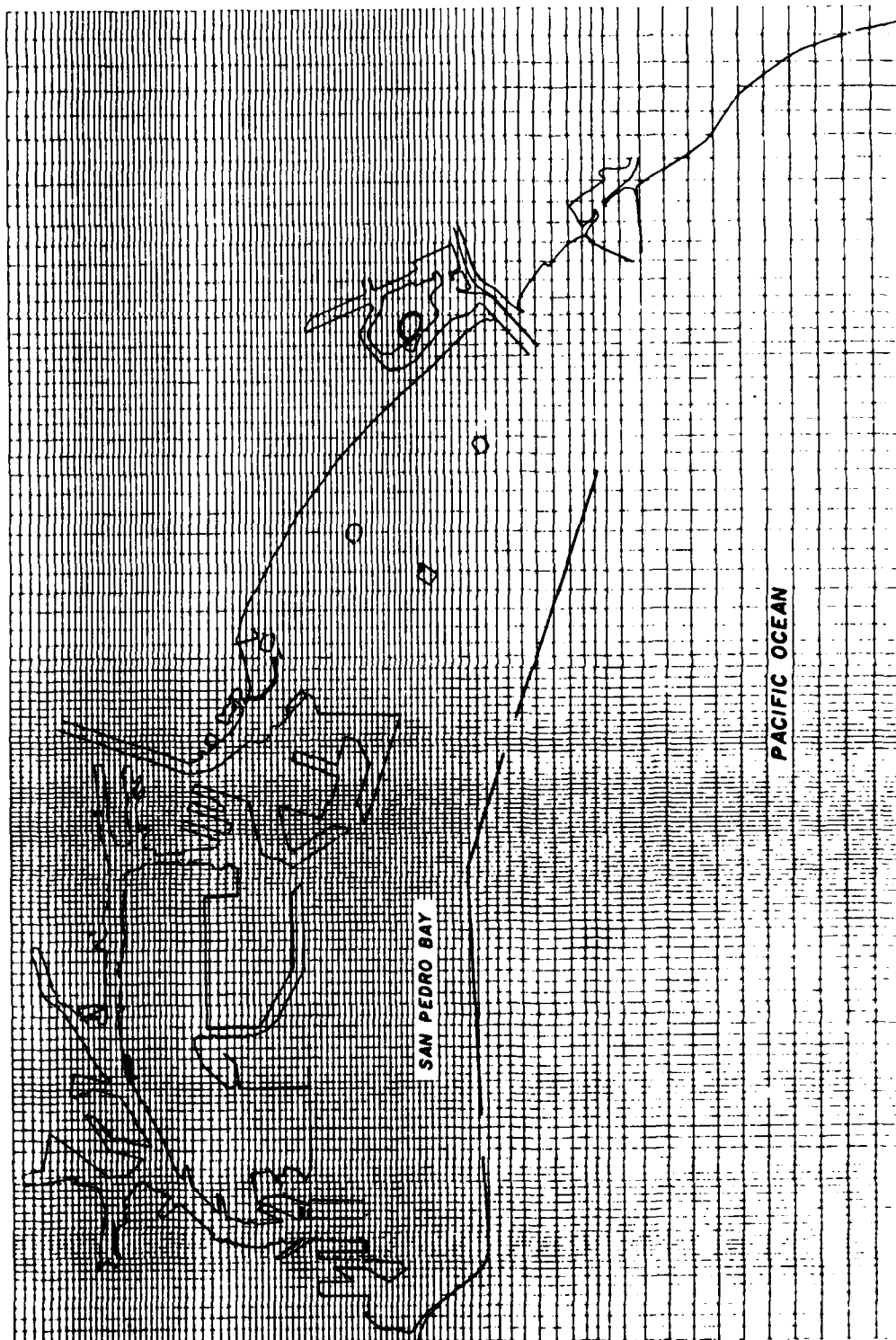


Figure 7. Grid for the tidal circulation model

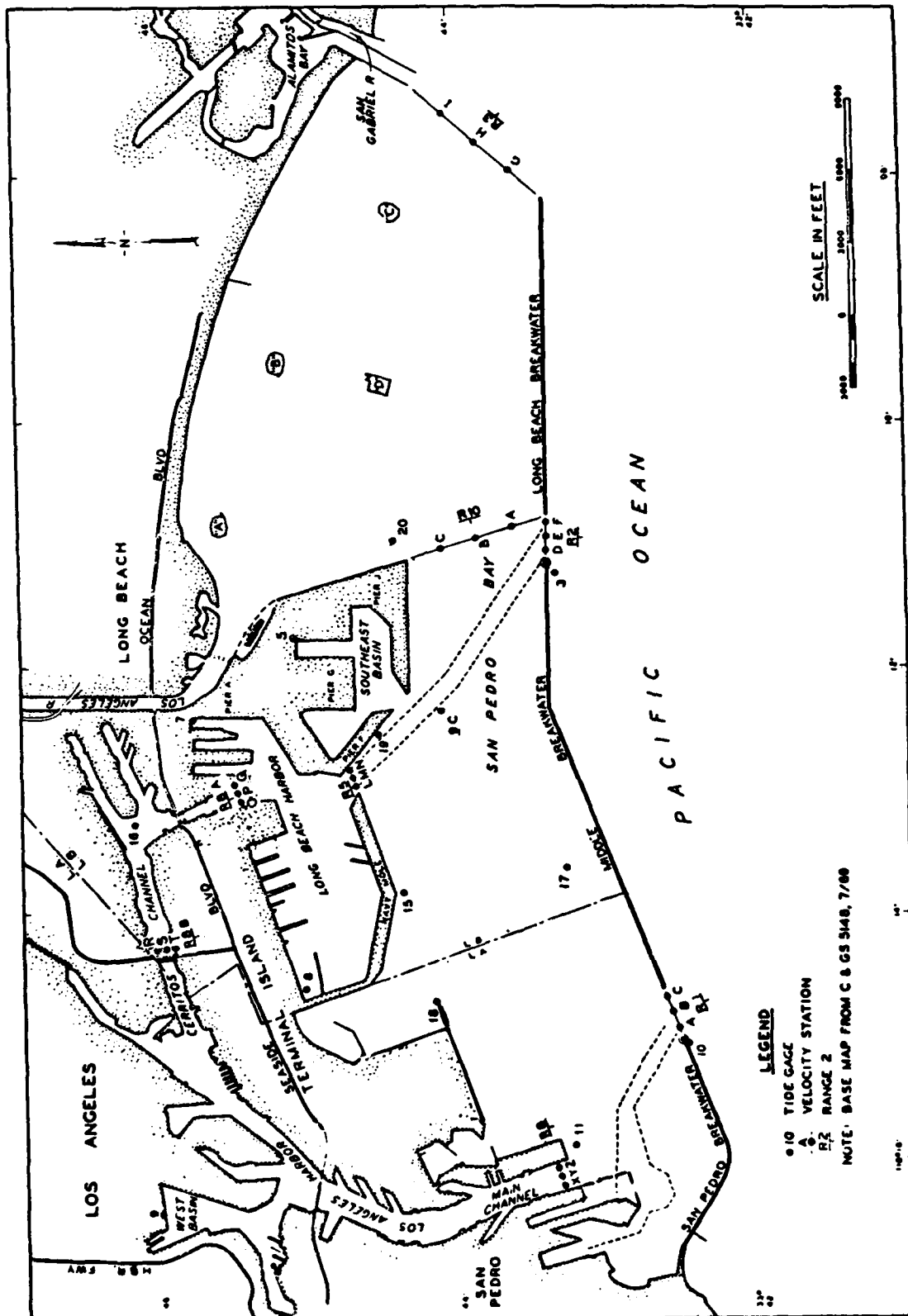


Figure 8. Gage, station, and range locations

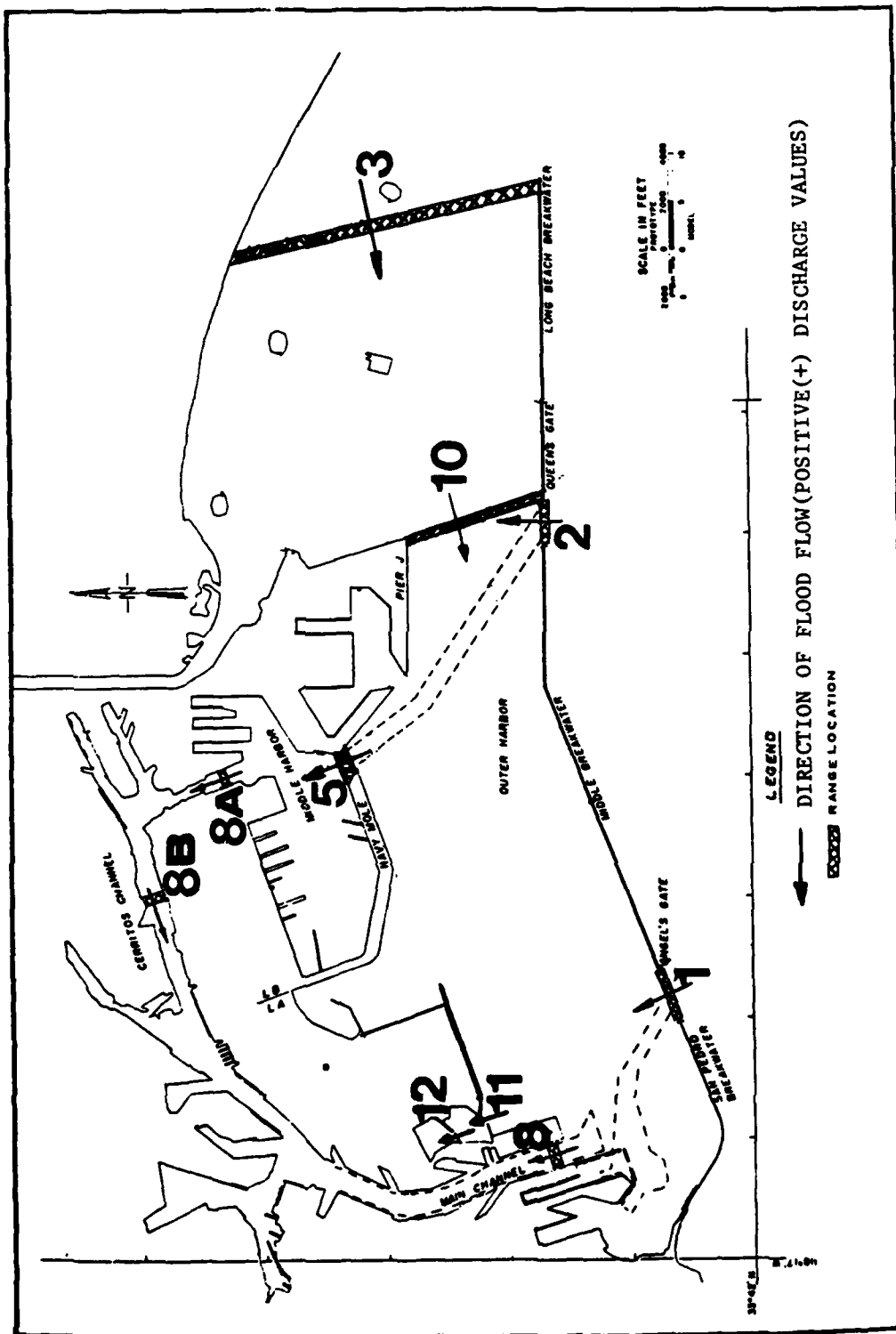


Figure 9. Locations of discharge and flow volume ranges

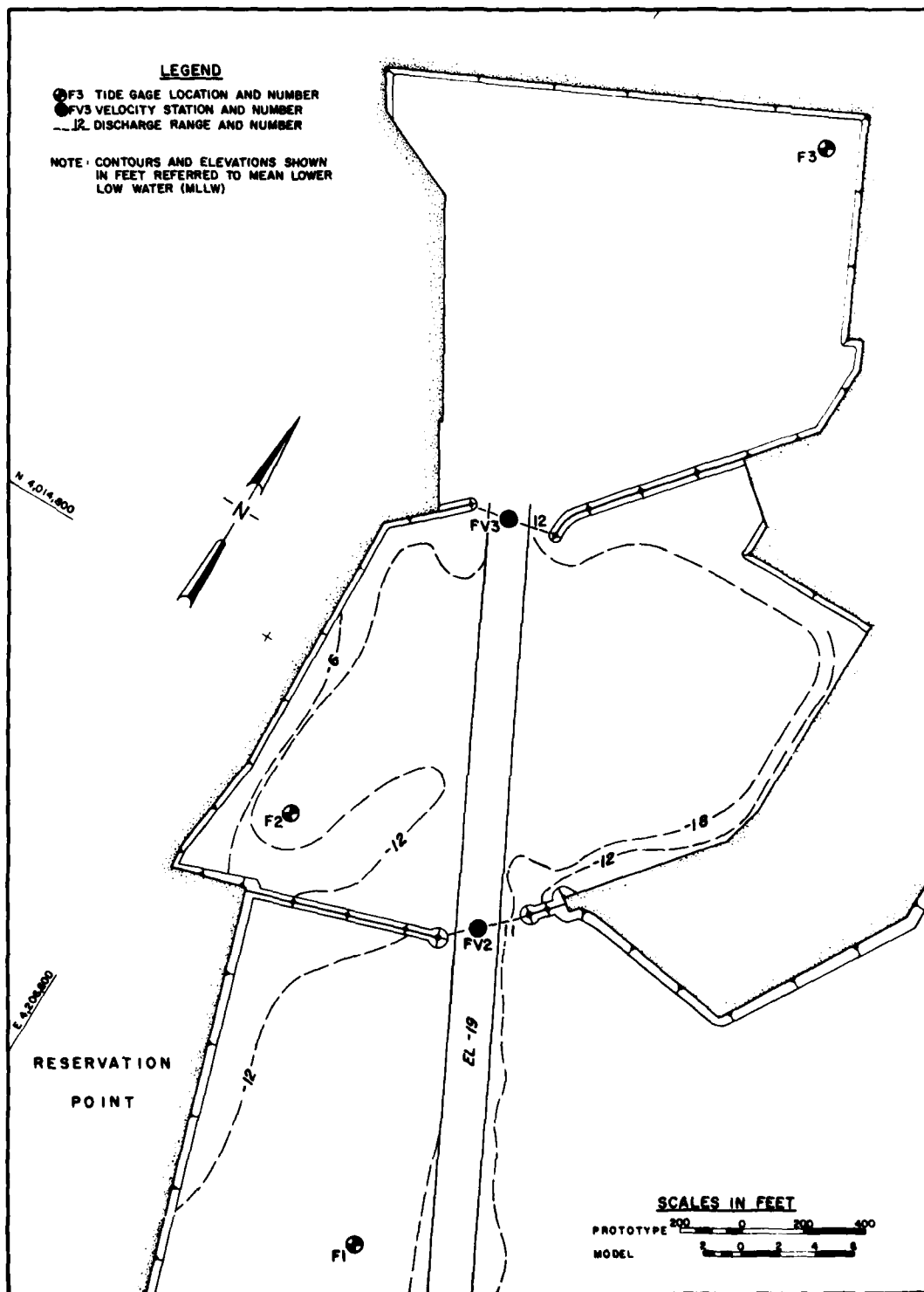


Figure 10. Existing condition gage locations

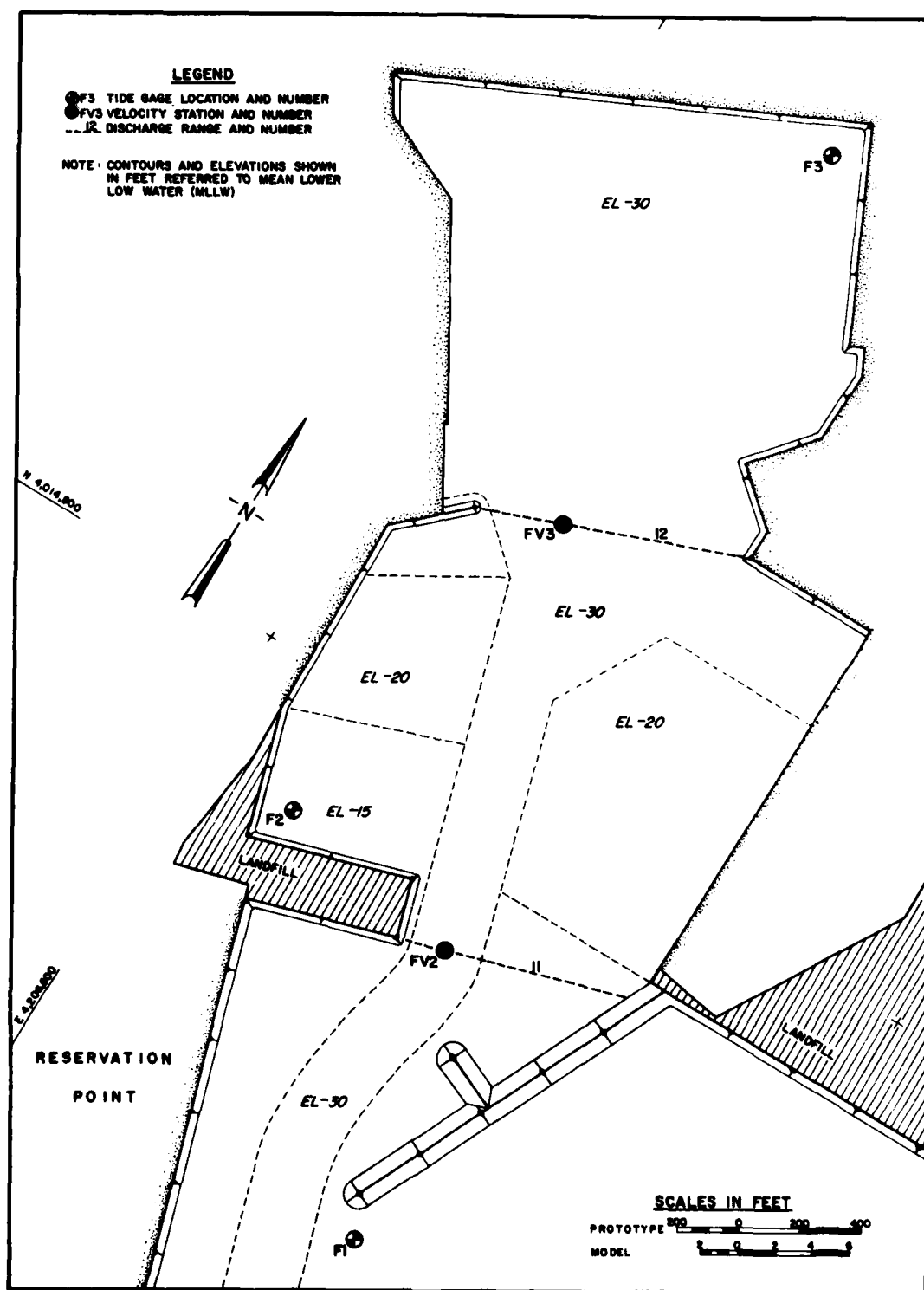


Figure 11. Plan 1L gage locations

and 8B-S in Plates 79 and 80) indicate no difference between existing conditions and Plan 1L. The influence of Plan 1L is limited to the immediate area in and around Fish Harbor. Sta FV2 (Plate 81) shows a reduction in velocities due to the widening of the entrance and increase in depth. Peak flood velocities are reduced from 0.24 to 0.09 ft/sec and peak ebb velocities from 0.25 to 0.10 ft/sec. Sta FV3 (Plate 82) shows a similar change as sta FV2 since the inner breakwater was removed and channel depths were increased. The plan reduces peak flood velocities from 0.10 to 0.04 ft/sec and peak ebb velocities from 0.11 to 0.05 ft/sec at sta FV2.

79. Tidal discharge. Hourly discharge values are plotted in Plates 83-91 for ranges 1, 2, 3, 5, 8, 8A, 8B, 11, and 12 (see Figure 9 for locations). There were no changes in discharge for these ranges.

80. Tidal flow volumes. Table 12 shows the average ebb and flood flow volumes through the discharge ranges and the net flow volumes, or differences between ebb and flood flow volumes. As shown in Table 12, there are no changes of any consequence in flow volumes. The change that occurs at range 11 indicates a slight decrease in flood and ebb flow volume due to the landfill near the entrance of Fish Harbor, which is just inside the range 11 location. The slight increase in flood and ebb flow volume at range 12 is due to the inclusion of more surface area bayward of range 12 when the inner breakwater is removed and the range line is extended laterally to the east side of Fish Harbor.

81. Velocity vector plots. Plates 92-99 present spring tide velocity vector plots that illustrate the tidal circulation for existing and Plan 1L conditions. The plots show velocity vectors at every second cell location of the model grid. Velocities less than 0.01 ft/sec drop out of the plots. Velocities within the 0.01 to 0.15 ft/sec range are within the triangular directional vector length. Velocities greater than the 0.15 ft/sec have the vector stem projecting down from the base of the vector head and can easily be sealed off.

82. Plates 92-95 show the tidal circulation for existing conditions at hour 36 (ebb flow condition), hour 42 (flood flow), hour 48 (ebb flow), and hour 54 (flood flow), respectively. As shown on the flood flow velocity vector plots in the vicinity of Fish Harbor (Plates 93 and 95), velocities approached Fish Harbor from Angel's Gate. Some of the flow was then deflected by Reservation Point and flowed southward and westward around Reservation

Point. Ebb flow in the vicinity of Fish Harbor could follow two paths, dependent on antecedent conditions. Plate 92 shows ebb velocities from Fish Harbor flowing along Reservation Point in a southward direction. Plate 94 shows ebb velocities being totally swept to the east of Fish Harbor.

83. Plates 96-99 show the same sequence of velocity vector plots for Plan 1L as described for existing conditions. Plates 97 and 99 show flood flow conditions, with flood velocities now approaching Fish Harbor along Reservation Point due to the Plan 1L jetty structure rather than from the southwest (compare Plates 93 and 97). Plates 96 and 98 show ebb flow exiting southward along Reservation Point for both ebb flow conditions. A comparison of Plates 94 and 98 shows that ebb flow for Plan 1L deflects the existing condition eddy along Reservation Point indicating a trend for all ebb flows for Plan 1L to move south along Reservation Point with the possibility to move eastward, as shown in Plate 94.

84. Dye movement. Dye (representing a conservative substance) was injected into the entire Fish Harbor basin with a concentration of 10 ppt at hour 18 of the numerical simulation. The movement of the dye was then traced for the remainder of the simulation (through hour 70). Plates 100-109 show contours of the dye as it dispersed from Fish Harbor for the spring tide condition. Prototype data are not yet available to calibrate the dye dispersion and relative comparisons between existing conditions and Plan 1L are made. It is anticipated that data to calibrate this part of the numerical model will be available in the near future. However, relative comparisons of existing and Plan 1L conditions will aid in examining the mechanism by which Fish Harbor is flushed by tidal action and changes caused by the Plan 1L.

85. Plates 100-104 show contours of dye at hours 31 (high water), 37 (low water), 56 (high water), 62 (low water), and 68 (high water), respectively, for existing conditions. Plates 105-109 follow the same sequence for Plan 1L. Comparison of hour 31 (Plates 100 and 105) for existing and Plan 1L conditions at high water (one tidal cycle after the dye simulation was begun, or 13 hours) shows that a slug of fresh water had penetrated into Fish Harbor during the flood flow, while fresh water (i.e., 0.0 concentration) was not penetrating into the harbor for Plan 1L. A dilute concentration of dye was located along Reservation Point for existing conditions (Plate 100), which was evidently a remnant of the previous ebb tide while no such remnant exists for Plan 1L. These data suggest that for existing conditions, inflow into Fish

Harbor approached from the southeast and exited southwesterly along Reservation Point, while inflow and outflow for Plan 1L were confined along Reservation Point, with a part of the ebb flow from Fish Harbor reentering the harbor on flood flow for the Plan 1L condition. For the following low water (hour 37, Plates 101 and 106), a larger southward extension of the ebb dye plume was indicated for existing conditions than for Plan 1L. High water at hour 56 (compare Plates 102 and 107) shows more increased penetration of fresh water into Fish Harbor for the existing condition than that for Plan 1L. Following ebb flow at hour 62 (compare Plates 103 and 108), concentration contours are more broadly distributed overall for the existing condition. The final comparison at hour 68, during high water (Plates 104 and 109), shows lower concentrations in Fish Harbor for existing conditions than for Plan 1L.

86. Throughout the comparison it can be noted that at low water the contours inside Fish Harbor were similar between existing conditions and Plan 1L, indicating that strong mixing was not occurring. This is probably attributable to the low tidal currents in the basin. Table 13 shows the average concentration inside Fish Harbor for each time interval discussed. High-water concentrations were lower than low-water concentrations for both conditions. For the last high water at hour 68, the average concentration in Fish Harbor was 7.1 ppt for existing conditions and 8.5 ppt for Plan 1L. For the previous low water (hour 62), the average concentration was 9.2 for existing conditions and 9.3 for Plan 1L. The low-water concentrations are about equal for existing conditions and Plan 1L, indicating that mixing was weak for both existing conditions and Plan 1L, even though a trend for better water exchange for existing conditions can be noted by comparing concentrations at each successive high water.

PART V: CONCLUSIONS

87. Results of the prototype data acquisition and analysis portion of the investigation indicated:

- a. Maximum wave-height amplification (for long-period waves greater than 24.3 sec) calculated from the prototype wave data occurred over the 50- to 70-sec-period range and over the 100- to 150-sec-period range for the inner harbor area.
- b. Maximum wave-height amplification (for long-period waves greater than 24.3 sec) calculated from the prototype wave data for the outer harbor area occurred over broader period bands of 50-90 sec and 100-200 sec.
- c. The maximum significant wave heights observed were 0.68 ft in the outer harbor and 0.48 ft in the inner harbor.

88. Based on the results of the three-dimensional physical hydraulic model investigation reported herein, it was concluded that:

- a. Existing conditions are characterized by rough and turbulent wave conditions, particularly in the lee of each entrance, in both the outer and inner harbors during periods of storm wave attack.
- b. The 1,200-ft-long breakwater of the originally proposed improvement plan (Plan I) appeared promising initially; however, additional testing indicated excessive wave heights along the vertical wall adjacent to the eastern commercial fishing area.
- c. The improvement plans tested involving a reduction in the length of the breakwater (Plans 2-4B) will not meet the established wave-height criteria (maximum wave heights of 1.5 ft in the commercial fishing basins and 1.0 ft in the recreational boating area).
- d. Of the improvement plans tested involving a revetment along the vertical wall adjacent to the eastern commercial fishing basin and/or the installation of spurs on the breakwater, several plans (Plan 1E and Plans 1H-1L) met the established wave-height criteria.
- e. Of the improvement plans that met the established wave-height criteria, Plans 1J and 1L appeared optimum. Plan 1J required 50 ft less spur length than Plan 1L; however, Plan 1L provided a much larger protected area for mooring small craft in the lee of the breakwater.

89. Based on the results of the numerical harbor oscillation study reported herein, it was concluded that:

- a. Prototype amplification data and numerical amplification data for existing conditions indicated resonant conditions near

similar periods, but the prototype results were not as sharply peaked and covered a broader period band.

- b. Periods of maximum wave-height amplification for proposed improvement Plan 1L were shifted from the period range above 100 sec to the period range below 80 sec in comparison with existing conditions.
- c. Long-period wave energy in the shifted resonant peaks for Plan 1L decreased by amounts ranging from 45 to 93 percent at sta 8, 11, and 13.
- d. Based on the results of the short-period sea and swell model results, prototype data analysis results, and the numerical harbor resonance results, Plan 1L is recommended for protection of the harbor against incident short- and long-period wave attack.

90. Based on the results of the numerical tidal circulation study, it was concluded that:

- a. No changes in tidal elevation or phases were noted between existing conditions and Plan 1L. Plan 1L provided no impediment to complete filling of the basin.
- b. Velocity changes between existing conditions and Plan 1L were limited to the immediate Fish Harbor region, with no changes noted at other stations throughout the remainder of LA-LB Harbors. Generally, velocities in the entrance to Fish Harbor were reduced due to widening the entrance channel and increasing channel depths.
- c. Tidal discharges and tidal flow volumes were not changed significantly in Fish Harbor or at any other location in the LA-LB Harbors as a result of Plan 1L.
- d. Tidal circulation patterns indicated a slight shift in flood flow patterns approaching Fish Harbor due to the jetty structure of Plan 1L. Ebb flow from Fish Harbor exited along Reservation Point and moved southward for Plan 1L. Existing condition ebb flow patterns showed flow exited Fish Harbor along Reservation Point a portion of the time and could exit eastward along the new landfill, dependent on antecedent conditions. Therefore Plan 1L partially changed ebb flow patterns near Fish Harbor.
- e. Tidal flushing characteristics of Fish Harbor were changed somewhat by Plan 1L, although due to the relatively low velocities, dye concentrations at successive low waters were similar for existing conditions and Plan 1L.

REFERENCES

Chen, H. S., and Mei, C. C. 1974. "Oscillations and Wave Forces in an Offshore Harbor (Applications of the Hybrid Finite Element Method to Water-Wave Scattering)," Report No. 190, Massachusetts Institute of Technology, Cambridge, Mass.

Hales, L. Z. 1976 (May). "Transmission of Wave Energy Through and Overtopping of the Long Beach, California, Breakwater; Hydraulic Model Investigation," Miscellaneous Paper H-76-10, US Army Engineer Waterways Experiment Station, Vicksburg, Miss.

Houston, J. R. 1976 (Jul). "Numerical Modeling of Resonant Oscillations in Deep Draft Harbors," Research Report H-76-1, US Army Engineer Waterways Experiment Station, Vicksburg, Miss.

Keulegan, G. H. 1950 (May). "The Gradual Damping of a Progressive Oscillatory Wave with Distance in a Prismatic Rectangular Channel" (Unpublished data), US Bureau of Standards, Washington, DC.

National Marine Consultants. 1960 (Dec). "Wave Statistics for Seven Deep-Water Stations Along the California Coast," Contract Report for US Army Corps of Engineer Districts, Los Angeles and San Francisco.

Outlaw, D. G., et al. 1977 (Feb). "Los Angeles and Long Beach Harbors Model Study; Model Design," Technical Report H-75-4, Report 4, US Army Engineer Waterways Experiment Station, Vicksburg, Miss.

Seabergh, W. C., and Outlaw, D. G. 1984 (Jul). "Los Angeles and Long Beach Harbors Model Study; Numerical Analysis of Tidal Circulation for the 2020 Master Plan," Miscellaneous Paper CERC-84-5, US Army Engineer Waterways Experiment Station, Vicksburg, Miss.

Stevens, J. C., et al. 1942. "Hydraulic Models," Manuals of Engineering Practice No. 25, American Society of Civil Engineers, New York.

US Army Engineer Waterways Experiment Station, Coastal Engineering Research Center. 1984. Shore Protection Manual, Vicksburg, Miss.

Table 1
Wave Characteristics at Fish Harbor Entrance

Incident Wave Characteristics at LA-LB Breakwater*		Wave Characteristics at Fish Harbor Entrance due to:	
Period, sec	Height, ft	Wave Diffraction Through Angel's Gate	Overtopping of and Transmission Through the LA-LB Breakwater
		Period, sec	Height, ft
5	4	5	1.6
7	4	7	1.6
	8		3.3
	12		4.9
9	4	9	1.6
	8		3.3
	12		4.9
	16		6.6
11	4	11	1.7
	8		3.4
	12		5.0
13	4	13	1.4
	8		2.8
	12		4.2
15	4	15	1.4
	8		2.8
17	4	17	1.5
	8		3.0
19	4	19	1.5
	8		3.0
		5	0.6
		7	0.9
			1.2
			2.0
		9	1.1
			1.7
			2.7
			5.2
		11	1.3
			2.3
			5.2
		13	1.2
			1.9
			4.9
		15	1.4
			3.3
		17	1.1
			2.0
		19	1.1
			2.3

* After application of refraction-shoaling coefficients.

Table 2
Wave Heights for Existing Conditions
+5.4 ft swl

Direction deg	Test Wave Period sec	Height ft	Wave Height, ft														
			1	2	3	4	5	6	7	8	9	10	11	12	13	14	15
162	5.0	2.0	0.9	0.7	<0.1	0.3	0.1	0.1	<0.1	0.3	<0.1	<0.1	<0.1	0.1	0.1	<0.1	0.1
	7.0	5.0	2.6	1.8	0.4	1.0	0.9	0.3	0.9	0.7	0.4	0.2	0.2	0.3	0.1	0.2	0.2
	9.0	3.0	1.4	1.4	0.4	1.6	0.7	1.0	0.2	0.5	0.2	0.3	0.1	0.2	0.4	0.2	0.5
		7.0	4.9	4.2	0.7	4.1	1.3	1.6	1.0	1.5	0.4	0.5	0.3	0.5	0.7	0.4	1.0
	11.0	5.0	4.0	2.6	1.4	1.2	1.3	1.1	0.5	1.6	0.6	0.6	0.6	0.7	0.6	0.6	0.3
	13.0	5.0	4.5	2.5	1.7	2.8	1.9	2.0	2.9	2.3	0.7	1.6	0.7	3.2	0.6	0.5	0.9
	15.0	3.0	4.1	3.6	0.5	2.6	1.7	1.2	3.4	2.2	0.4	2.1	0.9	1.0	0.7	0.7	0.7
	17.0	3.0	2.4	1.1	1.1	2.1	1.8	0.6	2.1	0.7	0.5	0.4	0.2	0.7	0.2	0.5	0.6
	19.0	3.0	4.9	1.5	0.5	2.5	1.3	0.9	2.8	0.9	1.1	1.1	0.4	0.4	0.3	0.6	0.4
	118	8.0	3.0	2.8	1.0	0.6	1.0	0.5	0.9	0.2	0.4	0.1	0.2	0.1	<0.1	<0.1	<0.1

Table 3
Wave Heights for Plan 1
+5.4 ft swl

Test Move			Wave Height, ft																			
Direction	Period sec	Height ft	Gage 1	Gage 2	Gage 3	Gage 4	Gage 5	Gage 6	Gage 7	Gage 8	Gage 9	Gage 10	Gage 41	Gage 12	Gage 13	Gage 14	Gage 15	Gage 16	Gage 17	Gage 18	Gage 19	Gage 20
162	5.0	2.0	1.1	0.7	0.4	0.1	0.1	<0.1	<0.1	0.3	0.2	0.3	0.1	<0.1	0.1	<0.1	<0.1	<0.1	0.1	0.1	<0.1	0.1
	7.0	5.0	2.1	0.5	0.5	0.1	0.1	0.2	0.1	0.3	0.6	0.3	0.2	0.1	0.1	0.2	0.1	0.1	0.1	0.3	0.1	0.1
	9.0	3.0	2.2	0.5	0.3	0.2	0.4	0.1	0.2	0.1	0.1	0.3	0.2	0.2	0.1	0.2	0.1	0.1	0.1	0.3	0.1	0.1
		7.0	5.3	1.6	1.4	0.7	1.0	0.9	0.4	0.7	0.8	0.8	0.5	0.5	0.8	0.6	0.3	0.4	0.9	0.4	0.6	0.4
	11.0	5.0	1.9	1.6	0.5	0.4	0.6	0.5	0.1	0.5	0.9	0.4	0.7	0.5	0.5	0.7	0.5	0.4	0.4	0.6	0.3	0.6
	13.0	5.0	2.8	2.0	0.5	0.2	0.3	0.3	0.4	0.5	0.5	0.9	0.3	0.5	0.5	0.5	0.5	0.5	0.5	0.4	0.2	0.1
	15.0	3.0	3.5	2.1	0.6	0.4	0.6	0.8	0.6	0.7	1.1	1.2	0.4	0.6	0.6	0.6	0.7	0.3	0.5	0.7	0.7	0.2
	17.0	3.0	1.9	1.0	0.4	0.4	0.6	0.3	0.3	1.3	0.6	1.0	0.4	0.3	0.9	0.7	0.7	0.2	0.4	0.3	0.3	0.2
	19.0	3.0	1.4	0.5	0.2	0.1	0.2	0.3	0.2	0.2	0.5	0.6	0.2	0.2	0.3	0.2	0.2	0.1	0.4	0.2	0.2	0.4

Table 4
Wave Heights for Plan 2
+5.4 ft swl

[illegible]

Table 5

Wave Heights for Plan 3

+5.4 ft swl

[illegible]

Table 6
Wave Heights for Plan 4
+5.4 ft swl

Test Wave			Wave Height, ft																			
Direction deg	Period sec	Height ft	Cage 1	Cage 2	Cage 3	Cage 4	Cage 5	Cage 6	Cage 7	Cage 8	Cage 9	Cage 10	Cage 11	Cage 12	Cage 13	Cage 14	Cage 15	Cage 16	Cage 17	Cage 18	Cage 19	Cage 20
162	5.0	2.0	0.7	0.6	0.3	0.2	0.1	0.1	0.1	0.3	0.4	0.2	0.3	0.2	0.1	0.2	0.1	0.1	0.1	0.1	0.2	0.2
	7.0	5.0	1.3	0.8	0.3	0.3	0.4	0.8	0.4	0.7	1.4	0.3	0.4	0.2	0.5	0.5	0.2	0.3	0.8	0.2	0.2	0.1
	9.0	3.0	1.3	0.5	0.4	0.3	0.1	0.1	0.3	0.2	0.3	0.3	0.3	0.2	0.2	0.2	0.1	0.1	0.1	0.1	0.2	0.1
	7.0	4.2	2.0	0.8	0.8	0.4	0.5	1.1	1.0	0.8	1.0	0.9	0.9	0.6	0.8	0.7	0.3	0.2	0.4	0.4	0.6	0.4
	11.0	5.0	1.6	2.4	0.5	0.3	0.6	0.7	0.1	0.7	1.1	0.5	0.9	0.6	0.8	0.7	0.3	0.2	0.4	0.4	0.6	0.4
	13.0	5.0	2.0	1.6	0.5	0.5	0.6	0.4	0.3	0.8	0.8	1.2	0.6	0.6	0.5	0.5	0.7	0.4	0.5	0.3	0.2	0.1
	15.0	3.0	3.3	2.3	0.6	1.0	0.4	0.8	0.8	0.6	1.1	1.3	1.1	0.4	1.5	0.8	0.8	0.8	1.0	0.8	0.9	0.4
	17.0	3.0	1.4	1.1	0.2	0.8	0.9	0.6	0.4	1.3	1.1	0.9	0.8	0.3	0.6	0.7	0.5	0.3	0.5	0.2	0.3	0.2
	19.0	3.0	1.0	0.7	0.2	0.2	0.2	0.2	0.3	0.2	0.3	0.3	0.2	0.2	0.3	0.3	0.2	0.2	0.1	0.3	0.2	0.2

Table 7
Wave Heights for Plans 1-1J and Plans 4A-4B for
Test Waves from 162 deg
+5.4 ft swl

Plan	Test Wave		Wave Height, ft				
	Period sec	Height ft	Gage 21	Gage 22	Gage 23	Gage 24	Gage 25
1	15.0	3.0	3.2	2.7	1.8	1.2	1.7
1A			3.2	1.9	1.6	1.0	1.6
1B			3.0	2.2	1.5	0.7	1.4
1C			3.0	2.2	1.7	0.5	1.2
1D			1.8	1.3	1.1	0.6	0.3
1E			1.5	1.1	1.0	0.6	0.3
1F			2.1	1.5	0.8	0.9	2.0
1G			2.0	0.9	1.1	1.0	0.9
1H			1.4	1.1	0.9	0.7	0.4
1I			1.5	1.1	1.1	1.0	0.6
1J			1.5	1.5	1.3	1.0	0.9
4A			2.9	2.2	1.6	0.7	0.8
4B			3.0	2.1	1.7	0.8	0.7
1J	9.0	7.0	0.7	1.5	1.2	0.7	0.8
	11.0	5.0	0.4	0.8	0.7	0.5	0.8
	13.0	5.0	0.6	0.8	0.7	0.4	0.8
	17.0	3.0	1.2	1.0	0.6	0.6	0.5

Table 8
Comparison of Wave Heights for Plans 1J-1L
for Test Waves from 162 deg
+5.4 ft swl

Test Wave			Wave Height, ft					
Plan	Period sec	Height ft	Gage 21	Gage 22	Gage 23	Gage 24	Gage 25	Gage 26
1J	15.0	3.0	1.5	1.5	1.3	1.0	0.9	--
1K			0.7	1.0	0.8	0.7	1.1	0.8
1L			1.1	1.3	1.0	0.6	1.1	0.9
1J	9.0	7.0	0.7	1.5	1.2	0.7	0.8	--
	11.0	5.0	0.4	0.8	0.7	0.5	0.8	--
	13.0	5.0	0.6	0.8	0.7	0.4	0.8	--
	17.0	3.0	1.2	1.0	0.6	0.6	0.5	--
1L	9.0	7.0	0.4	0.9	0.7	0.2	0.4	1.2
	11.0	5.0	0.8	1.3	1.1	0.2	1.2	1.3
	13.0	5.0	0.5	0.6	0.6	0.6	0.9	1.2
	17.0	3.0	1.0	1.2	0.7	0.6	0.5	0.7

Table 9

Wave Heights for Plan 1J
+5.4 ft swl

Test Wave			Wave Height, ft																				
Direction deg	Period sec	Height ft	Gage 1	Gage 2	Gage 3	Gage 4	Gage 5	Gage 6	Gage 7	Gage 8	Gage 9	Gage 10	Gage 11	Gage 12	Gage 13	Gage 14	Gage 15	Gage 16	Gage 17	Gage 18	Gage 19	Gage 20	
162	5.0	2.0	1.0	0.8	0.5	<0.1	<0.1	<0.1	<0.1	0.4	0.5	0.3	0.1	0.1	<0.1	<0.1	0.1	<0.1	0.1	0.2	0.1	0.2	<0.1
	7.0	5.0	2.0	0.6	0.6	0.2	0.1	0.3	<0.1	0.3	0.5	0.3	0.3	<0.1	0.3	0.4	0.1	0.1	0.3	0.3	0.3	<0.1	
	9.0	3.0	1.5	0.5	0.3	0.3	<0.1	0.1	0.1	0.1	0.2	0.2	0.2	0.1	0.2	0.2	<0.1	0.1	0.1	<0.1	0.1	<0.1	
	7.0	7.0	4.3	1.3	1.0	0.6	0.2	0.3	0.4	0.6	0.6	0.9	0.5	0.6	0.8	0.8	0.2	0.4	0.2	0.3	0.4	0.2	
	11.0	5.0	1.5	1.3	0.6	0.3	0.7	0.5	0.1	0.6	1.0	0.4	0.4	0.4	0.5	0.6	0.4	0.3	0.5	0.3	0.3	0.2	
	13.0	5.0	2.2	2.1	0.6	0.4	0.5	0.3	0.2	0.6	0.4	0.6	0.5	0.4	0.6	0.4	0.5	0.3	0.4	0.1	0.2	0.2	
	15.0	3.0	3.3	2.0	0.6	0.4	0.8	0.5	0.3	0.7	0.9	0.3	0.7	0.6	0.6	0.6	0.6	0.3	0.5	0.6	0.7	0.2	
	17.0	3.0	1.5	0.8	0.3	0.8	0.7	0.4	0.6	1.5	0.4	0.4	0.4	0.7	0.3	0.4	0.7	0.7	0.3	0.3	0.4	0.3	
	19.0	3.0	1.2	0.3	0.2	0.2	0.5	0.3	0.2	0.6	0.3	0.4	0.2	0.4	0.2	0.2	0.2	0.2	0.2	0.3	0.4	0.2	
	118	4.0	3.0	3.5	1.0	0.5	0.1	0.1	<0.1	0.1	0.3	0.5	0.2	0.1	0.1	0.2	0.1	0.1	0.1	<0.1	0.2	0.2	0.1

Table 10

Wave Heights for Plan 1L
+5.4 ft swl

Test Wave			Wave Height, ft																				
Direction deg	Period sec	Height ft	Gage 1	Gage 2	Gage 3	Gage 4	Gage 5	Gage 6	Gage 7	Gage 8	Gage 9	Gage 10	Gage 11	Gage 12	Gage 13	Gage 14	Gage 15	Gage 16	Gage 17	Gage 18	Gage 19	Gage 20	
162	5.0	2.0	1.0	0.8	0.5	0.1	<0.1	<0.1	<0.1	0.4	0.5	0.2	<0.1	0.2	0.2	<0.1	0.1	0.1	<0.1	0.1	0.1	0.2	<0.1
	7.0	5.0	1.5	0.7	0.4	0.2	0.2	<0.1	<0.1	0.2	0.4	0.3	0.3	0.1	0.2	0.1	0.2	0.1	<0.1	0.3	0.1	<0.1	<0.1
	9.0	3.0	1.4	0.6	0.3	0.2	<0.1	0.1	0.1	<0.1	0.2	0.1	0.2	0.1	0.3	0.2	<0.1	0.1	0.1	<0.1	0.2	0.1	<0.1
	11.0	7.0	4.6	1.3	0.9	0.6	0.3	0.5	0.3	0.5	0.7	0.6	0.5	0.5	0.9	0.6	0.3	0.4	0.6	0.3	0.5	0.2	0.2
	13.0	5.0	1.6	1.3	0.5	0.3	0.6	0.3	0.1	0.5	0.8	0.3	0.3	0.1	0.4	0.4	0.4	0.4	0.6	0.3	0.3	0.3	0.3
	15.0	3.0	1.9	2.2	0.5	0.3	0.3	0.2	0.4	0.8	0.4	0.7	0.6	0.5	0.6	0.5	0.4	0.5	0.4	0.3	0.1	0.2	0.2
	17.0	3.0	3.3	1.8	0.8	0.4	0.8	0.9	0.5	0.7	1.1	0.5	0.6	0.2	0.7	0.4	0.4	0.3	0.5	0.5	0.4	0.3	0.3
	19.0	3.0	1.5	0.7	0.2	0.4	0.6	0.4	0.7	0.3	0.8	0.3	0.4	0.7	0.7	0.6	0.2	0.7	0.4	0.3	0.4	0.3	0.3
	4.0	3.0	0.9	0.4	0.3	0.2	0.5	0.2	0.3	0.3	0.4	0.3	0.2	0.2	0.2	0.2	0.3	0.3	<0.1	0.2	0.2	0.2	0.1
	118	4.0	3.0	3.5	1.0	0.4	0.1	0.1	0.1	0.1	0.4	0.5	0.2	0.3	0.2	0.2	0.2	0.1	0.1	0.1	0.3	0.3	0.1

Table 11
Dates for Data Acquisition Intervals 1-6

<u>Data Acquisition Interval</u>	<u>Date</u>
1	14 Oct 82 - 17 Nov 82
2	17 Nov 82 - 15 Dec 82
3	15 Dec 82 - 18 Jan 83
4	18 Jan 83 - 14 Feb 83
5	14 Feb 83 - 14 Mar 83
6	14 Mar 83 - 13 Apr 83

Table 12
Averaged* Flow Volumes (10^6 cu ft)
for One Spring Tidal Cycle

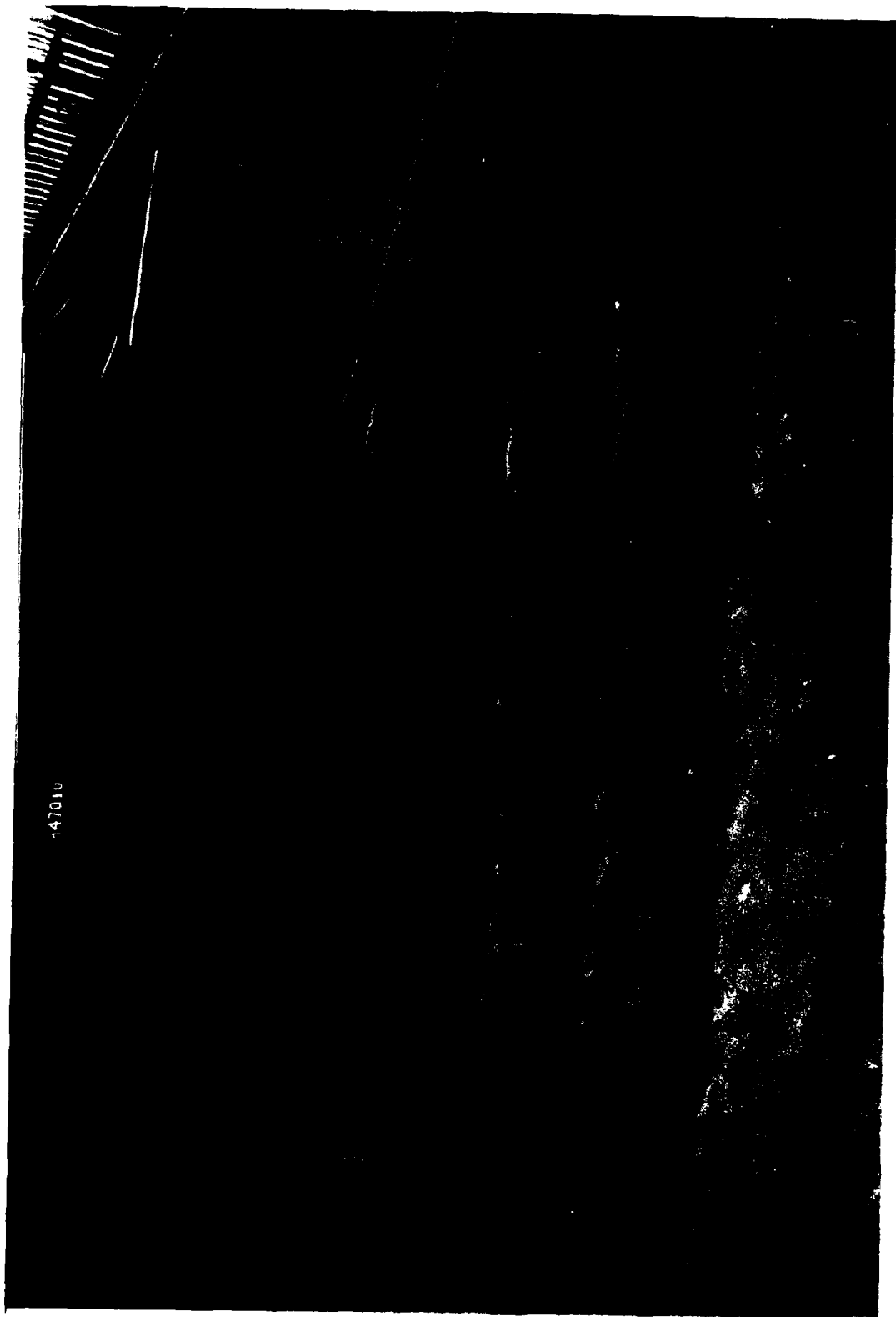
<u>Existing Conditions</u>				<u>Plan 1L</u>		
<u>Range</u>	<u>Flood</u>	<u>Ebb</u>	<u>Net</u>	<u>Flood</u>	<u>Ebb</u>	<u>Net</u>
1	1,267	-1,065	202	1,269	-1,063	206
2	838	-709	129	836	-709	127
3	805	-1,138	-333	802	-1,138	-336
5	332	-326	6	332	-326	6
8	156	-164	-8	156	-164	-8
8A	135	-128	7	135	-128	7
8B	76	-69	7	76	-69	7
10	0	-331	-331	0	-333	-333
11	20	-20	0	19	-19	0
12	8	-8	0	9	-9	0

* Averaged over four tidal cycles.

Table 13
Average Dye Concentration in Fish Harbor

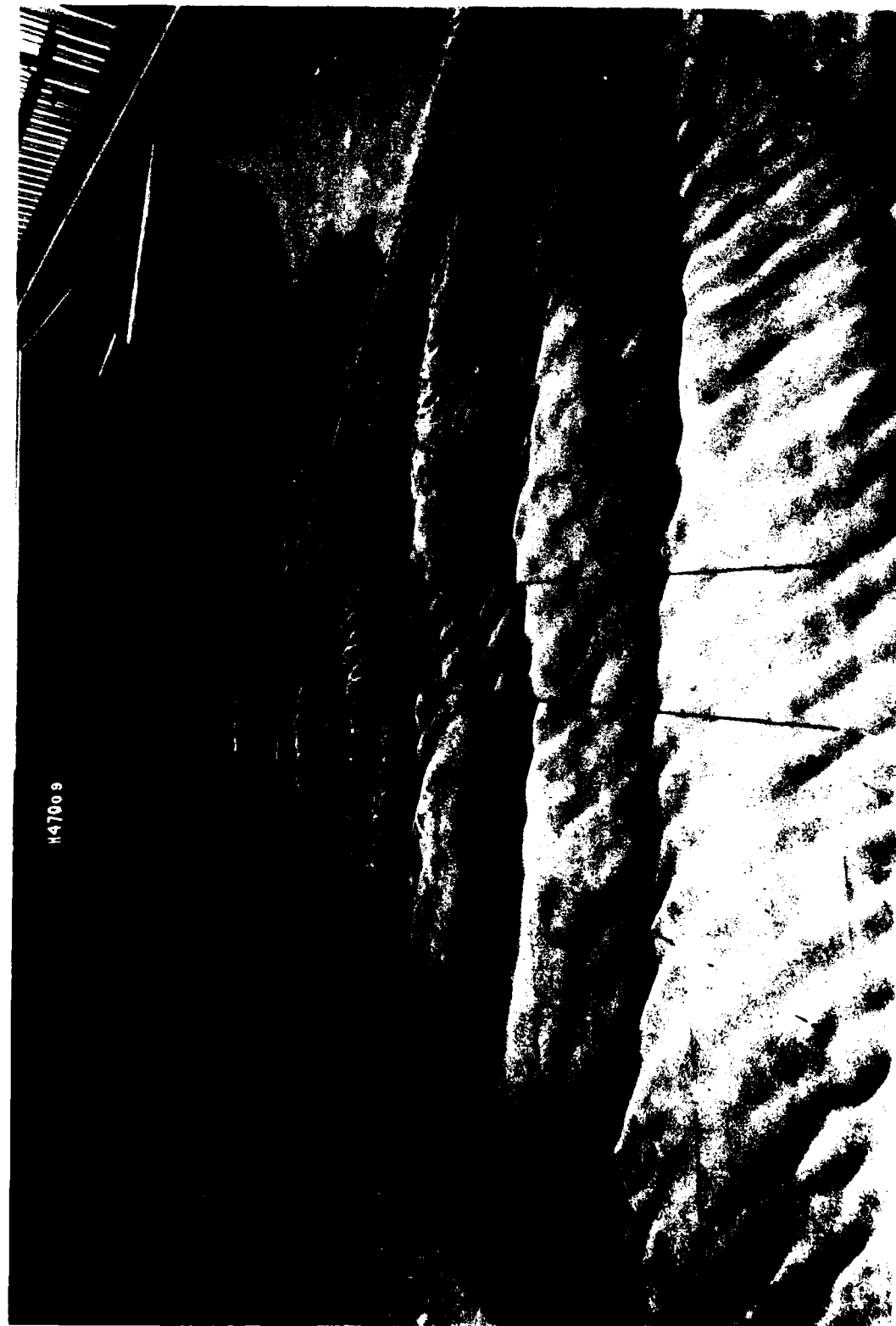
<u>Time, hr</u>	<u>Existing Conditions</u>		<u>Plan 1L</u>
	<u>Dye Concentration, ppt*</u>		<u>Dye Concentration, ppt</u>
31 (high water)	8.2	9.0	
37 (low water)	9.9	9.9	
56 (high water)	7.3	8.6	
62 (low water)	9.2	9.3	
68 (high water)	7.1	8.5	

* ppt = part per thousand.



47010

Photo 1. Typical wave patterns for existing conditions; 7-sec, 5-ft waves from 162 deg



H4700 9

Photo 2. Typical wave patterns for existing conditions; 9-sec, 7-ft waves from 162 deg



Photo 3. Typical wave patterns for existing conditions; 11-sec, 5-ft waves from 162 deg

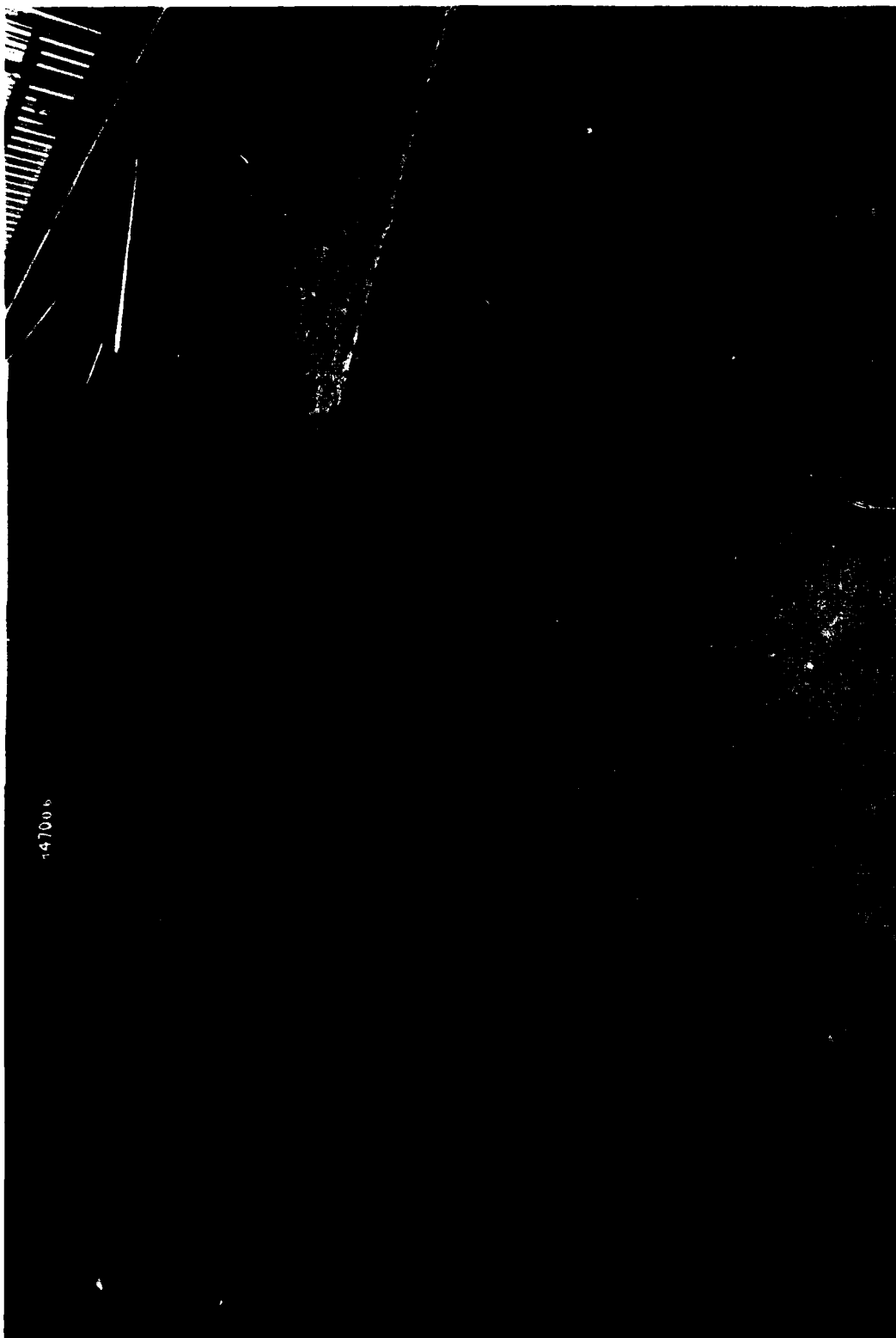


Photo 4. Typical wave patterns for existing conditions; 15-sec, 3-ft waves from 162 deg



Photo 5. Typical wave patterns for existing conditions; 4-sec, 3-ft waves from 118 deg



Photo 6. Typical wave patterns for Plan 1; 7-sec, 5-ft waves from 162 deg

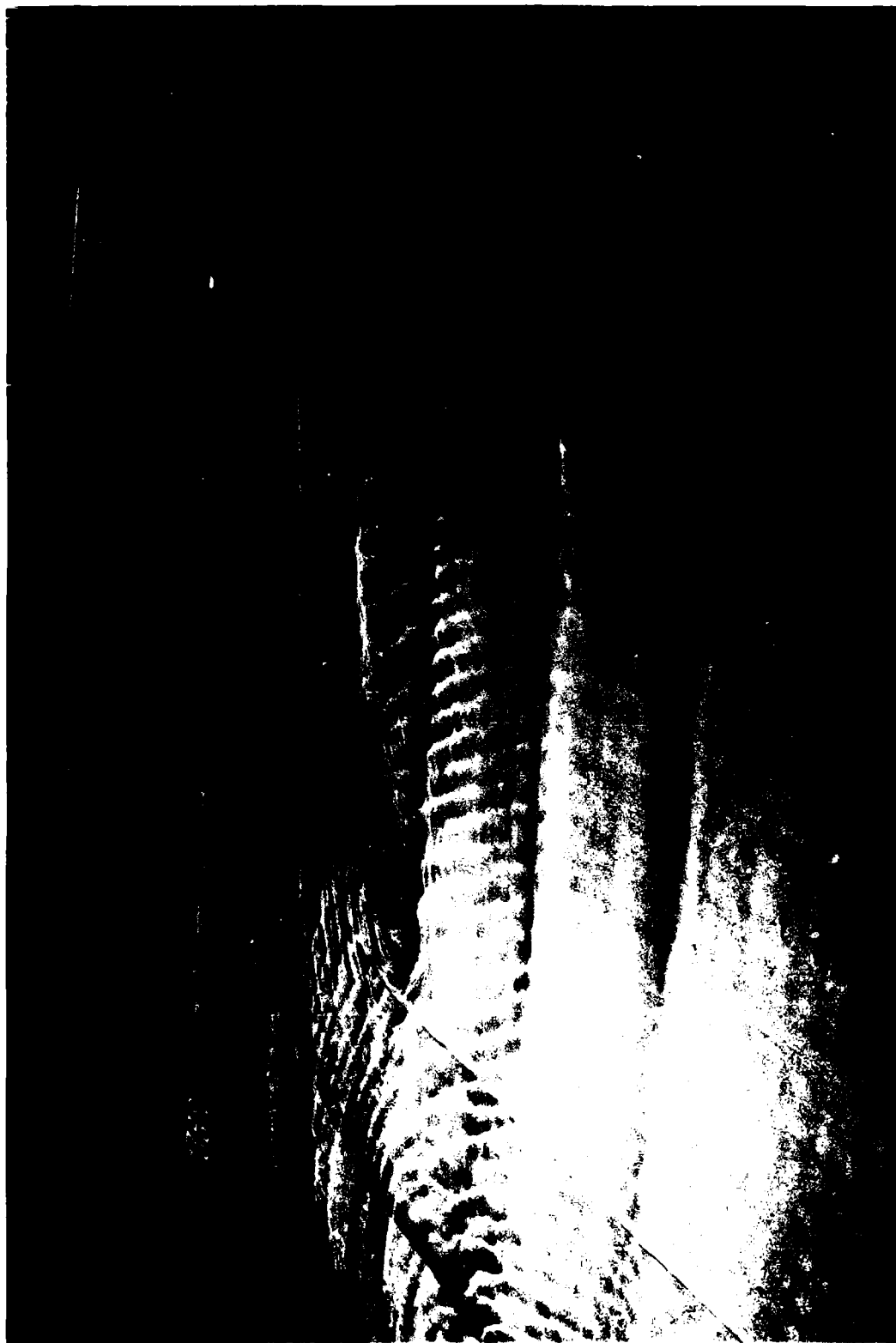


Photo 7. Typical wave patterns for Plan 1; 9-sec, 7-ft waves from 162 deg



Photo 8. Typical wave patterns for Plan 1; 11-sec, 5-ft waves from 162 deg

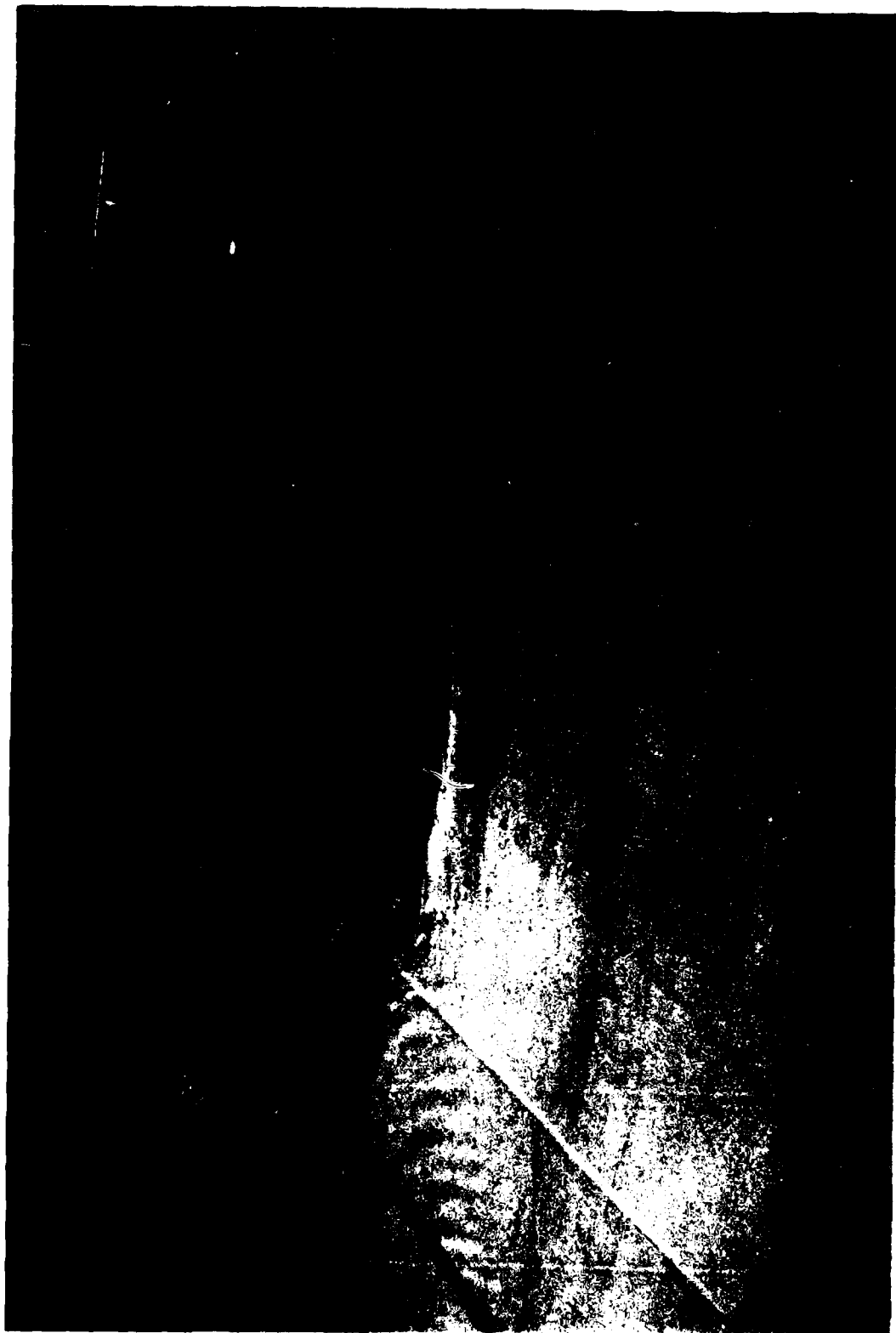


Photo 9. Typical wave patterns for Plan 1; 15-sec, 3-ft waves from 162 deg



Photo 10. Typical wave patterns for Plan 1L; 7-sec, 5-ft waves from 162 deg

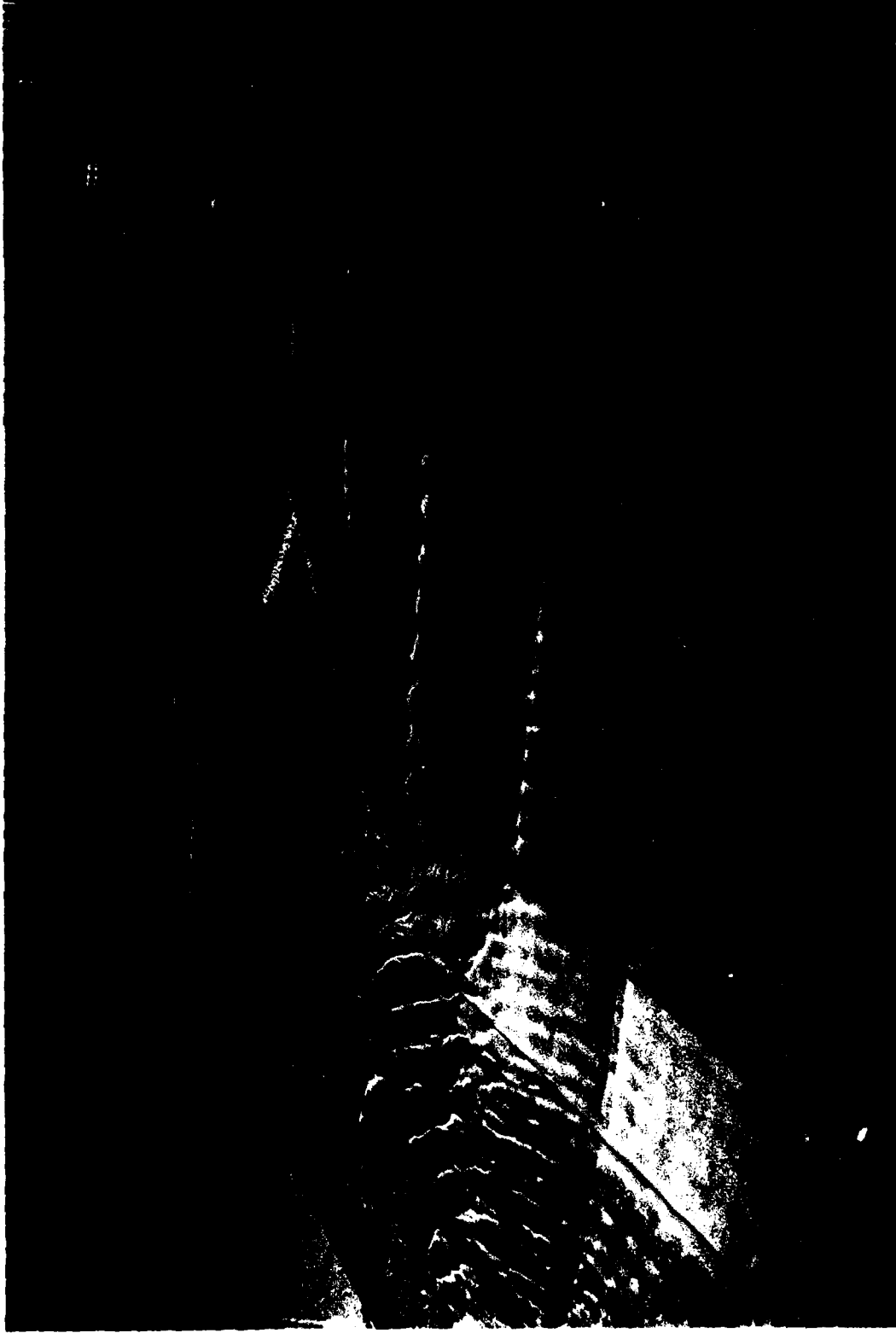


Photo 11. Typical wave patterns for Plan 11; 9-sec, 7-ft waves from 162 deg

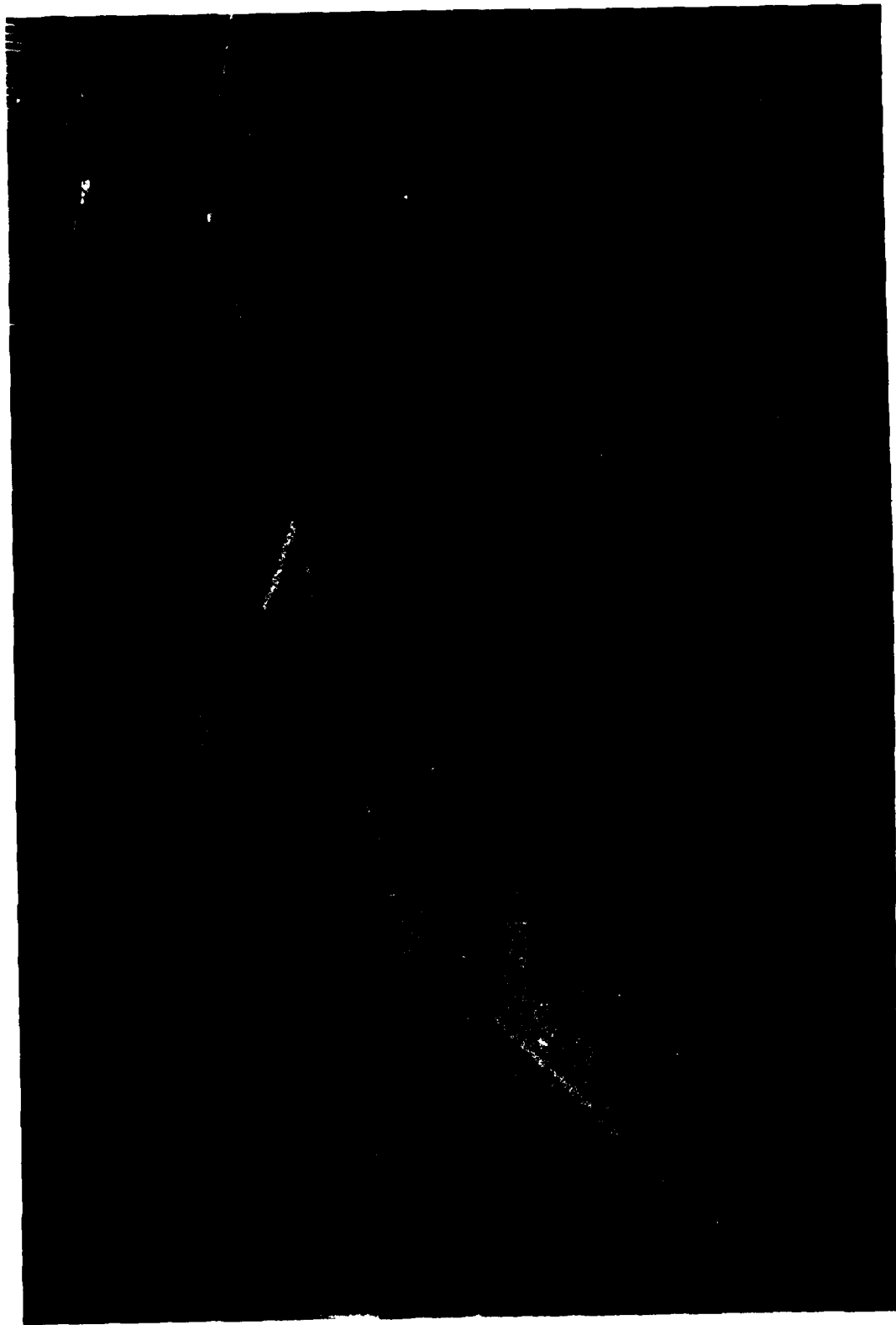


Photo 12. Typical wave patterns for Plan 11; 11-sec, 5-ft waves from 162 deg

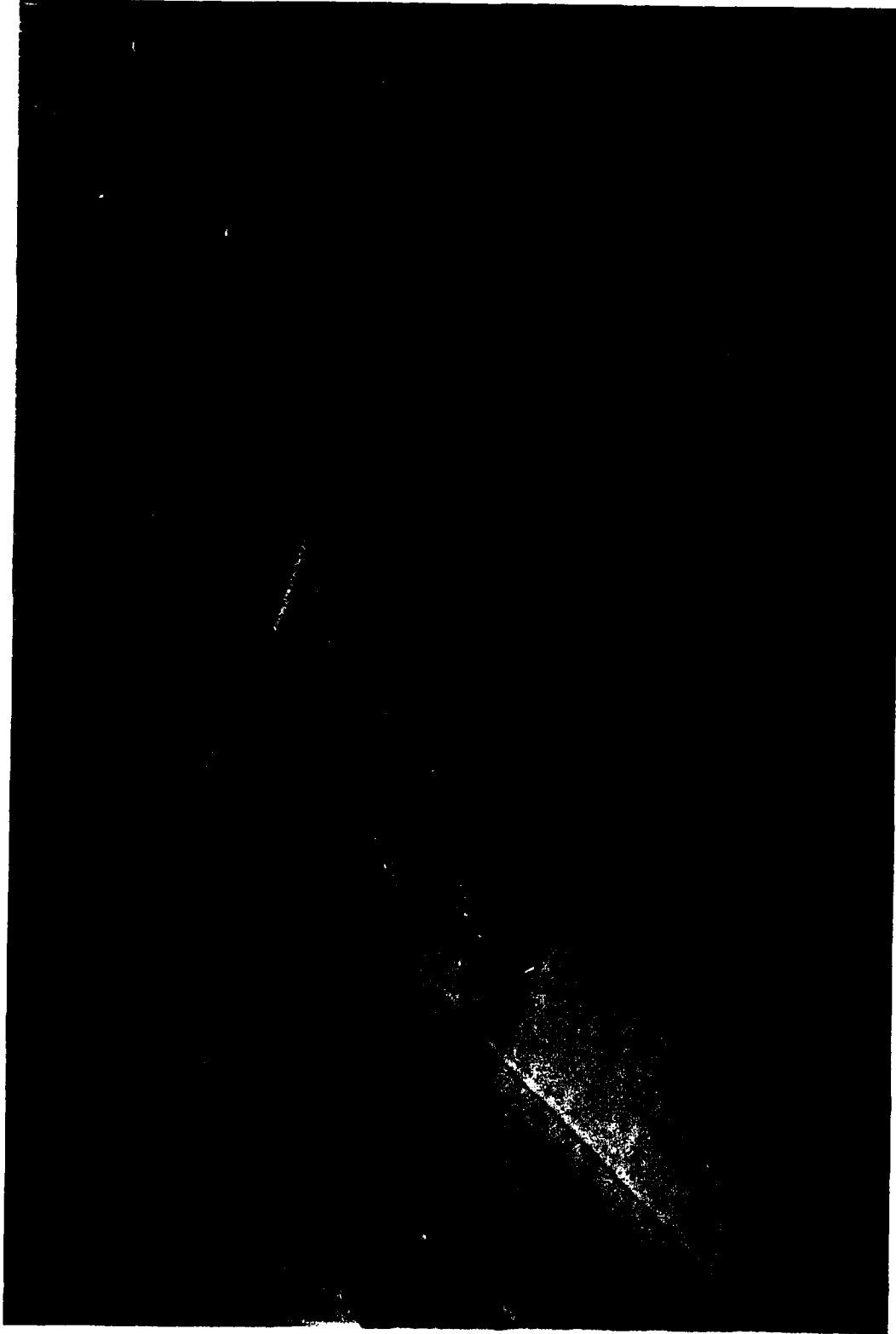


Photo 13. Typical wave patterns for Plan 1L; 15-sec, 3-ft waves from 162 deg

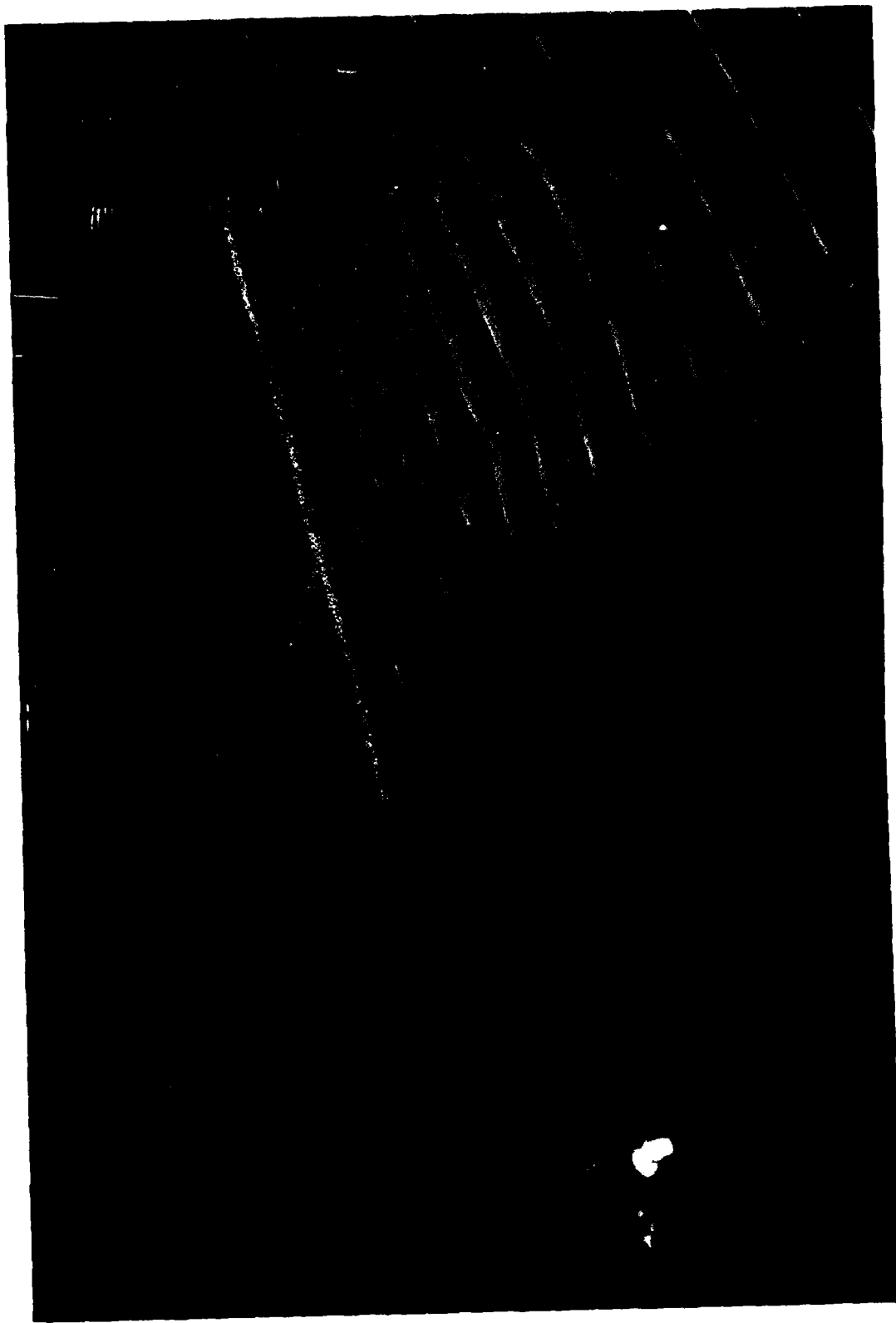


Photo 14. Typical wave patterns for Plan 11; 4-sec, 3-ft waves from 118 deg

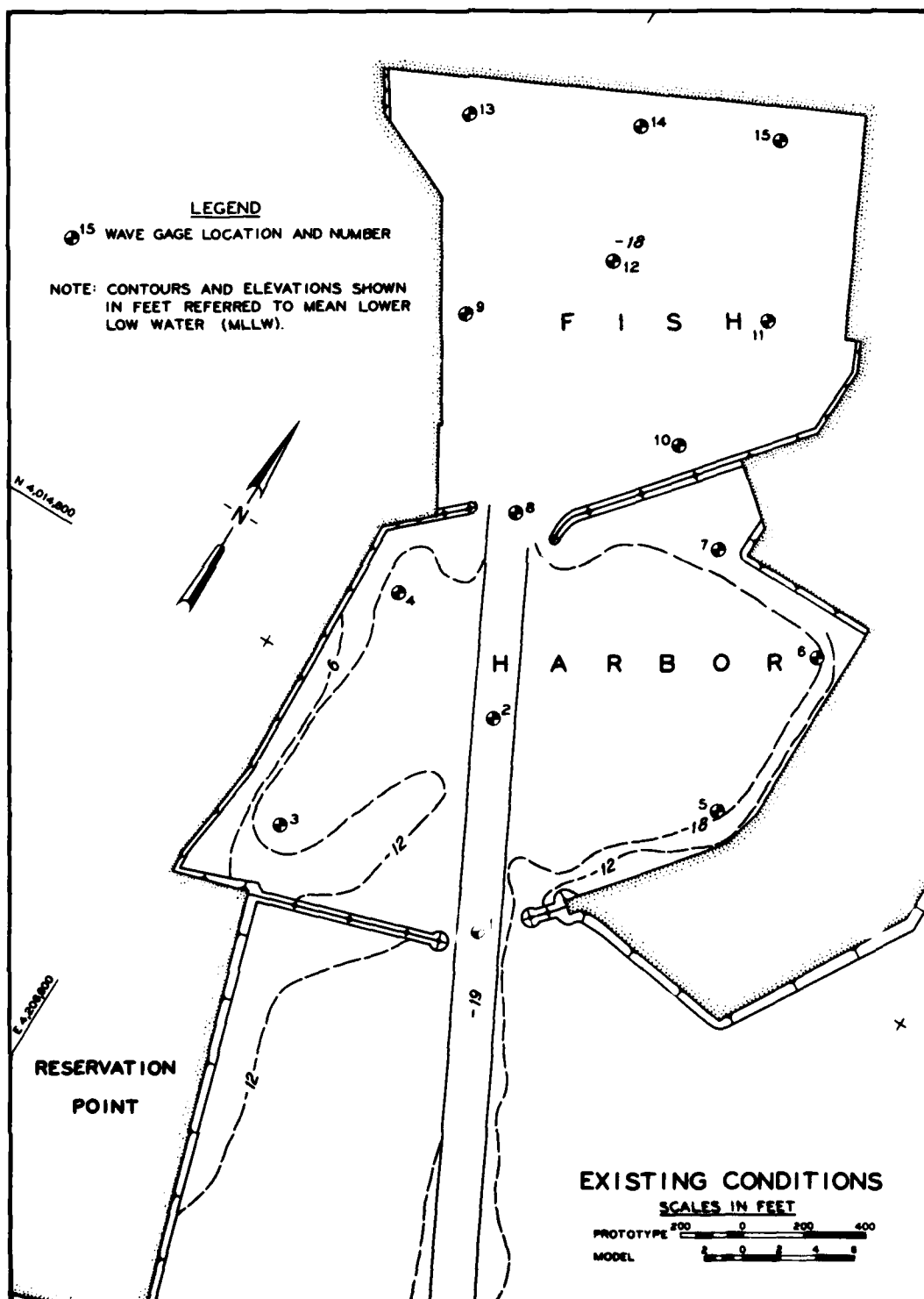


PLATE I

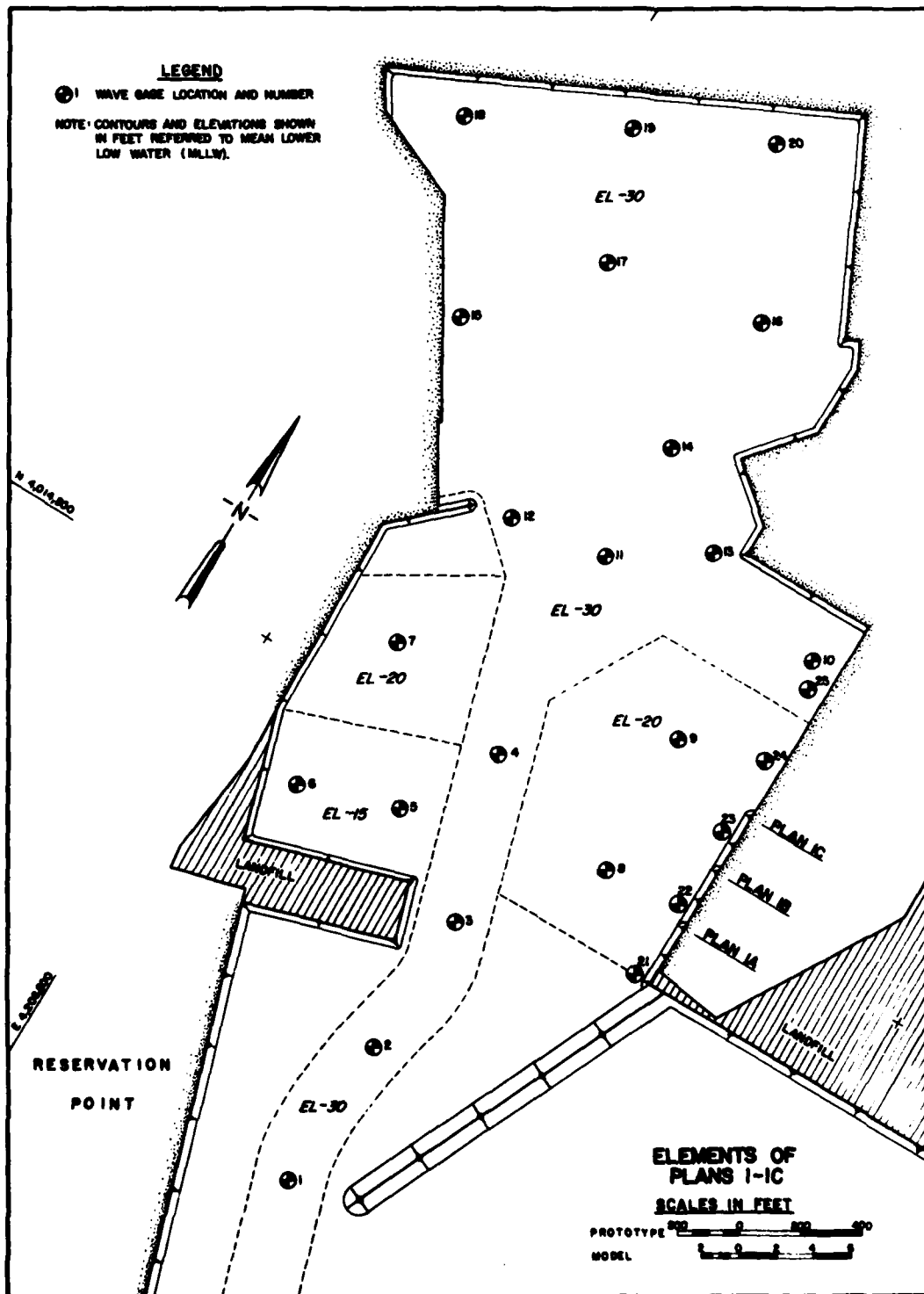


PLATE 2

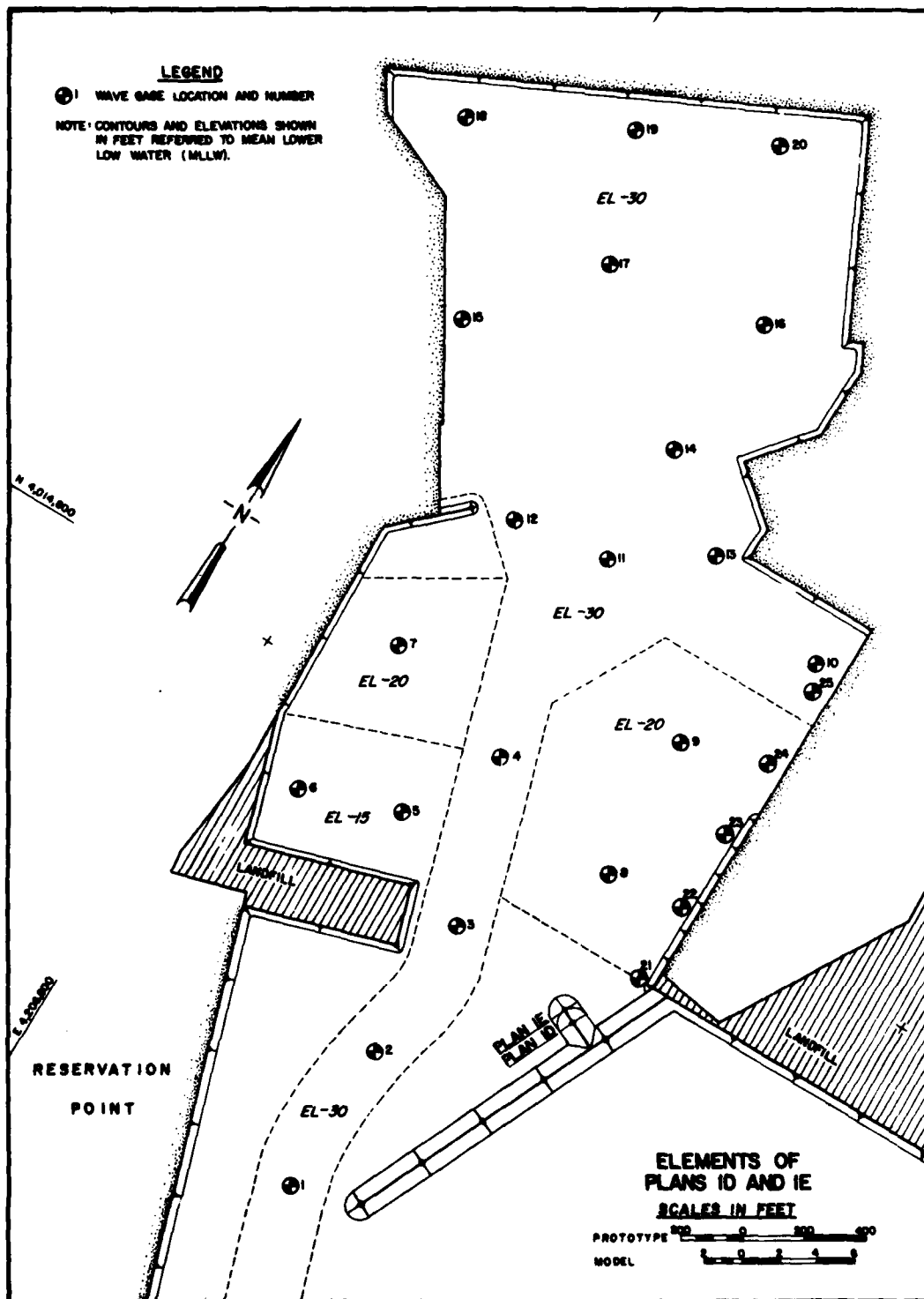


PLATE 3

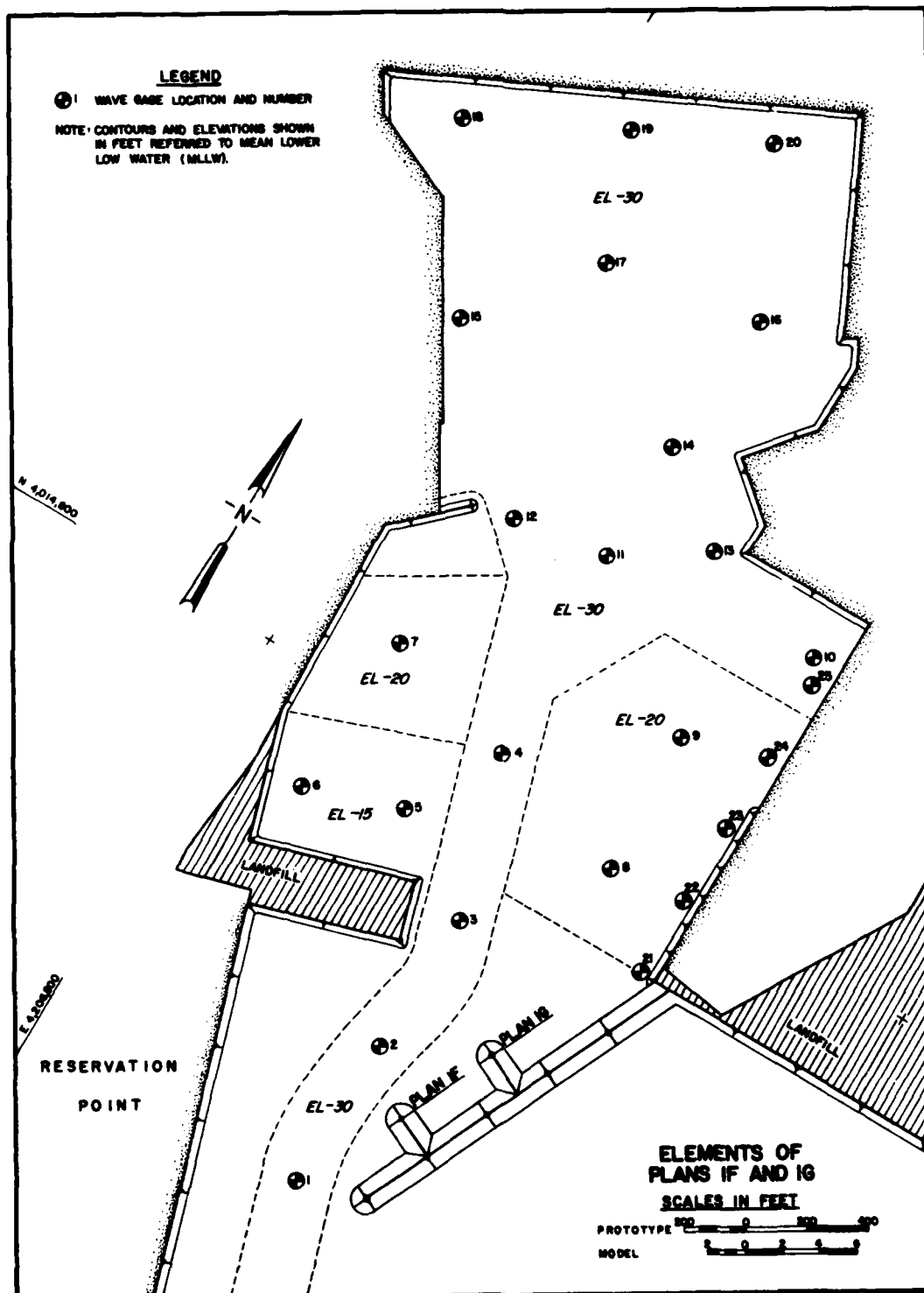
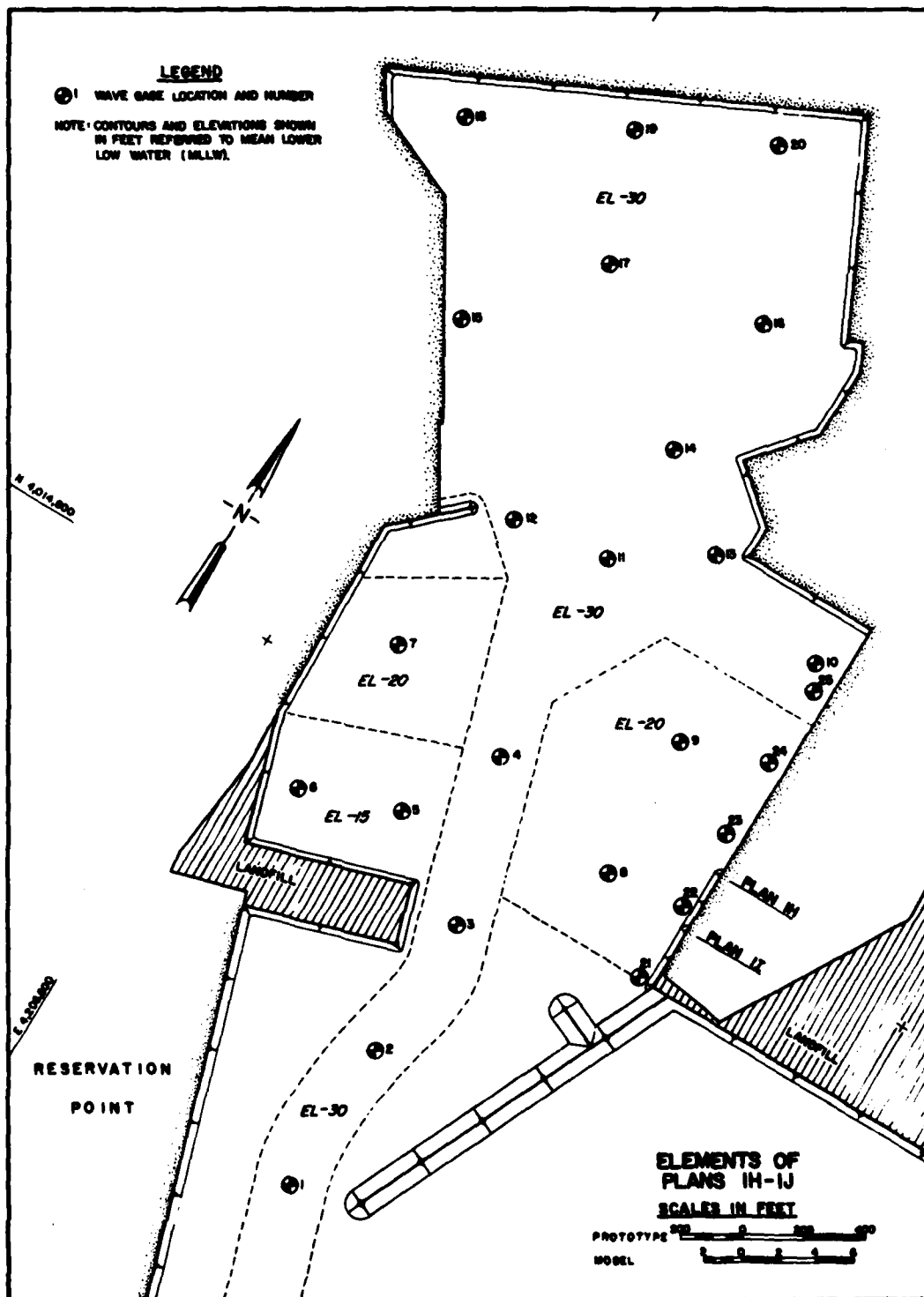


PLATE 4



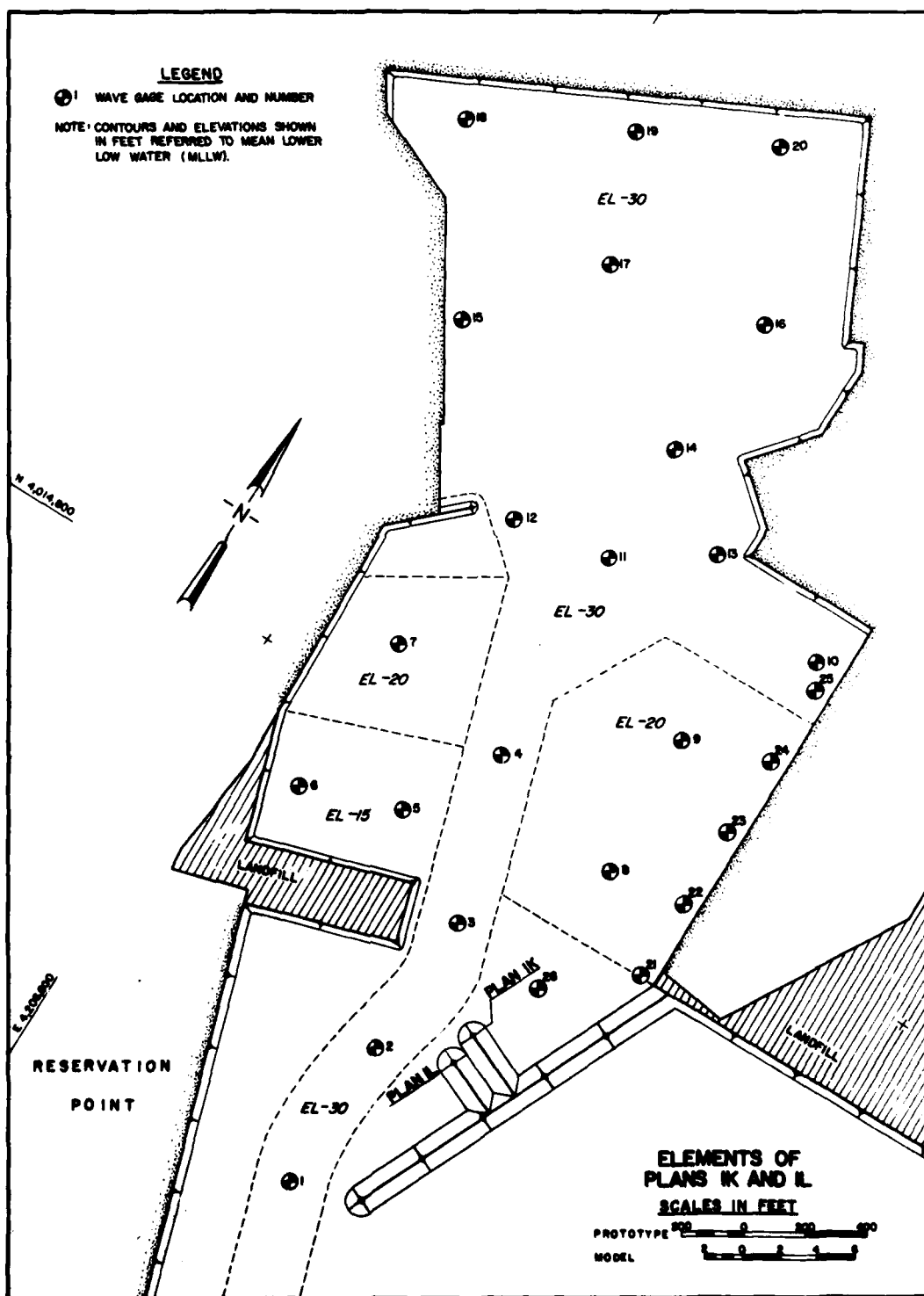
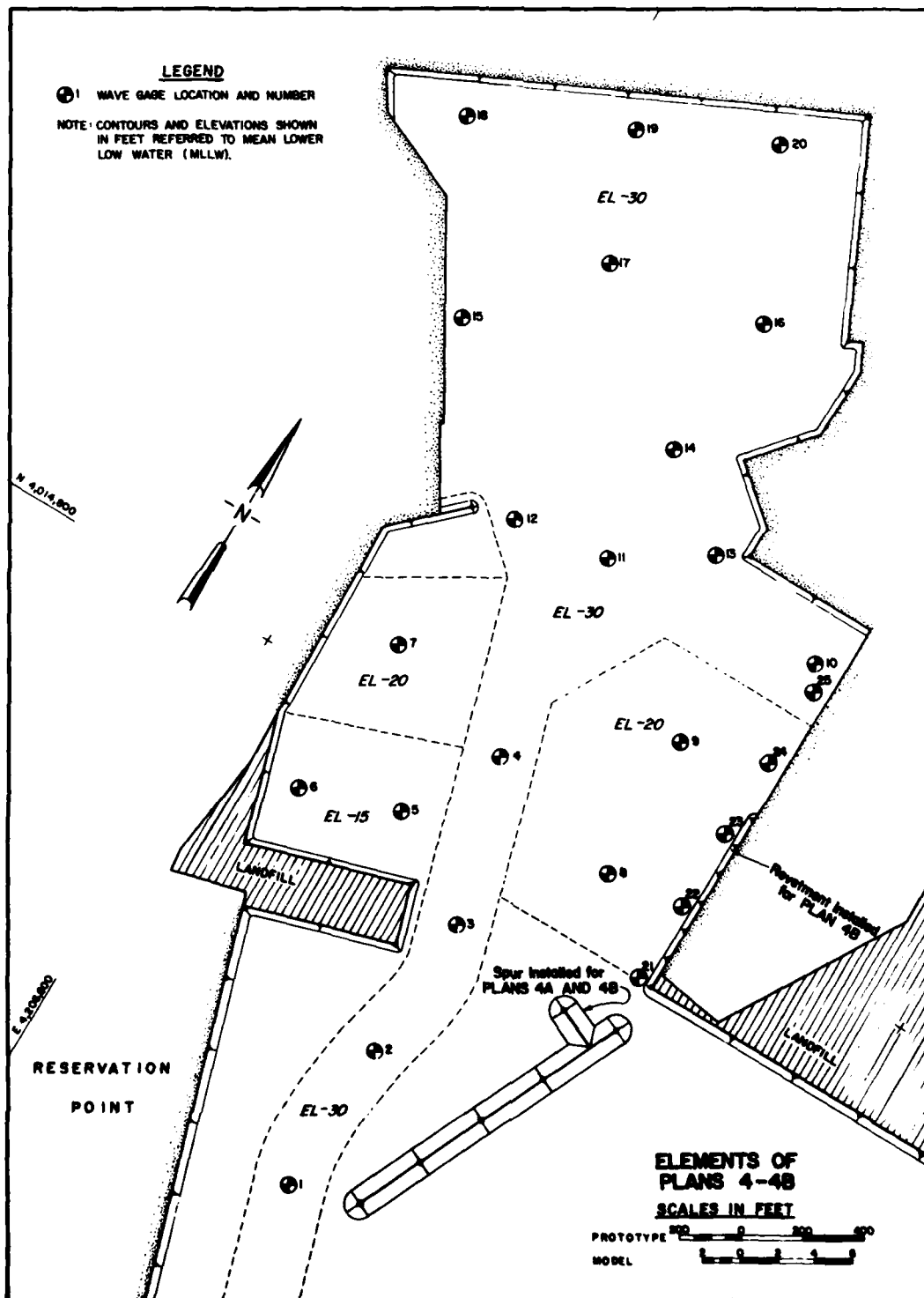
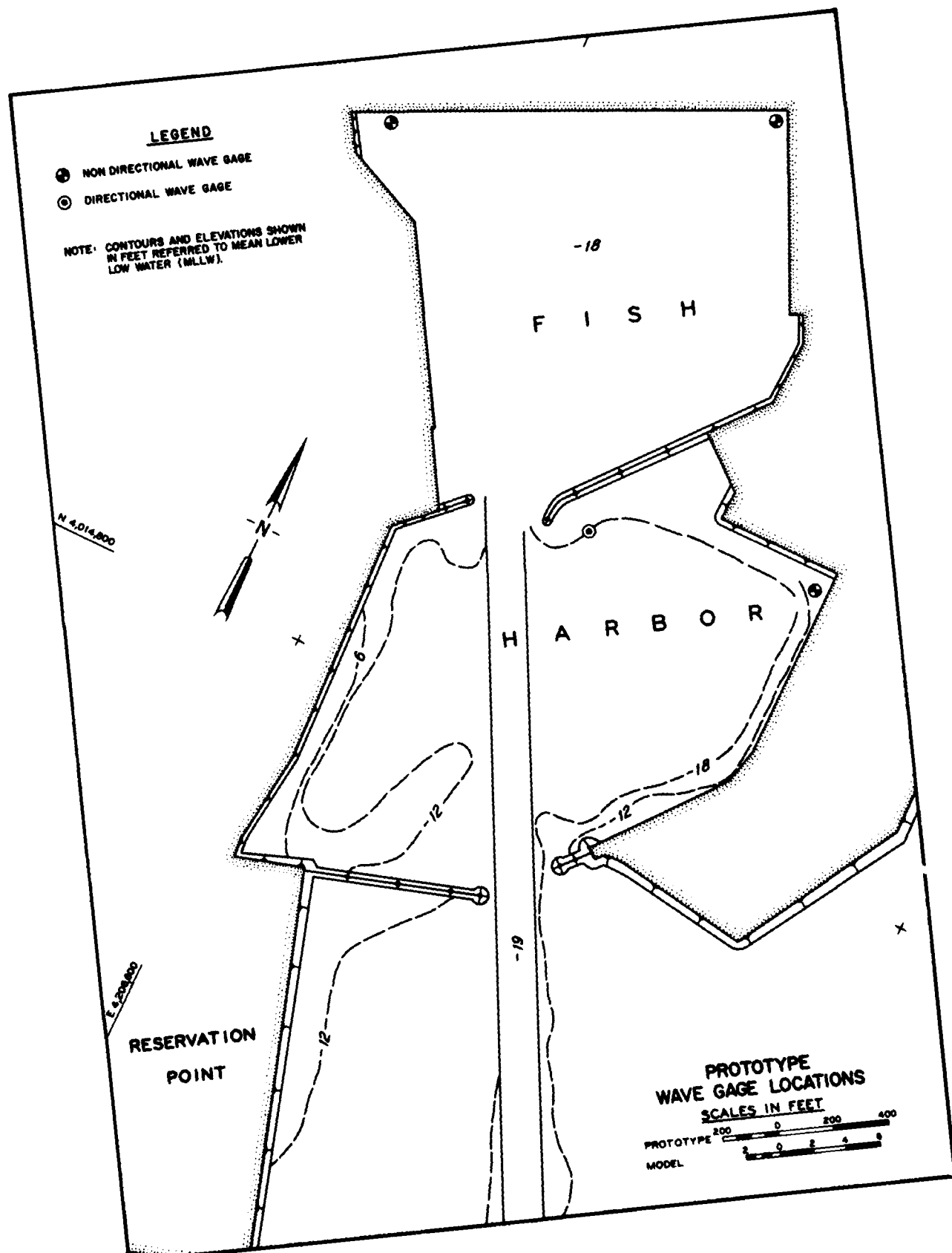
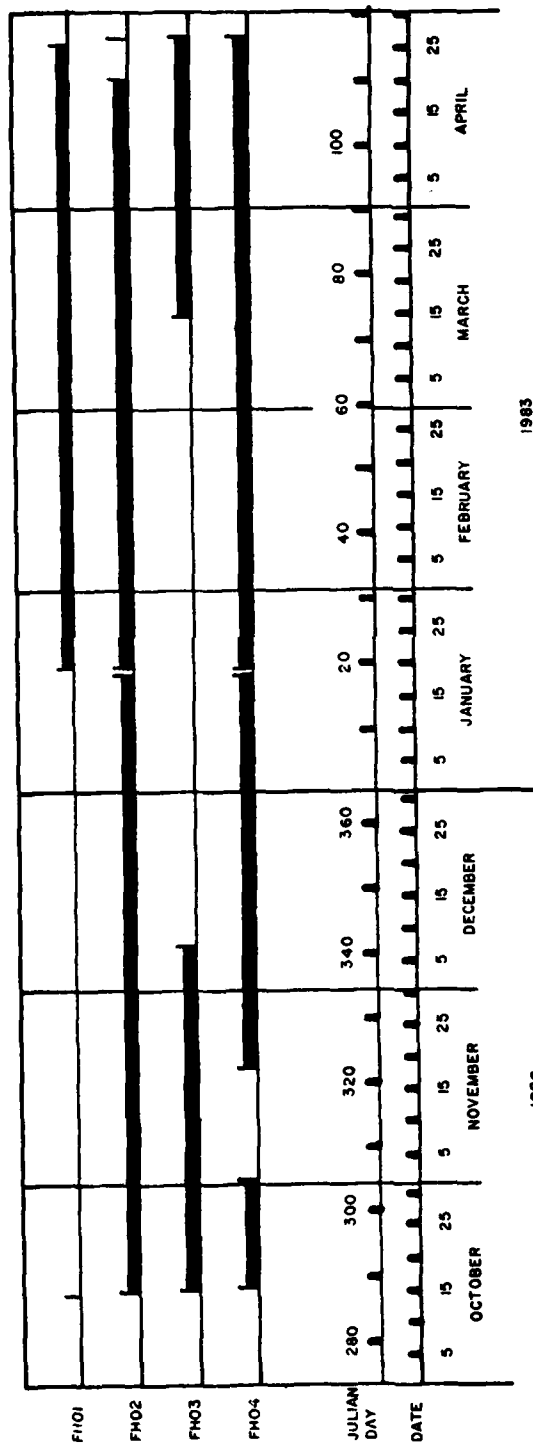


PLATE 6

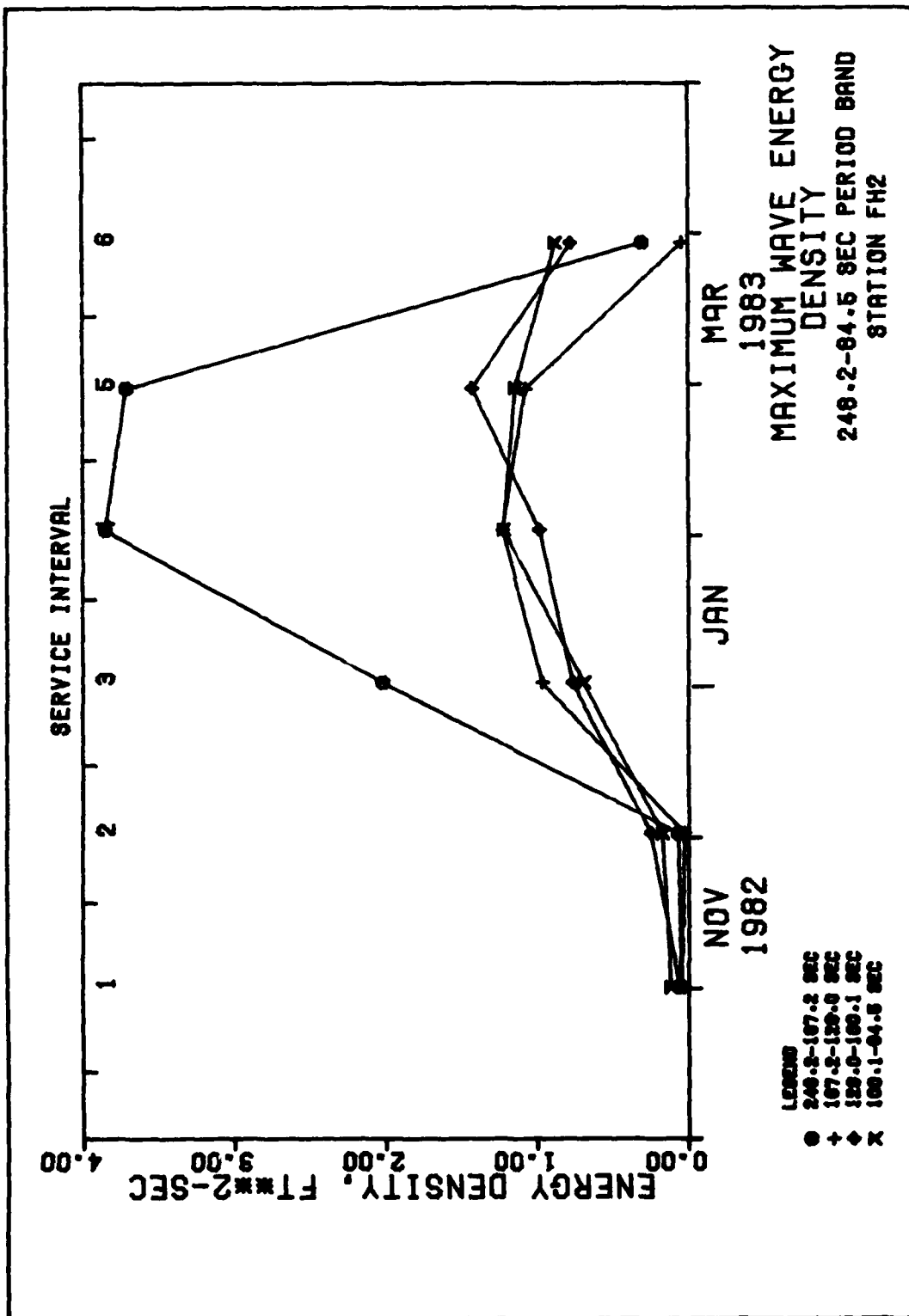


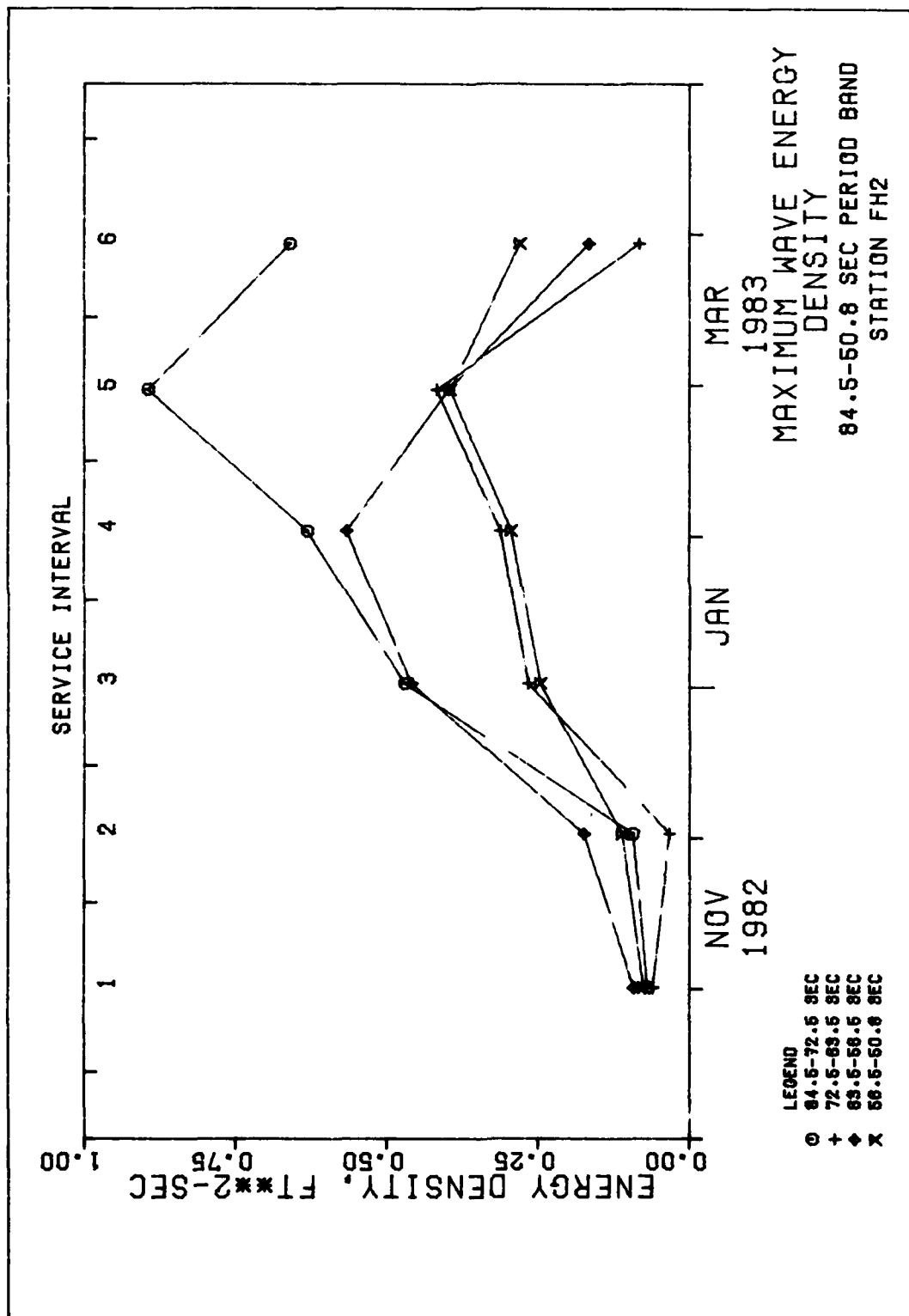




WAVE GAGE OPERATIONAL STATUS OCTOBER 1982 - APRIL 1983

GAGE OPERATING





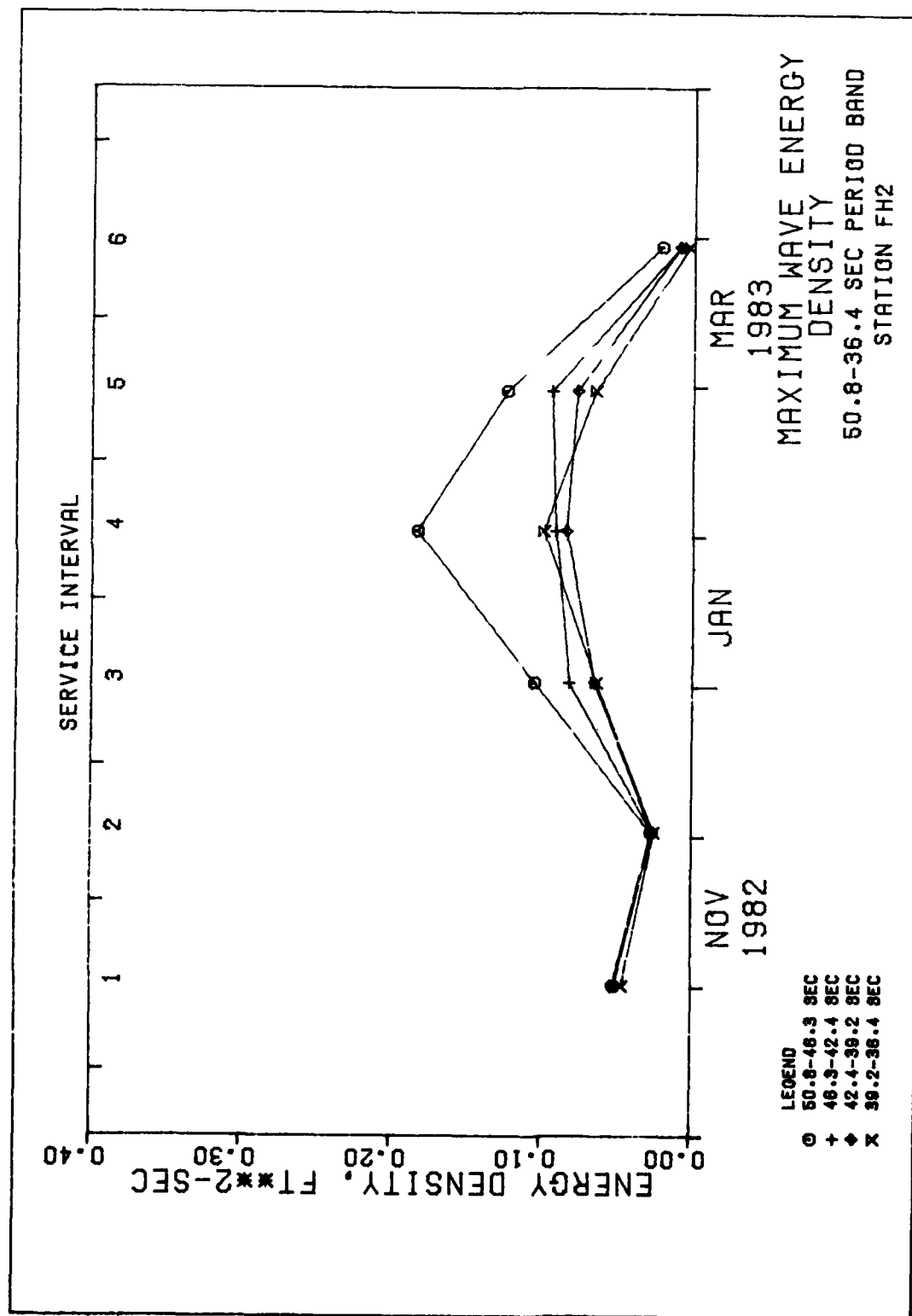
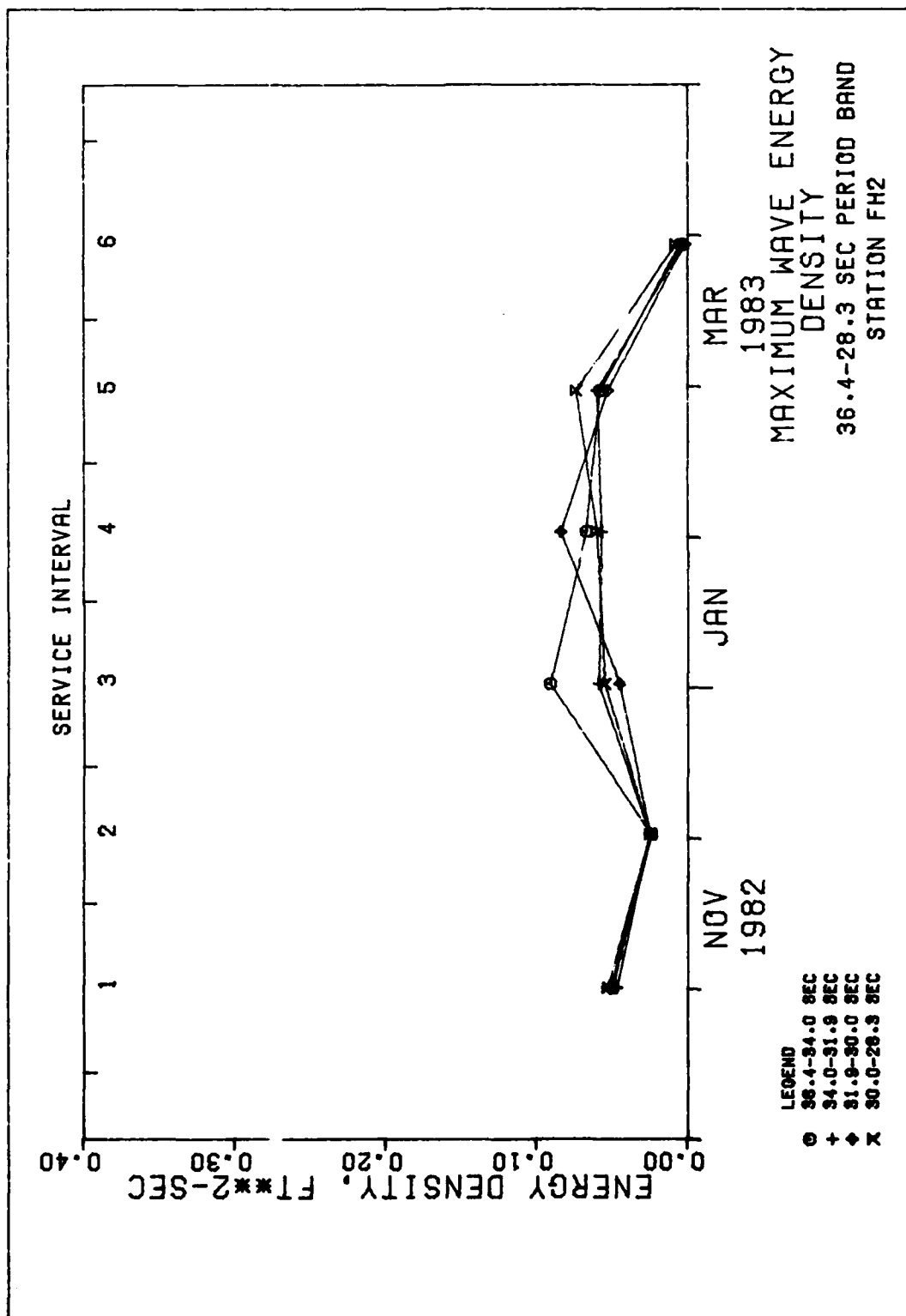
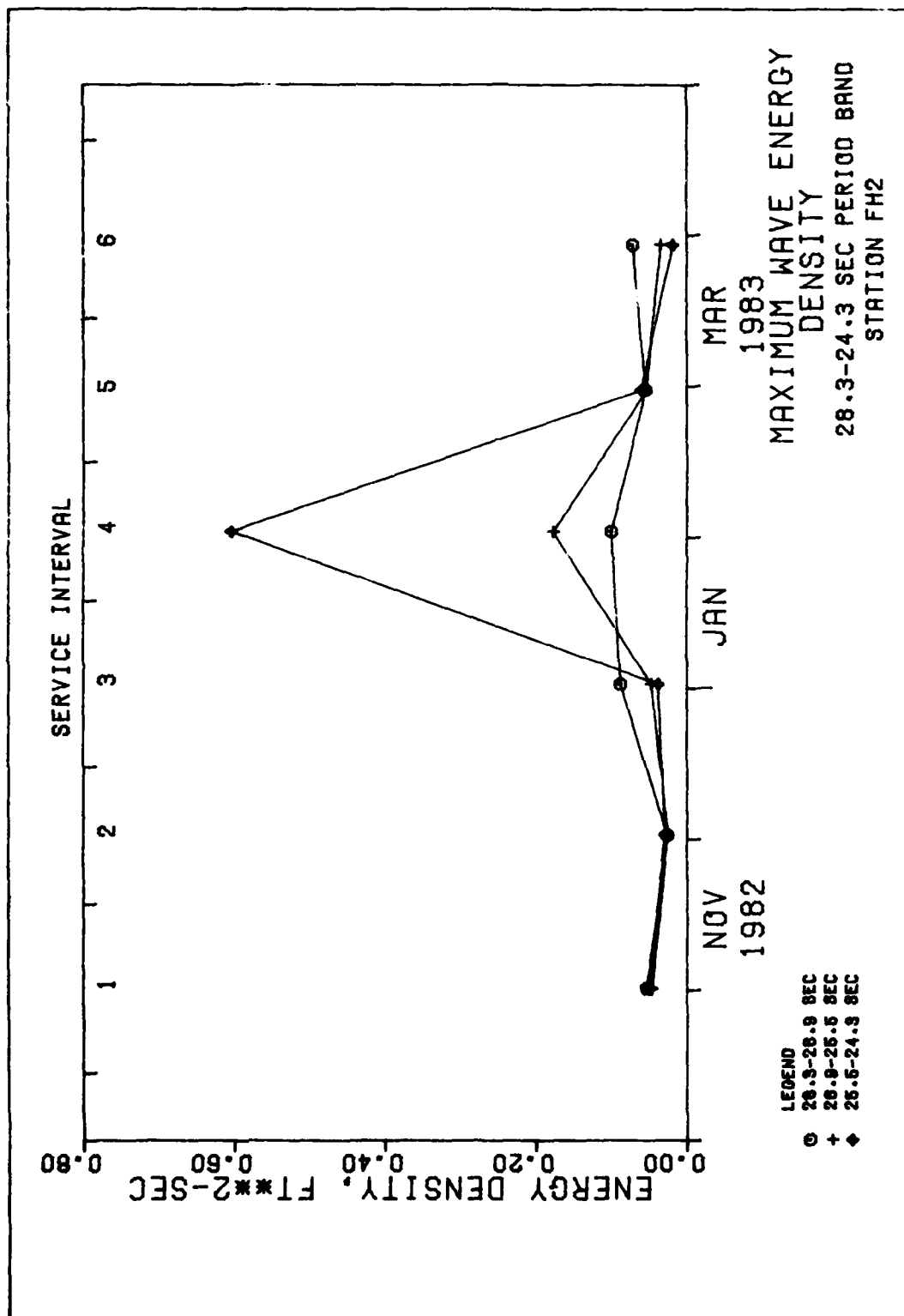
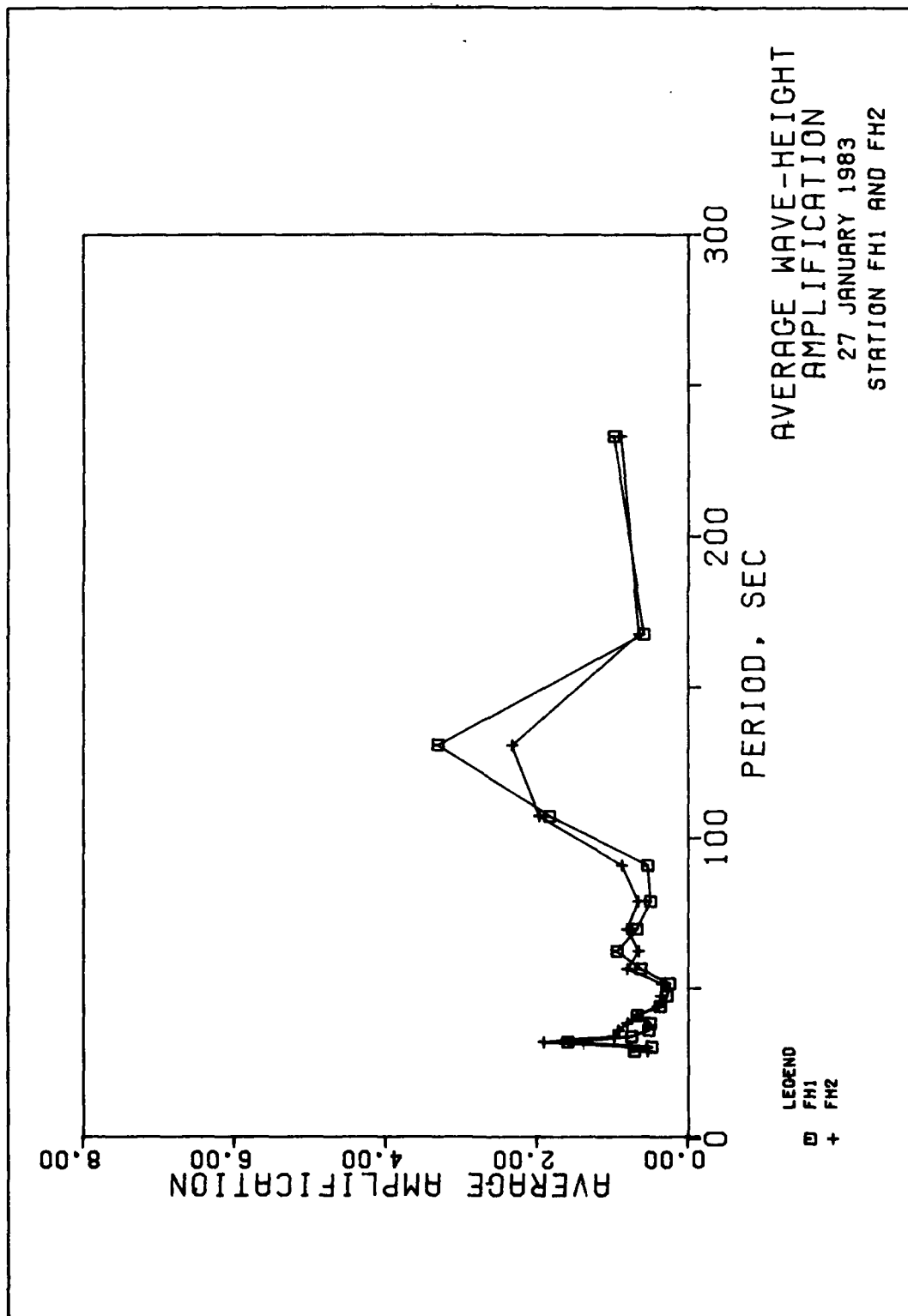
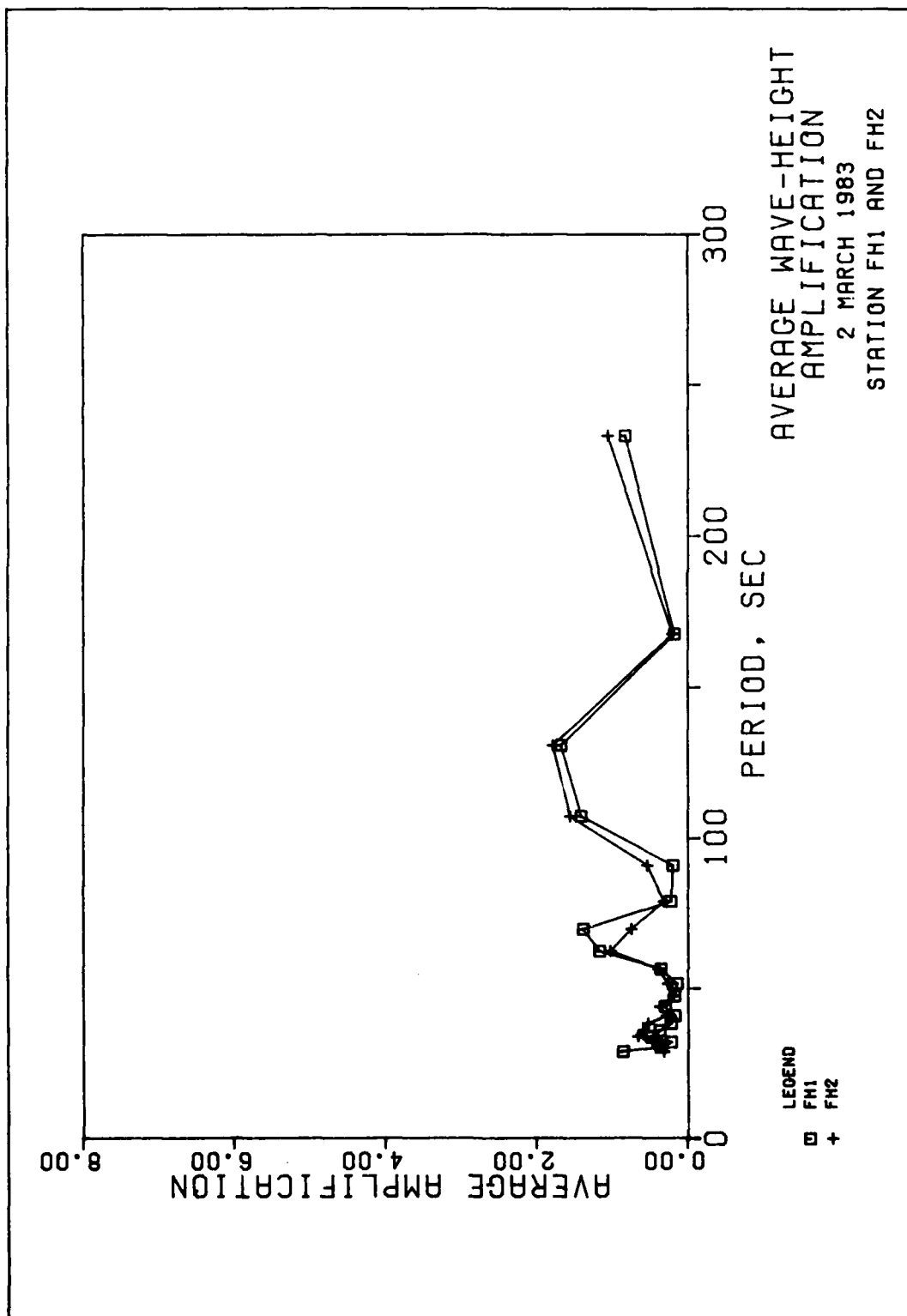


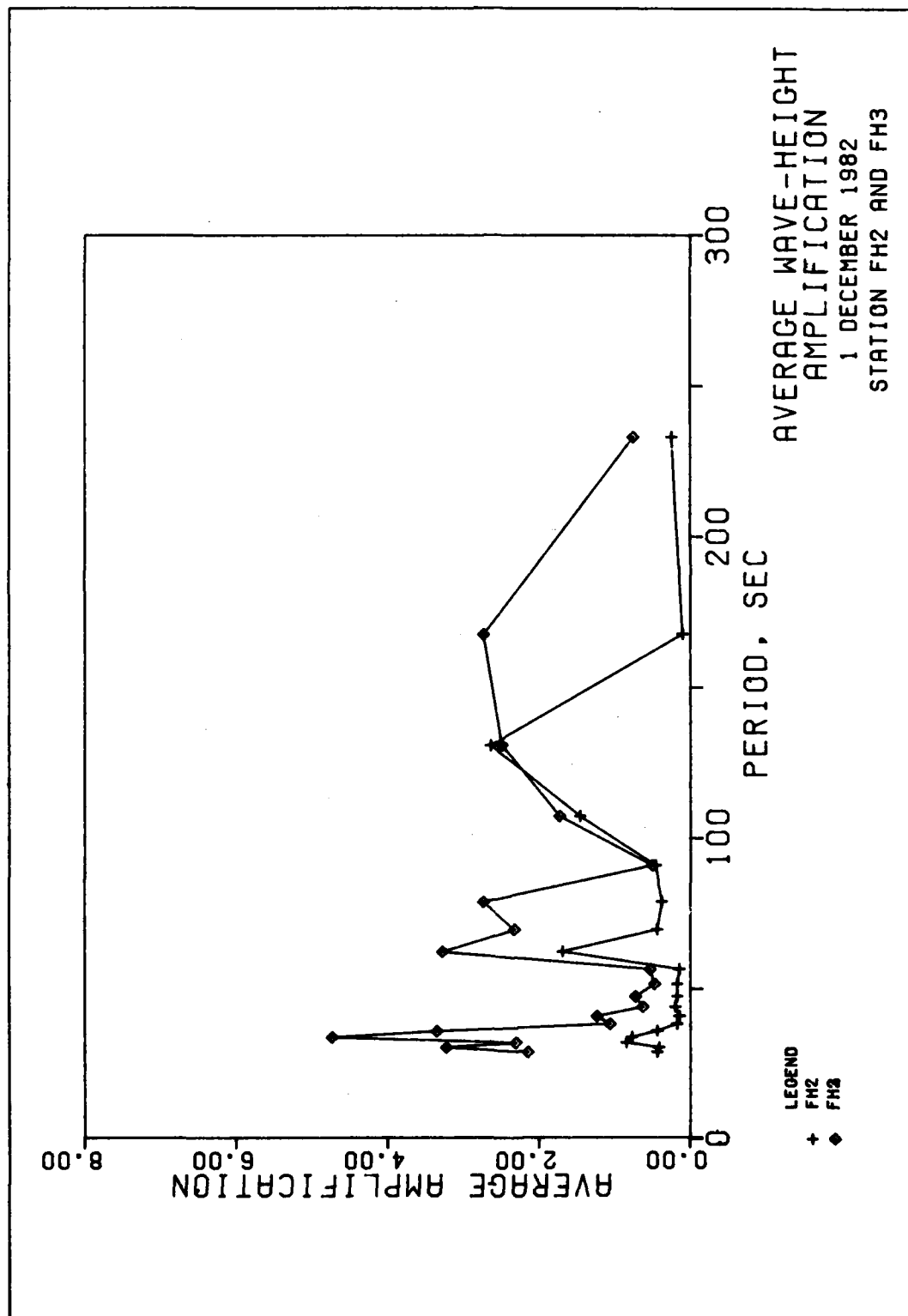
PLATE 14

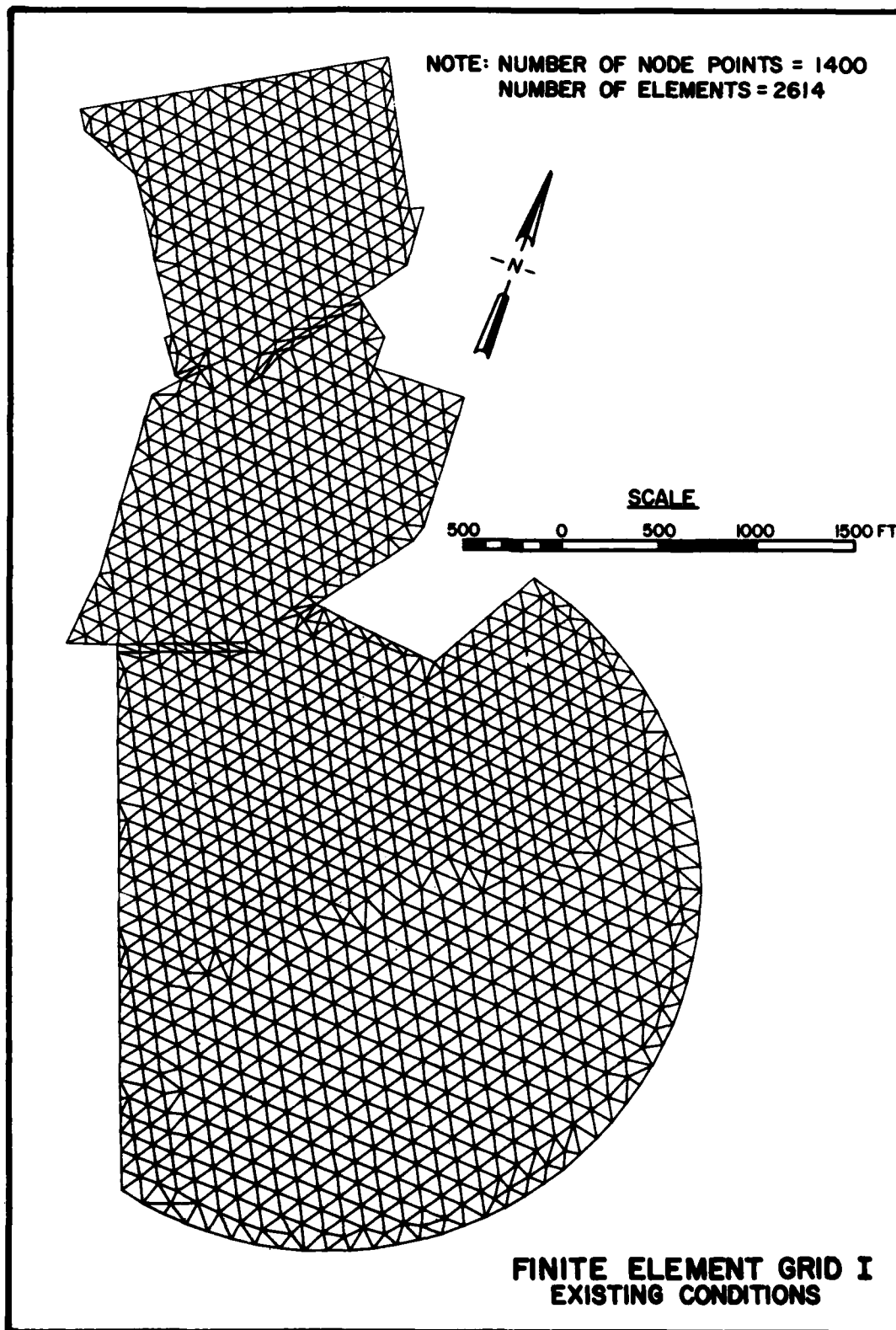


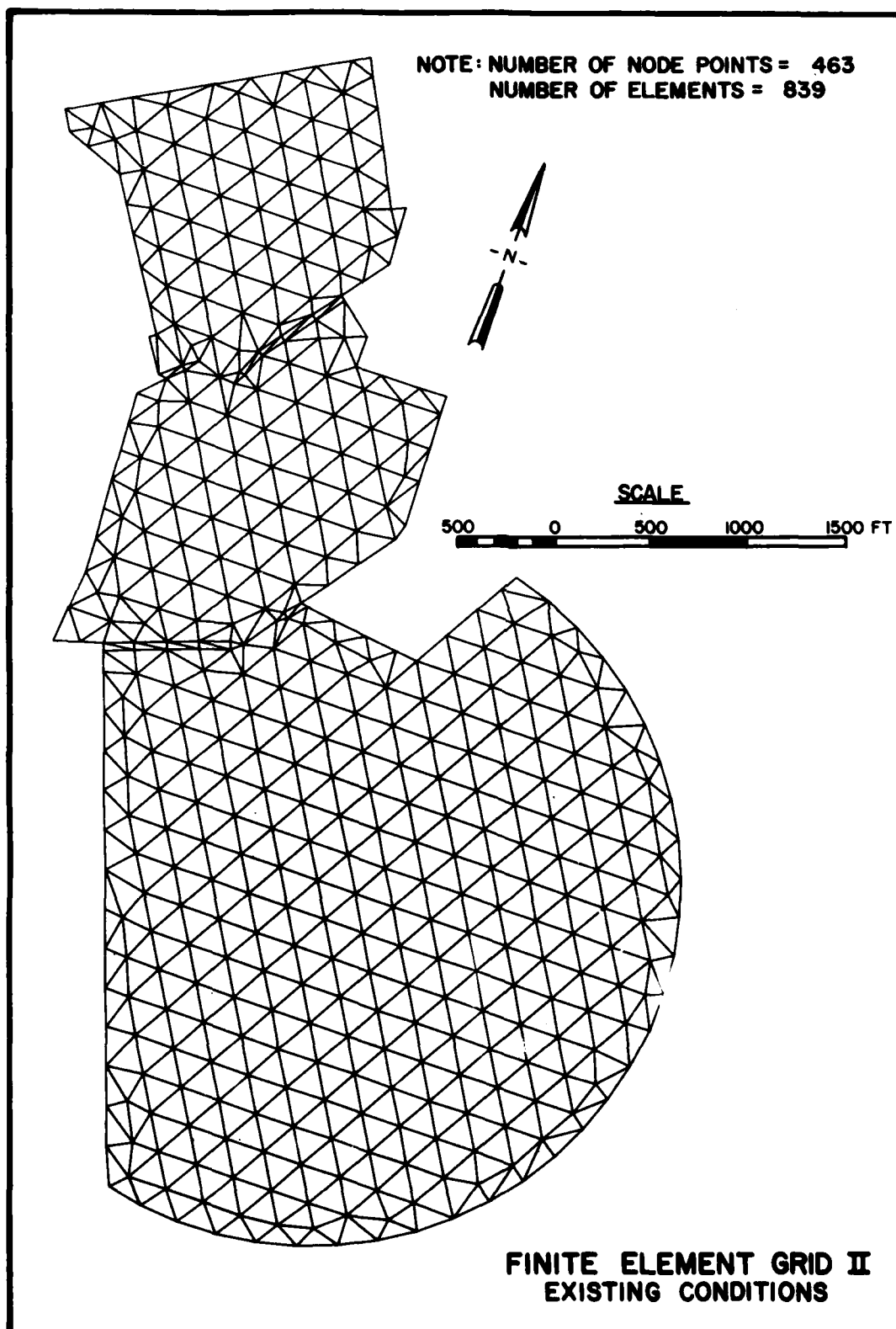


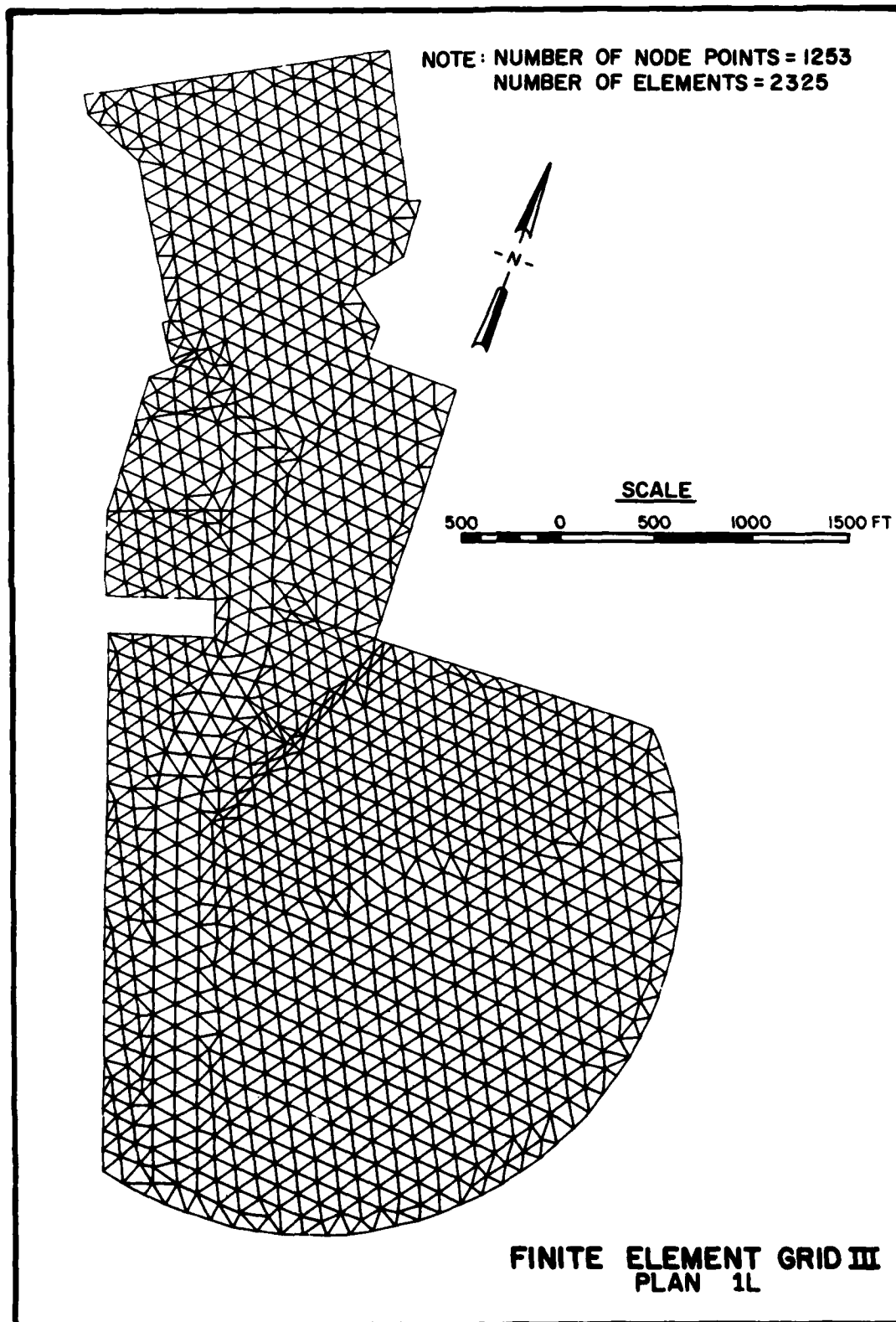


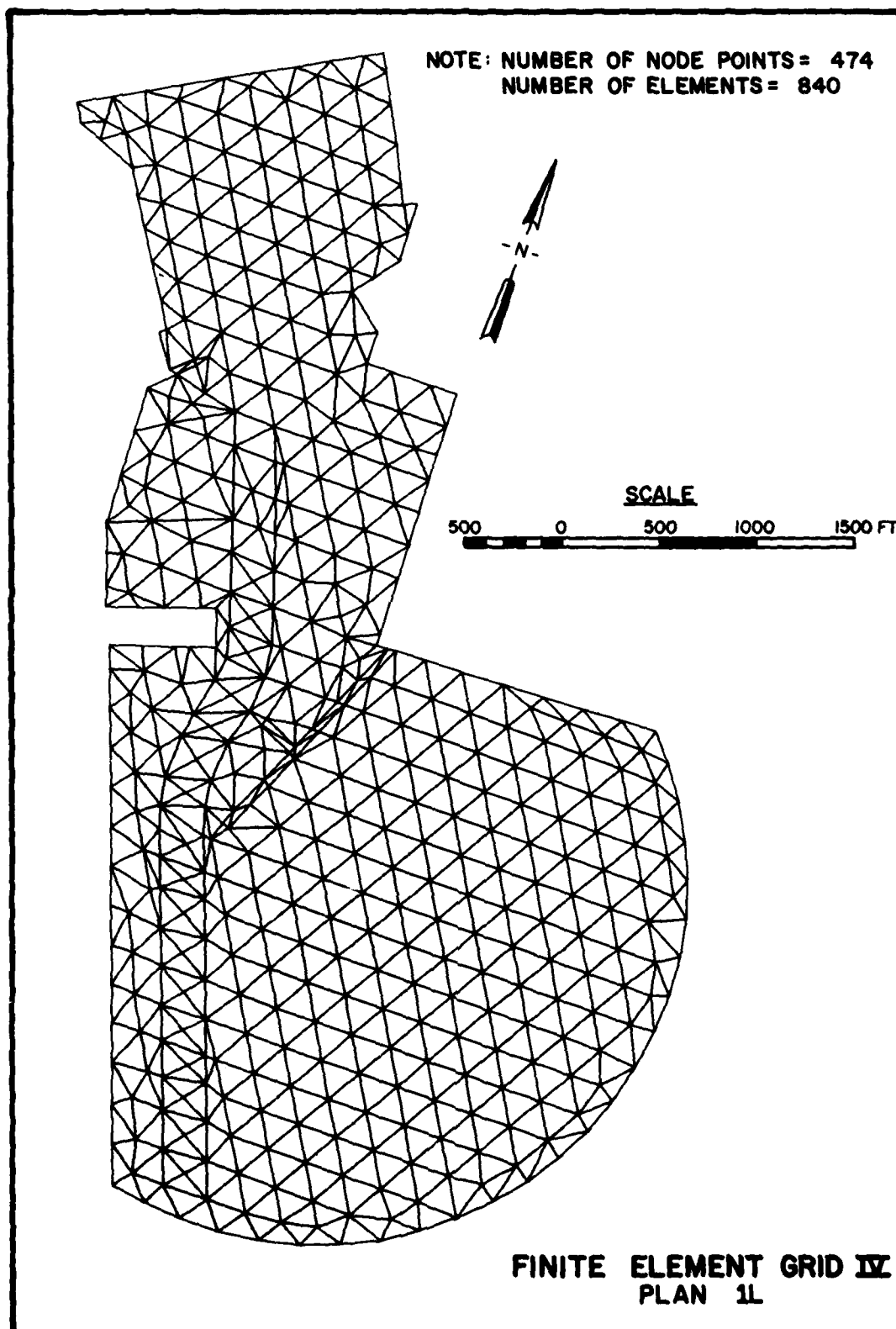












AD A157 888

EFFECTS OF PROPOSED HARBOR MODIFICATIONS ON WAVE
CONDITIONS HARBOR RESONANCE (U) COASTAL ENGINEERING
RESEARCH CENTER VICKSBURG MS R R BOTTIN ET AL. JUN 85
CERC-85-2

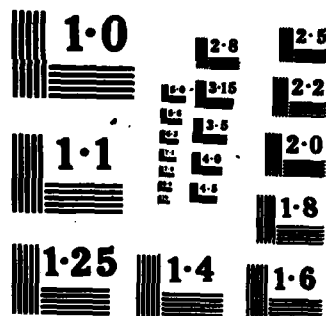
22

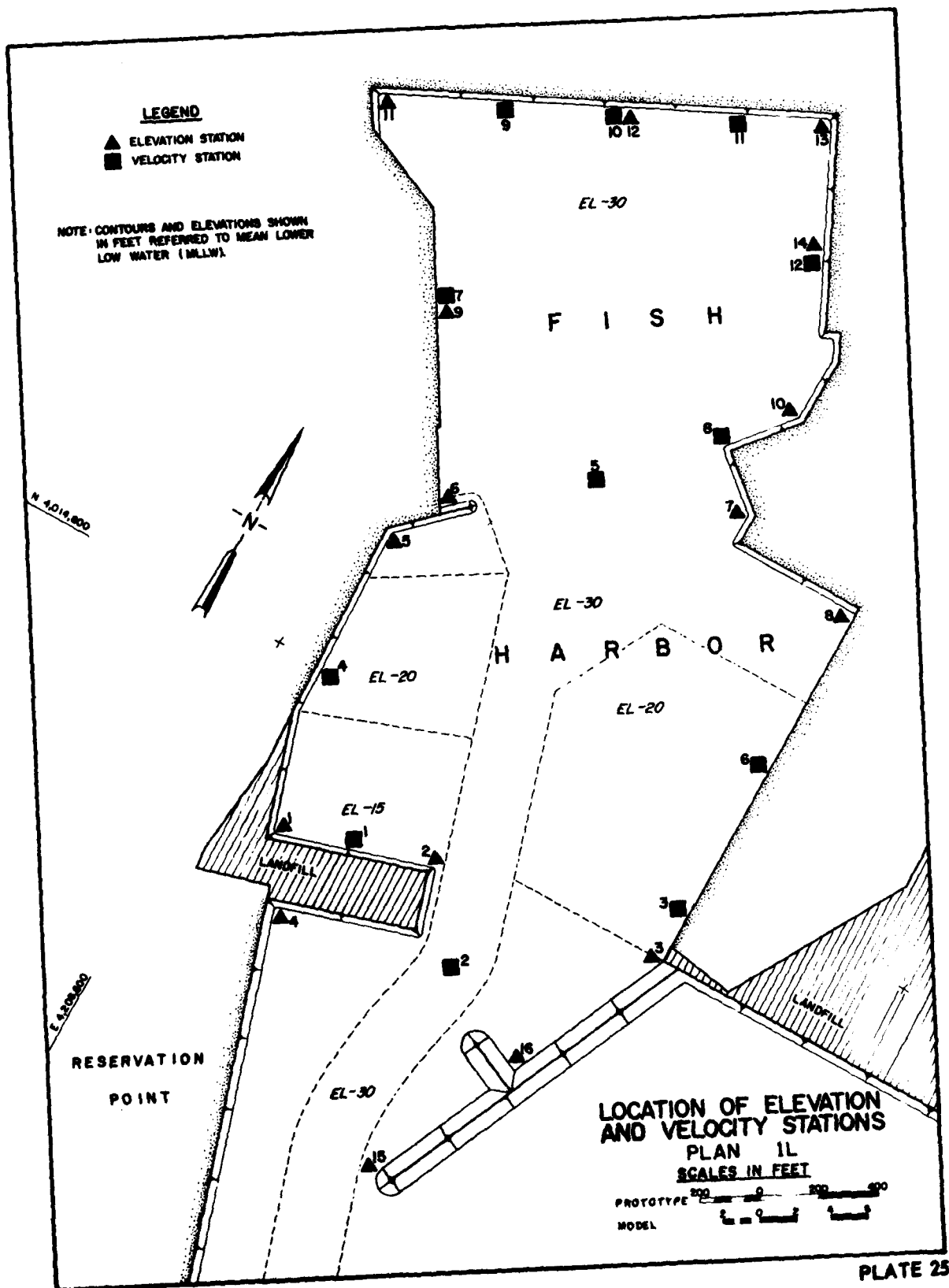
UNCLASSIFIED

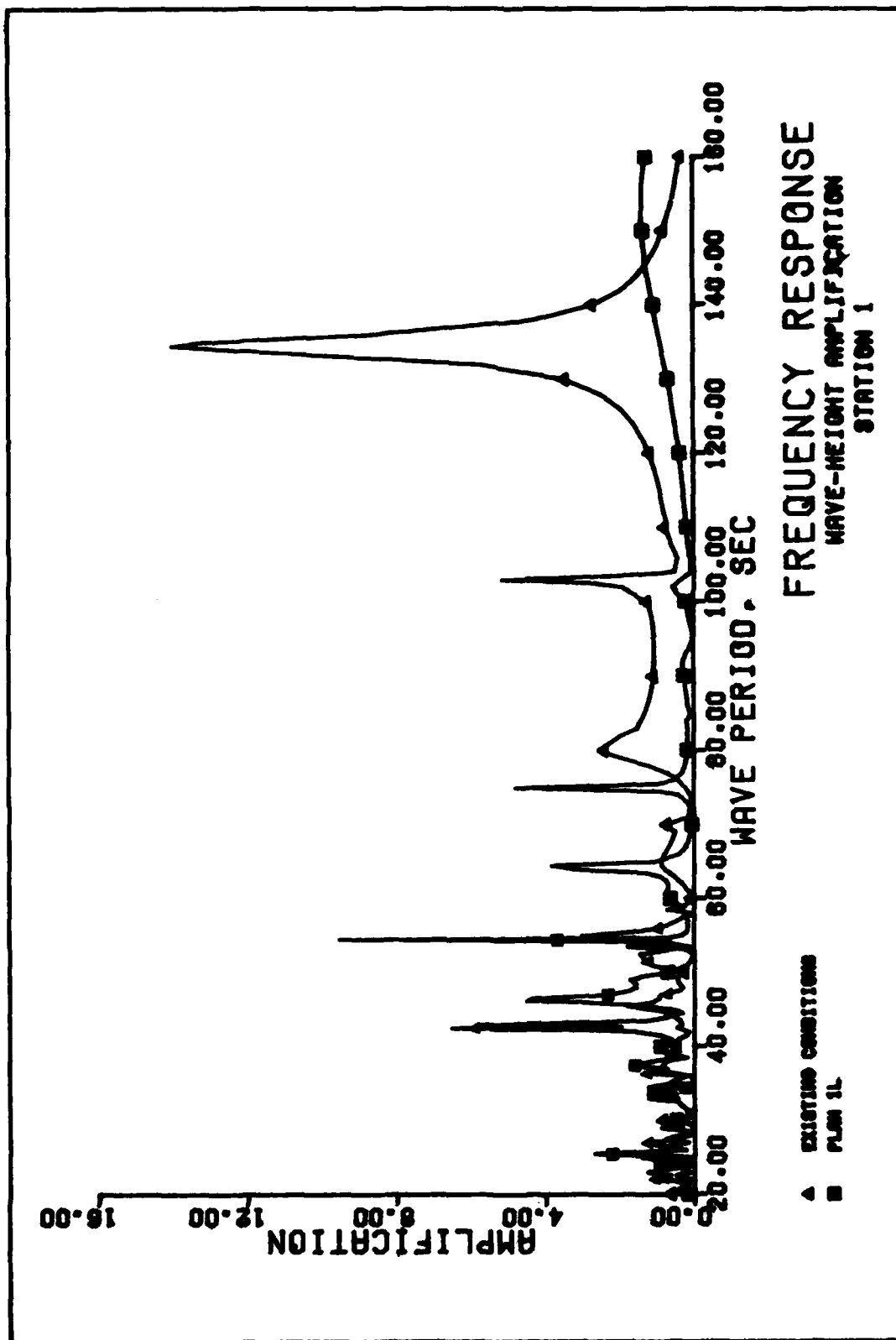
F/G 13/2

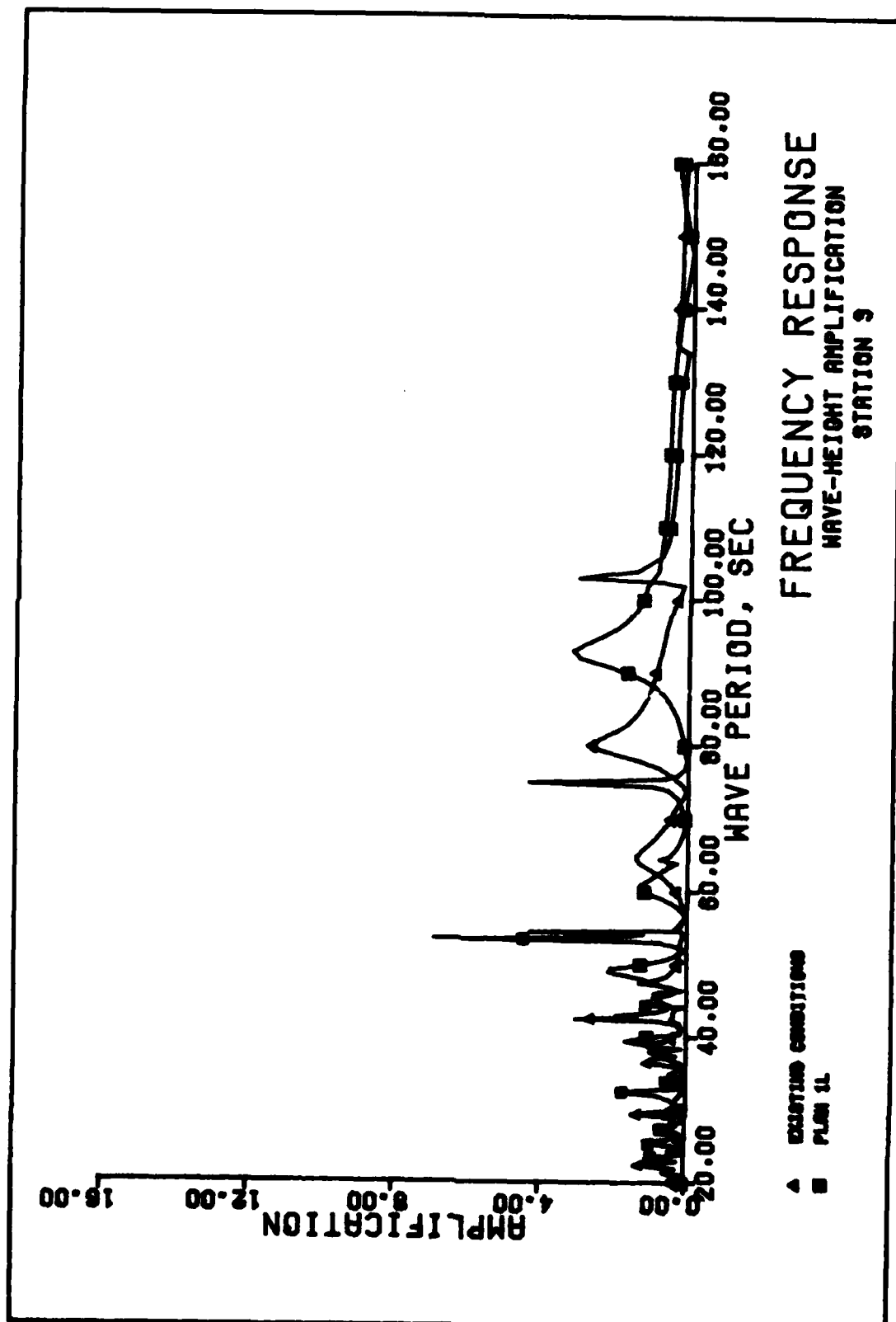
NL

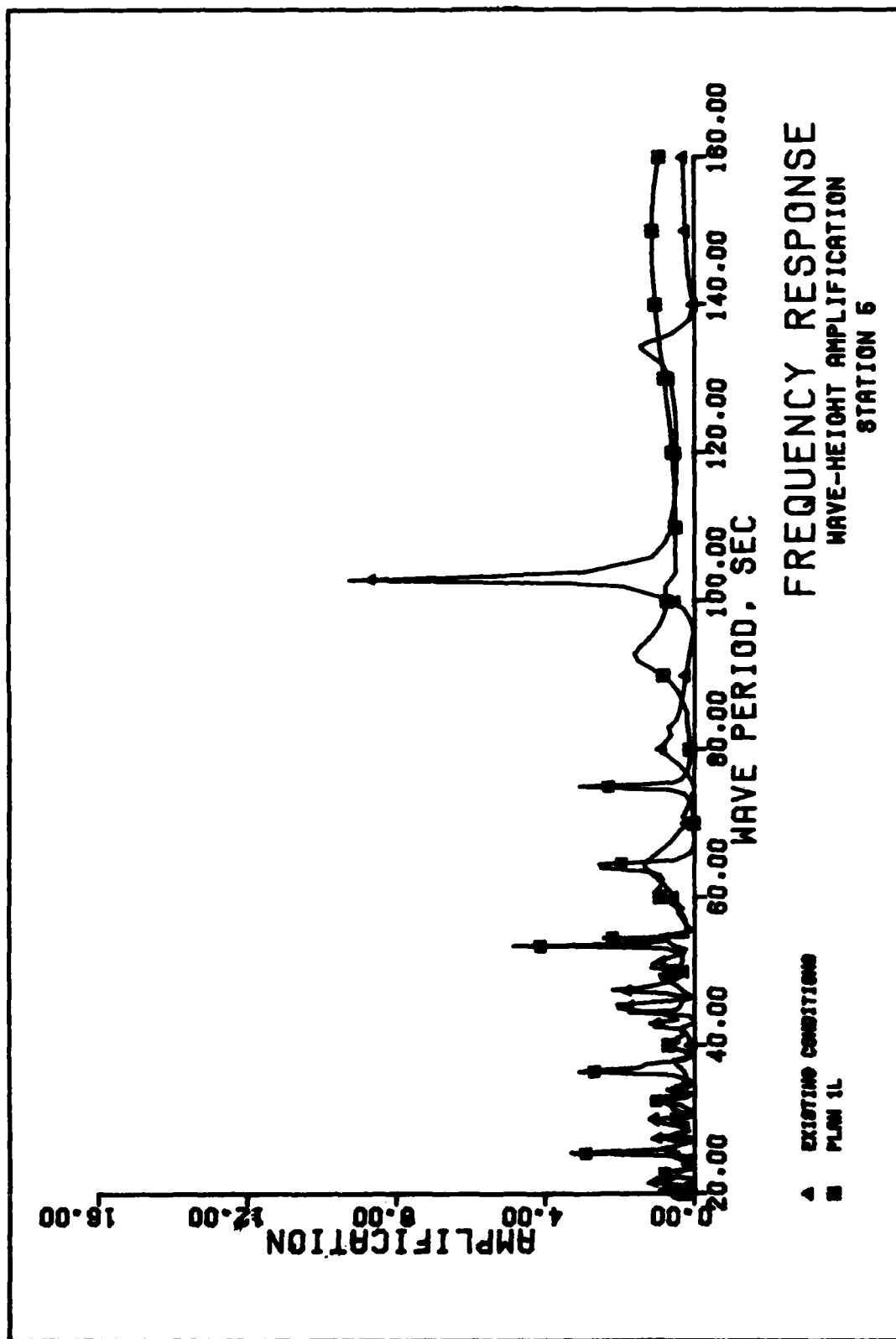
END
DATE
FILMED
JUN 85

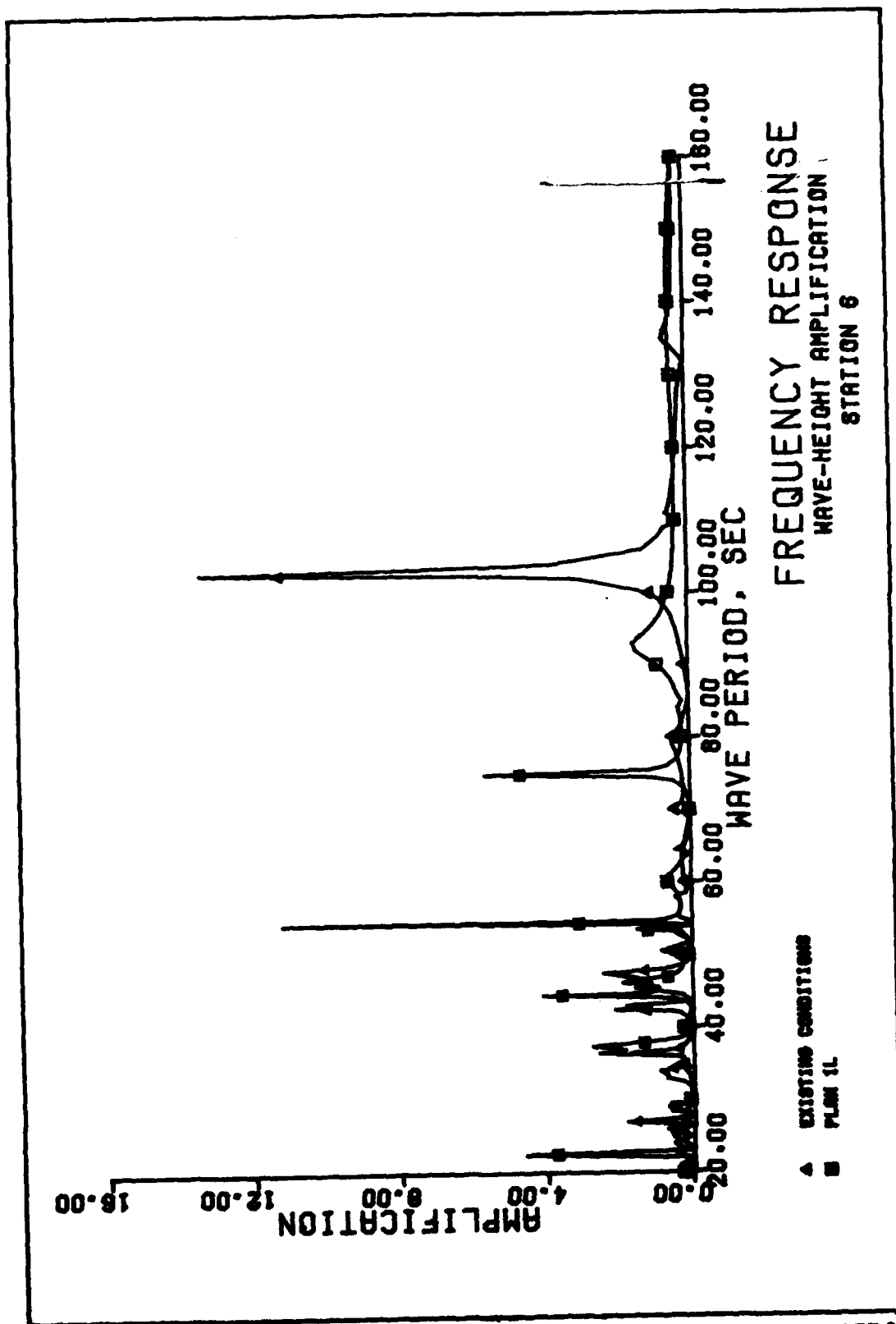


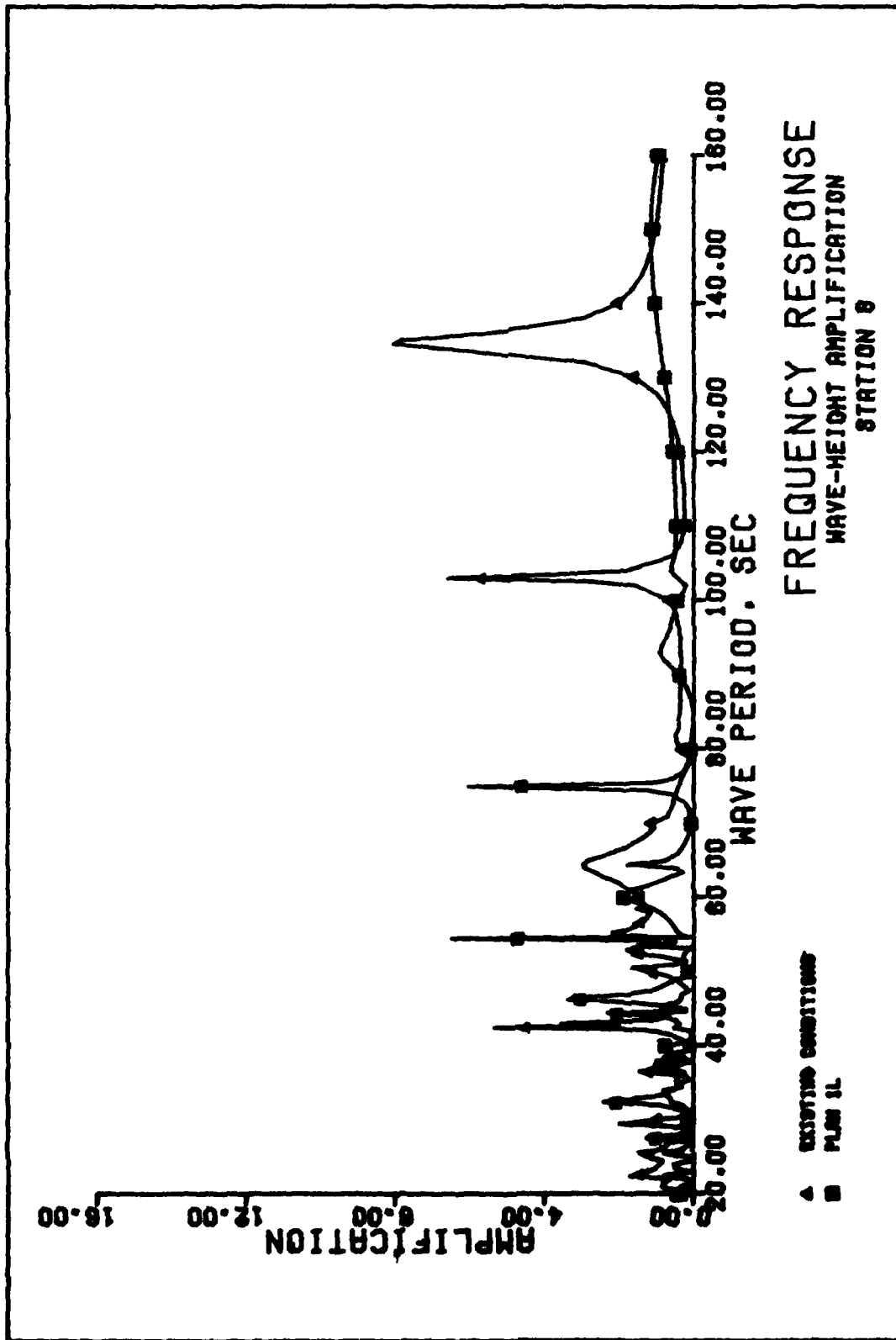


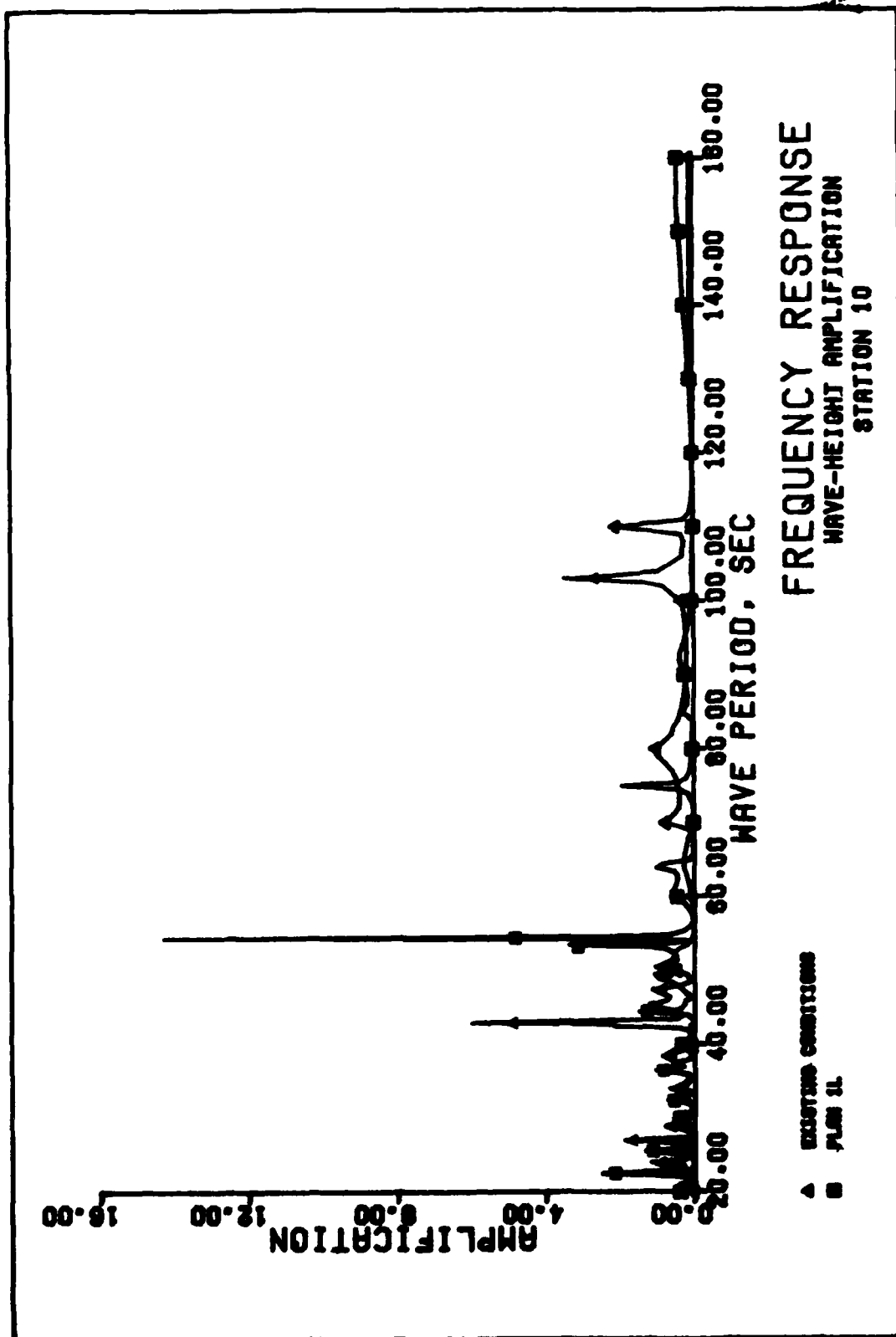


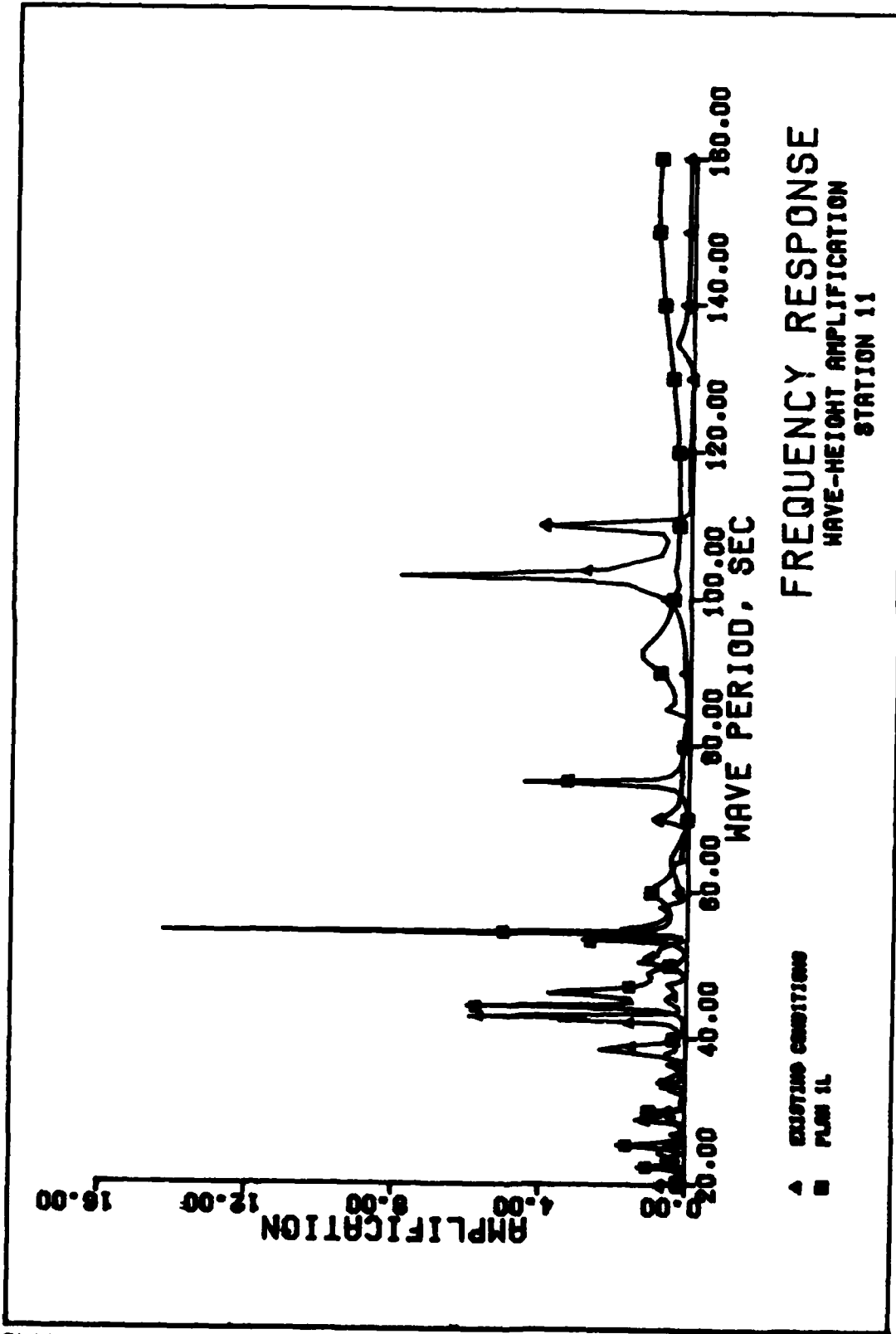


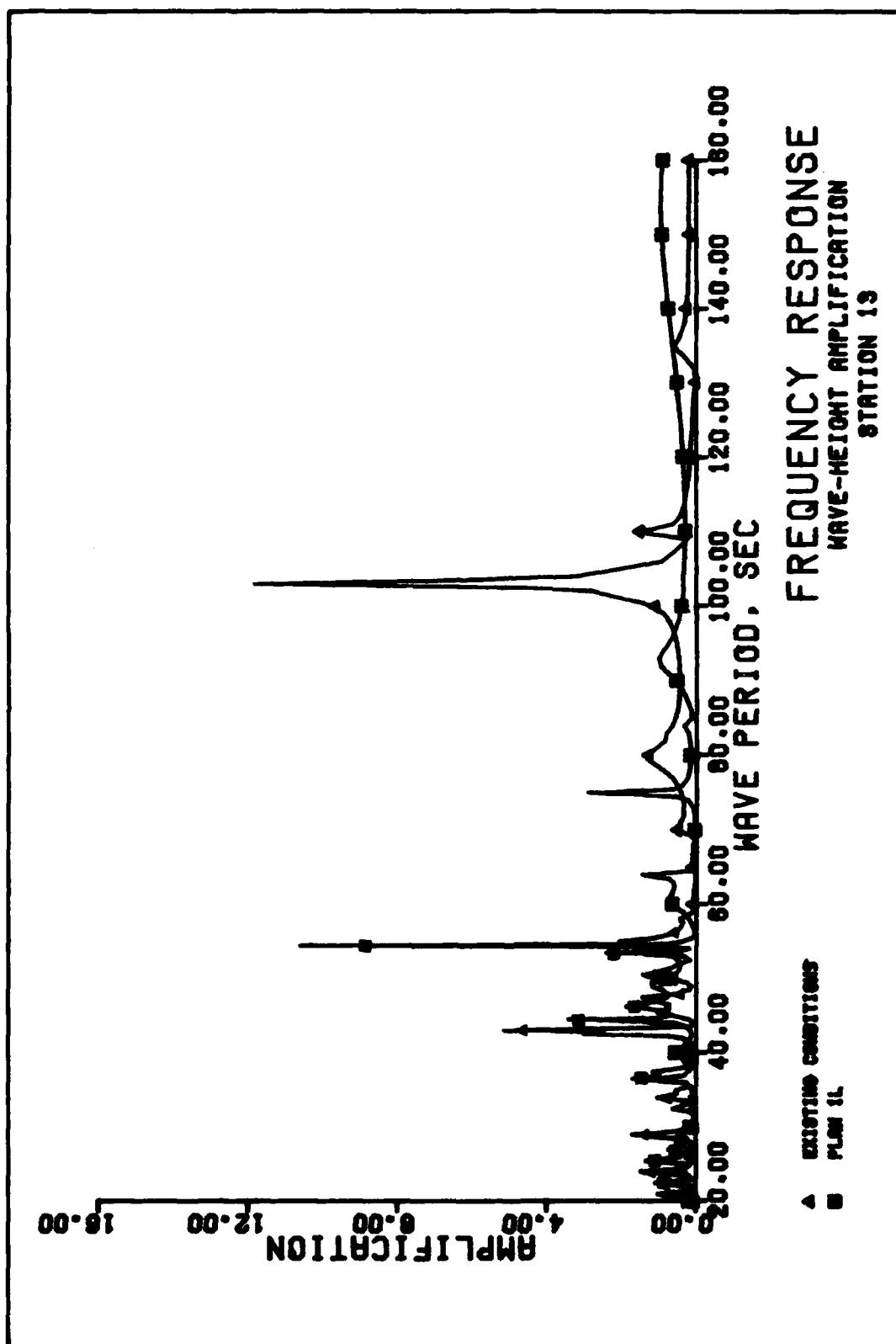


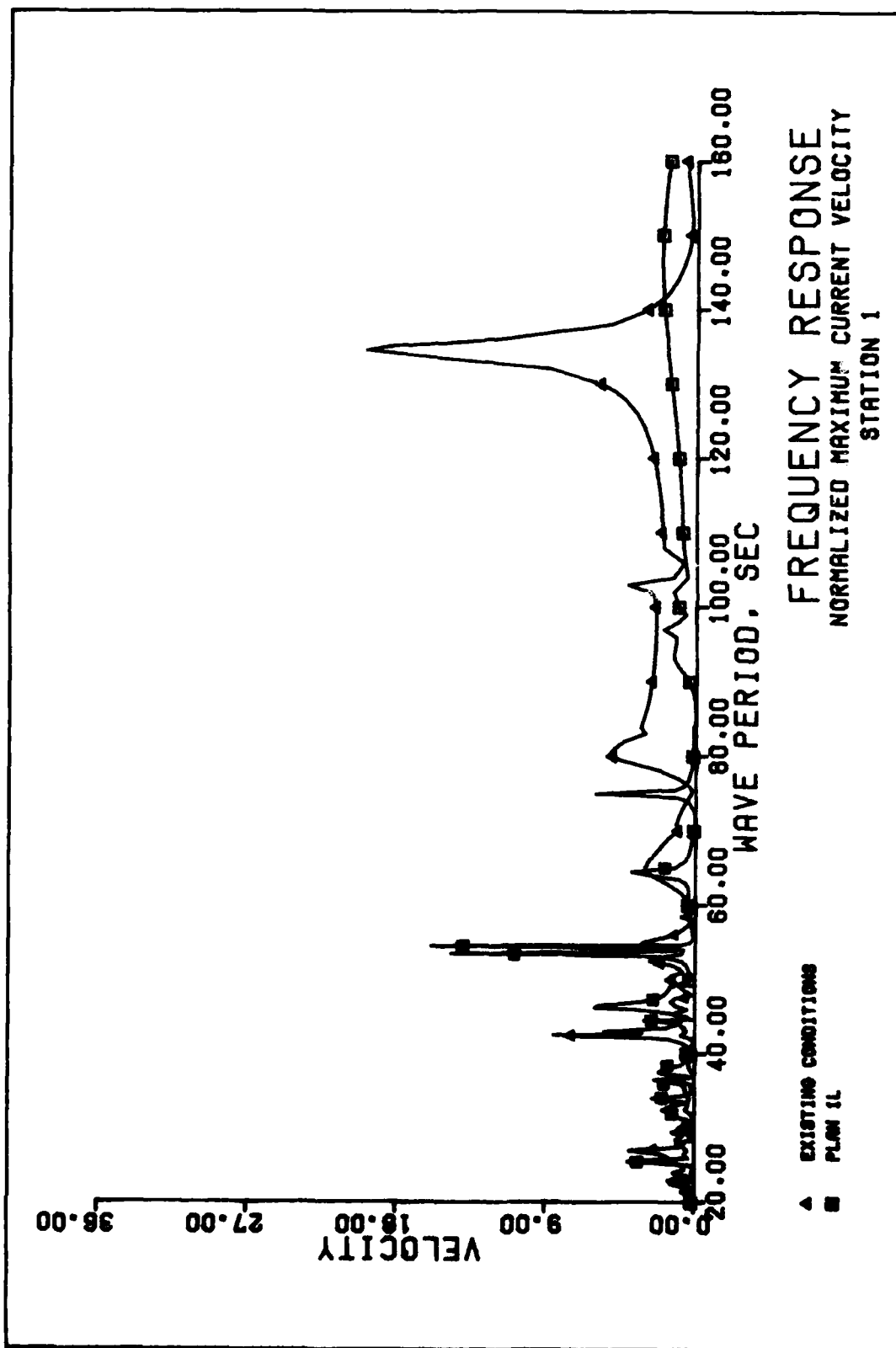


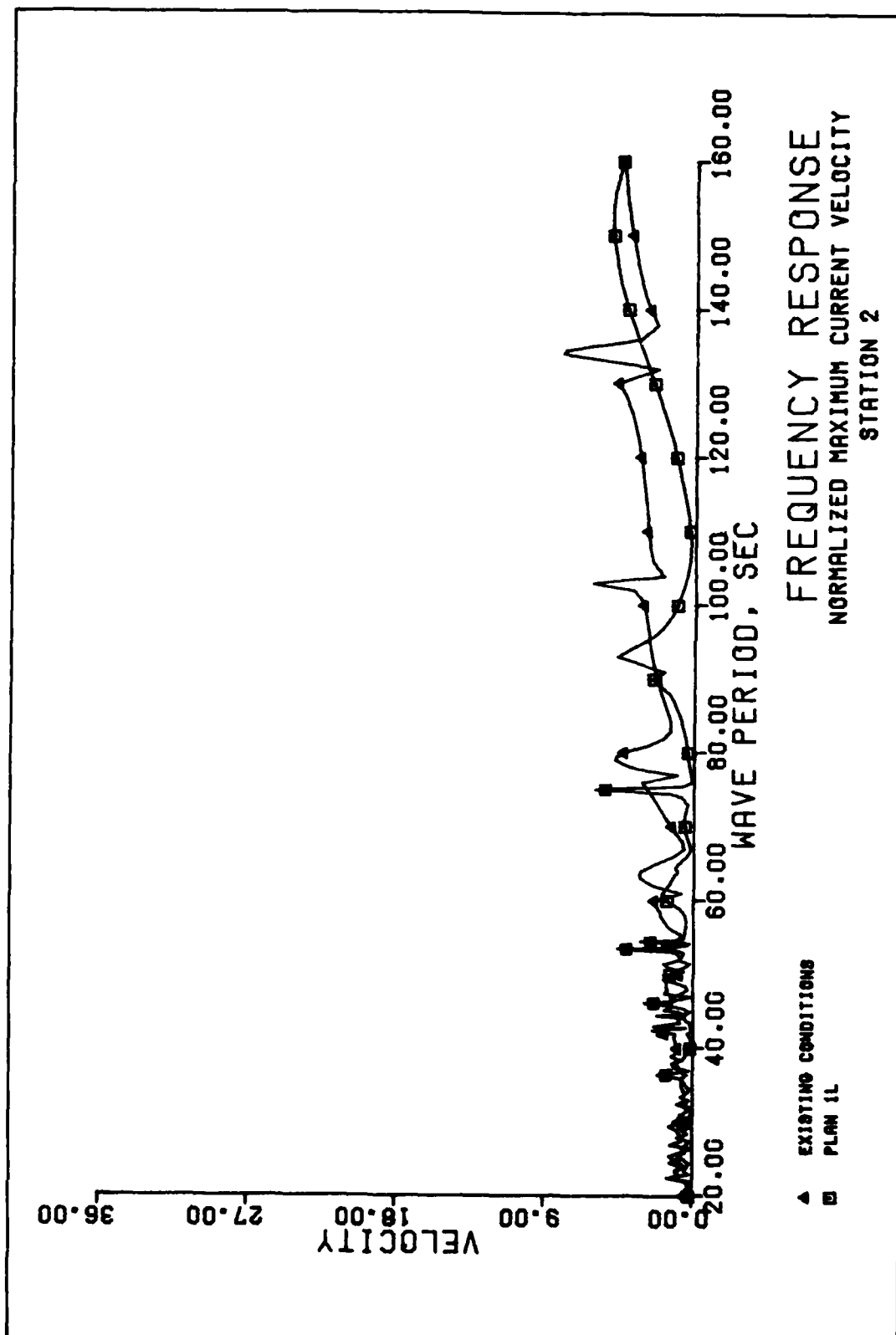


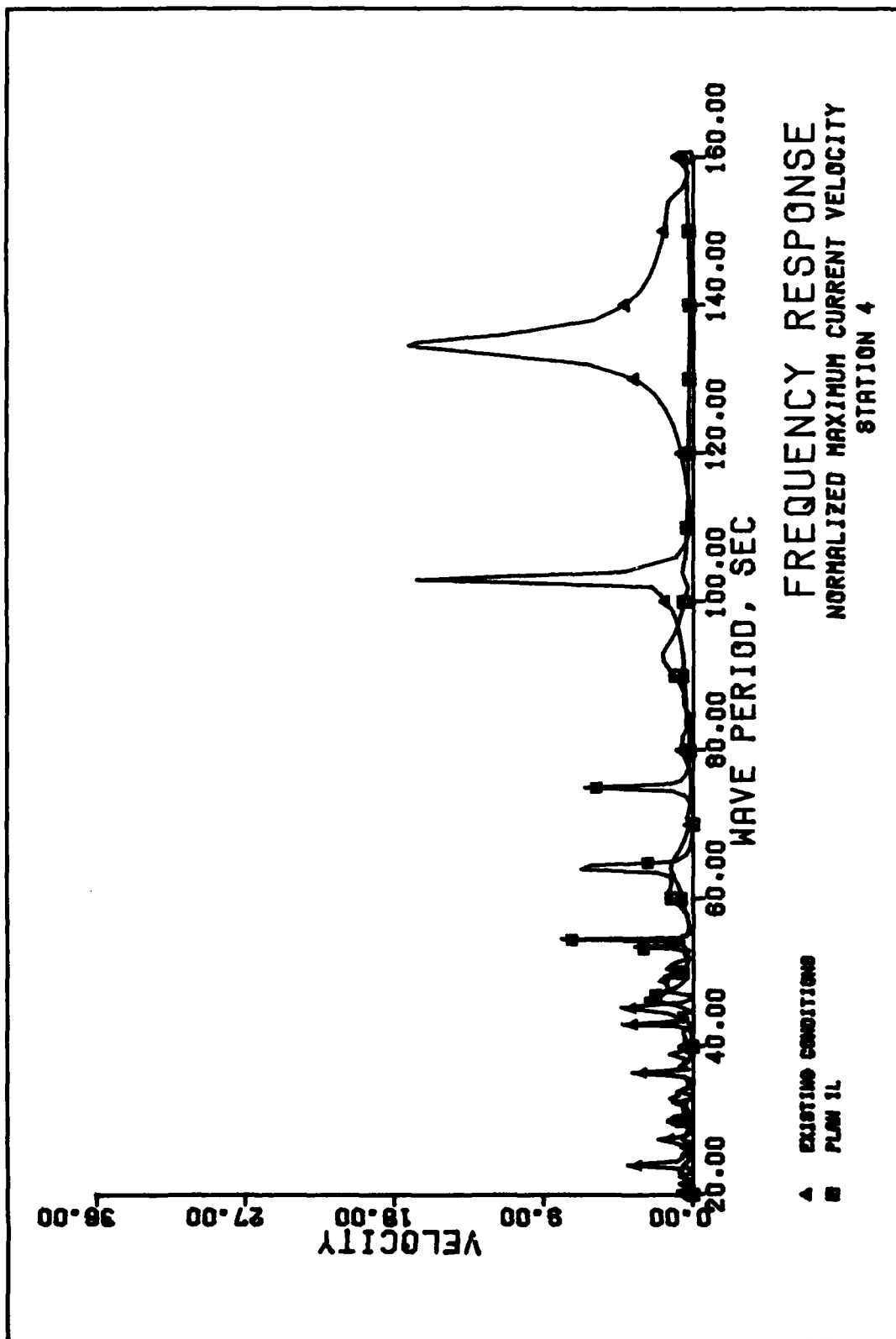


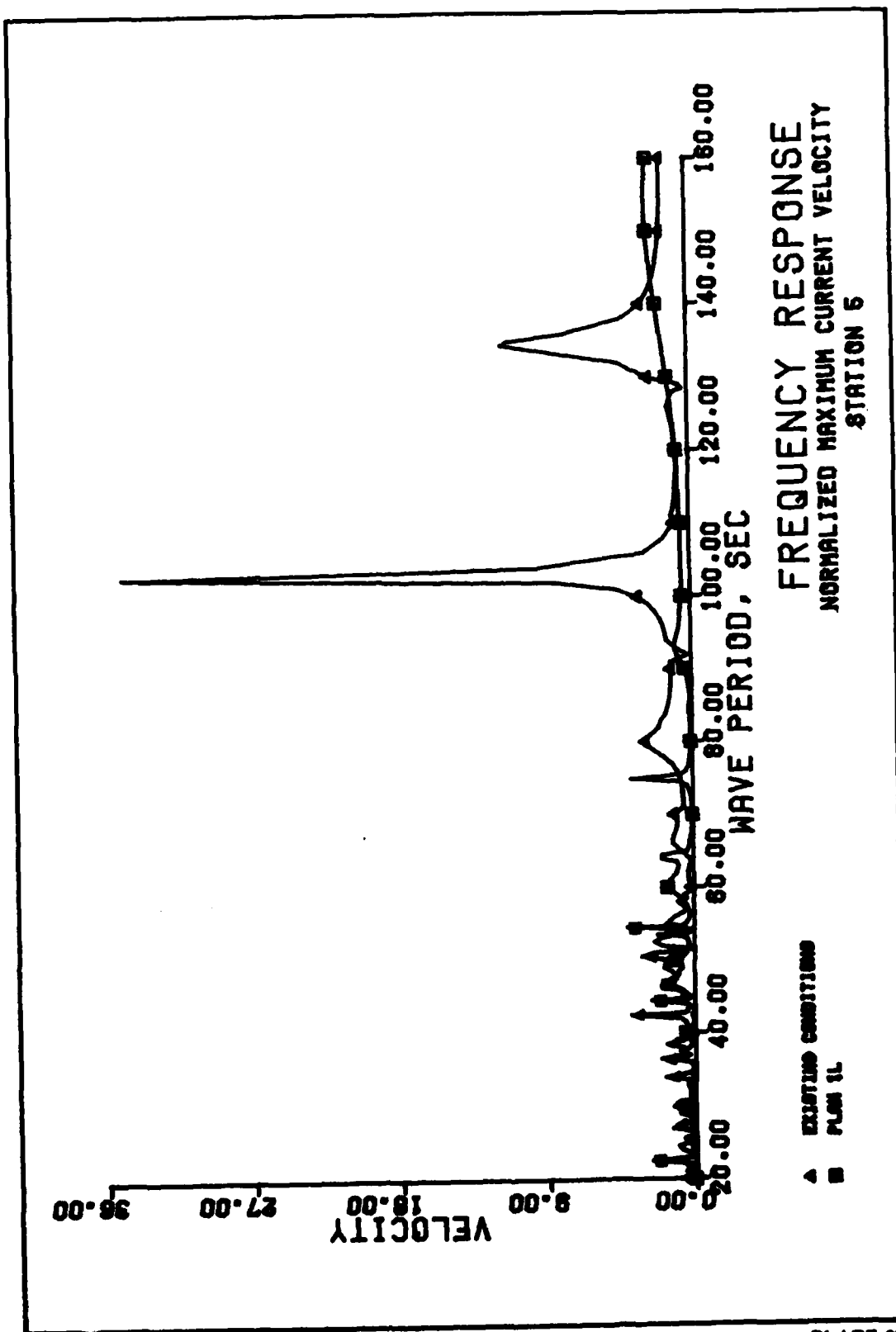


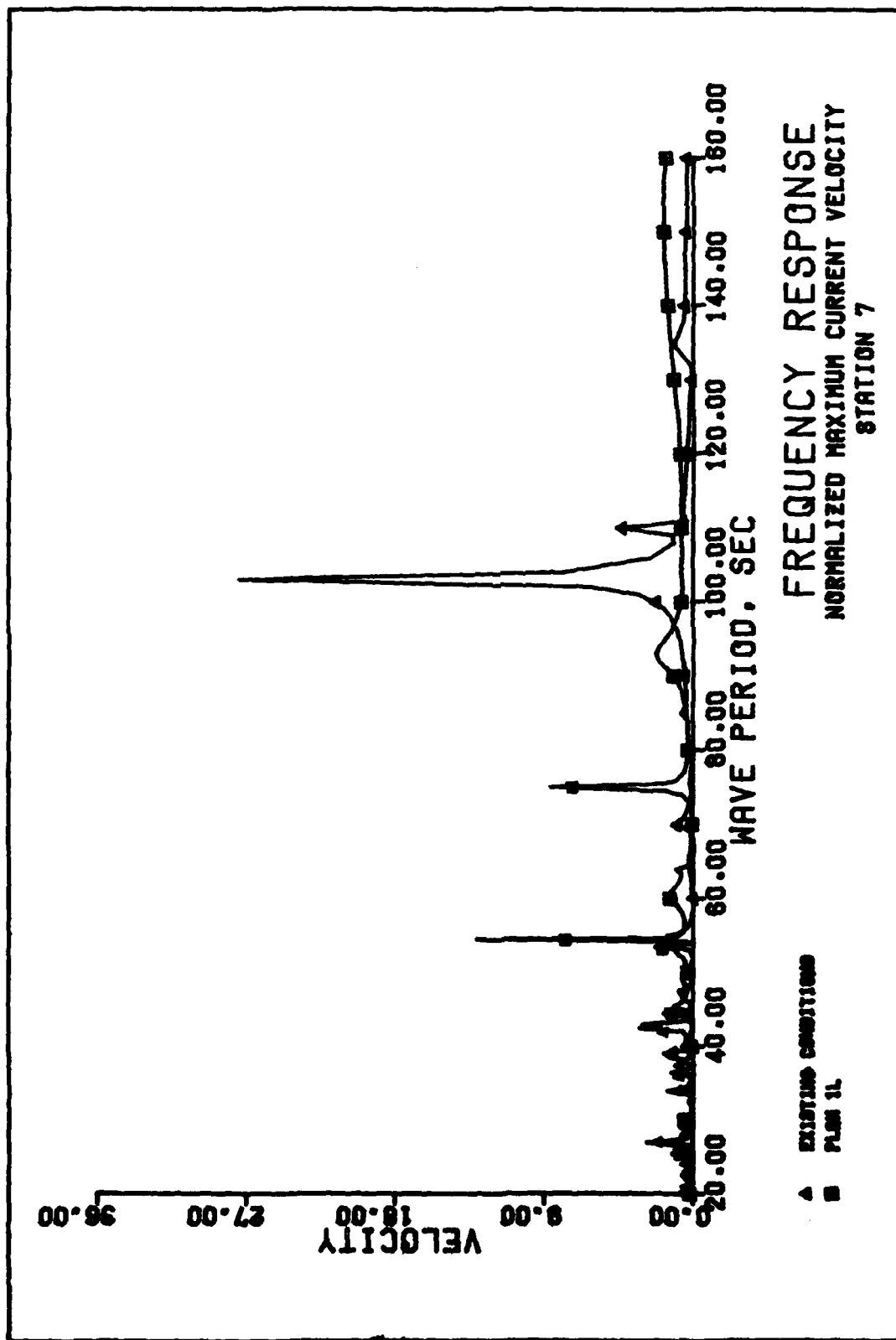


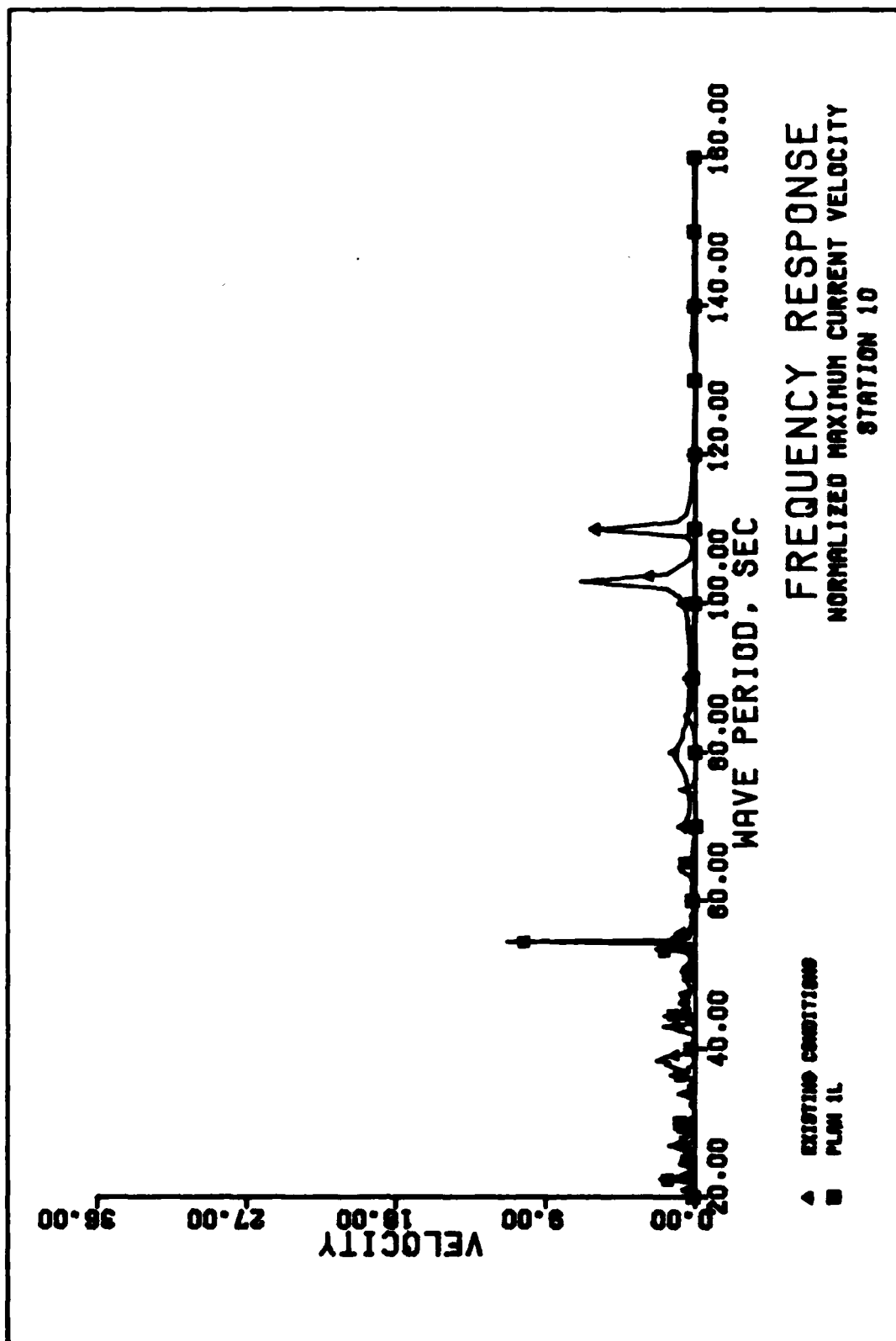


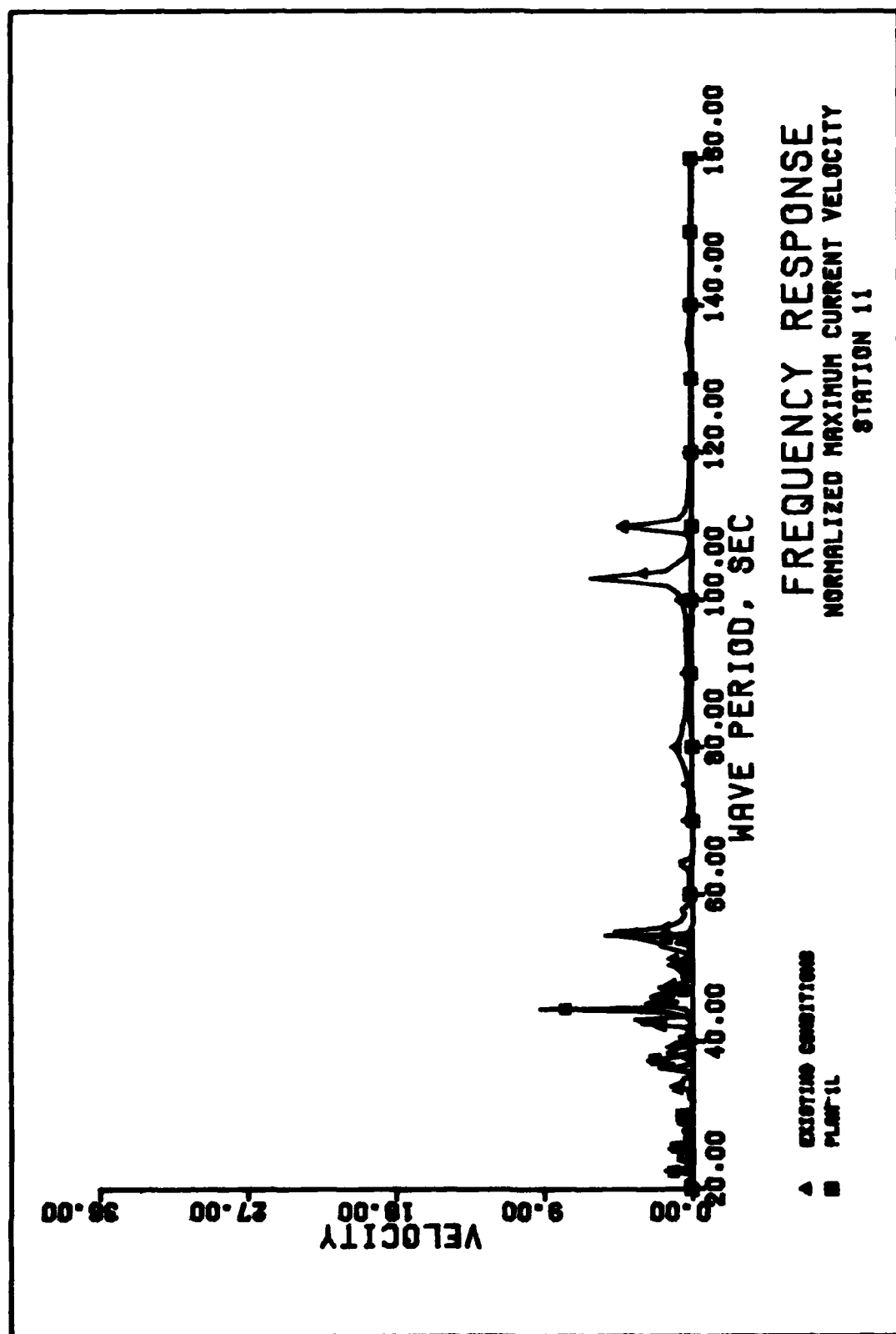


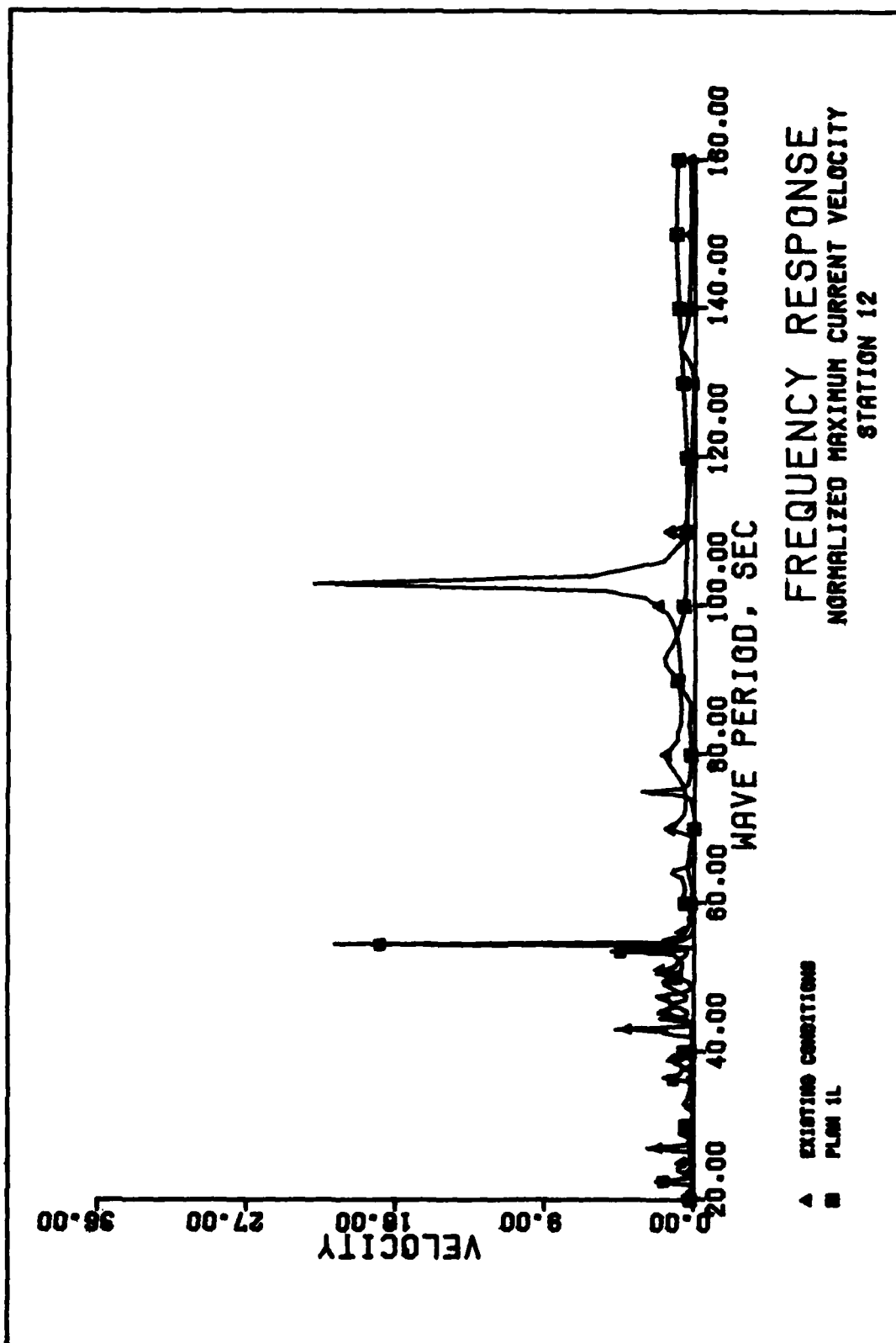












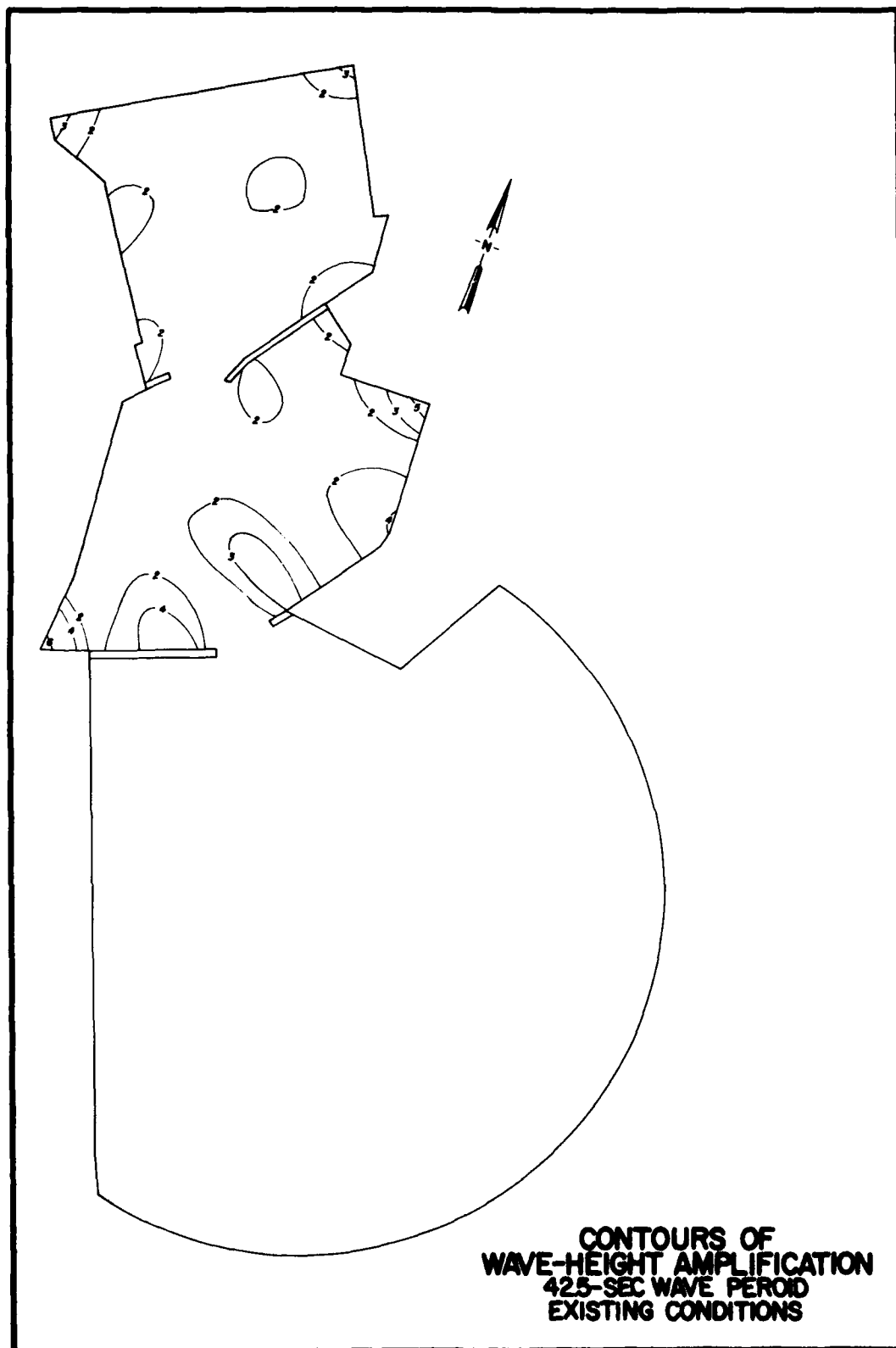
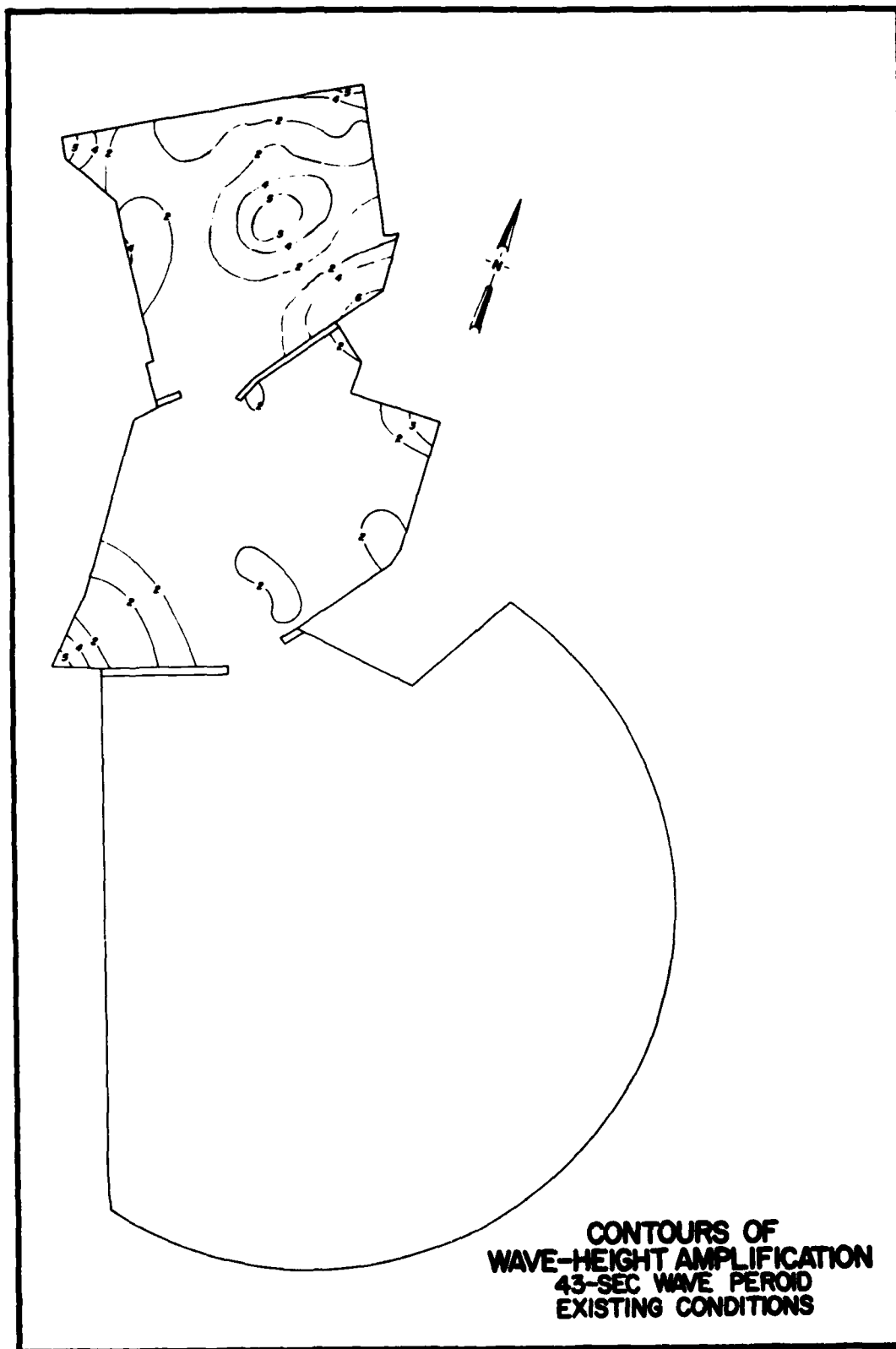
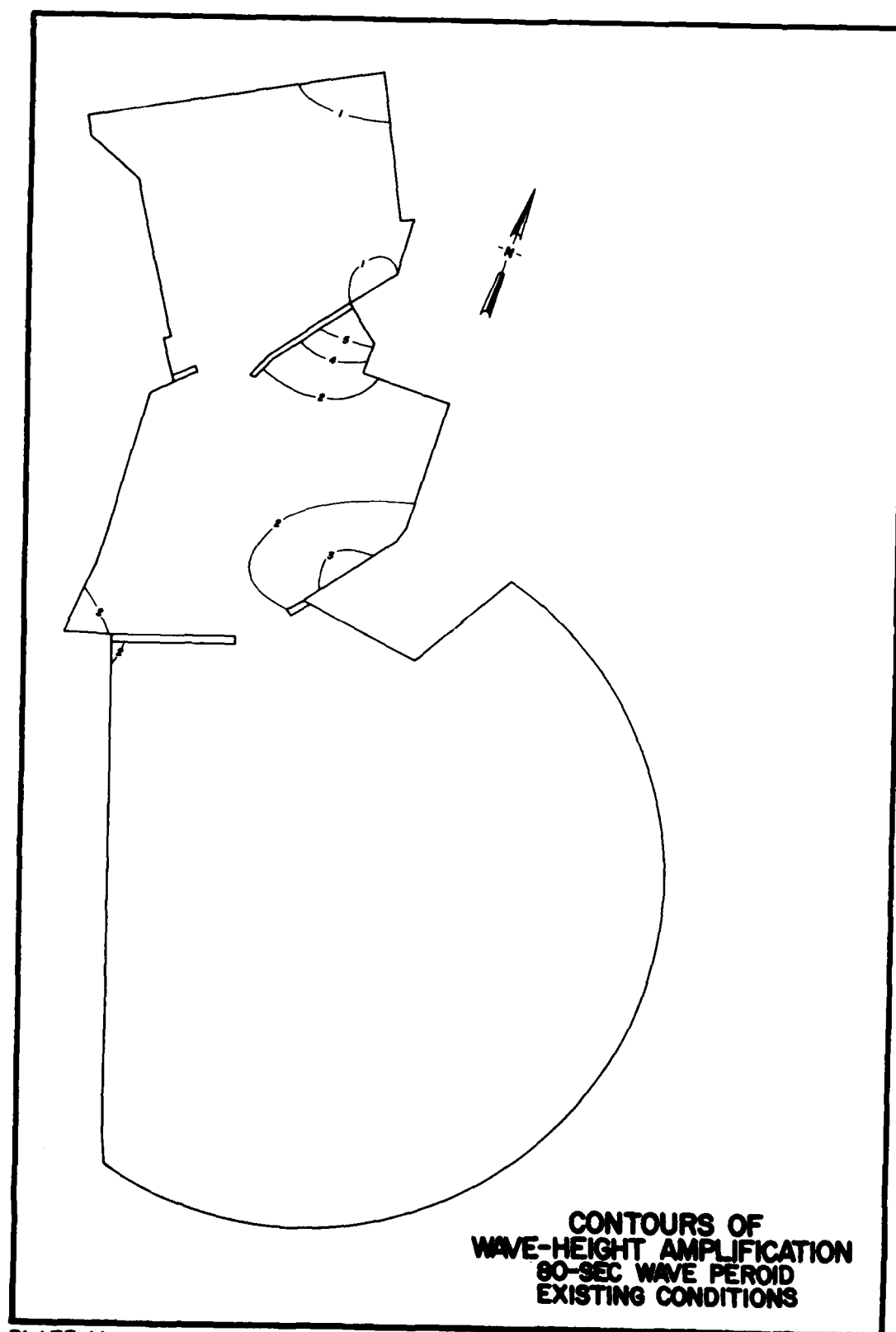
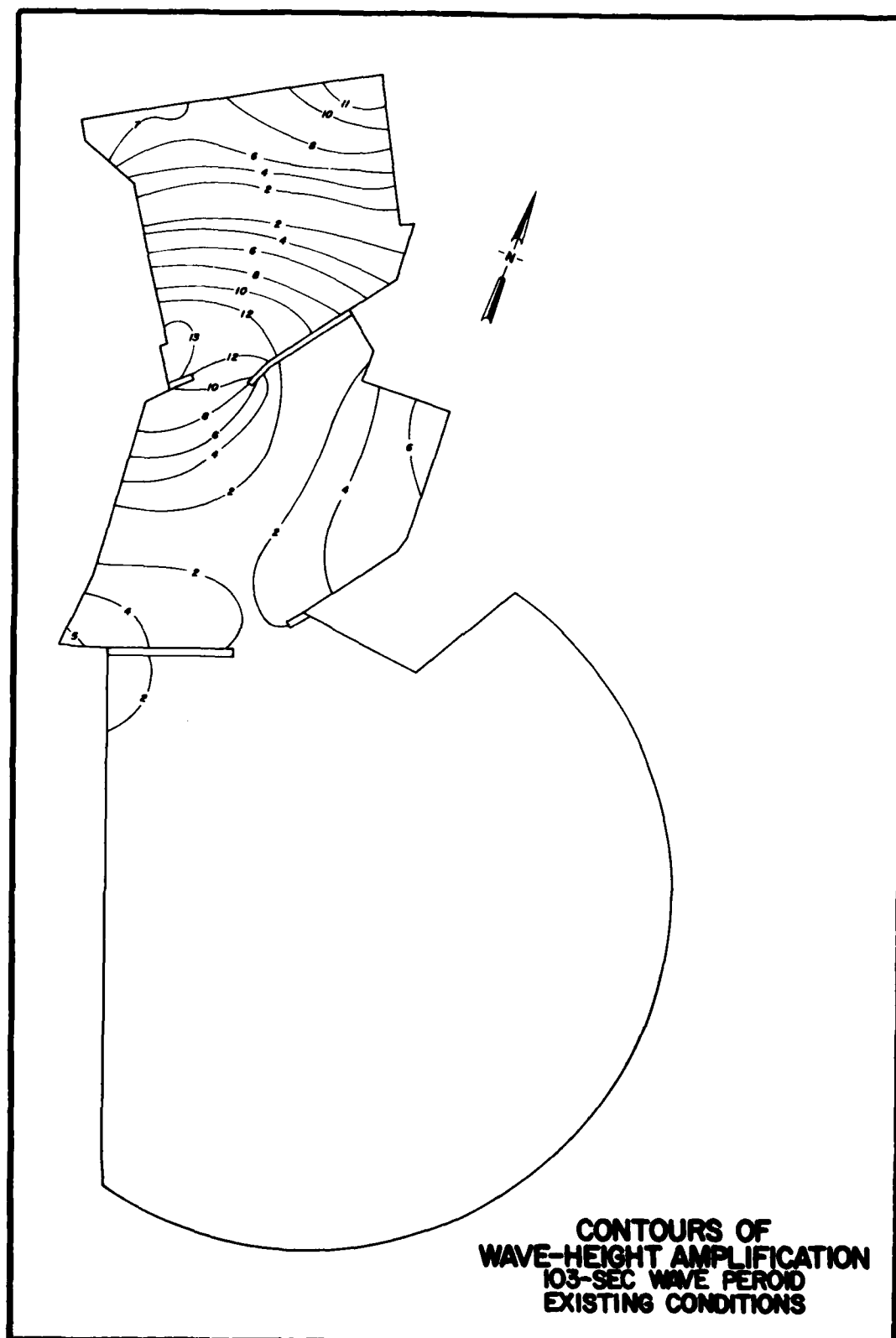
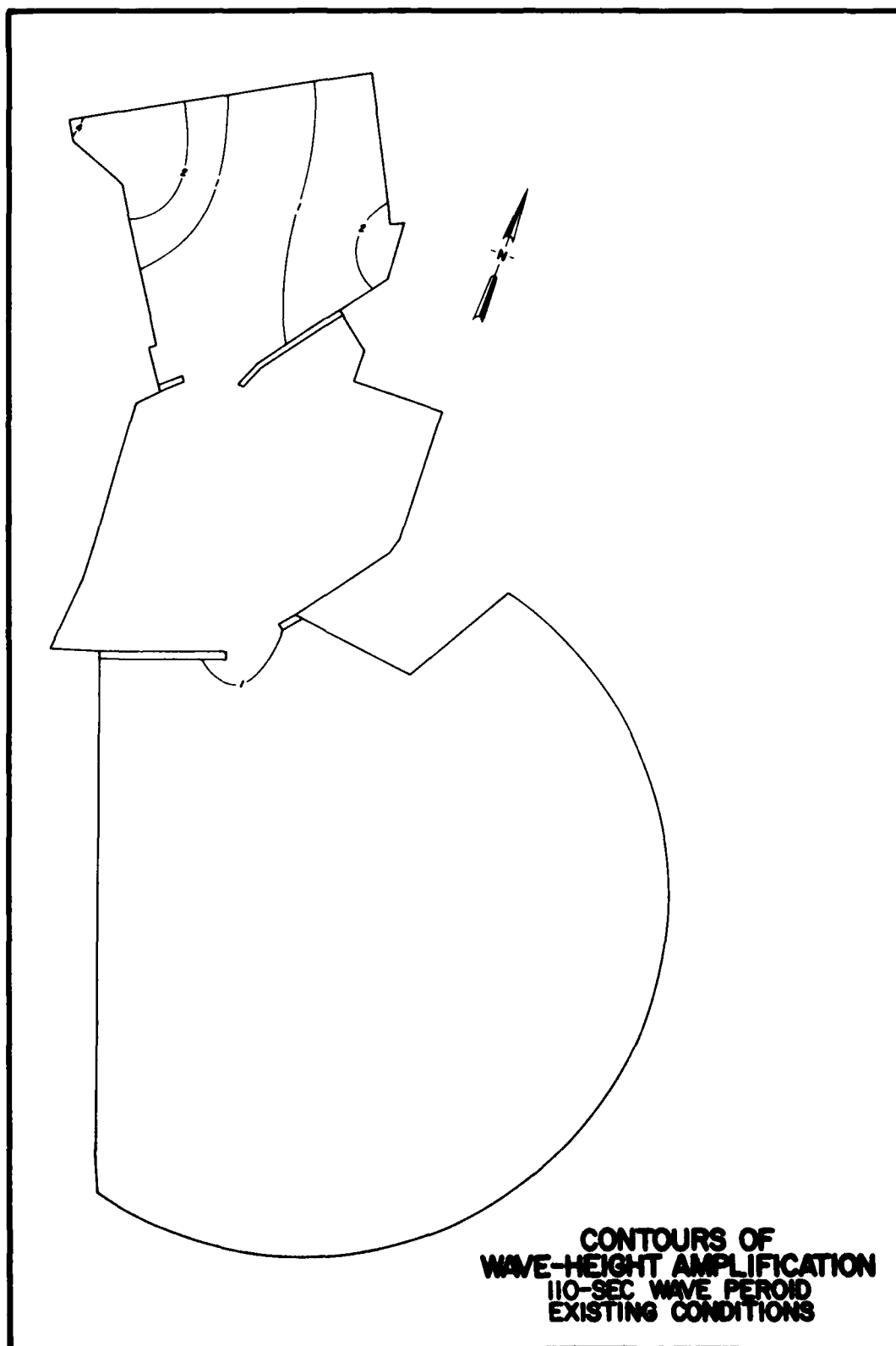


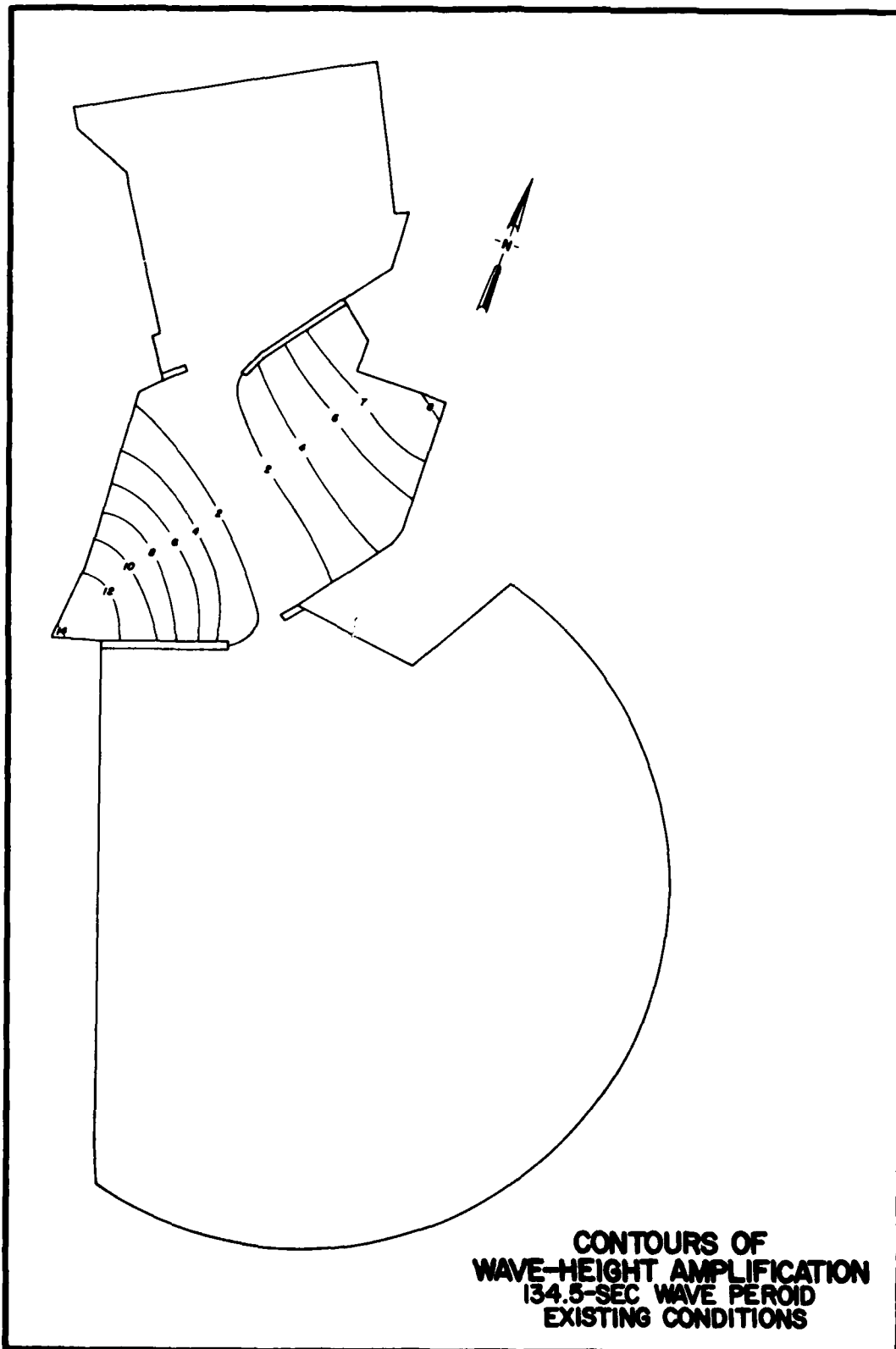
PLATE 42

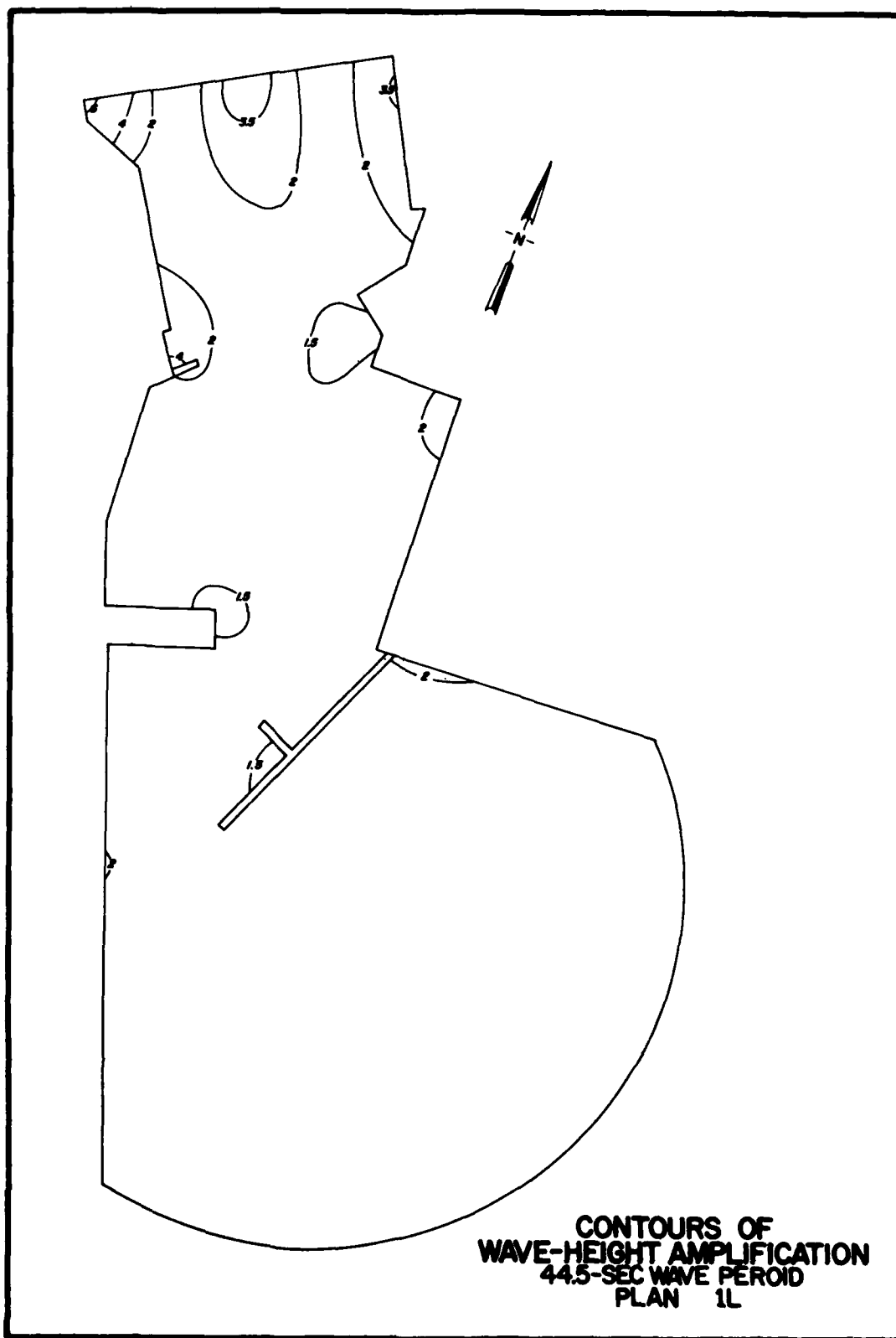


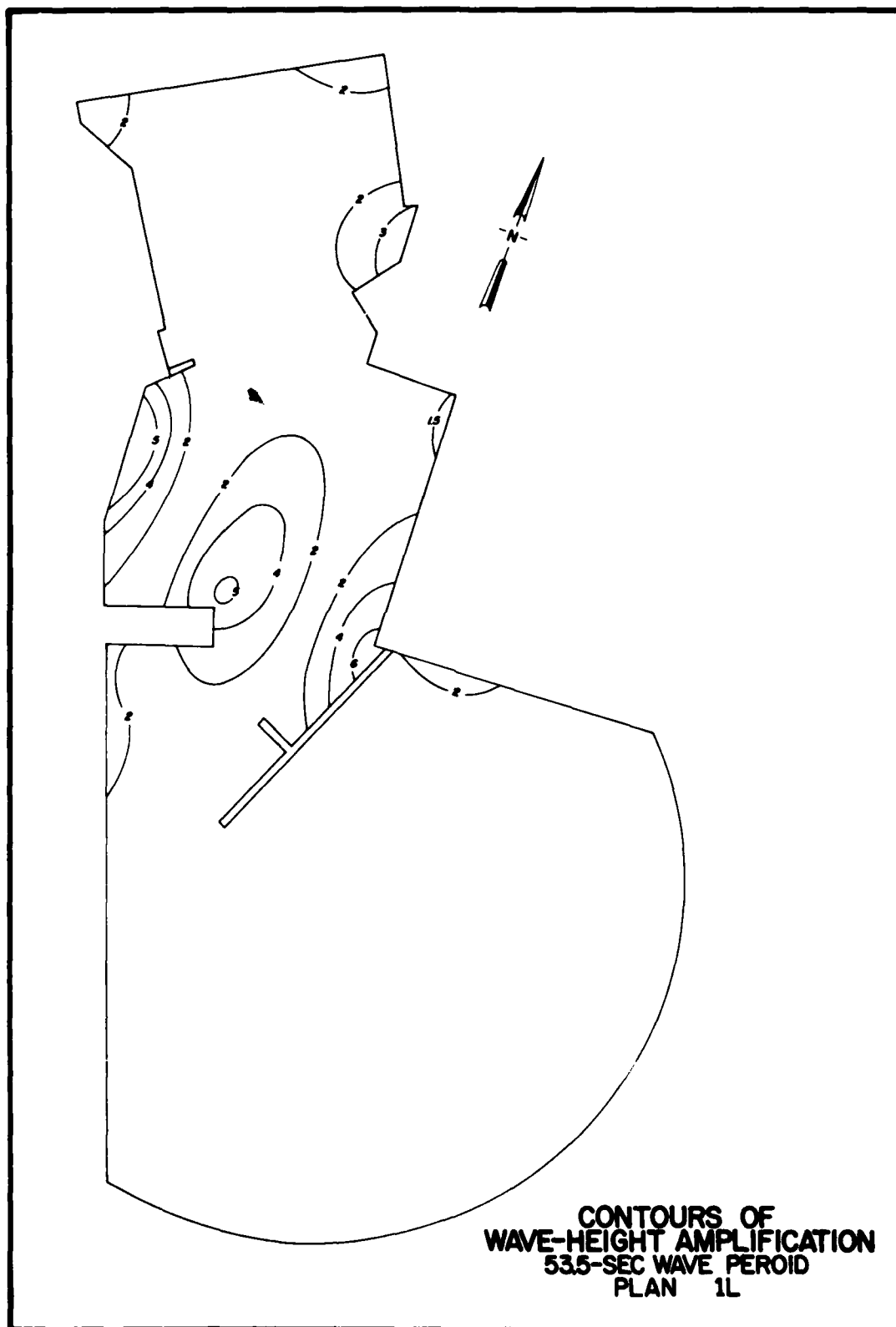


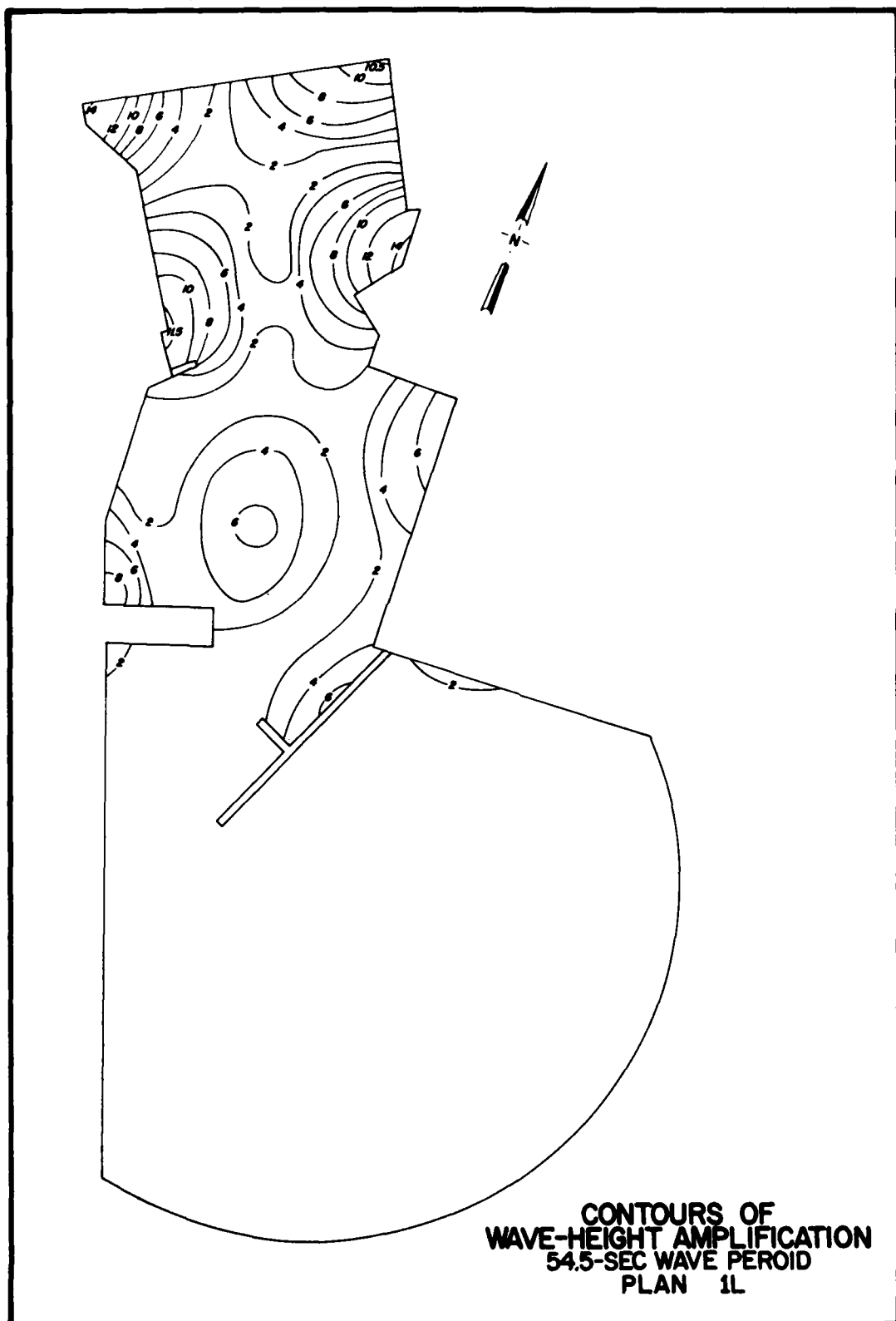


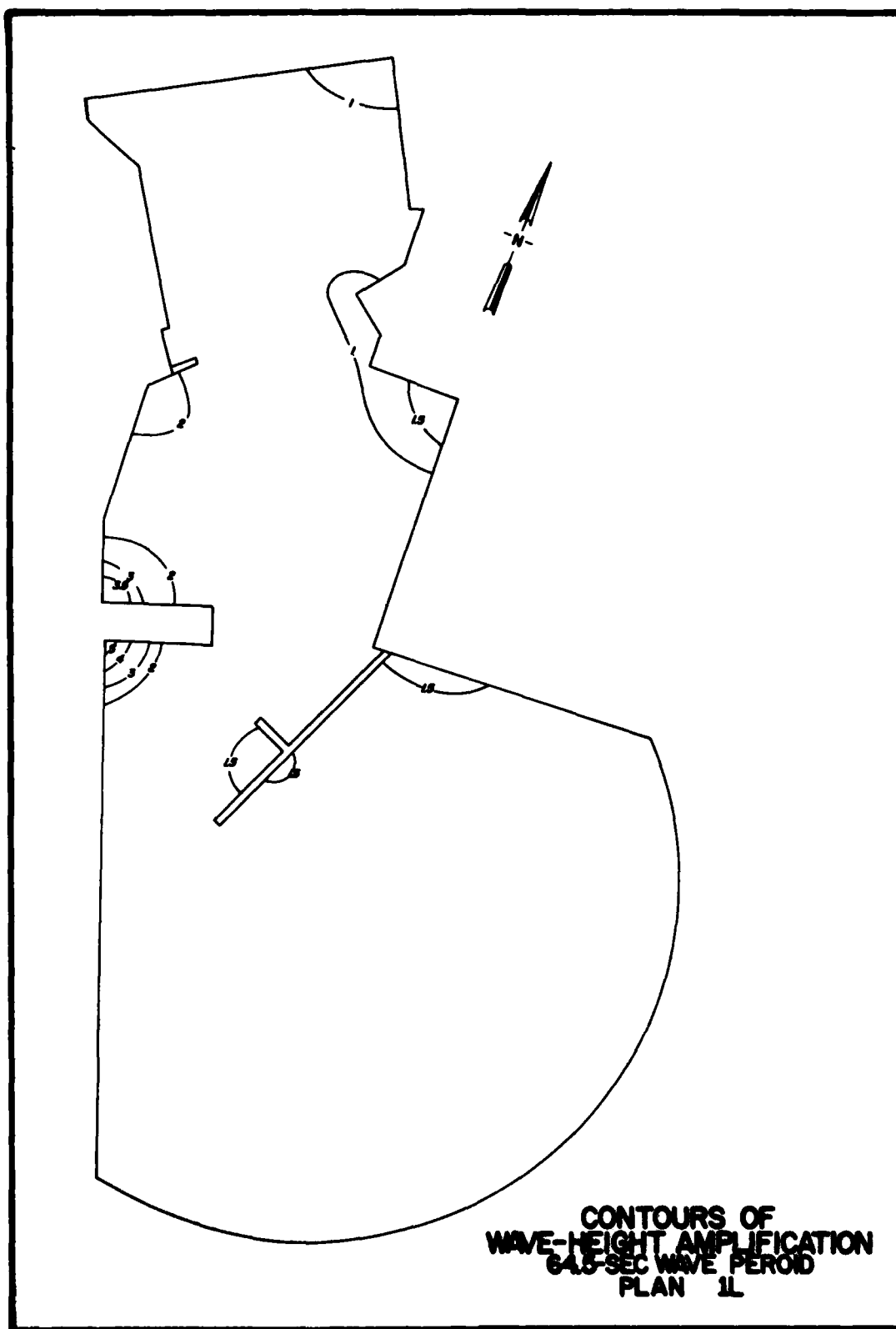


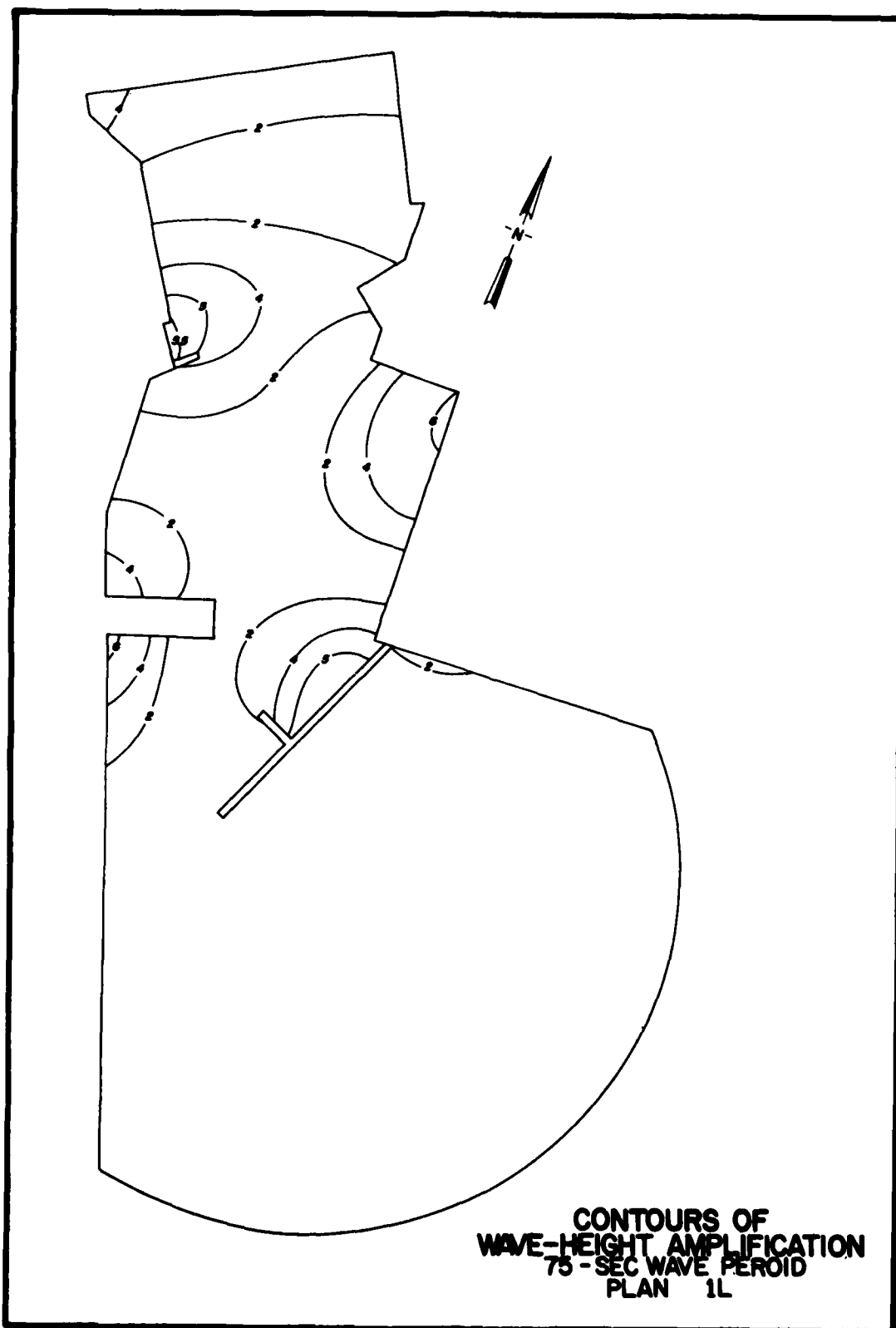


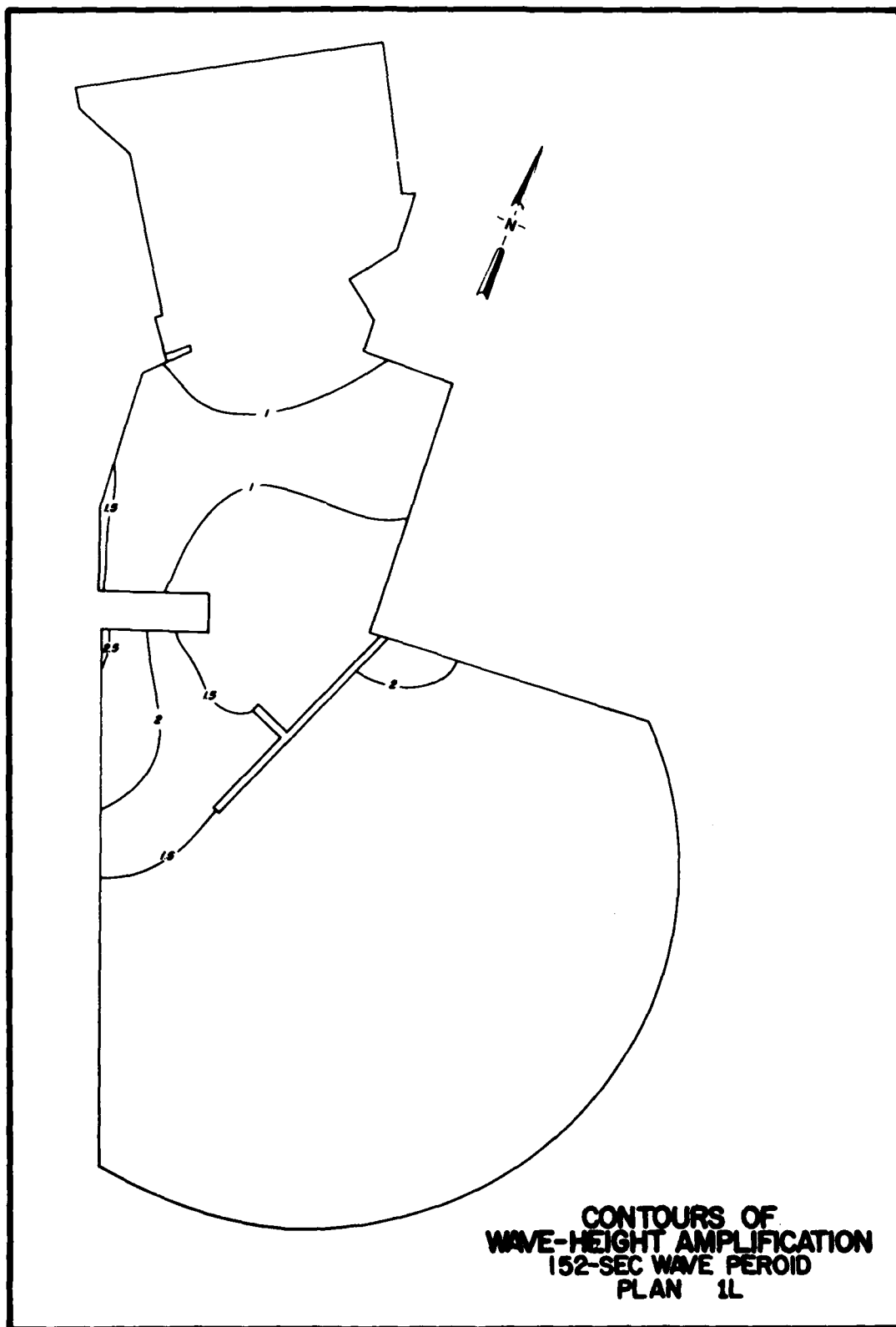


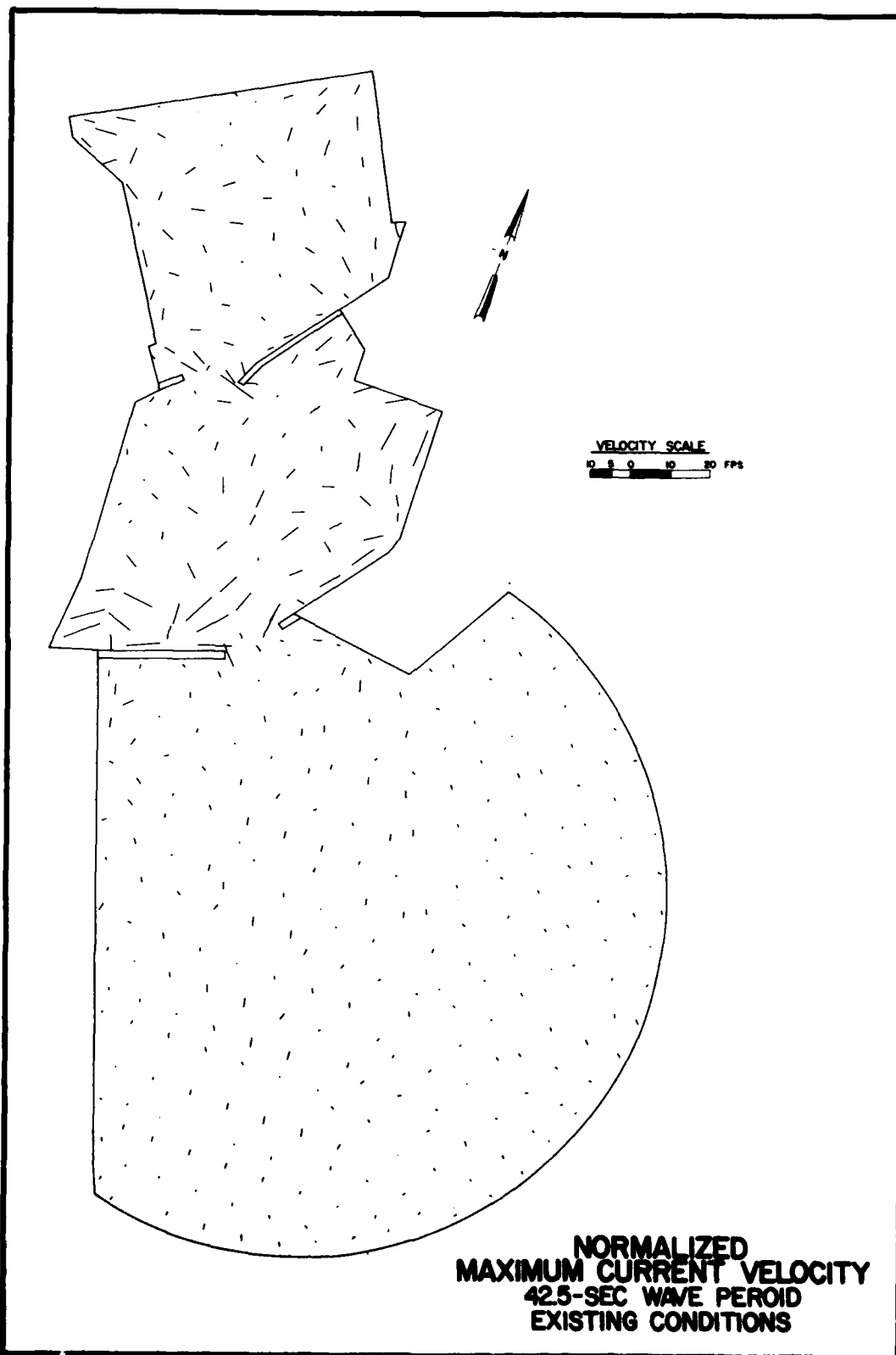


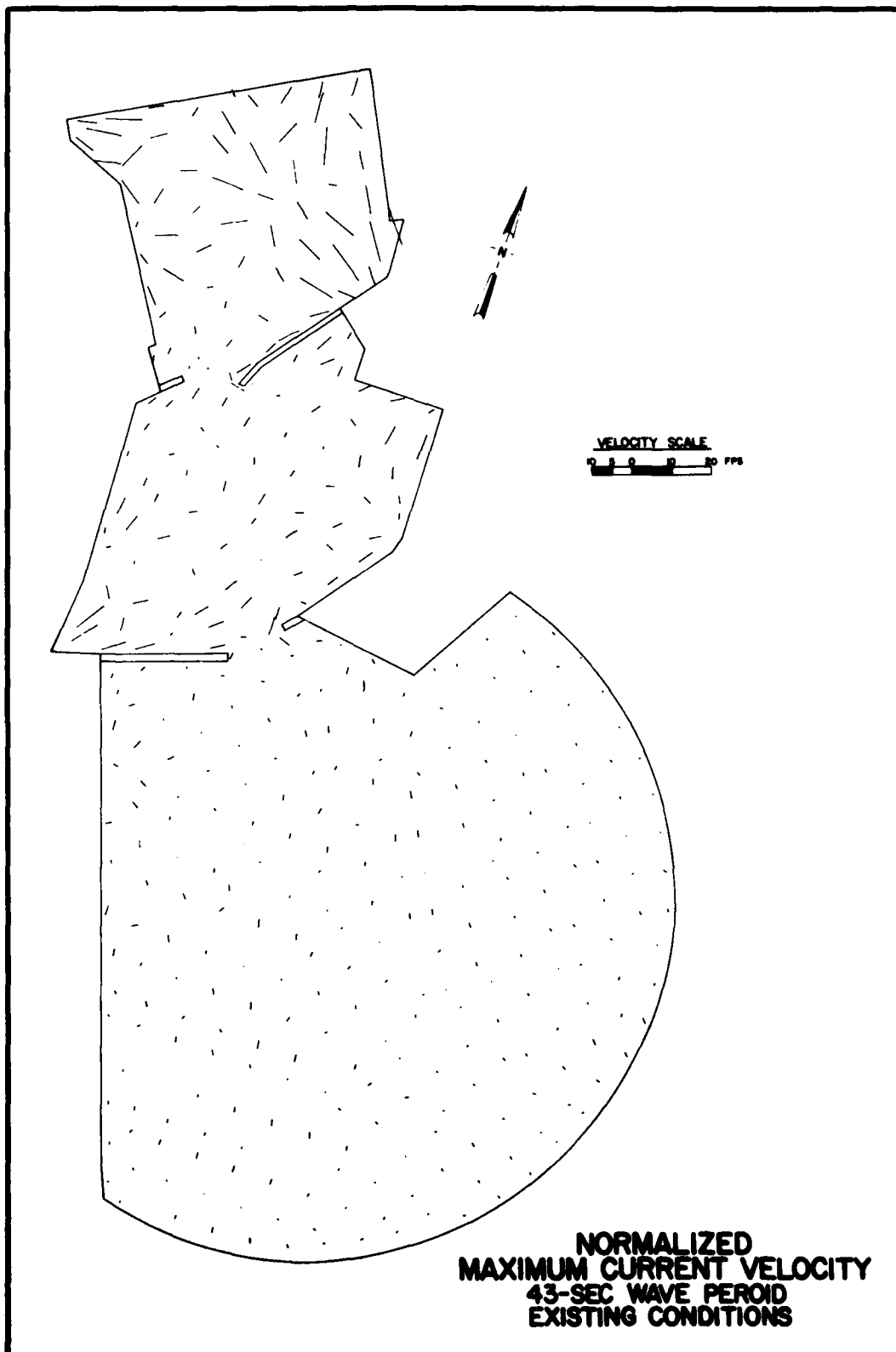












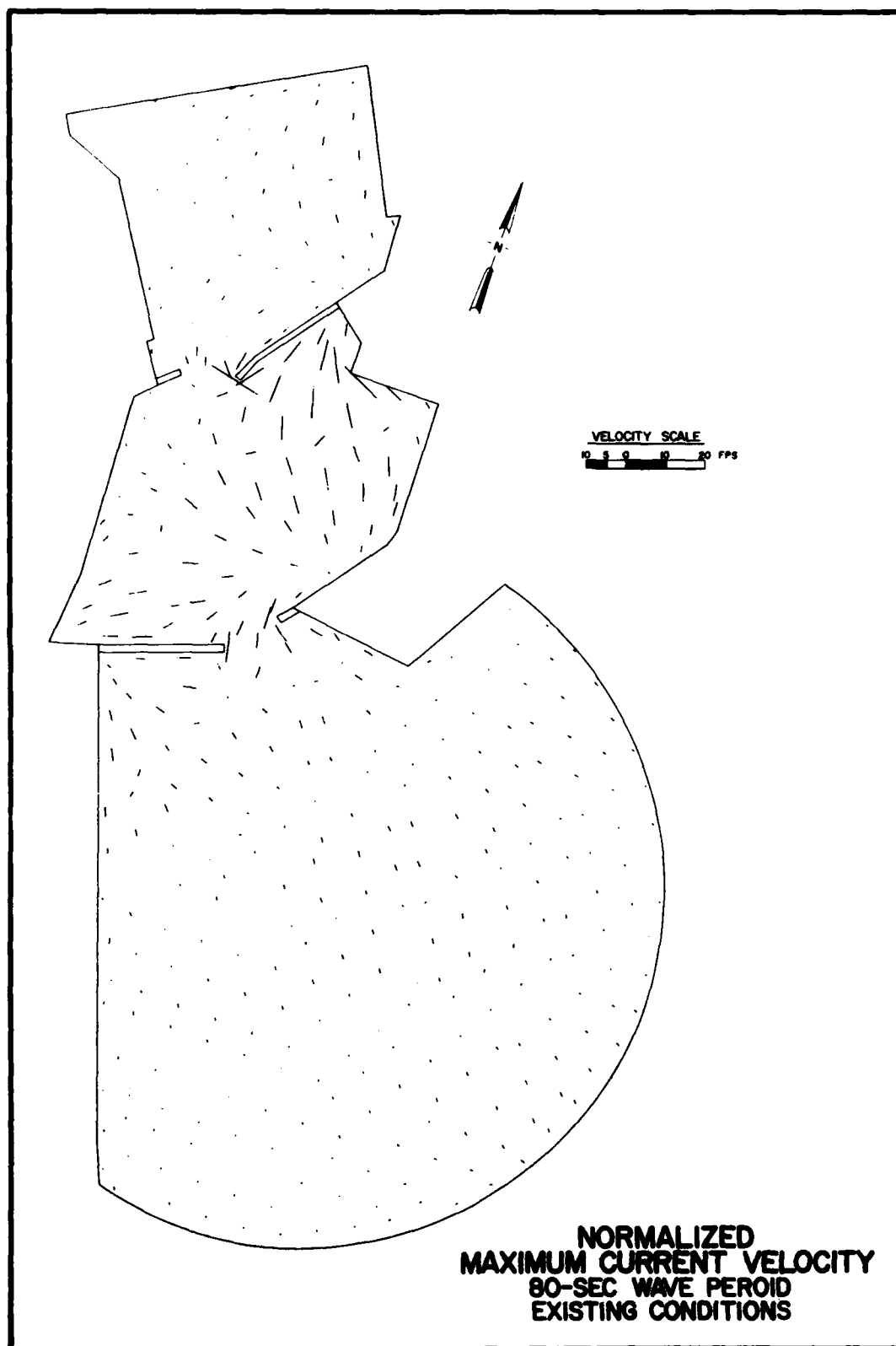
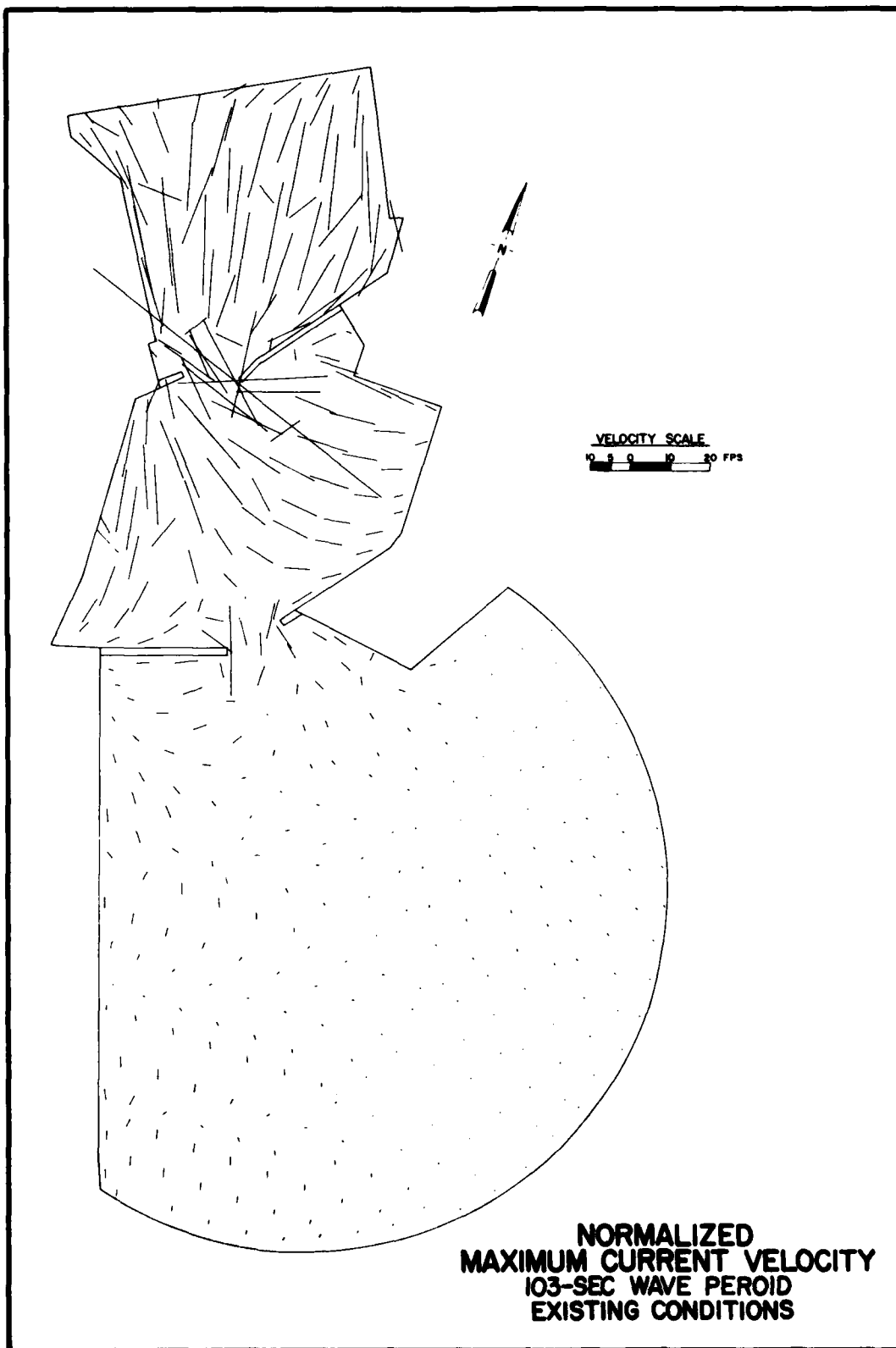
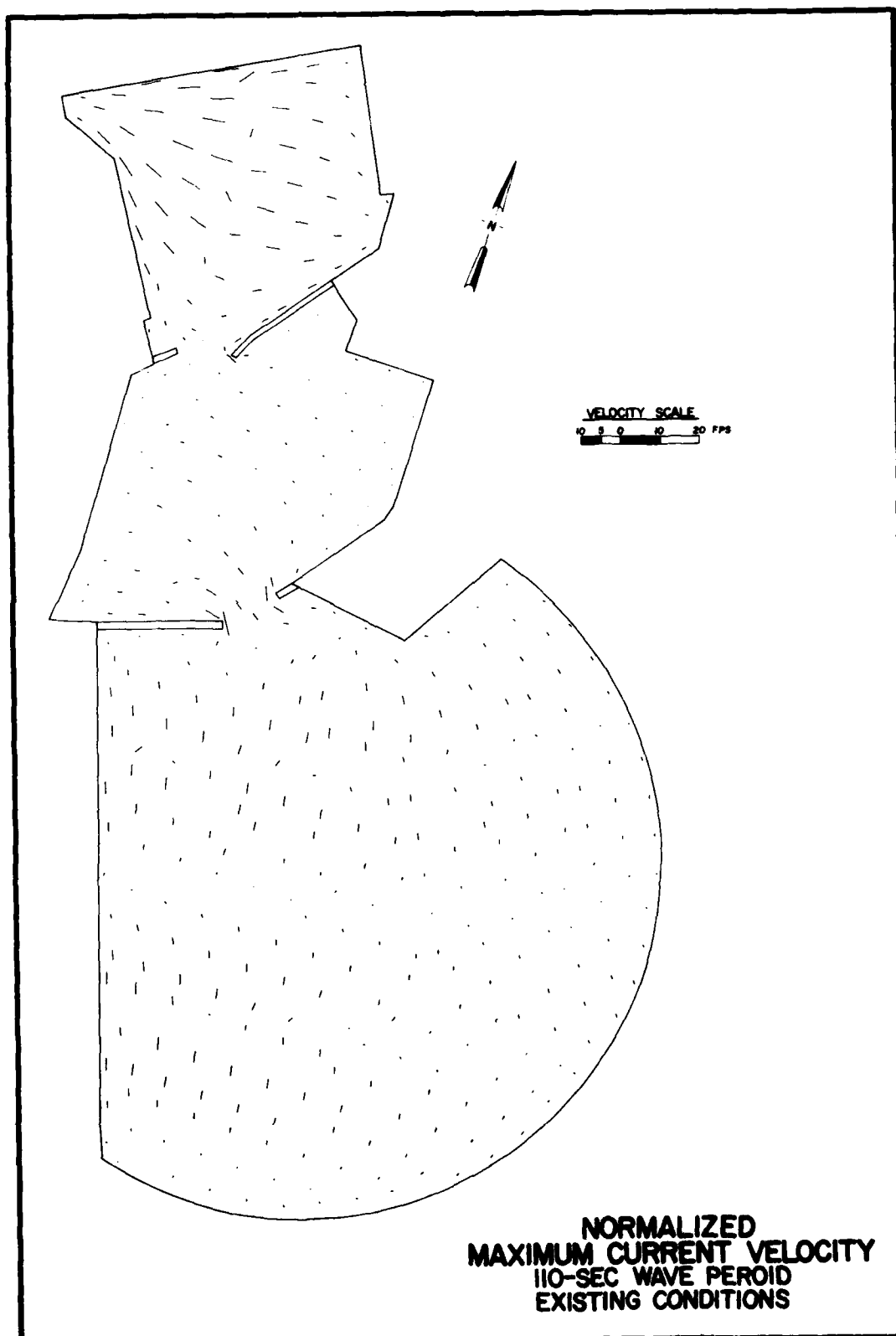
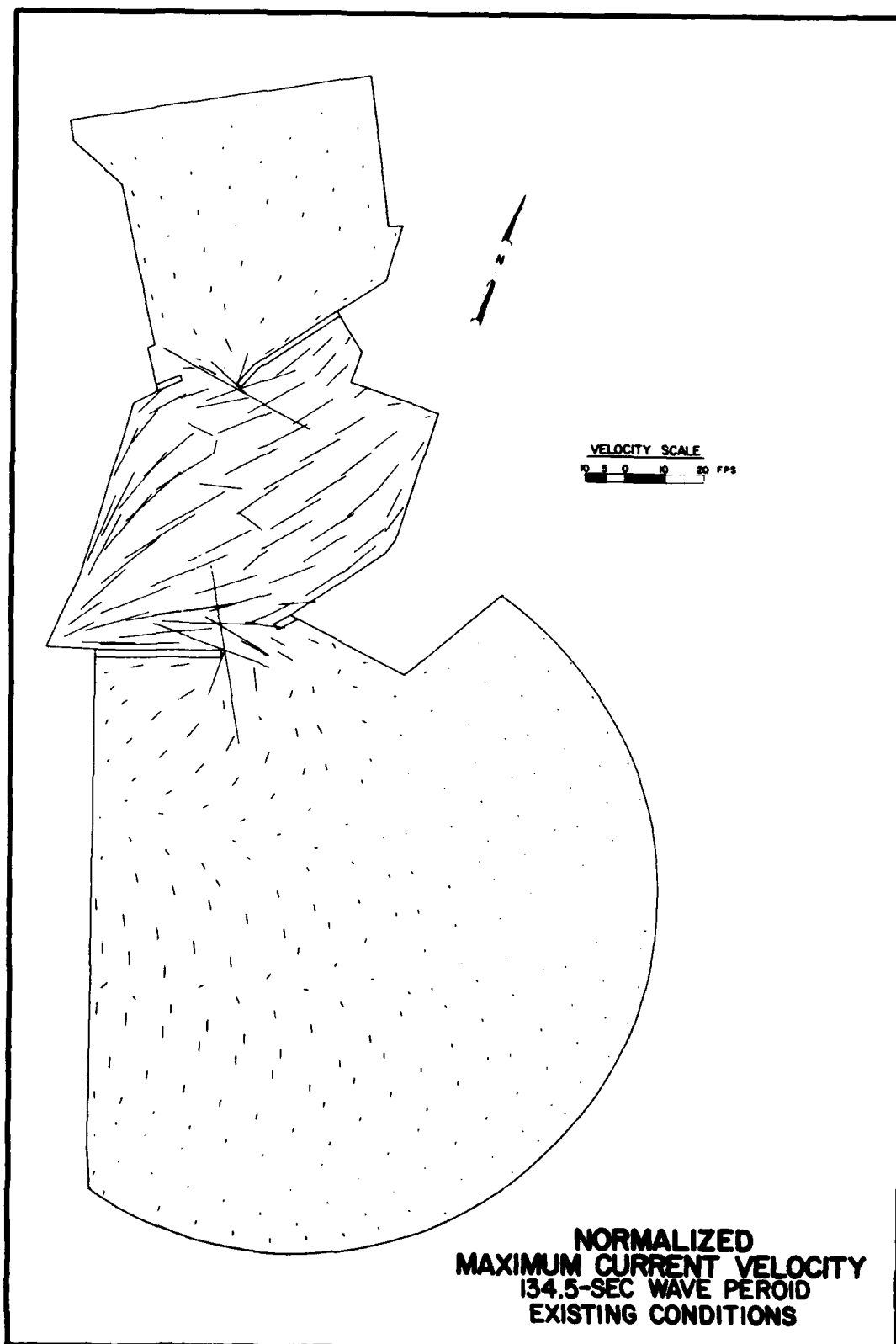
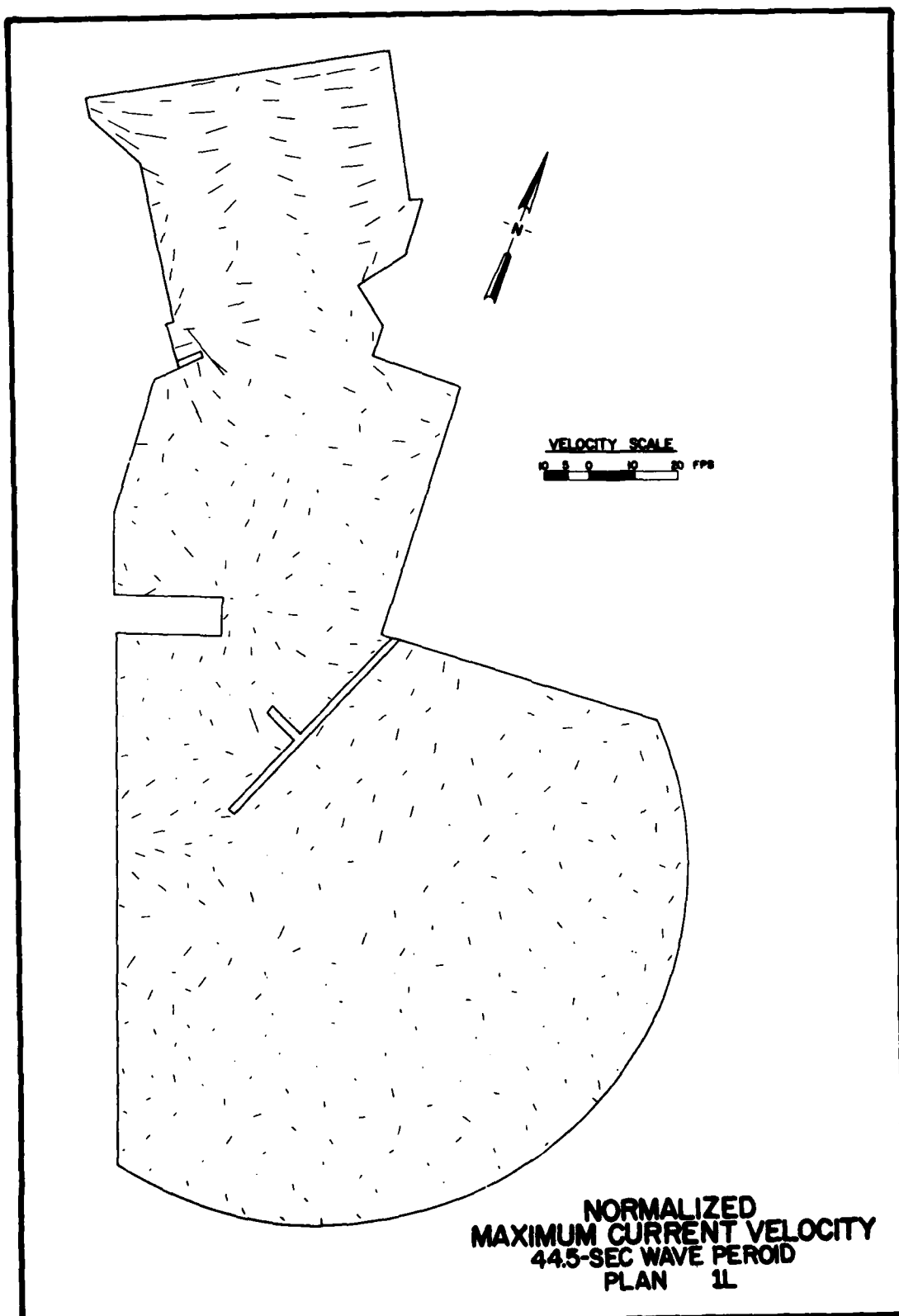


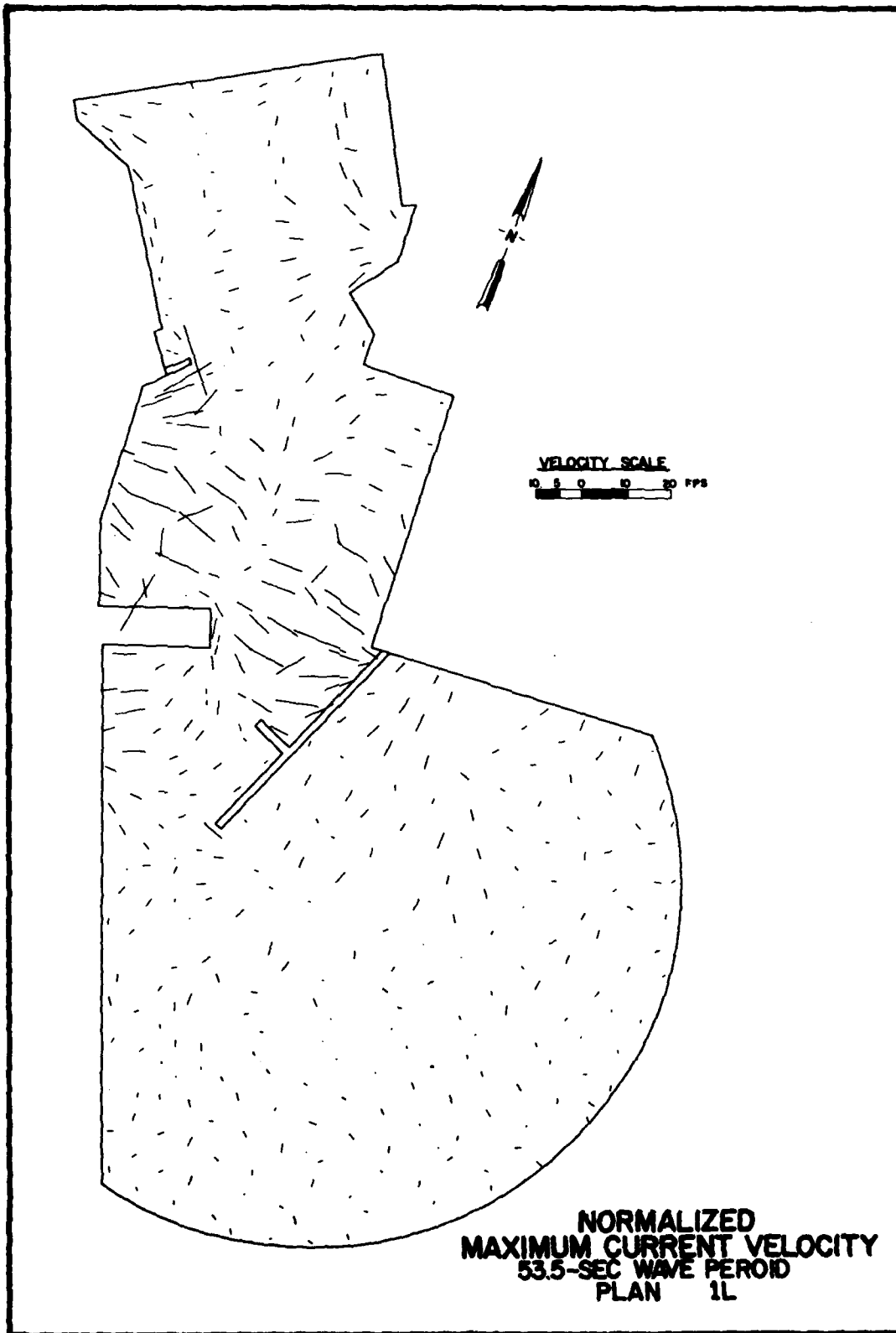
PLATE 56











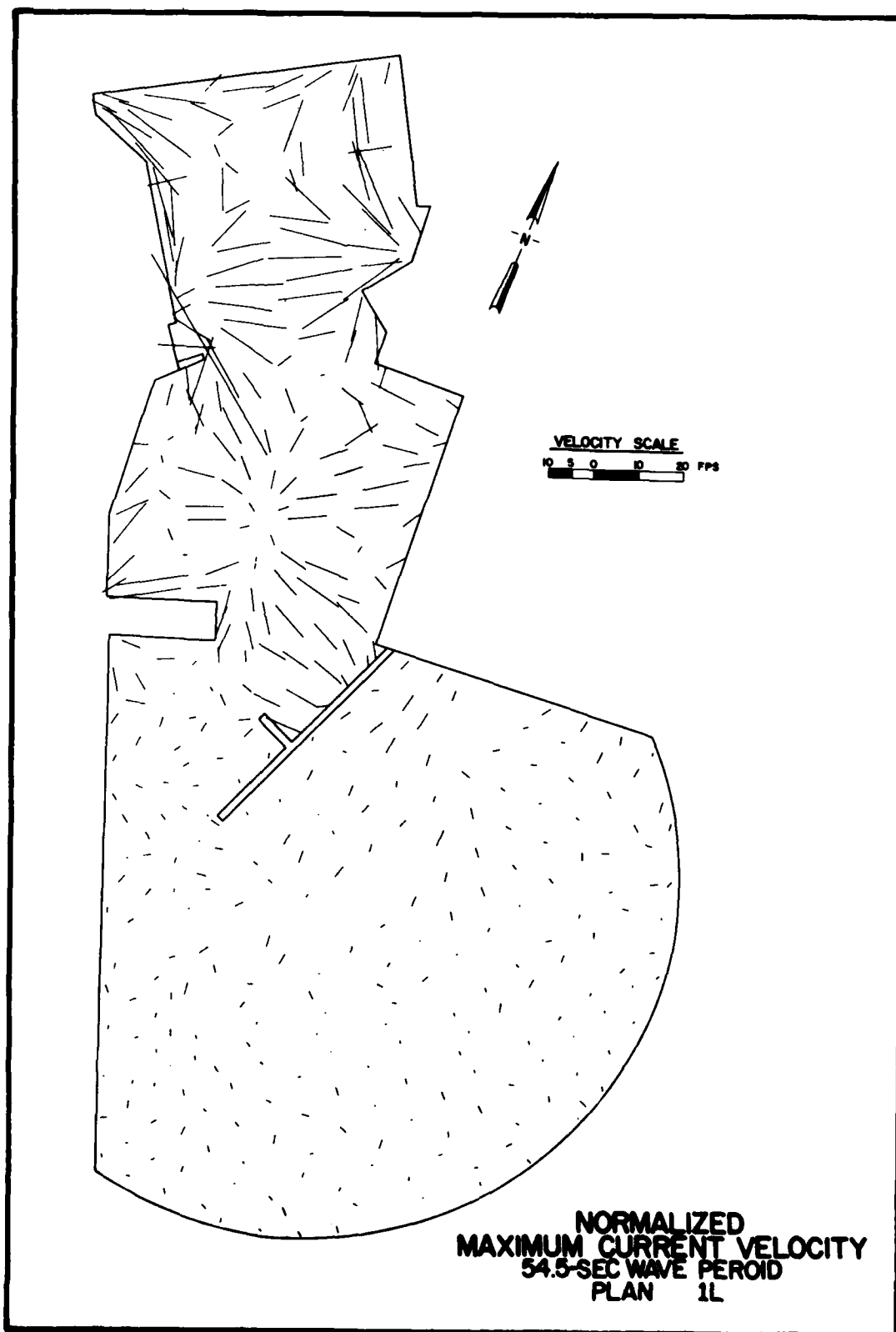
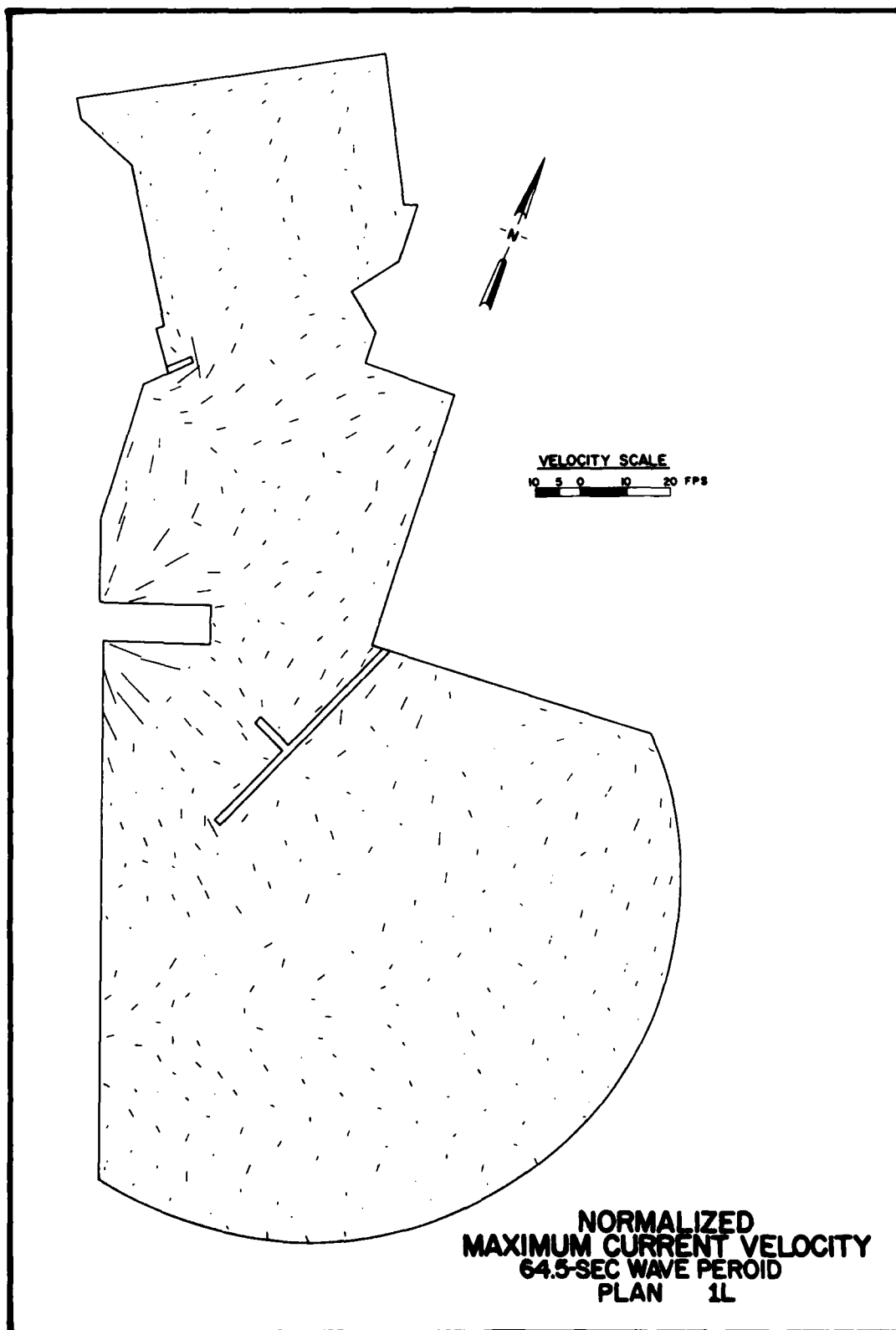
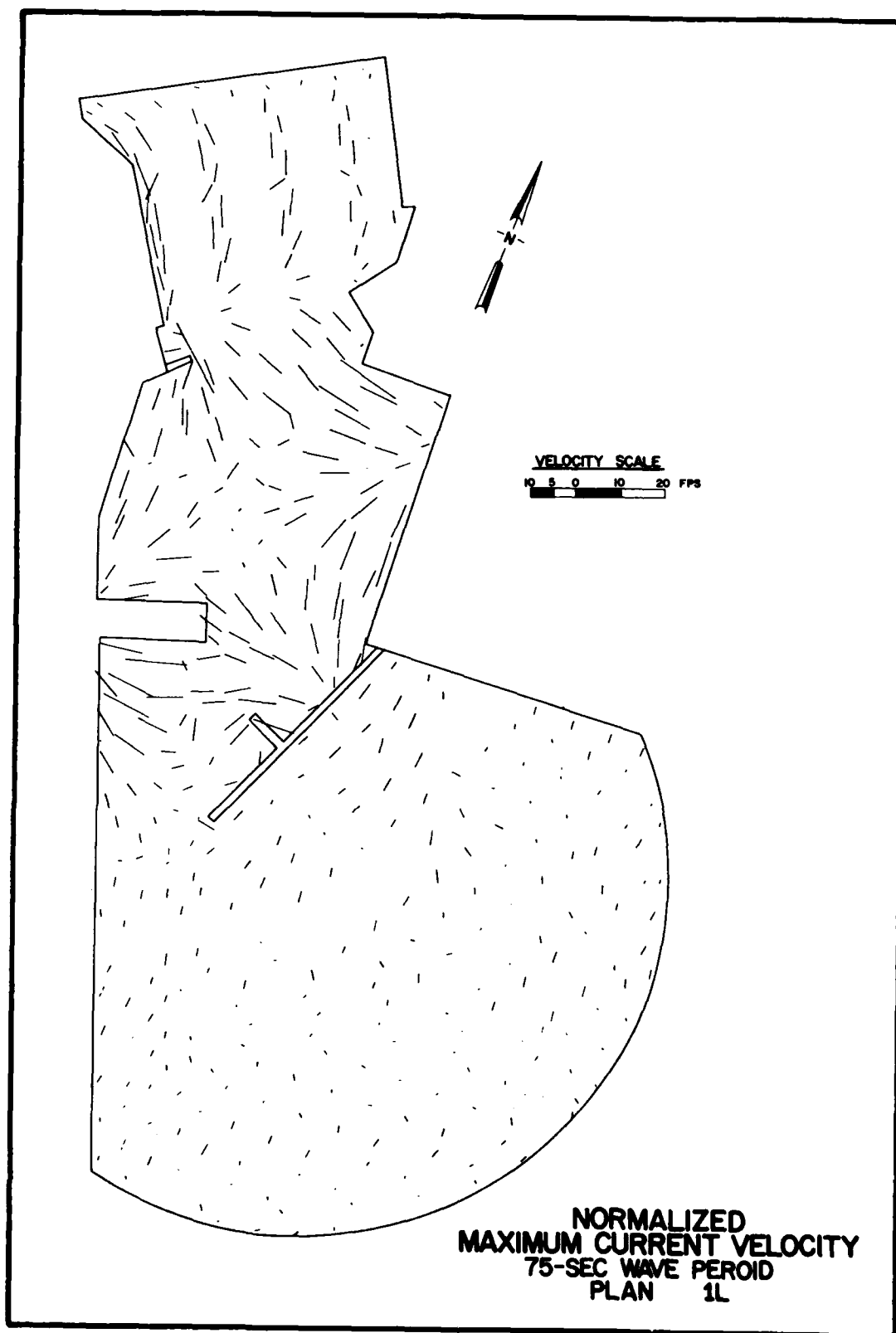
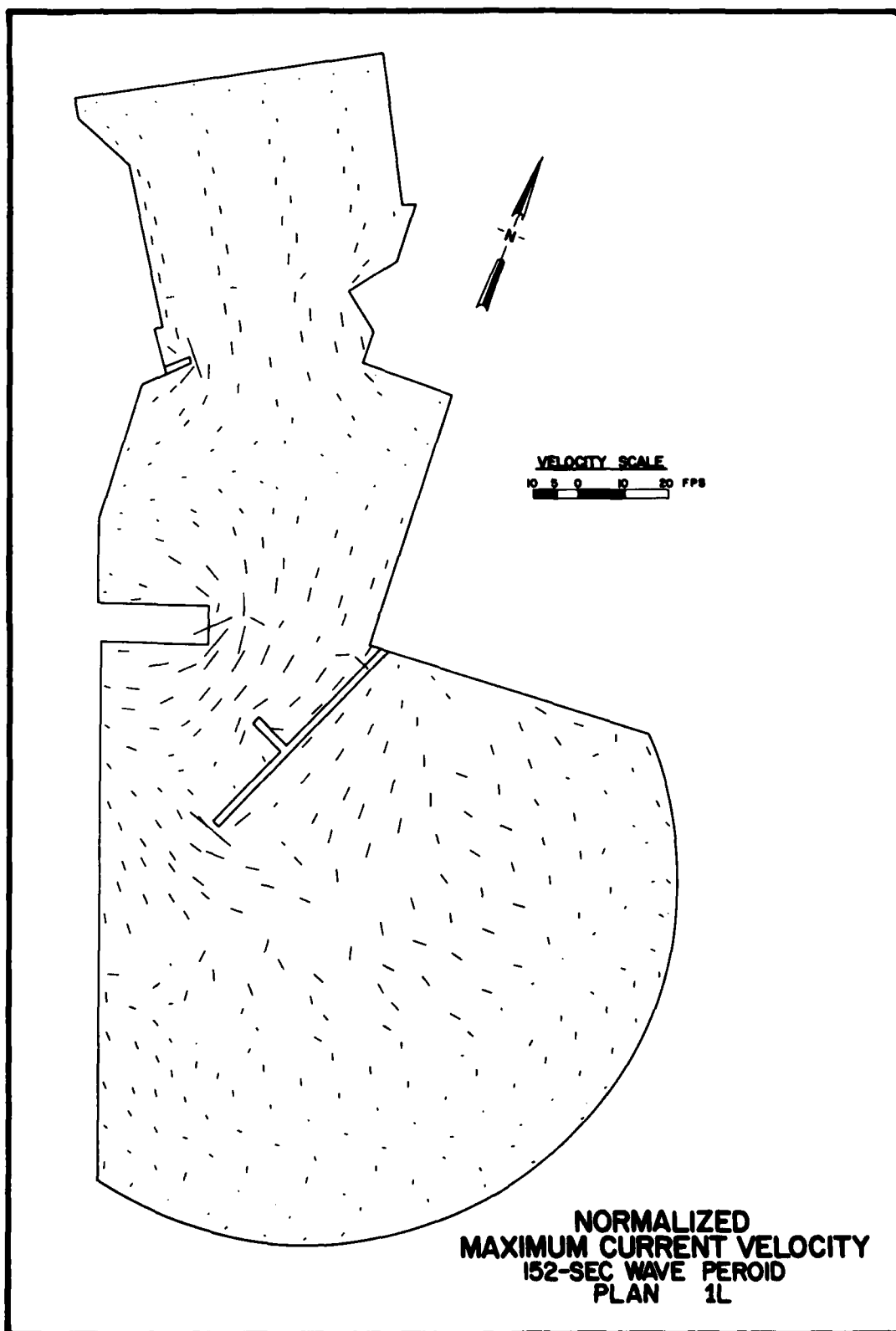
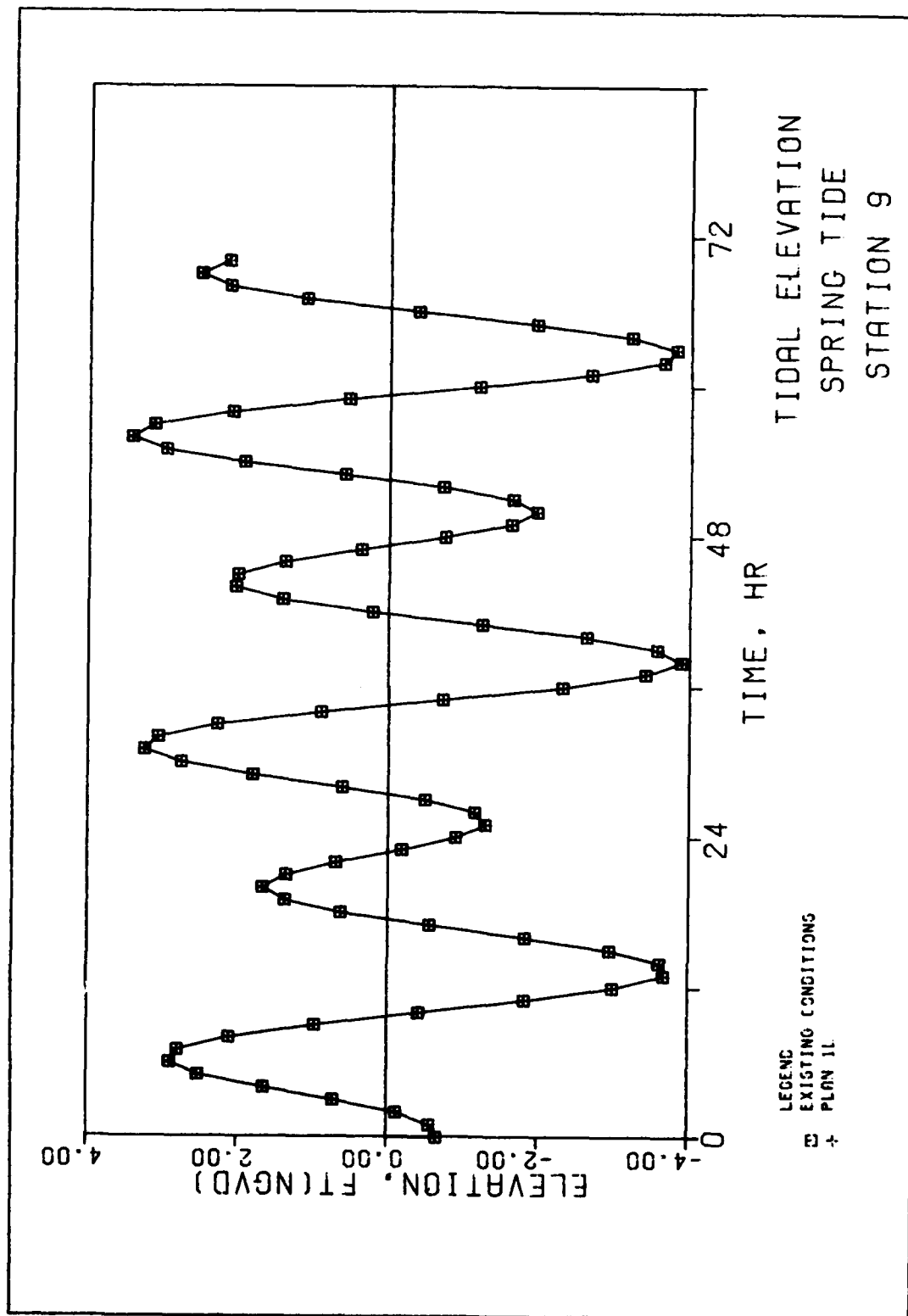


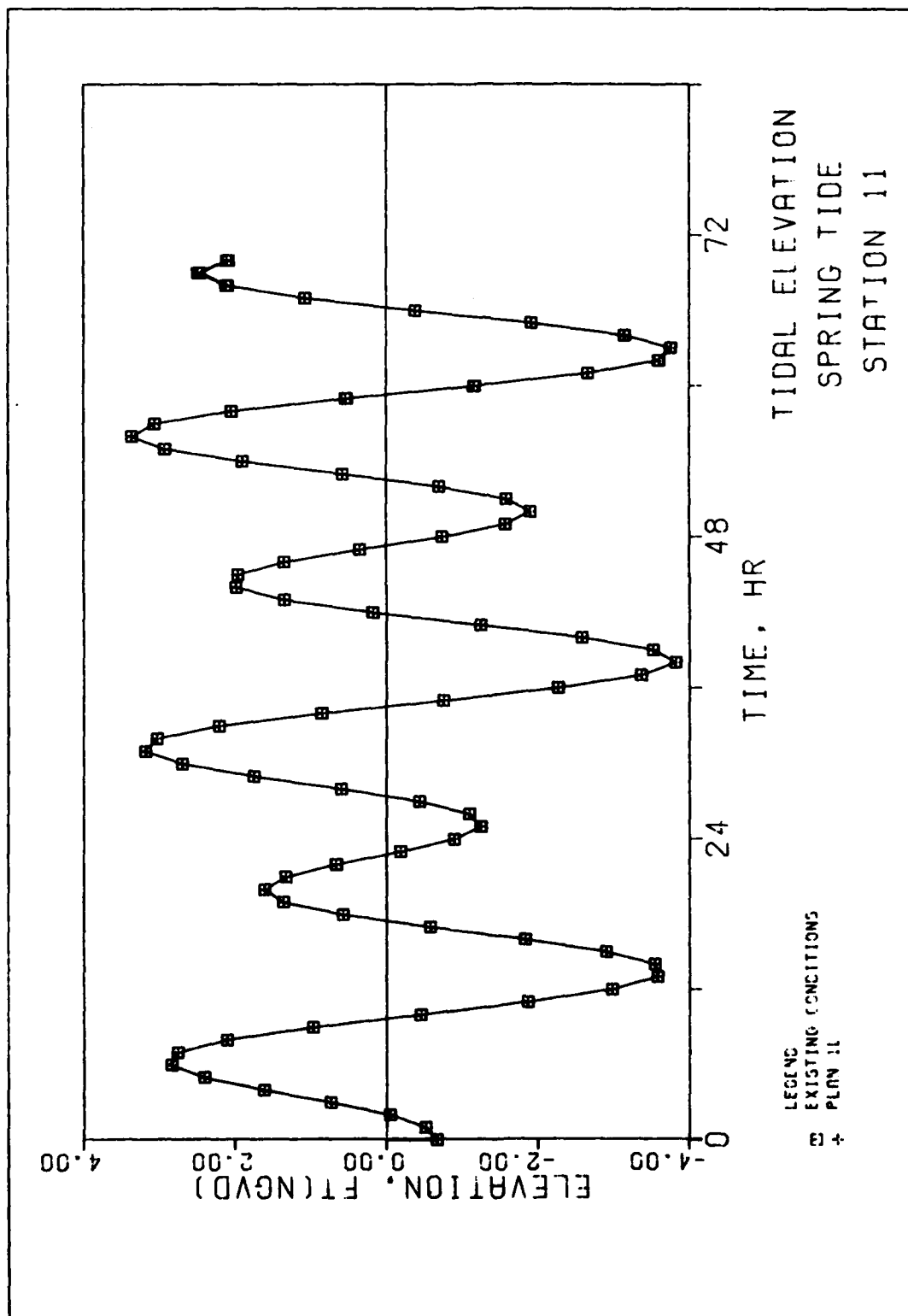
PLATE 62

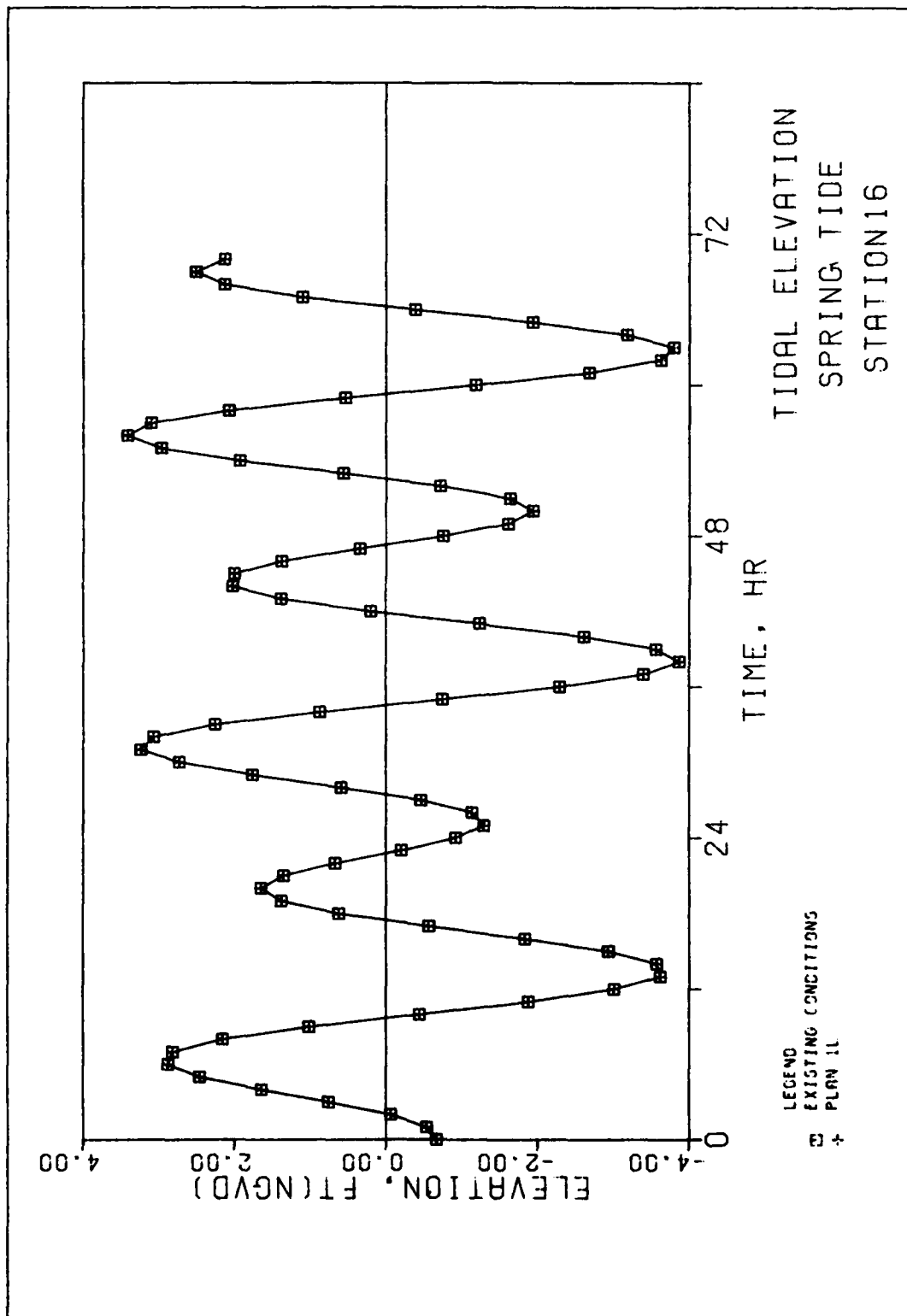


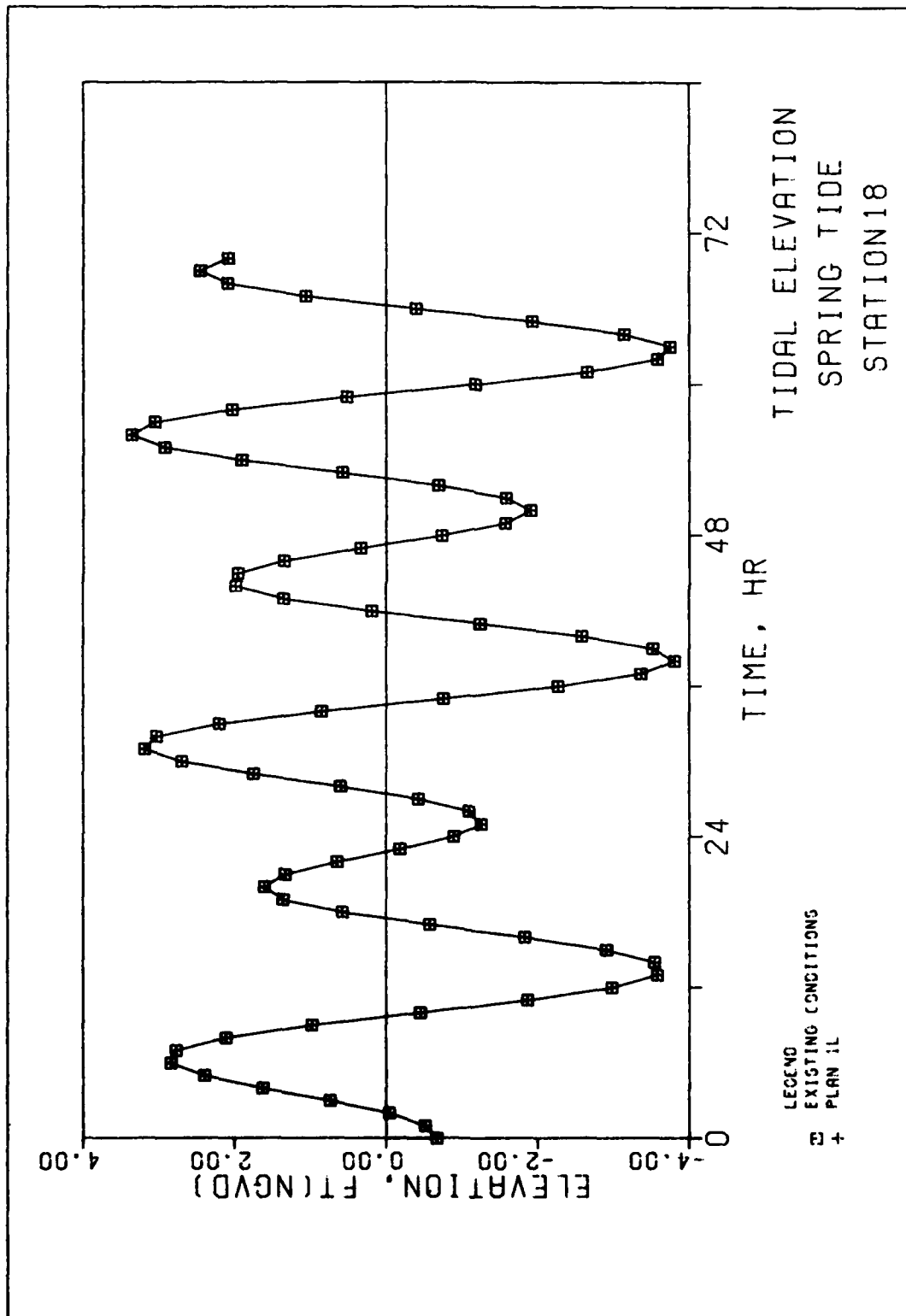


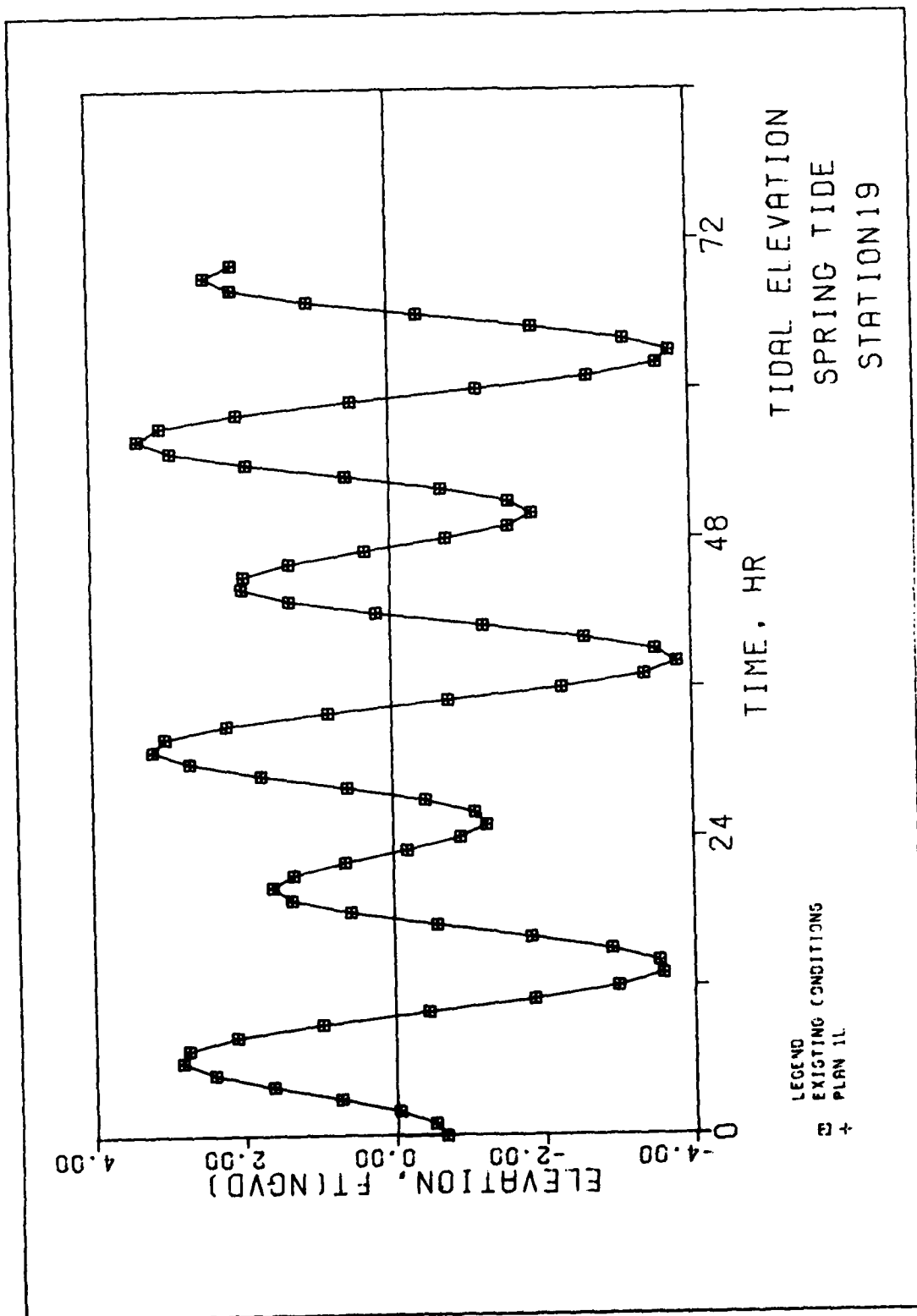


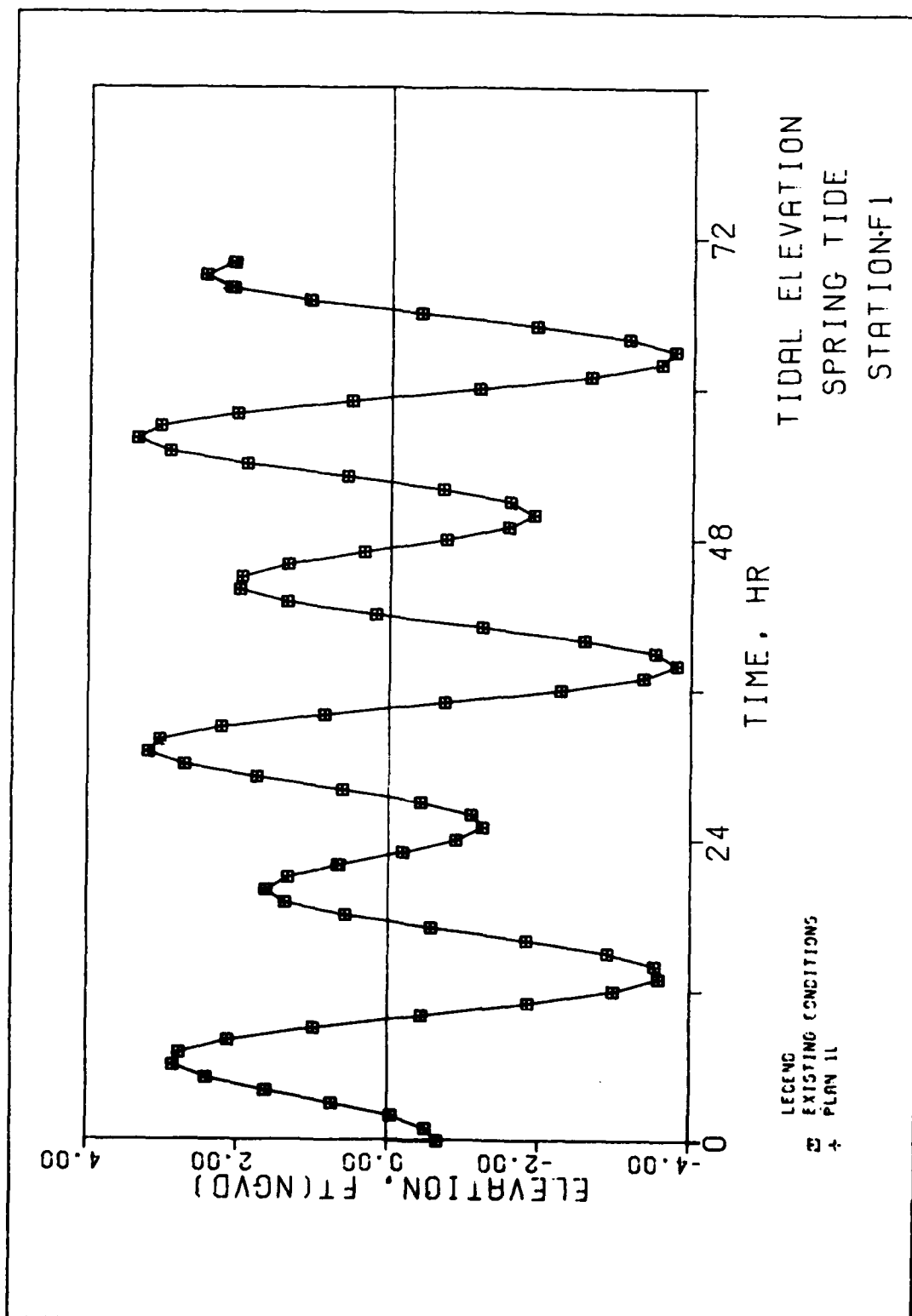


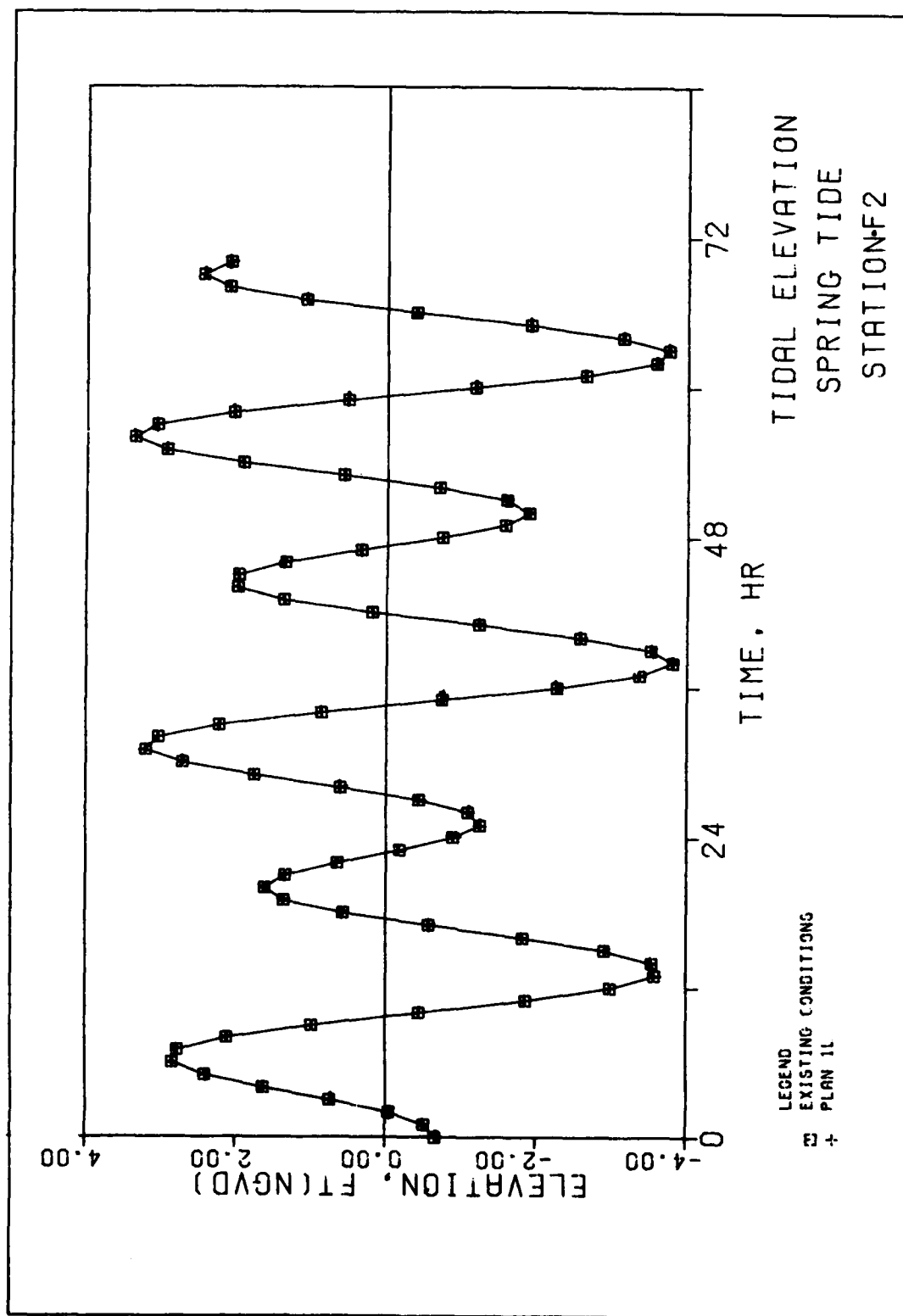


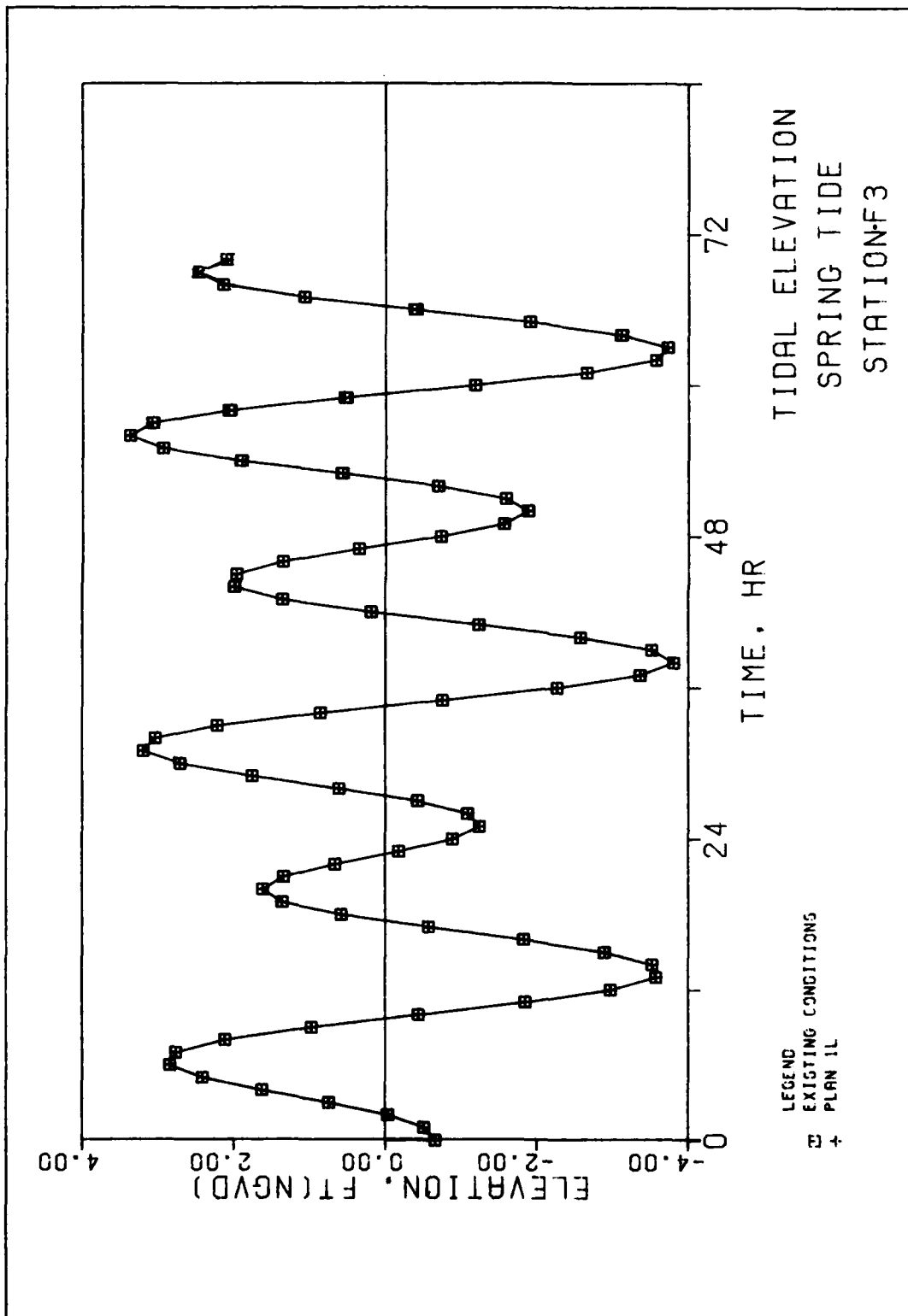












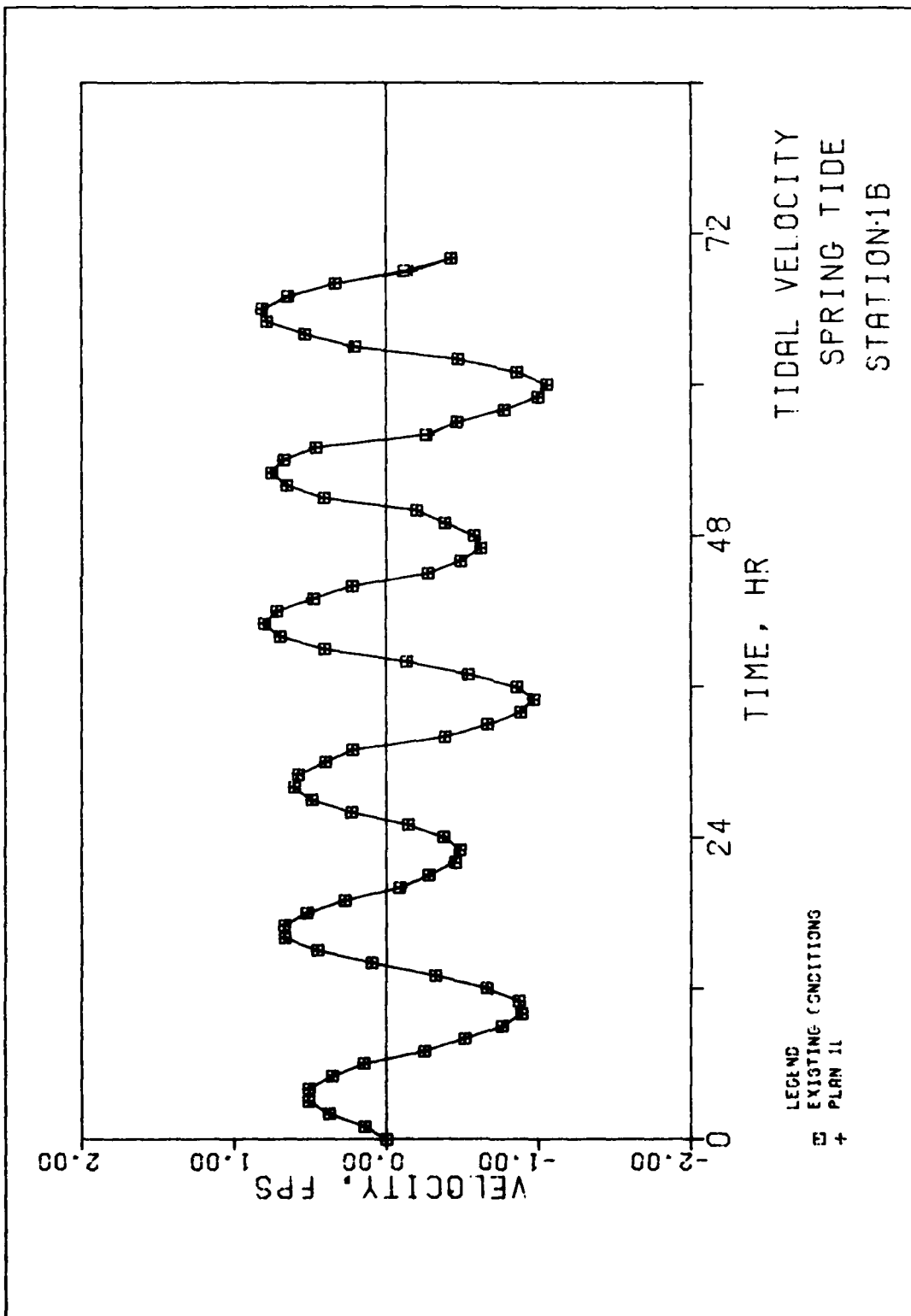
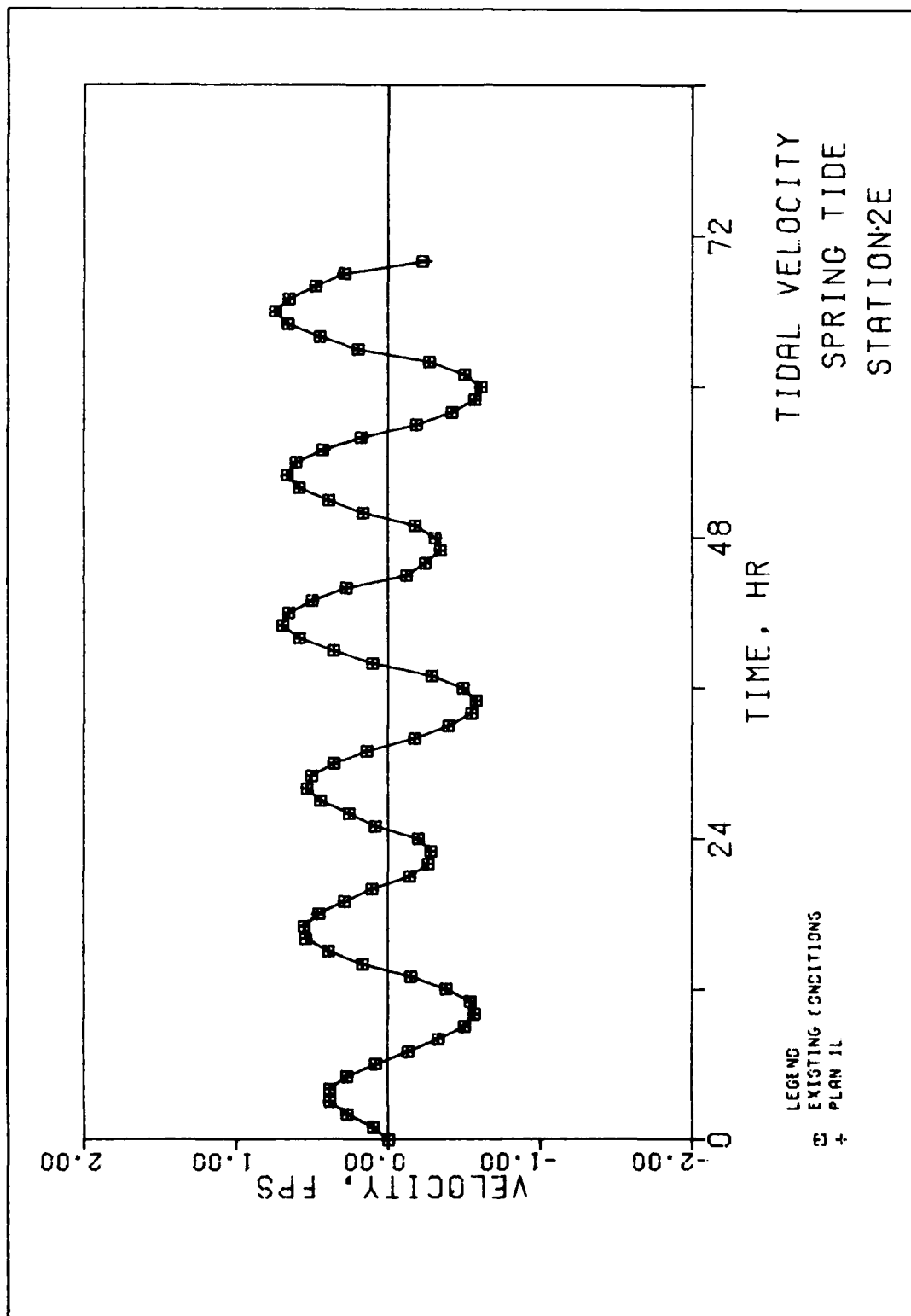


PLATE 74



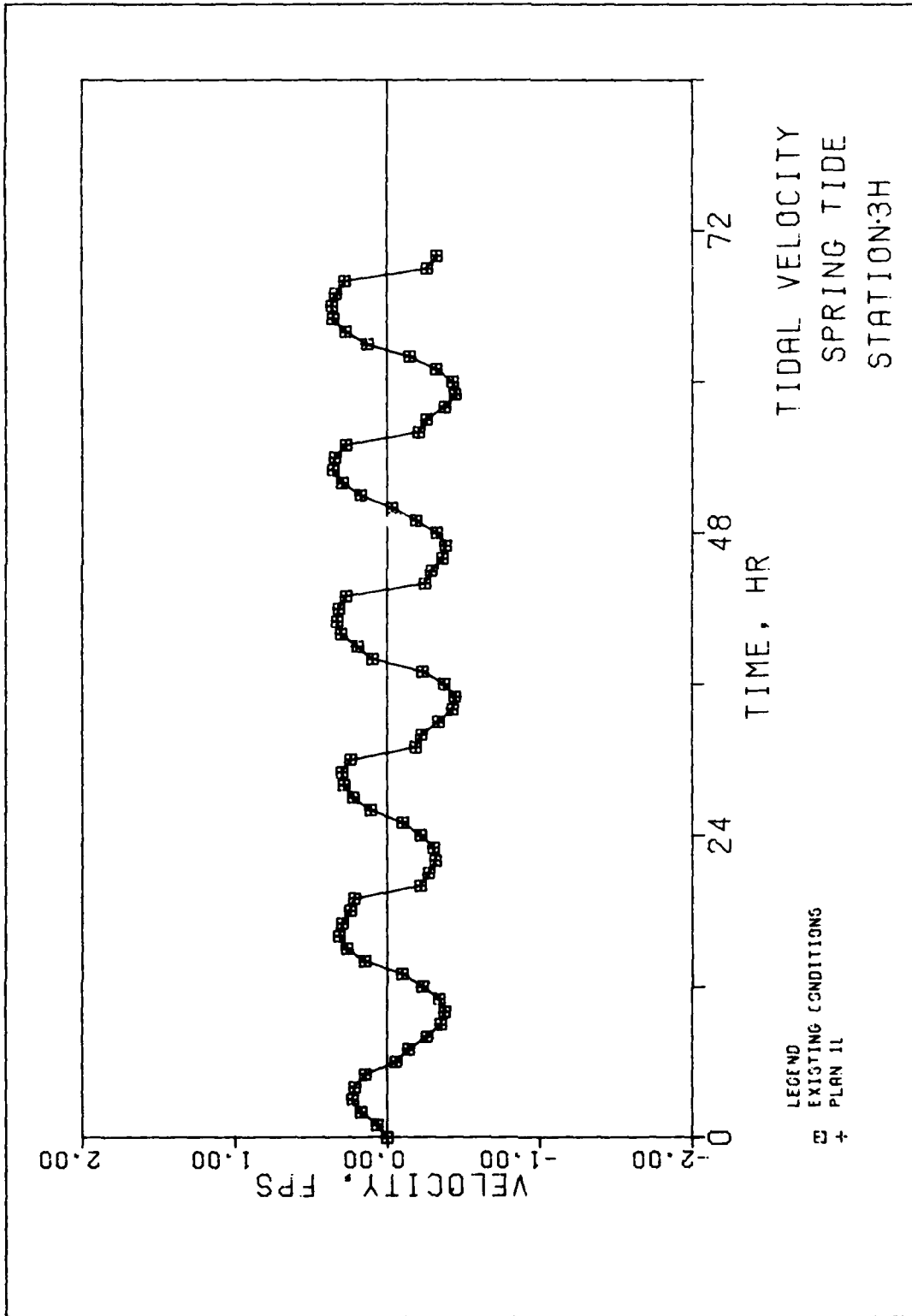
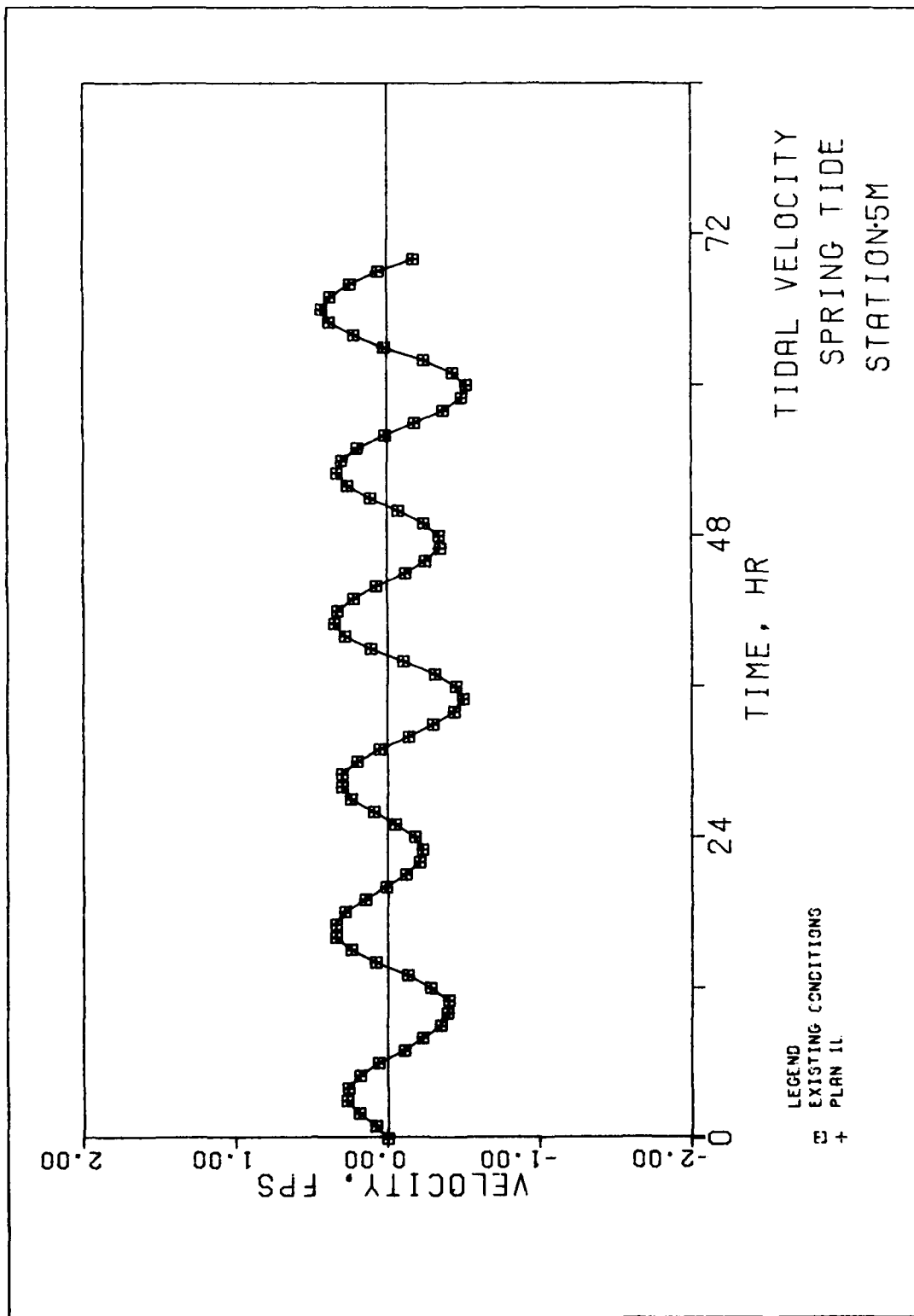
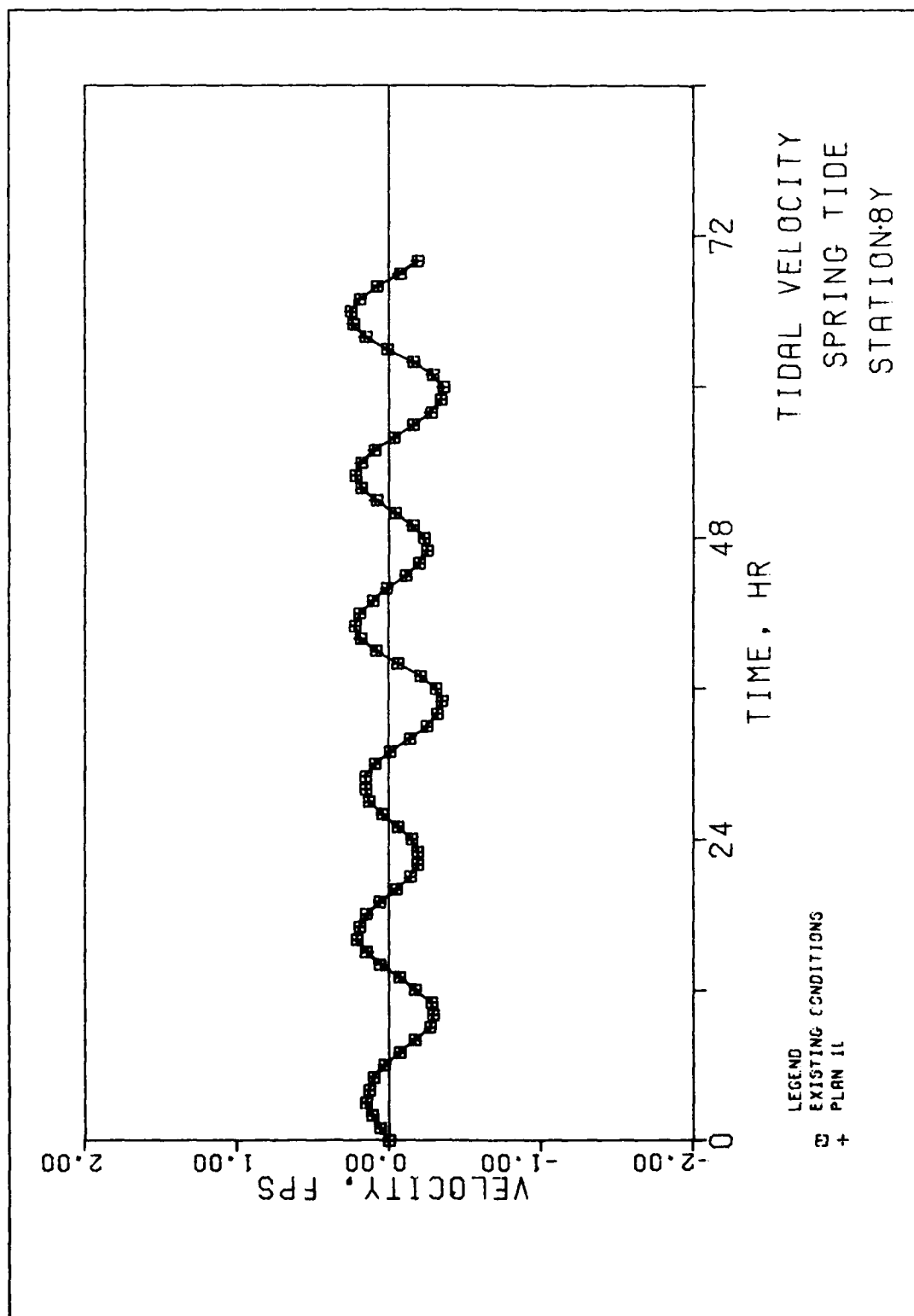
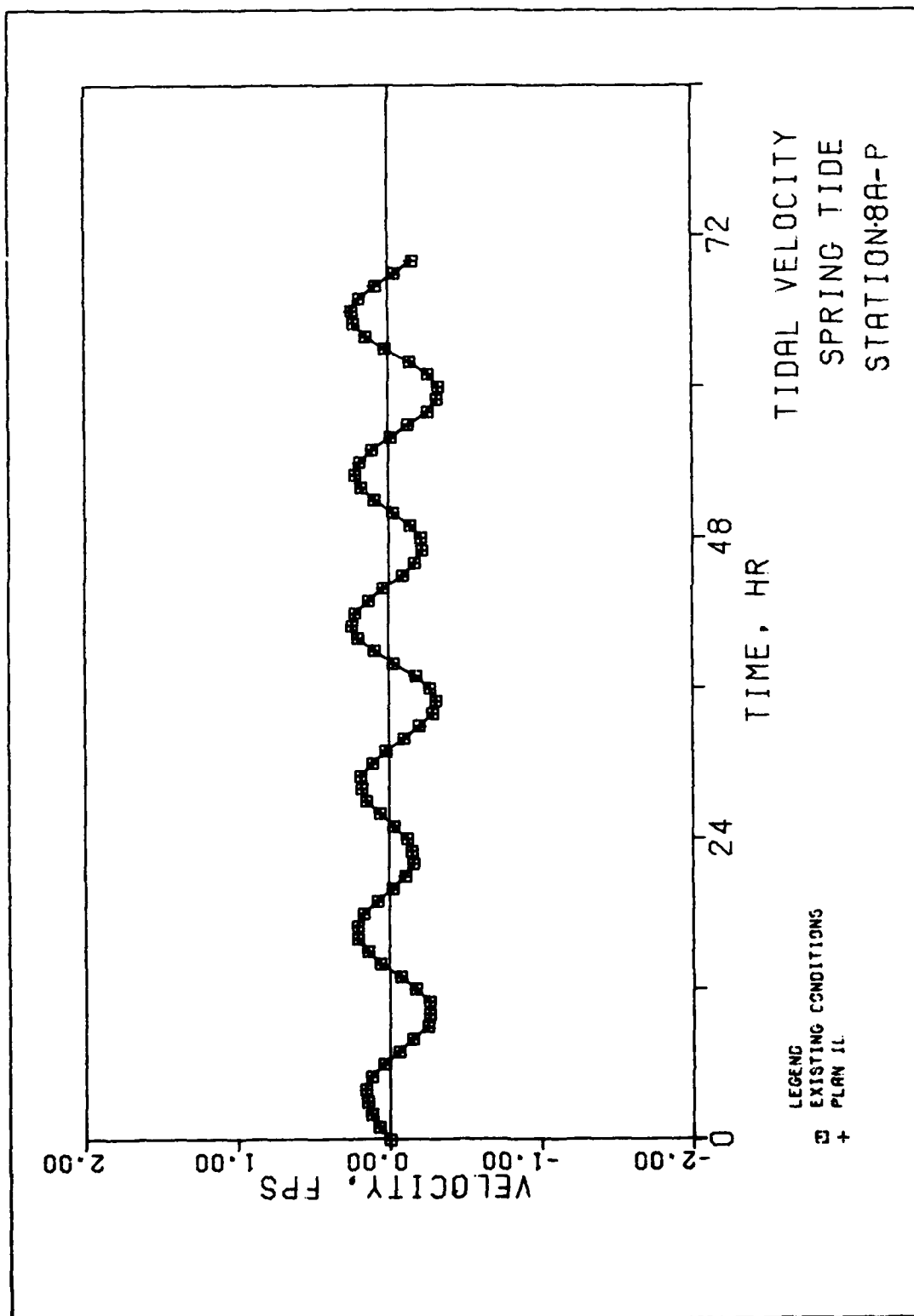
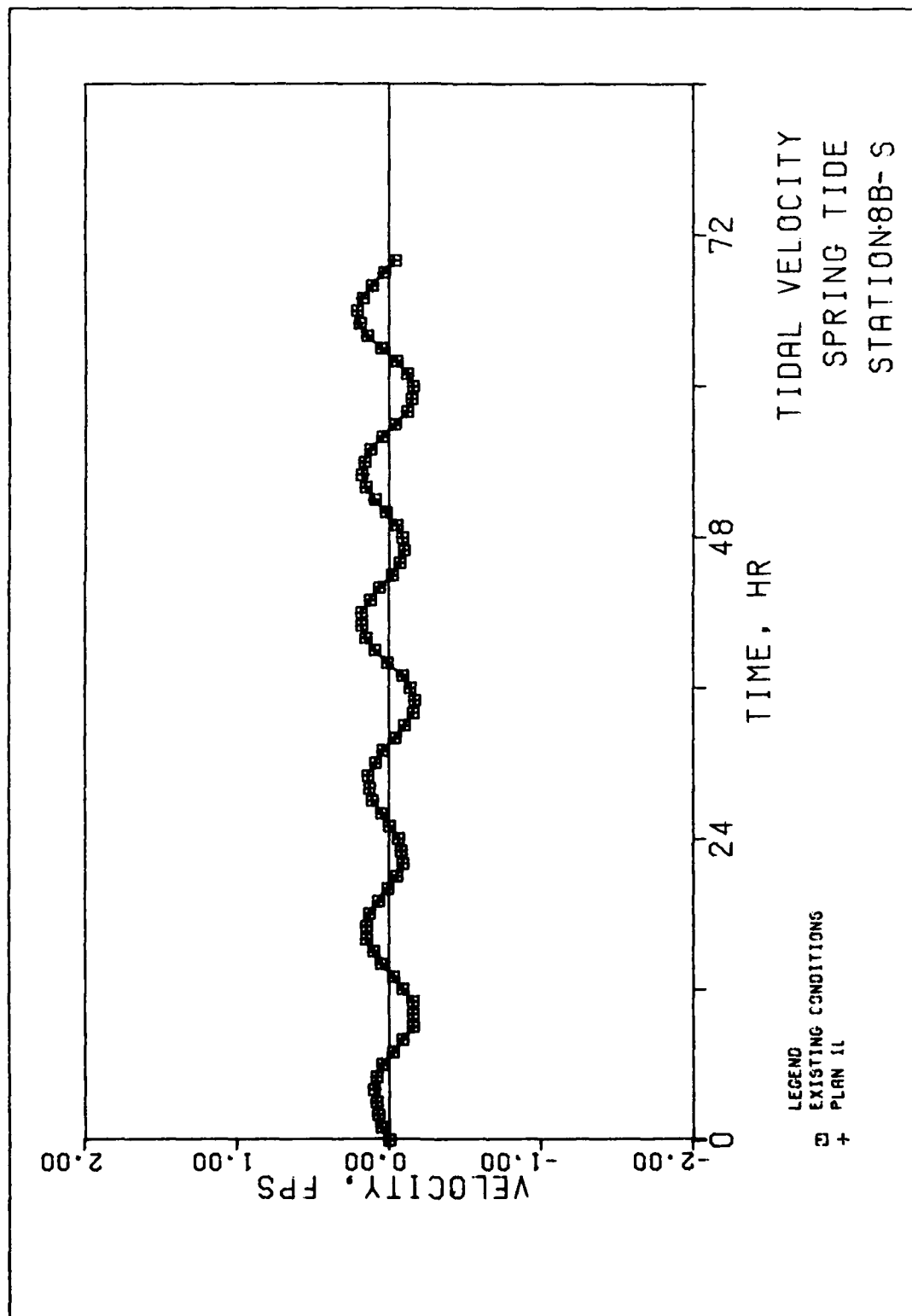


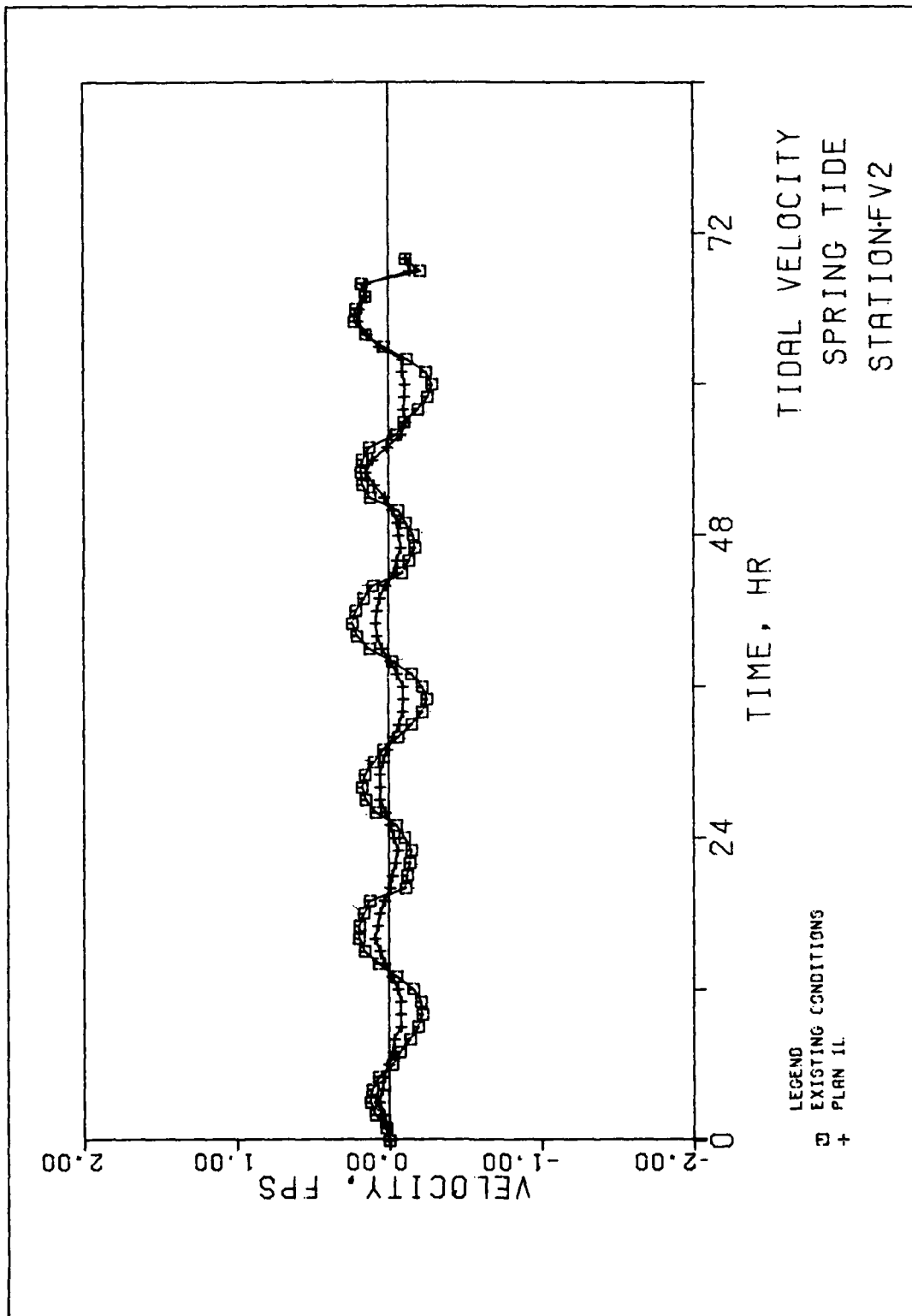
PLATE 76

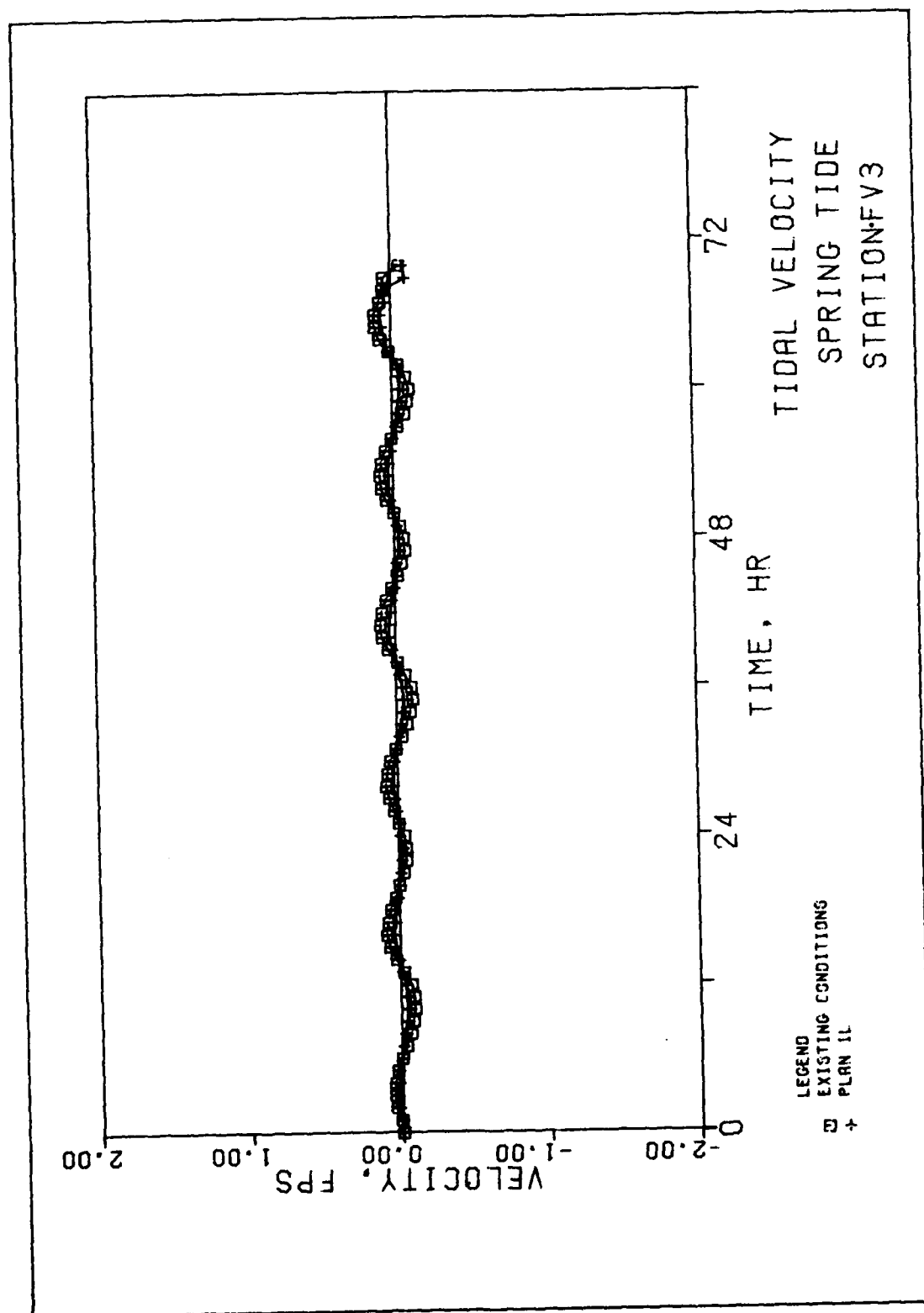


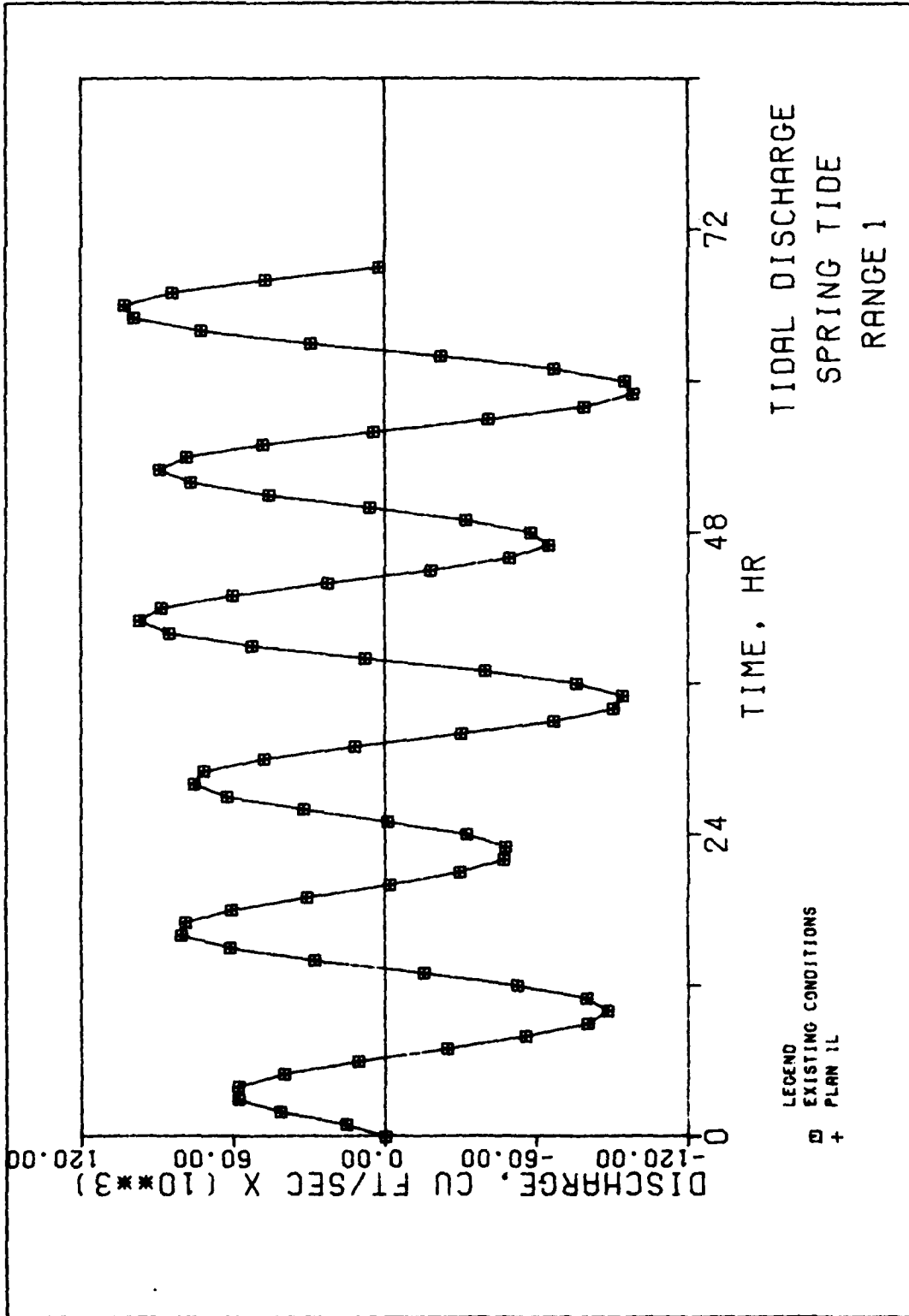


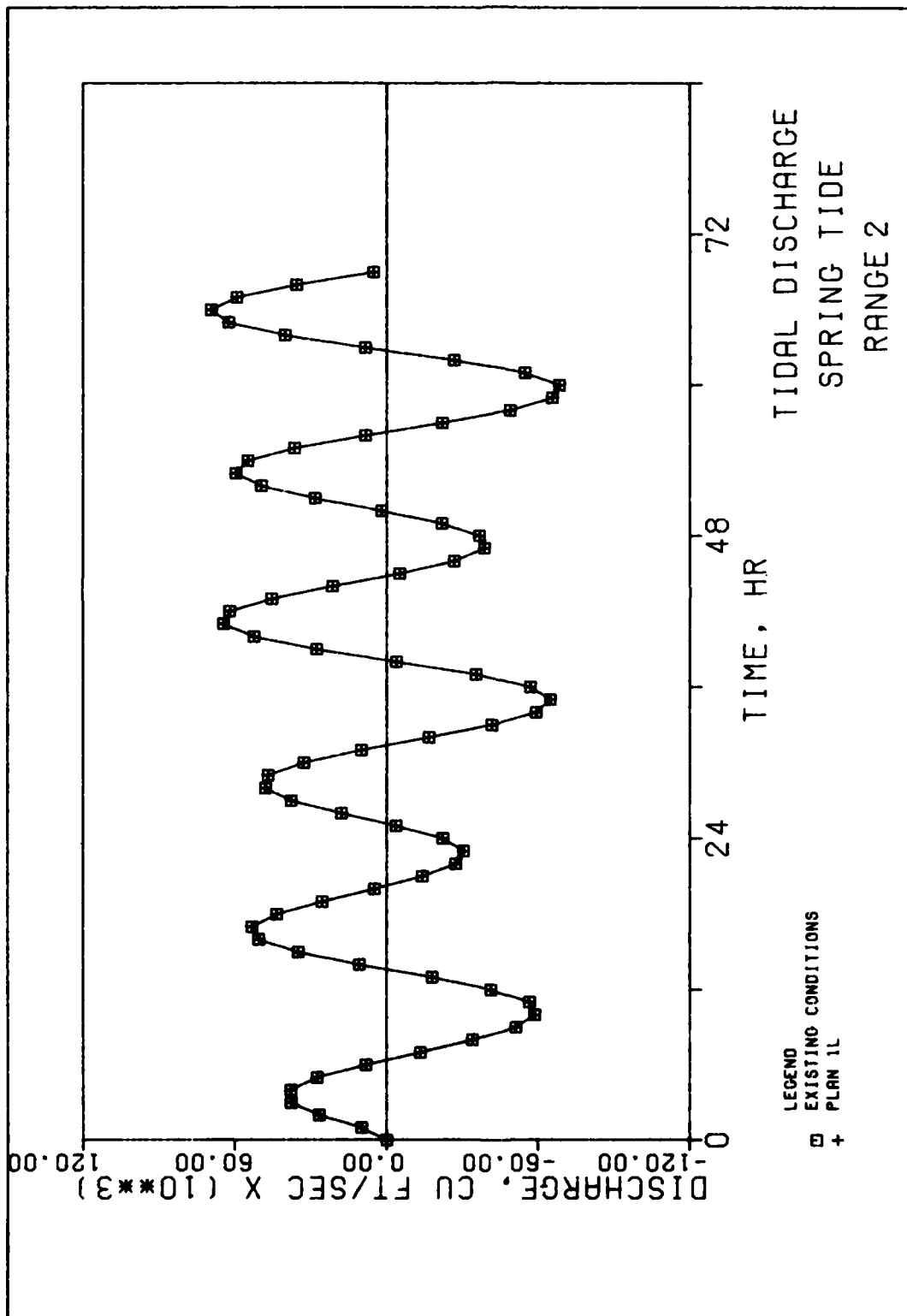


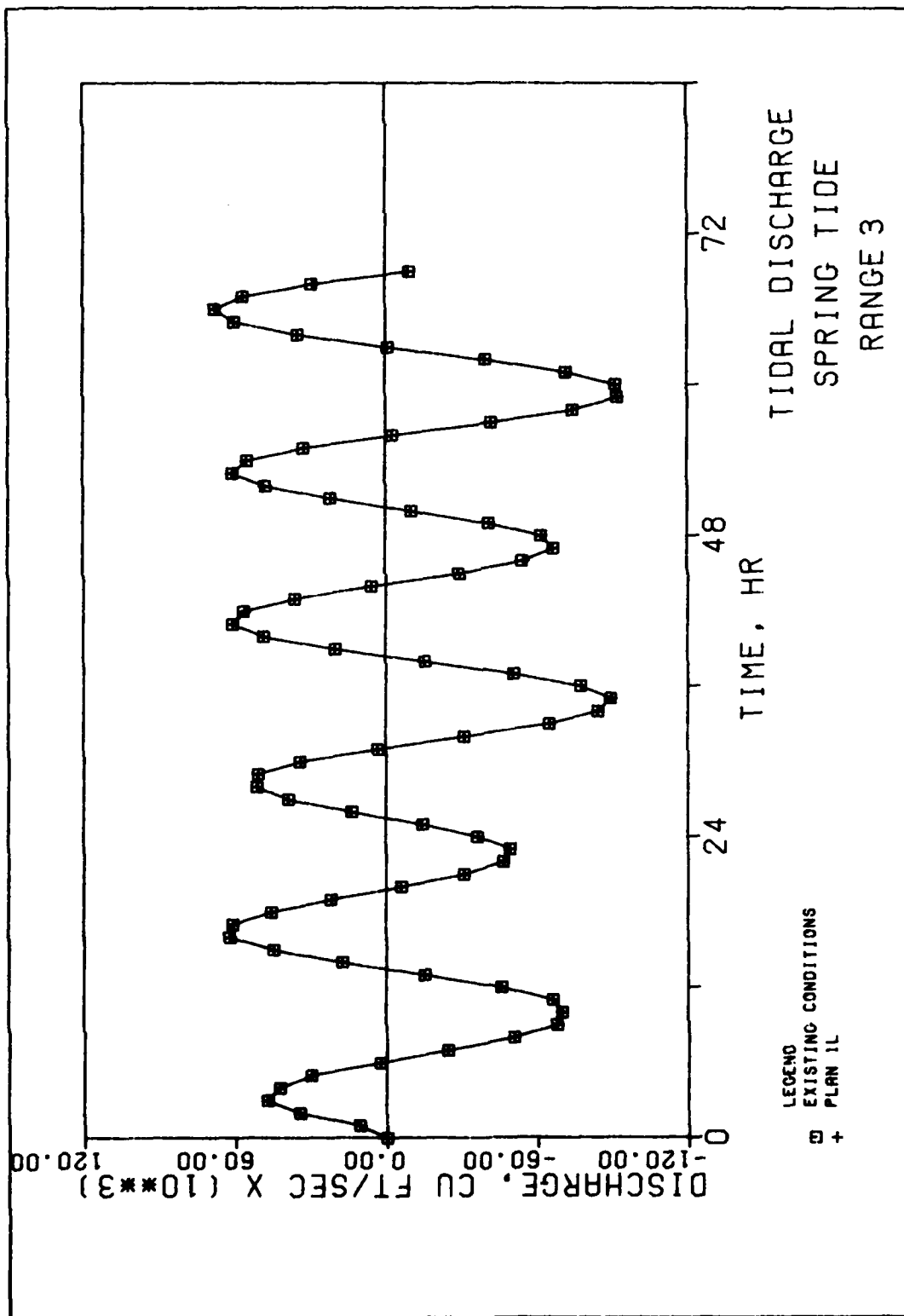


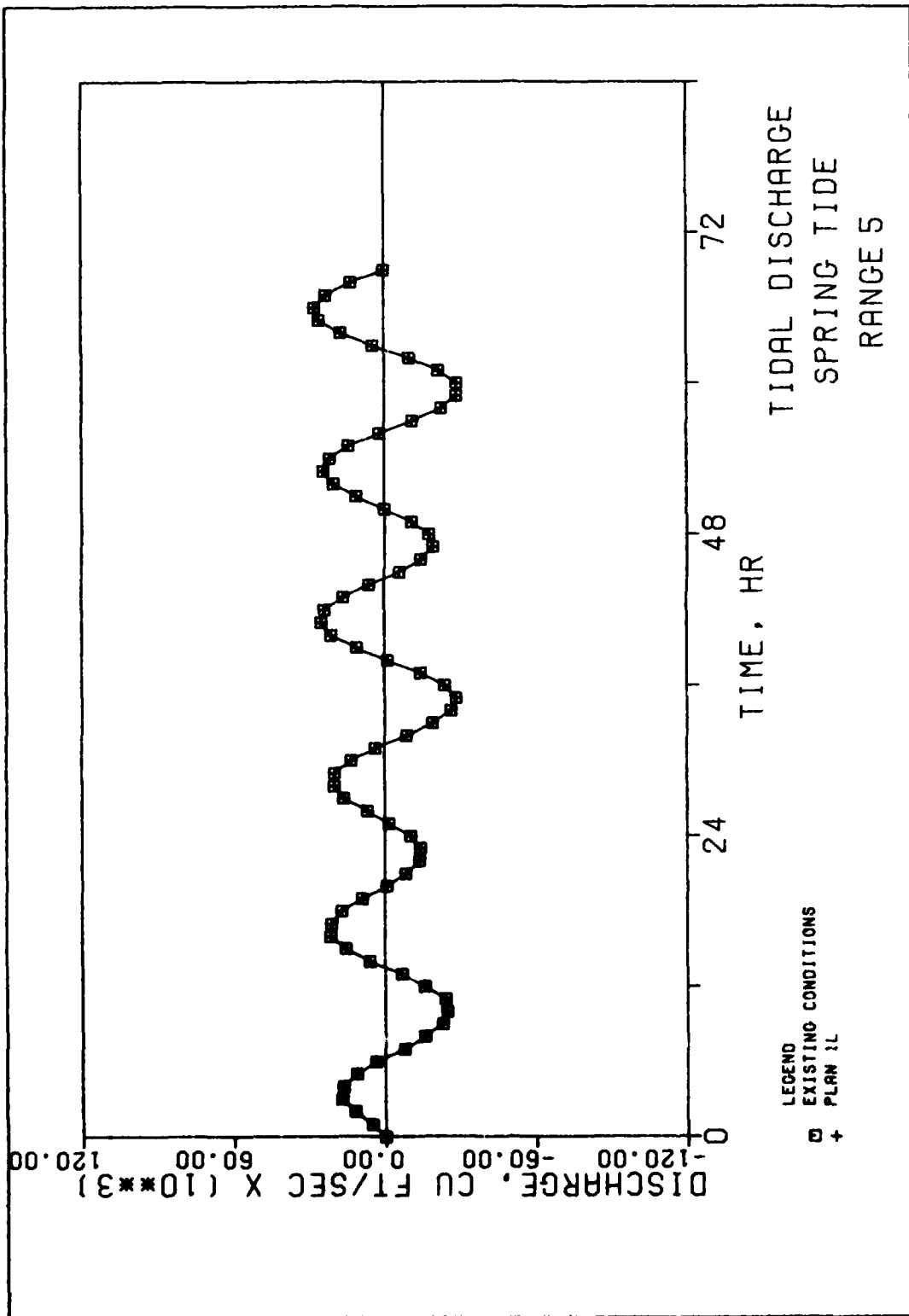


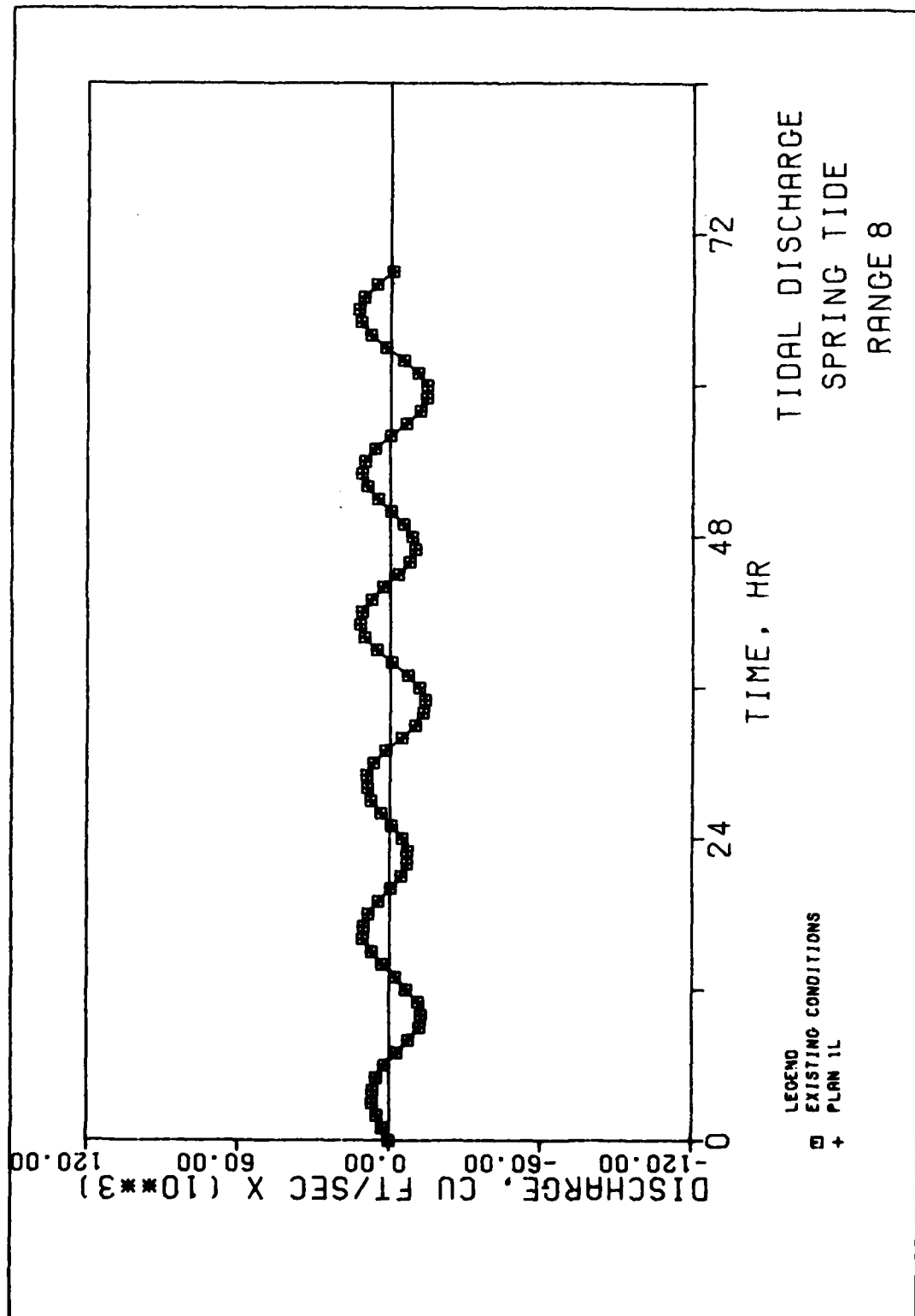


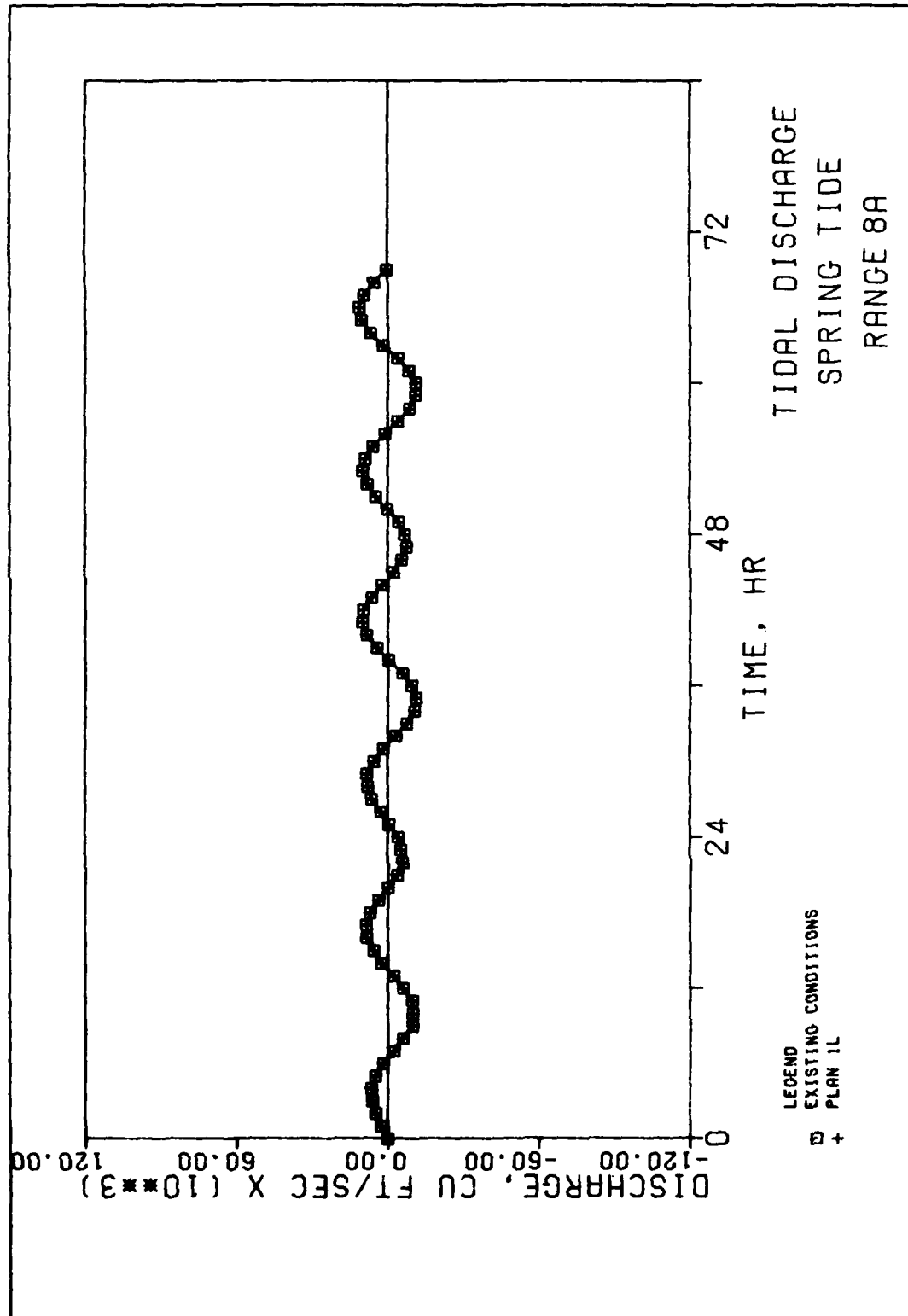


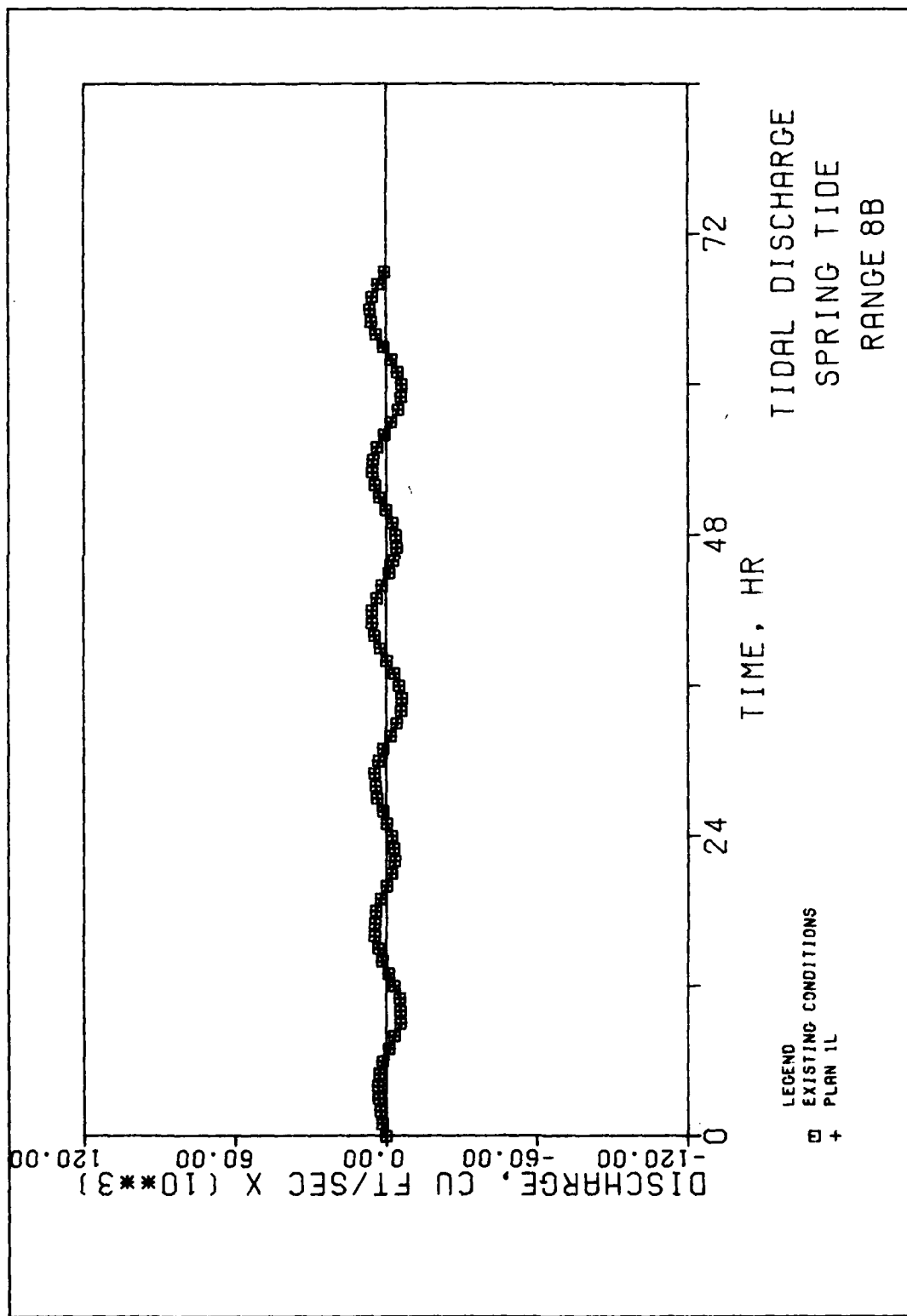


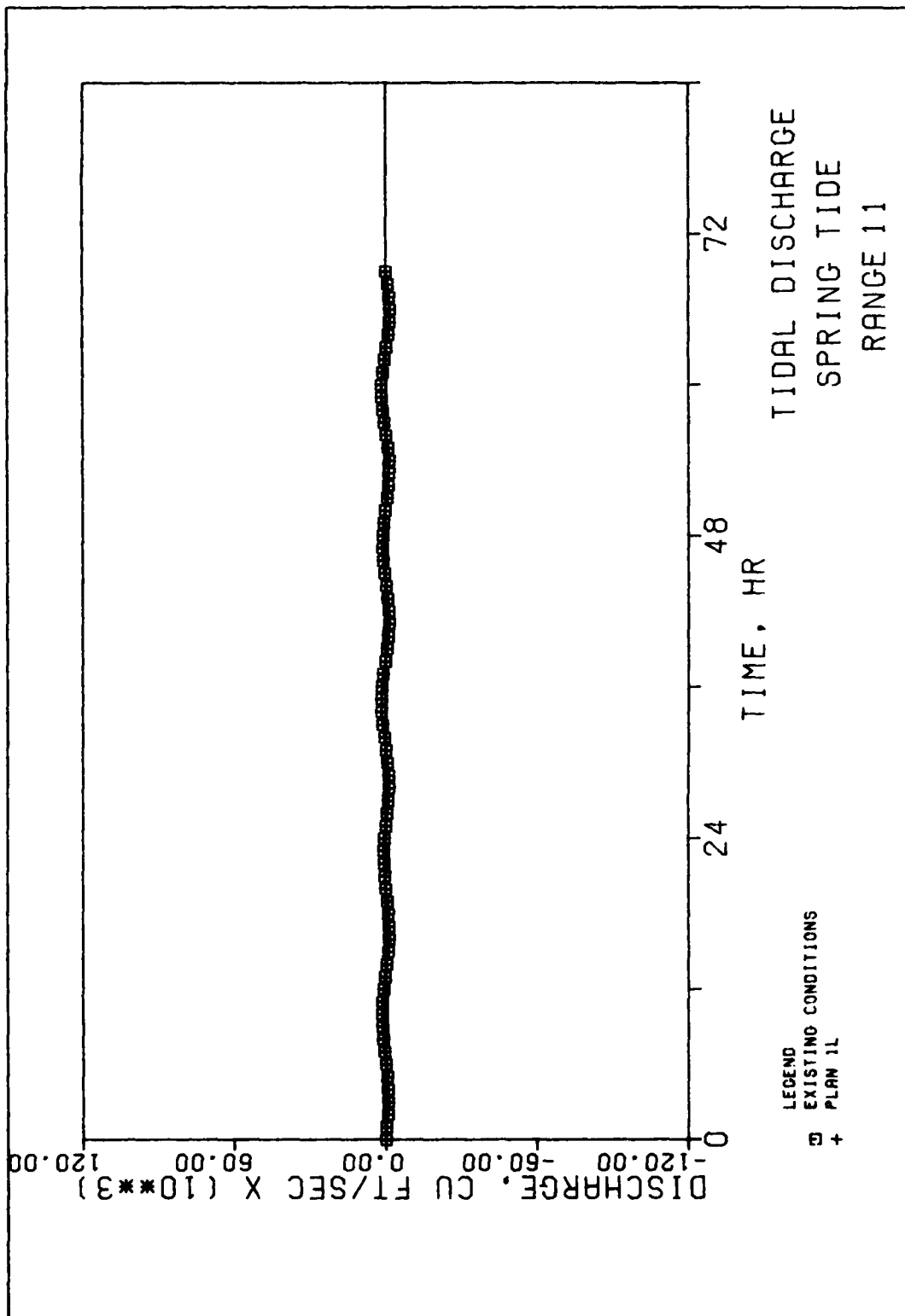


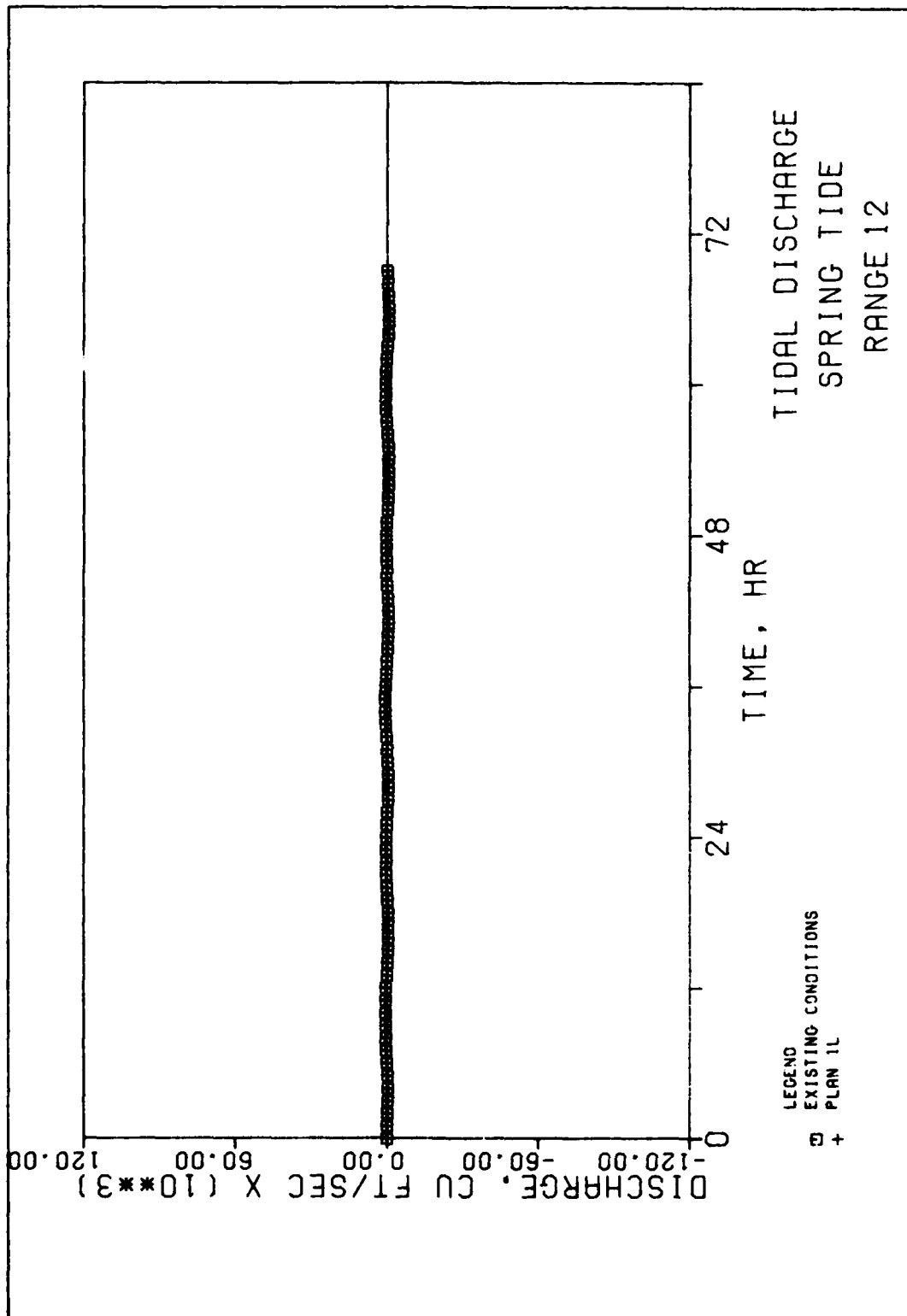


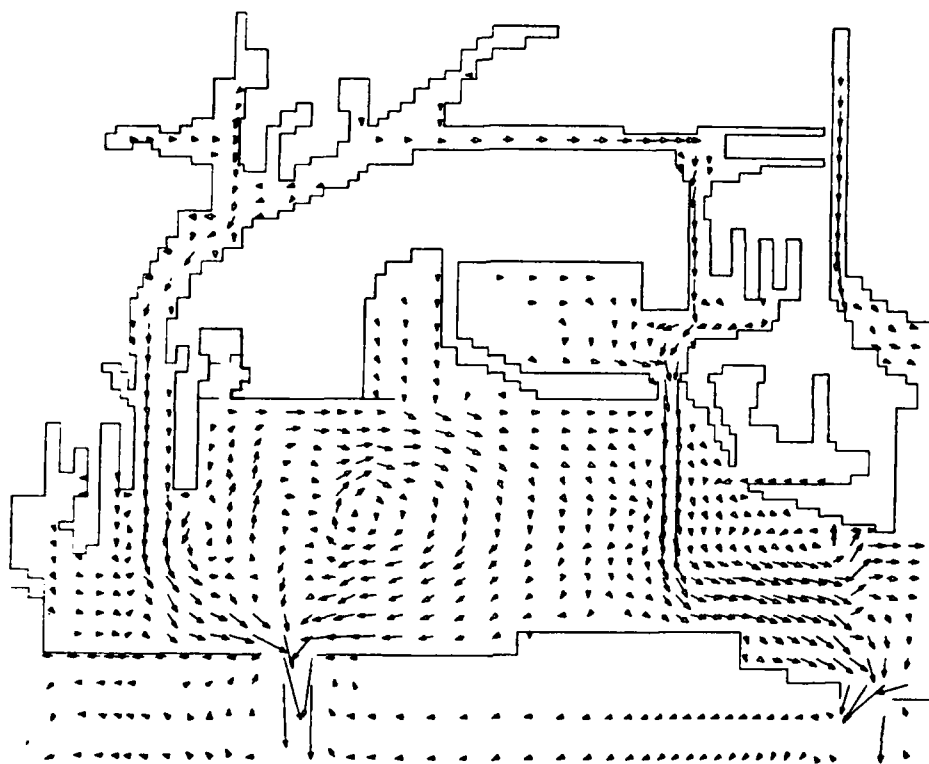








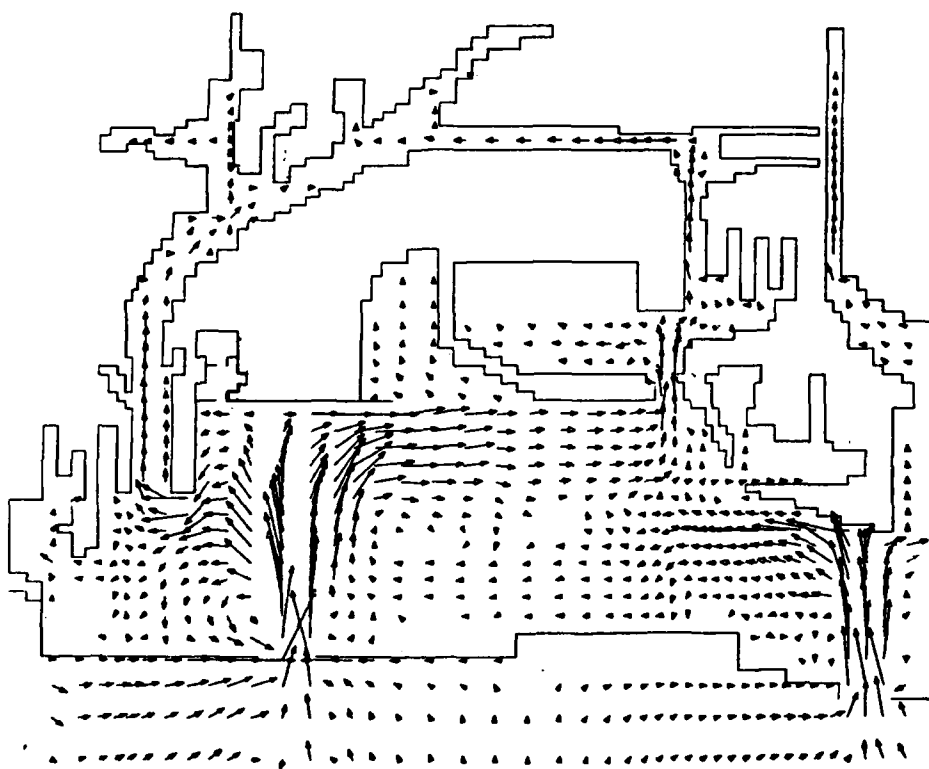




VELOCITY SCALE, FPS
1.0 0.5 0 1.0 2.0

SCALE IN FEET
X 1000
2 1 0 2 4

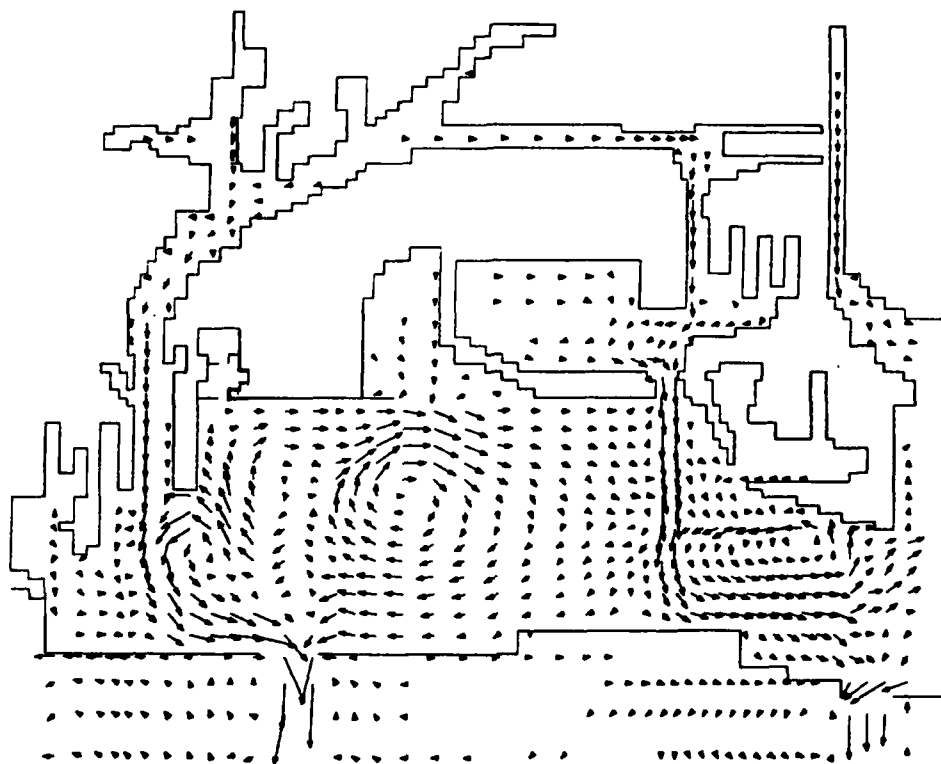
VELOCITY VECTOR PLOTS OF TIDAL CIRCULATION
EXISTING CONDITIONS
SPRING TIDE
HOUR 36



VELOCITY SCALE, FPS
1.0 0.5 0 1.0 2.0

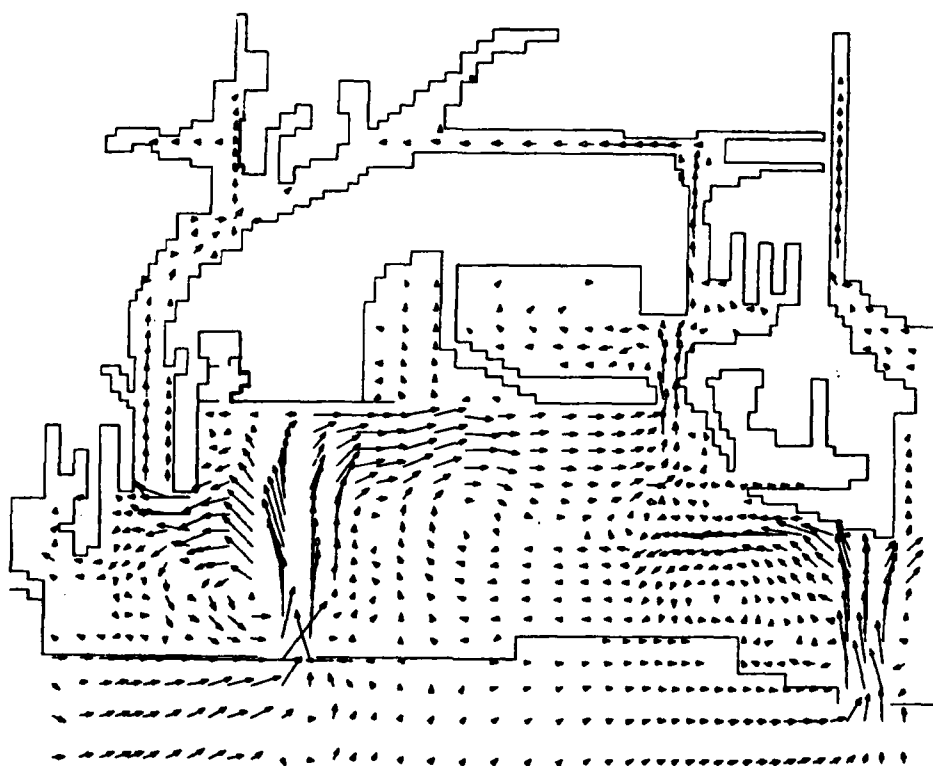
SCALE IN FEET
X 1000
2 1 0 2 4

VELOCITY VECTOR PLOTS OF TIDAL CIRCULATION
EXISTING CONDITIONS
SPRING TIDE
HOUR 42



VELOCITY SCALE, FPS SCALE IN FEET
 1.0 0.5 0 1.0 2.0 X 1000
 2 1 0 2 4

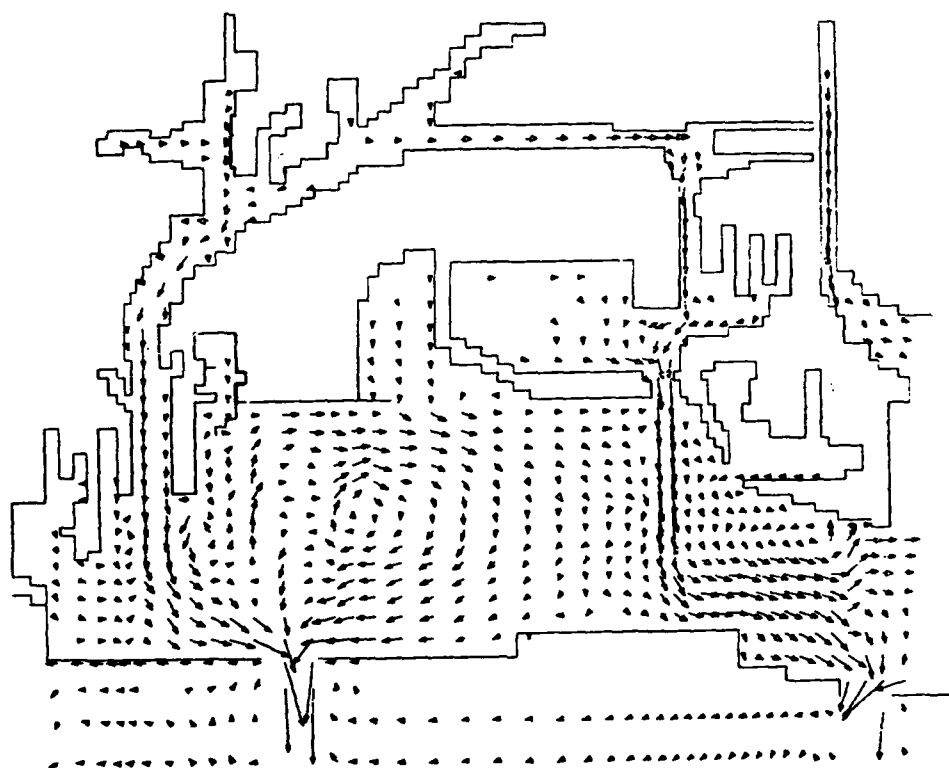
VELOCITY VECTOR PLOTS OF TIDAL CIRCULATION
 EXISTING CONDITIONS
 SPRING TIDE
 HOUR 48



VELOCITY SCALE, FPS
1.0 0.5 0 1.0 2.0

SCALE IN FEET
X 1000
2 1 0 2 4

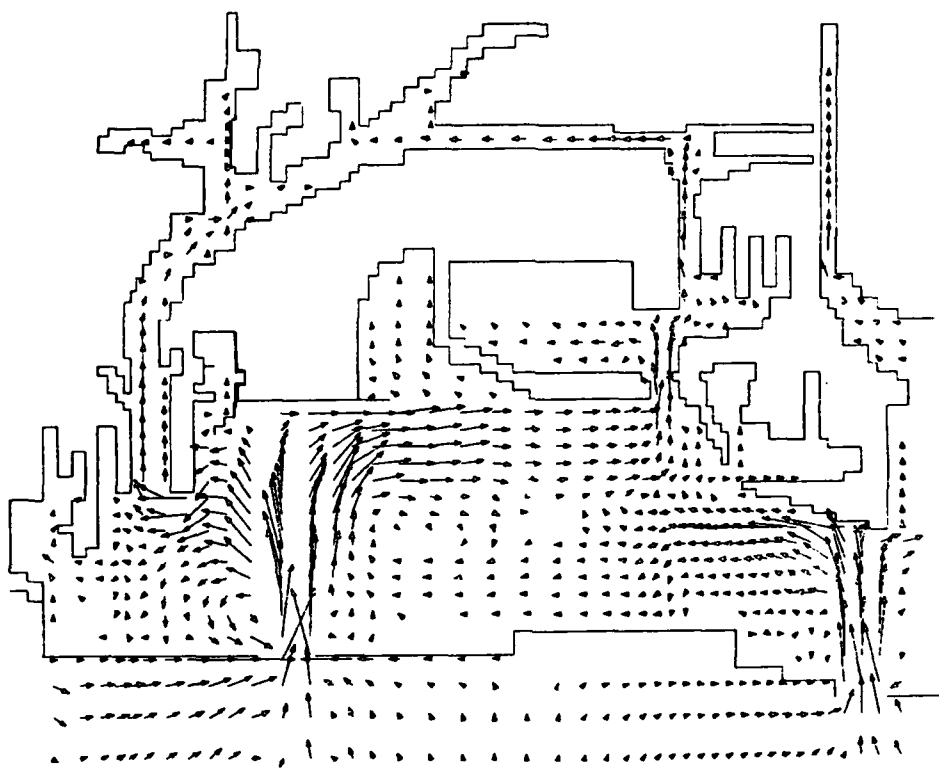
VELOCITY VECTOR PLOTS OF TIDAL CIRCULATION
EXISTING CONDITION
SPRING TIDE
HOUR 54



VELOCITY SCALE, FPS
1.0 0.5 0 1.0 2.0

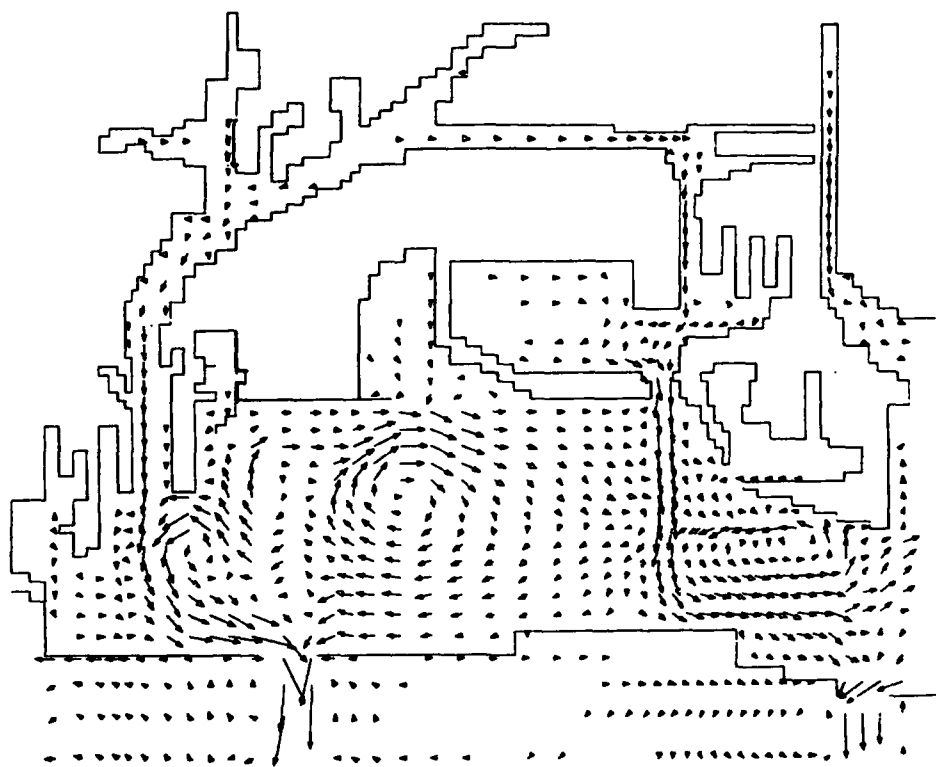
SCALE IN FEET
X 1000
2 1 0 2 4

VELOCITY VECTOR PLOTS OF TIDAL CIRCULATION
PLAN IL
SPRING TIDE
HOUR 36



VELOCITY SCALE, FPS SCALE IN FEET
1.0 0.5 0 1.0 2.0 X 1000
2 1 0 2 4

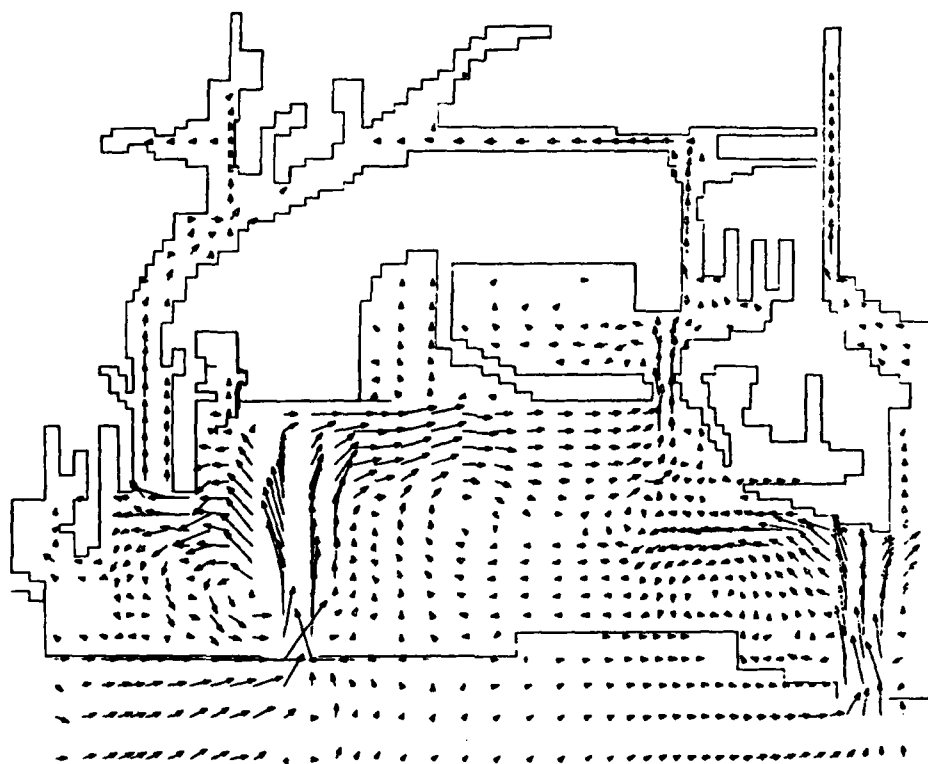
VELOCITY VECTOR PLOTS OF TIDAL CIRCULATION
PLAN 1L
SPRING TIDE
HOUR 42



VELOCITY SCALE, FPS
1.0 0.5 0 1.0 2.0

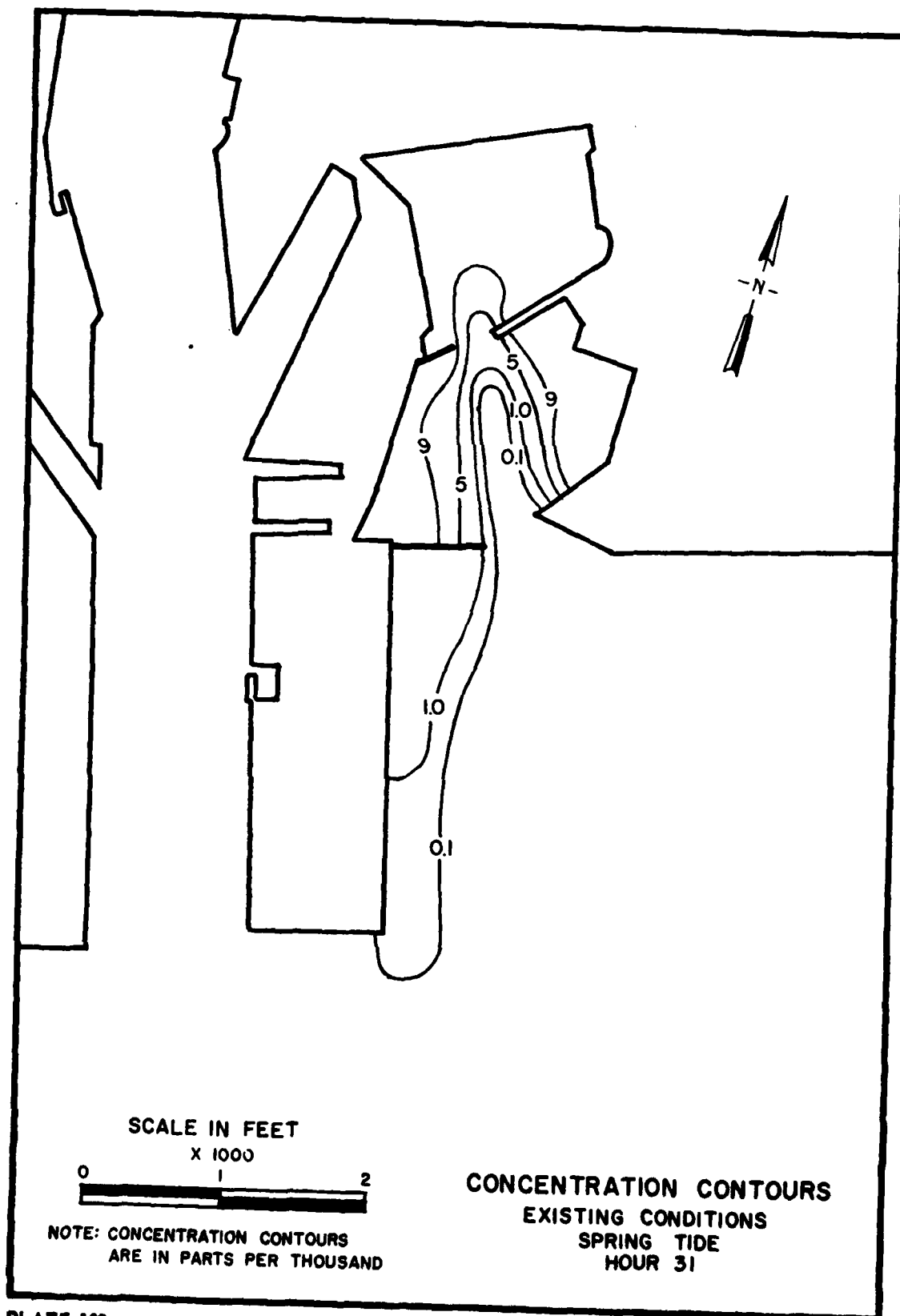
SCALE IN FEET
X 1000
2 1 0 2 4

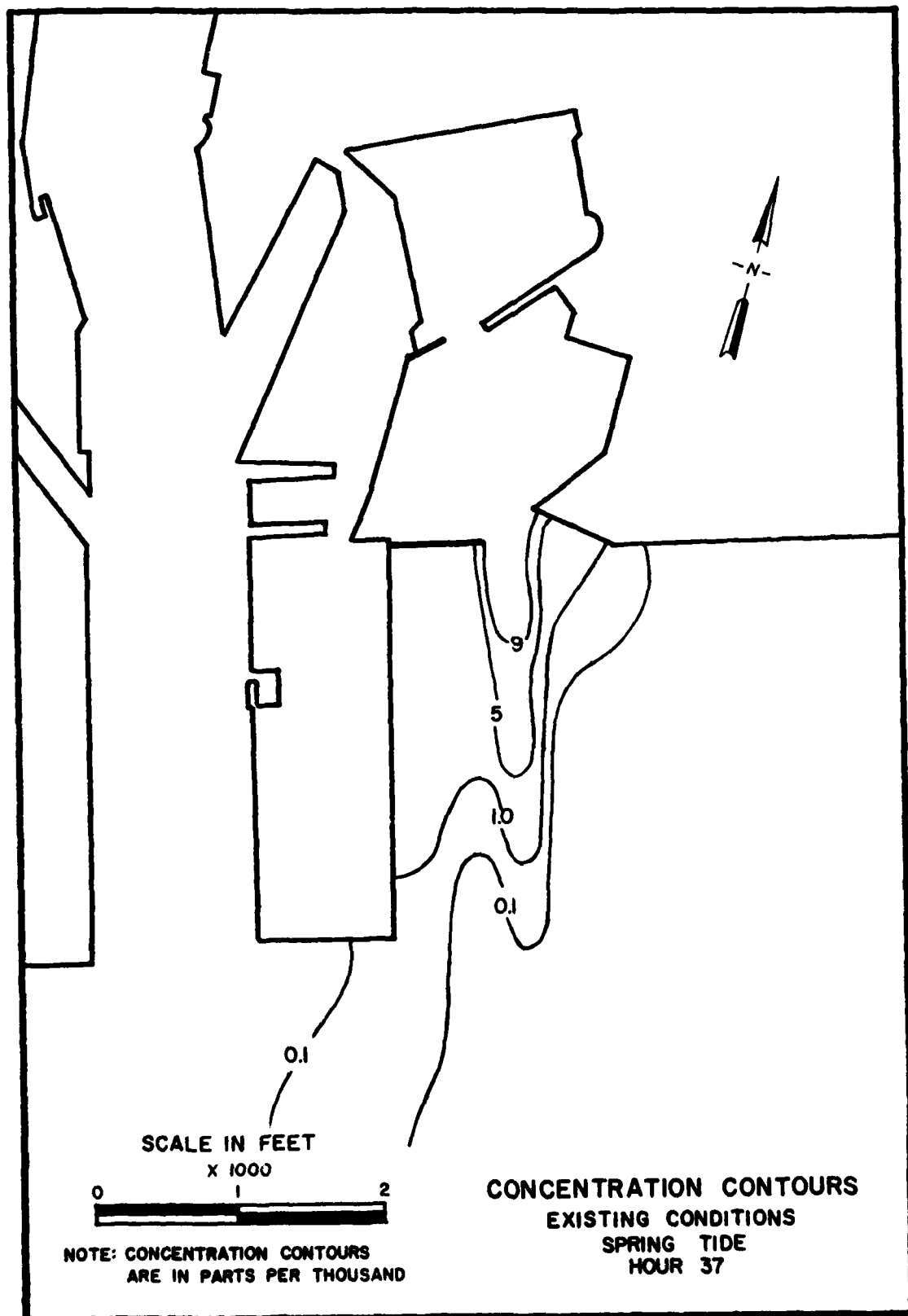
VELOCITY VECTOR PLOTS OF TIDAL CIRCULATION
PLAN IL
SPRING TIDE
HOUR 48

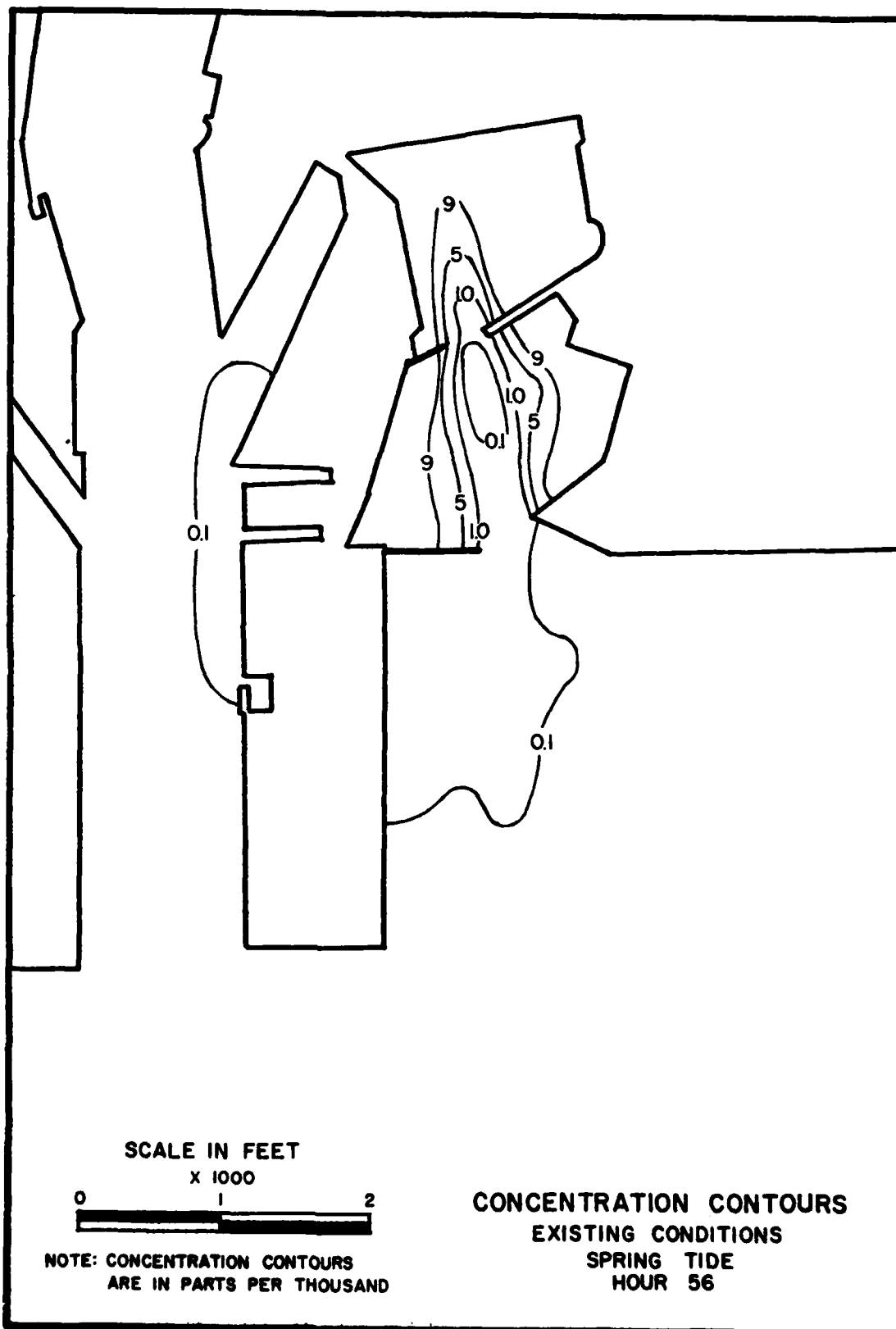


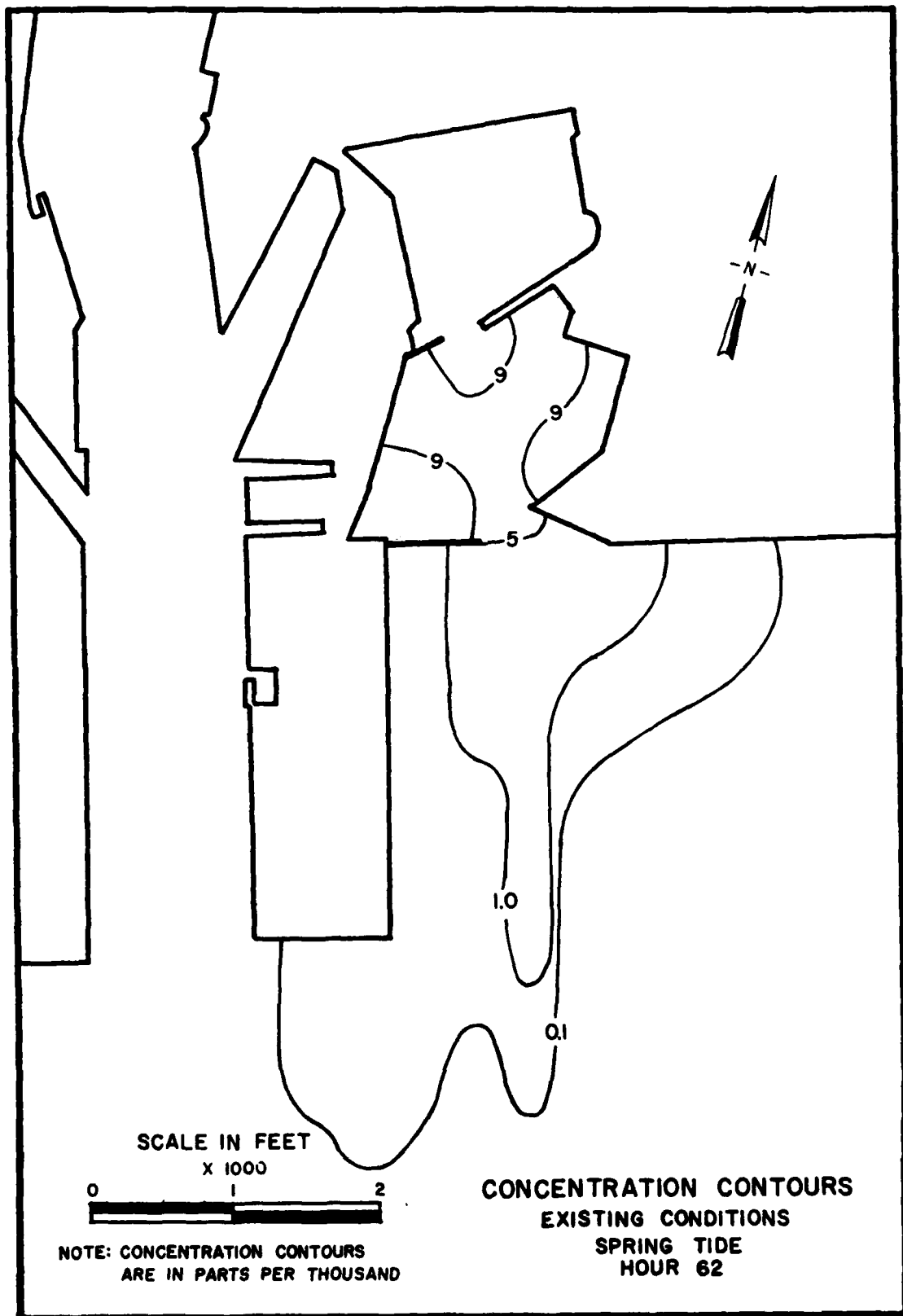
VELOCITY SCALE, FPS SCALE IN FEET
 1.0 0.5 0 10 2.0 X 1000
 2 1 0 2 4

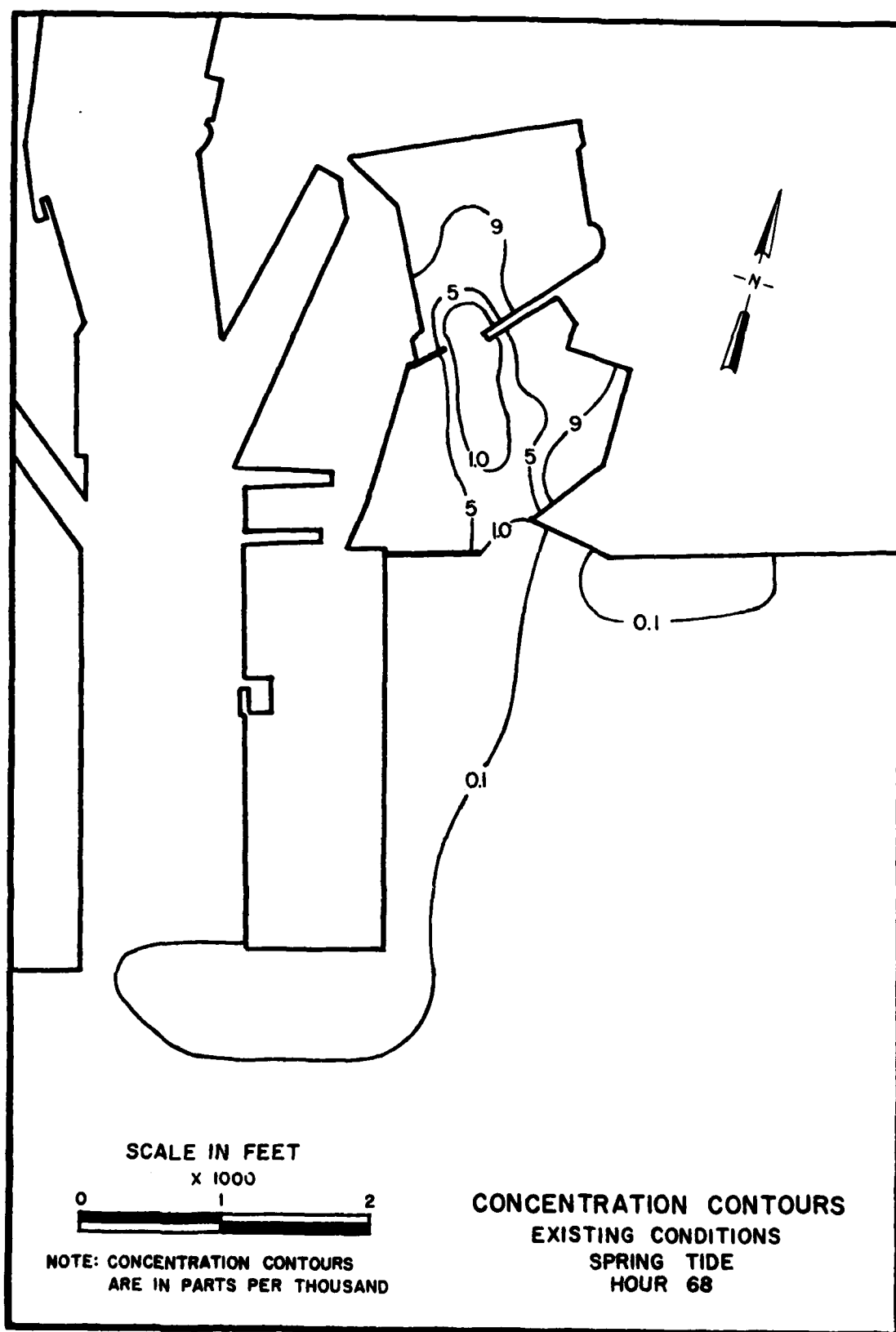
VELOCITY VECTOR PLOTS OF TIDAL CIRCULATION
 PLAN 1L
 SPRING TIDE
 HOUR 54

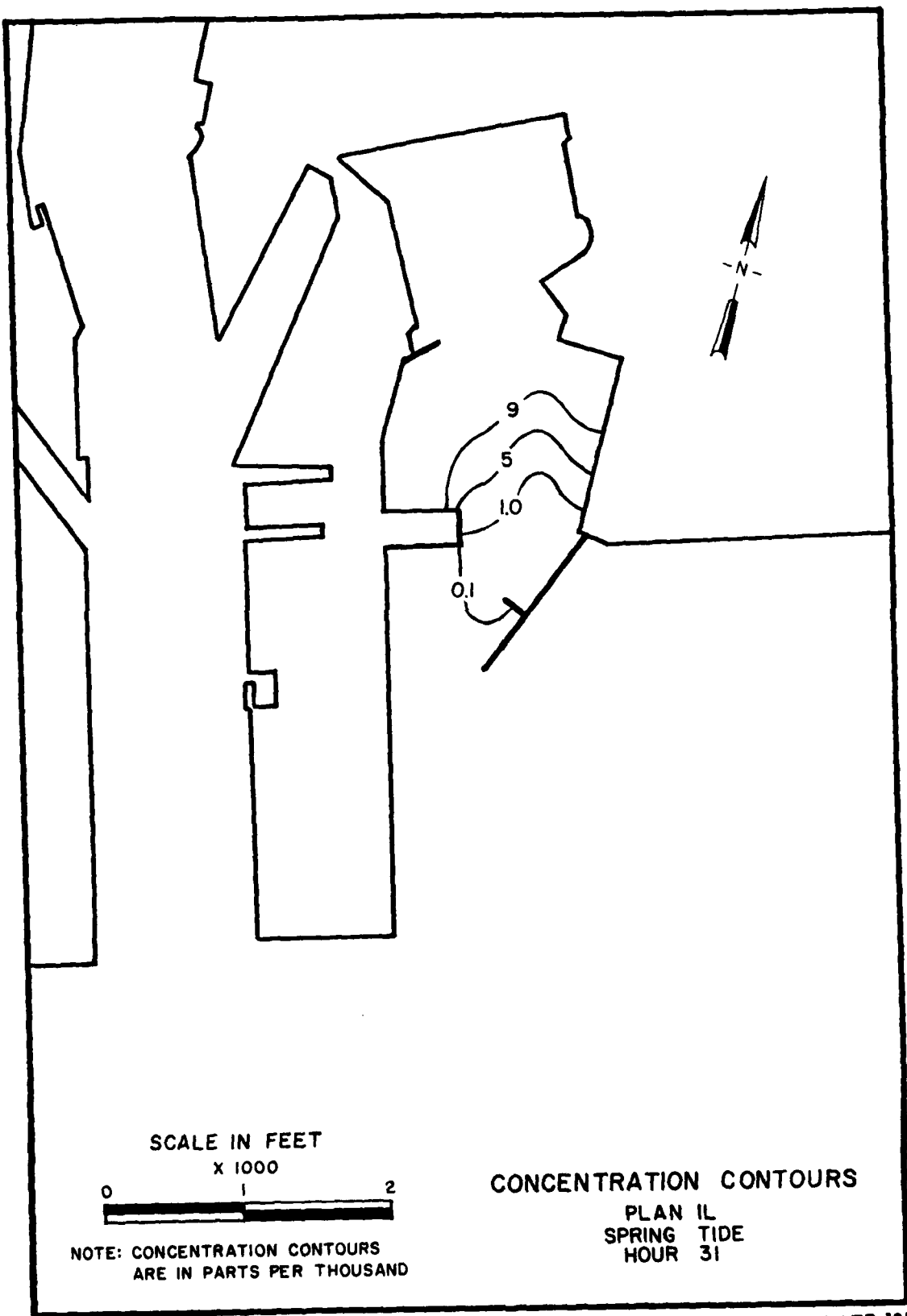








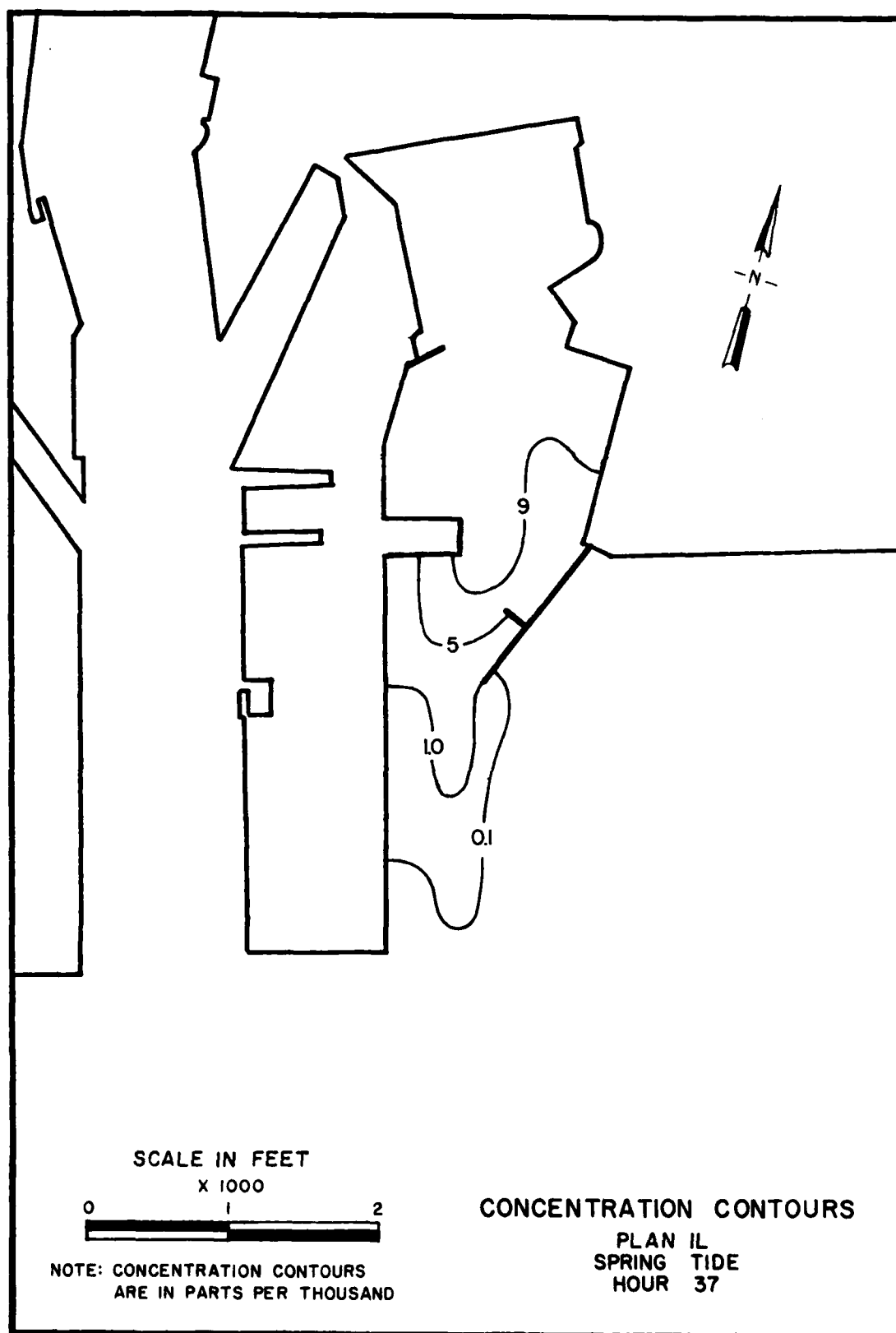


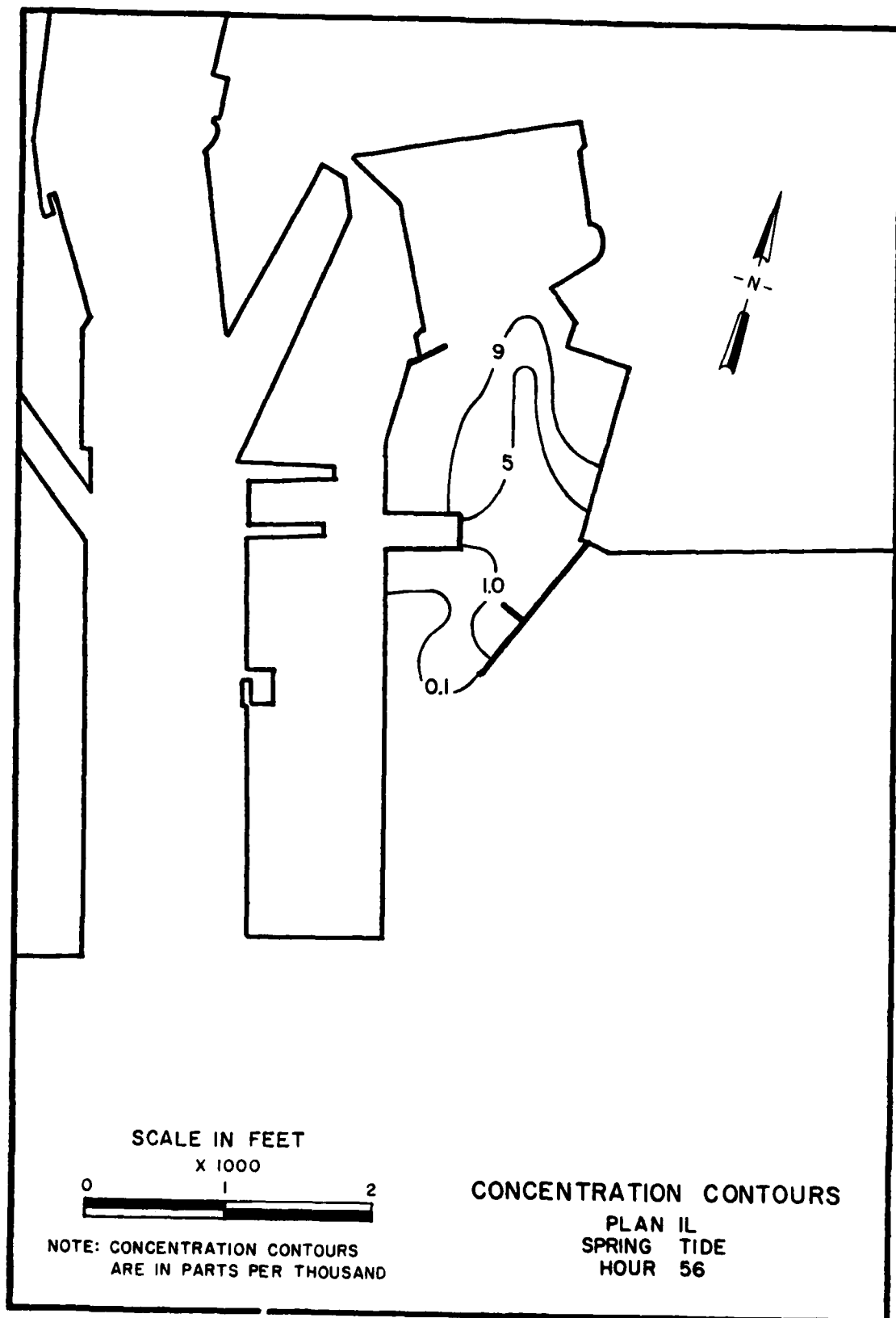


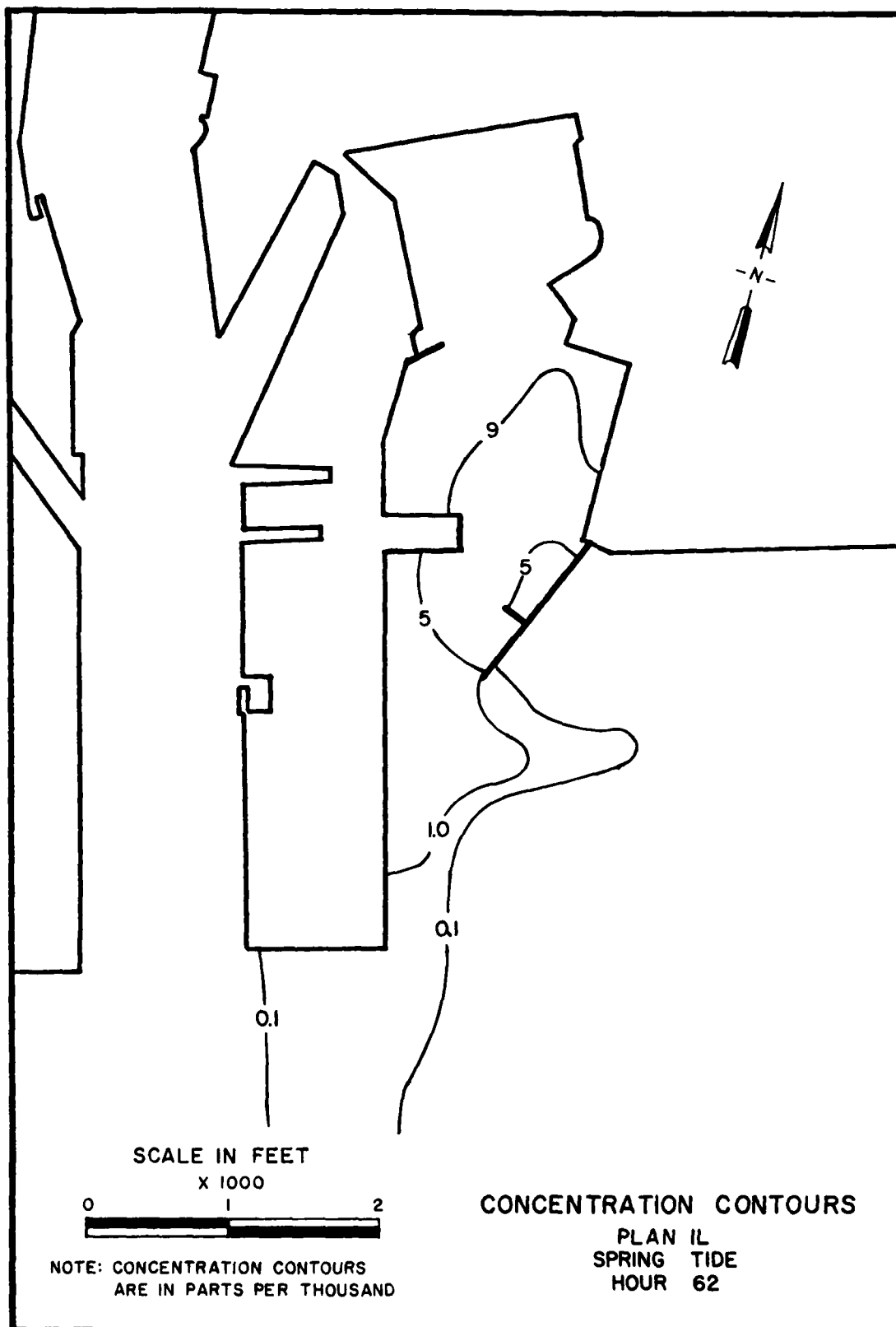
NOTE: CONCENTRATION CONTOURS
ARE IN PARTS PER THOUSAND

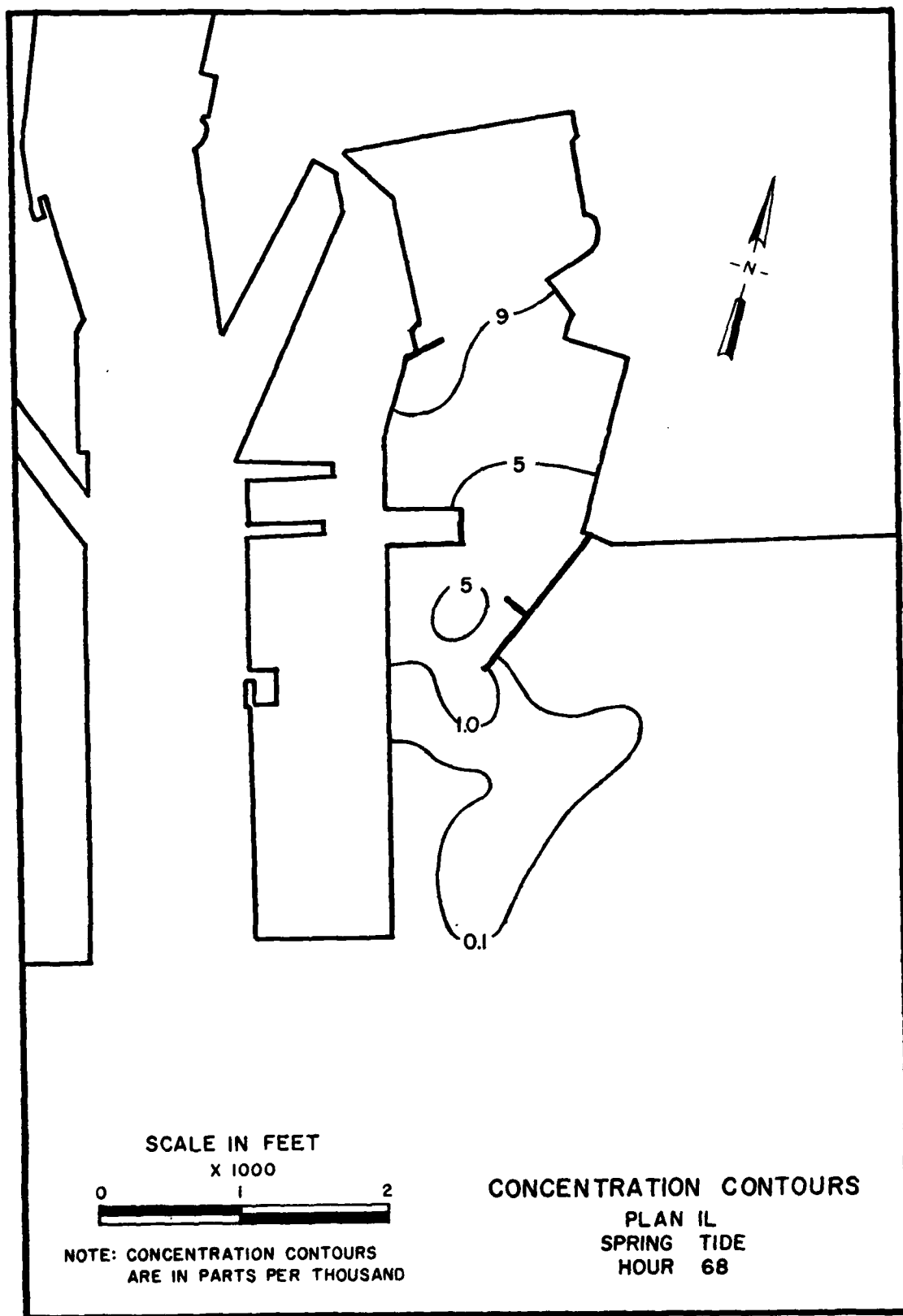
CONCENTRATION CONTOURS

PLAN 1L
SPRING TIDE
HOUR 31









APPENDIX A: NOTATION

APPENDIX A: NOTATION

a	Boundary of region A
A	Area of region inside a harbor
A_r	Area scale
b	Shallow-water orthogonal spacing
b_o	Deepwater orthogonal spacing
$(b_o/b)^{1/2}$	Refraction coefficient K_r
D	Wave sensor height, ft
E	Energy density
f	Frequency
g	Acceleration due to gravity, 32.3 ft/sec ²
h	Water depth, ft
H	Shallow-water wave height
H_{m0}	Significant wave height
H_n	Hankel function of the first kind of order n
H_o	Deepwater wave height
$H_{1/3}$	Significant wave height
i	Imaginary number
k	Wave number, ft ⁻¹
K_r	Refraction coefficient
K_s	Shoaling coefficient
n	Integer
n_a	Unit vector normal to boundary a
r	Spherical coordinate, ft
t	Time, sec
T	Time scale; record length

u	Velocity in x-direction, ft/sec
v	Velocity in y-direction, ft/sec
V_r	Velocity, scale
V_r	Volume, scale
w	Angular velocity, radians/sec
x	Cartesian coordinate, ft
y	Cartesian coordinate, ft
∇	Gradient, ft^{-1}
α_n	Unknown coefficient
Δt	Sampling interval, sec
η	Wave amplitude, ft
θ	Spherical coordinate, deg
ϕ	Total velocity potential, ft^2/sec
ϕ_a	Total velocity potential evaluated on boundary a , ft^2/sec
ϕ_I	Incident velocity potential, ft^2/sec
ϕ_R	Far-field velocity potential, ft^2/sec
ϕ_s	Scattered velocity potential, ft^2/sec

Subscripts

b	Energy density in a frequency band
j, m	Constants
p	Energy density spectra prior to correcting for pressure response
s	Sea surface energy spectra

DATE
FILMED
-8